JOURNAL OF BIOLOGICAL REGULATORS & HOMEOSTATIC AGENTS
Volume 32, No. 2, March - April, 2018

CONTENTS

EDITORIAL

LOW-GRADE CHRONIC INFLAMMATION MEDIATED BY MAST CELLS IN FIBROMYALGIA: ROLE OF IL-37

F. MASTRANGELO[1], I. FRYDAS[2], G. RONCONI[3], S.K. KRITAS[4], L. TETTAMANTI[5], AL. CARAFFA[6], C. D'OVIDIO[7], A. YOUNES[8], C.E. GALLENGA[9] and P. CONTI[10]

[1]Department of Medical Science and Biotechnology, University of Foggia, Foggia, Italy; [2]Faculty of Parasitology, Aristotle University of Thessaloniki, Macedonia, Greece; [3]UOS Clinica dei Pazienti del Territorio, Policlinico Gemelli, Rome, Italy; [4]Department of Microbiology and Infectious Diseases, Aristotle University of Thessaloniki, Macedonia, Greece; [5]Department of Medical and Morphological Science, University of Insubria, Varese, Italy; [6]Department of Pharmacology, University of Perugia, Perugia, Italy; [7]Section of Legal Medicine, Department of Medicine and Aging Sciences, University of Chieti-Pescara,Chieti, Italy; [8]Department of Anesthesiology, 'Santo Spirito' Hospital, Pescara, Italy; [9]Department of Biomedical Sciences and Specialist Surgery, Section of Ophthalmology, University of Ferrara, Italy; [10]Immunology Division, Postgraduate Medical School, University of Chieti-Pescara, Chieti, Italy

Received - January 22, 2018 -Accepted March 12, 2018

It has been observed that acute stress causes the activation of TH1 cells, while TH2 cells regulate and act on chronic inflammation. Fibromyalgia (FM) is a chronic, idiopathic disorder which affects about twelve million people in the United States. FM is characterized by chronic widespread pain, fatigue, aching, joint stiffness, depression, cognitive dysfunction and non-restorative sleep. The mechanism of induction of muscle pain and inflammation is not yet clear. In FM there is an increase in reactivity of central neurons with increased sensitivity localized mainly in the CNS. Mast cells are involved in FM by releasing pro-inflammatory cytokines, chemokines, chemical mediators, and PGD2. TNF is a cytokine generated by MCs and its level is higher in FM. The inhibition of pro-inflammatory IL-1 family members and TNF by IL-37 in FM could have a therapeutic effect. Here, we report for the first time the relationship between MCs, inflammatory cytokines and the new anti-inflammatory cytokine IL-37 in FM.

Fibromyalgia (FM) affects 2–4% of the population and is a complex high pain intensity disorder characterized by widespread pain and tenderness (1). In FM there is an increase in reactivity of central neurons with increased sensitivity localized mainly in the CNS. FM is due to an interaction between the sympathetic nervous system, neurotransmitters, external stressor and hormones. Therefore, FM affects the people physically, mentally and socially, since it is characterized by migraine, fatigue syndrome, morphological and/or functional muscular abnormalities, lower sleep and neuropathies.

It has been seen that exercise improves the disease, however the genesis of this disease is not clear (2).

Cytokines are important immune-modulators in the modulation of the hypothalamic-pituitary-adrenal axis (HPA) and certainly participate in the inflammation that takes part in this disease.

Patients with FM have higher levels of

Key words: fibromyalgia, mast cell, inflammation, cytokines, IL-37

Mailing address:
Prof. Pio Conti,
Postgraduate Medical School,
University of Chieti, Viale Unità d'Italia 73, Chieti, Italy
Tel./Fax: +39 0871 574136
e-mail: pconti@unich.it

0393-974X (2018)

inflammatory interleukin (IL)-1, IL-6, IL-18 and IL-33, and serotonin (3). This means that in this disease there is an immunological dysfunction of peripheral blood mononuclear cell phenotypes which can cause peripheral sensitization, pain, and fatigue syndrome (4). In addition, mast cells (MCs) and microglia are critically involved in the pathogenesis of neurodegenerative diseases including FM.

Inflammatory cytokines from the IL-1 family can cause high- and low-grade chronic inflammation. In fact, patients with FM present high levels of TNF, inflammatory IL-1 family members and IL-8. These cytokines contribute to the FM symptomatology. Activated MCs, along with other immune cells, produce inflammatory cytokines/chemokines, which participate in the pathological phenomena that occur in FM (5-7).

TNF is a potent inflammatory cytokine that is produced endogenously and exogenously by MCs and is capable of stimulating IL-1 on macrophages and other immune cells. In addition, TNF and IL-1 may regulate gene expression of other inflammatory cytokines including IL-6 and IL-33.

Inflammasome activation in MCs leads to the generation of IL-1, IL-6 and other cytokines. TNF and inflammatory IL-1 family members are the main instigators of inflammation and exacerbate many diseases. Thus, by inhibiting these cytokines, we can have an improvement in many inflammatory diseases.

Intense or prolonged nociceptive receptor activation can result in a protracted increase in the excitability of dorsal horn neurons, designated as central sensitization, where MCs play an important role (8).

In FM, most patients suffer from pain and have abnormalities in brain structure and function, with changes in the volume of gray matter. In this disease there is a reduced basal regional cerebral blood flow implicated in cognition, perception, sleep regulation, modulation of the stress response, memory and pain, all symptoms mediated by inflammatory cytokines generated by activated glial cells and MCs, and that occur in FM (9). In addition, in this disorder there is an augmentation of several immune cells, including NK cells, T cells, monocytes, and B cells. For example, natural killer T (NKT) cells and MCs have shown to be correlated with depression and therefore with FM (10-11). In addition, B cells increase and Th2 cells are activated in this disorder

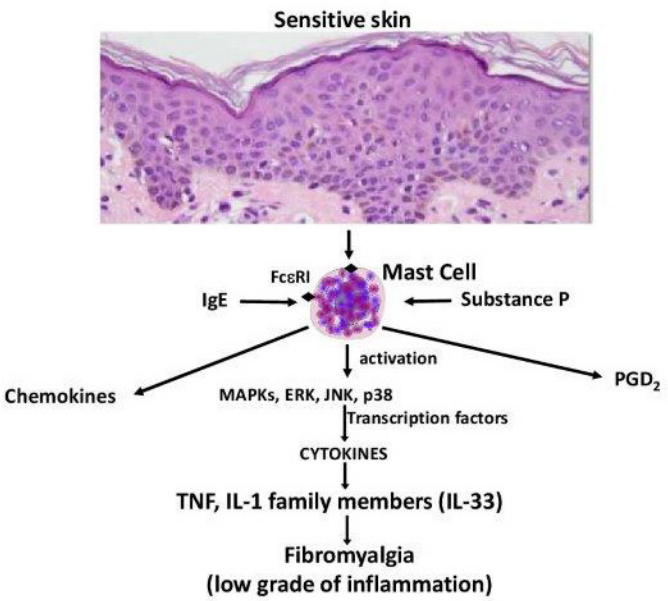

Fig. 1. *Mast cells are involved in sensitive skin and their activation, for example with Substance P or IgE, generates the release of inflammatory cytokines which participate in fibromyalgia low grade inflammation.*

(12). The activation of these immune cells leads to the generation of inflammatory cytokines including TNF and inflammatory IL-1 family members which can be inhibited by IL-37, the anti-IL1.

Mast cells

MCs derive from bone marrow $CD34^+/CD117^+/CD13^+$ pluripotent stem cells, the hematopoietic precursor cells which mature in the tissues and reside in virtually all vascularized organs.

MCs participate in innate and adaptive immune reactions, including allergic responses (13). They represent the "sentinels" of our body which defend us from infectious agents such as viruses, parasites, and bacteria. MCs neutralize various pathogens, fighting the external substances of the environment and micro-organisms. Activated MCs generate and release inflammatory substances that are harmful for the guest.

The activation of MCs with IgE leads to the release in a few seconds of substances such as histamine, heparin, tryptase, chymase, kinogenases, carboxypeptidase A3 and TNF; but these cells later can also release other inflammatory compounds such as cytokines, chemokines, NO, and PGD2 (14) (Fig. 1). The release of TNF and inflammatory IL-1 family members by MCs aggravates FM, an effect that can be partially inhibited by IL-37 (Fig.2).

Substance P and corticotropin-releasing hormone

Substance P (SP) and corticotropin-releasing hormone (CRH) are released from nociceptive afferent fibers and cause vasodilatation, increase capillary permeability, activate MCs and cause inflammatory responses. They are involved in stress, immune regulation, inflammation and neurotransmission. SP and CRH are found in high concentration on FM and are the stimulators of inflammatory cytokines on MCs (12).

IL-37

IL-37, or IL-1F7, is a new member of the IL-1 cytokine family with an anti-inflammatory activity (14) (Fig. 2). IL-37 binds IL-18 receptor alpha (IL-18Rα) chain and suppresses innate and acquired immunity. It prevents inhibition of IL-1, IL-6, IL-18, IL-33, and TNF and has therapeutic activity and a protective effect in animal models.

IL-37 down-regulates the expression of cJun, MAP kinase, p38α, STAT transcription factors and

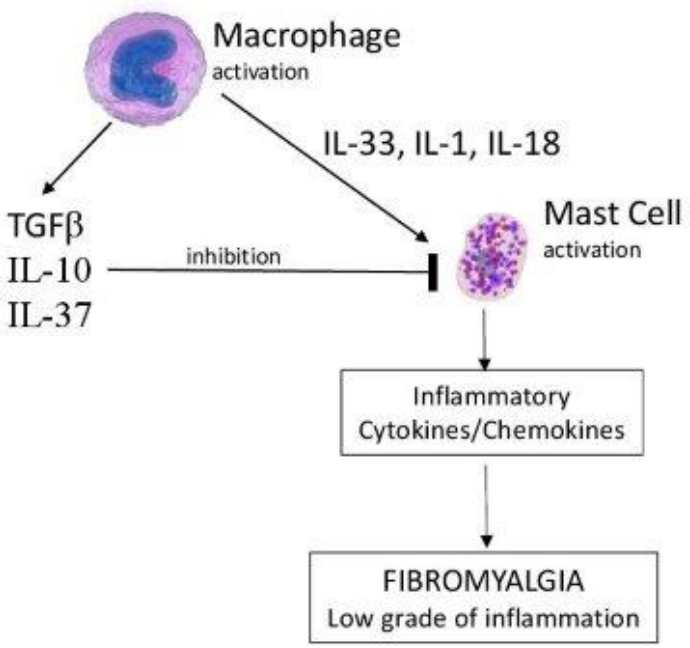

Fig. 2. *Activation of macrophages produces cytokines IL-33, IL-1, IL-18 which activate mast cells and partecipate in fybromyalgia. This effect can be inhibited by IL-37, IL-10 and TGFβ.*

p53, which are involved as proinflammatory signals. IL-37 could represent a new anti-inflammatory cytokine used as medication for FM where low-grade inflammation is present, since the current drugs used for this disease are ineffective and provoke harmful side effects.

CONCLUSION

In the light of these findings, we can conclude that MCs are deeply involved in FM as a source of inflammatory cytokines, and IL-37 could be used as a therapeutic cytokine which can offer benefit in this pathological disorder.

REFERENCES

1. Di Tommaso Morrison MC, Carinci F, Lessiani G, et al. Fibromyalgia and bipolar disorder: extent of comorbidity and therapeutic implications. J Biol Regul Homeost Agents 2017; 31(1):17-20.
2. Torgrimson-Ojerio B, Ross RL, Dieckmann NF, et al. Preliminary evidence of a blunted anti-inflammatory response to exhaustive exercise in fibromyalgia. J Neuroimmunol 2014; 277:160-67.
3. Arreola R, Becerril-Villanueva E, Cruz-Fuentes C, et al. Immunomodulatory effects mediated by serotonin. J Immunol Res 2015; 2015:354957.
4. Kopp S. Neuroendocrine, immune, and local responses related to temporomandibular disorders. Kopp S. J Orofac Pain 2001 Winter; 15(1):9-28.
5. Geenen R, Jacobs JW, Bijlsma JW. Evaluation and management of endocrine dysfunction in fibromyalgia. Rheum Dis Clin North Am 2002; 28(2):389-404.
6. Lawson K. Potential drug therapies for the treatment of fibromyalgia. Expert Opin Investig Drugs 2016; 25(9):1071-81.
7. McBeth J, Mulvey MR. Fibromyalgia: mechanisms and potential impact of the ACR 2010 classification criteria. Nat Rev Rheumatol 2012;
8. Borchers AT, Gershwin ME. Fibromyalgia: A Critical and Comprehensive Review Clin Rev Allergy Immunol 2015; 49(2):100-51.
9. Mullington JM, Hinze-Selch D, Pollmächer T. Mediators of inflammation and their interaction with sleep: relevance for chronic fatigue syndrome and related conditions. Ann N Y Acad Sci 2001; 933:201-10.
10. Thompson ME, Barkhuizen A. Fibromyalgia, hepatitis C infection, and the cytokine connection. Curr Pain Headache Rep 2003; 7(5):342-47.
11. Tsilioni I, Russell IJ, Stewart JM, Gleason RM, Theoharides TC. Neuropeptides CRH, SP, HK-1, and Inflammatory Cytokines IL-6 and TNF are increased in serum of patients with fibromyalgia syndrome, implicating mast cells. J Pharmacol Exp Ther 2016; 356(3):664-72.
12. Petra AI, Panagiotidou S, Stewart JM, Conti P, Theoharides TC. Spectrum of mast cell activation disorders. Expert Rev Clin Immunol 2014; 10(6):729-39.
13. Presta I, Guadagno E, Di Vito A, et al. Innate immunity may play a role in growth and relapse of chordoid meningioma. Int J Immunopathol Pharmacol 2017; 30(4):429-33.
14. Cavalli G, Dinarello CA. Suppression of inflammation and acquired immunity by IL-37. Immunol Rev 2018; 281(1):179-90.

PROTECTIVE EFFECT OF ERYTHROPOIETIN AGAINST LIPOPOLYSACCHARIDE-INDUCED INFLAMMATION AND MITOCHONDRIAL DAMAGE IN LIVER

G.X. ZHANG[1], Y.J. DU[2], X.H. LI[3], Z.T. FENG[4], H. ZHAO[1], Y. SUN[1], J.J. JIN[4] and X.J. LI[1]

[1]ICU, Ji Lin Tumor Hospital, Changchun, China; [2]Department of Nephropathy, The First Hospital of Jilin University, Changchun, China; [3]Department of Infection, The First Hospital of Jilin University, Changchun, China; [4]Life Sciences Institute, Jilin University, Changchun, China

Received July 23, 2017 – Accepted January 23, 2018

The first two authors contributed equally to this work

Recent studies have shown that liver dysfunction is an early event in sepsis. Pre-existing liver dysfunction is a risk factor for progression of infection to sepsis. However, the mechanism of the liver immune response in promoting sepsis and the importance of liver function are not completely understood. In the present study, we investigated the protective effect of erythropoietin (EPO) against mitochondrial dysfunction in a lipopolysaccharide (LPS)-induced sepsis model, and examined the underlying signaling mechanisms. Enzyme linked immunosorbent assay (ELISA) and reactive oxygen species (ROS) analysis were used to evaluate the levels of interleukin (IL)-1β and ROS. The effects of EPO on hepatic mitochondrial function were studied by detecting the mitochondrial DNA (mtDNA) copy number using real-time PCR (RT-PCR). To explore the mechanism of action of EPO in sepsis, protein expressions of IL-1β, caspase-1 and NLRP3 were assessed by Western blotting; liver histopathology and ultrastructure of liver mitochondria was examined by transmission electron microscopy. We found that LPS treatment increased serum IL-1β and ROS levels, the effect of which was attenuated by EPO. Moreover, LPS treatment also increased the mtDNA copy number and the protein expressions of IL-1β, caspase-1, and NLRP3, which were suppressed by EPO. Histological examination of liver showed LPS-induced cellular edema in hepatic lobules, lymphocytic infiltration and hepatocellular necrosis; these changes were also alleviated by EPO treatment. On electron microscopy, the size of hepatocellular mitochondria in the LPS group was smaller than that in the control group, and the changes were reversed by EPO in the LPS+EPO group. Our results suggest that EPO alleviated liver and mitochondrial damage induced by LPS, possibly *via* inhibition of NLRP3 signaling.

Severe sepsis is a leading cause of death worldwide, which results from the body's overwhelming response to infection. Severe sepsis is a complex syndrome which is typically associated with widespread tissue damage, organ failure, and even death (1). Management of complications of sepsis imposes significant strain on health care resources and the financial burden on the patients and their families. Development of newer, more effective therapeutic interventions for severe sepsis is a key imperative (2). Recent studies have reported a significant role of mitochondria in the

Key words: erythropoietin, lipopolysaccharide (LPS), liver damage, mitochondria,NLRP3

Mailing address:
Dr Xiu-Jiang Li,
ICU, Ji Lin Tumor Hospital,
1018 Huguang Street, Changchun 130012, China
Tel.: +86 18943008115
Fax: 0431-85879150
e-mail: zgxicu@163.com

0393-974X (2018)

pathophysiology of sepsis. In addition, studies have shown a correlation between the degree of mitochondrial dysfunction and treatment outcomes in patients with sepsis (3, 4). Mitochondria account for 98% of total body oxygen consumption. In addition to ATP production, mitochondria play a vital role in thermogenesis, thermoregulation, intracellular calcium regulation, and production of reactive oxygen species (ROS); these mechanisms are essential for the maintenance of vascular tone, oxygen sensing, and regulation of mitochondrial signaling in healthy state (5-8). However, the pathogenic mechanisms of mitochondrial dysfunction in sepsis have not been elucidated. Nevertheless, mitochondrial protection or acceleration of recovery of mitochondrial function represents a novel target intervention for treatment of sepsis (8, 9).

Lipopolysaccharide (LPS) located on the outer membrane of gram-negative bacteria is a prototypical trigger of sepsis, which stimulates immune responses by its interaction with membrane receptors, which in turn induces the generation of cytokines (10-12). Exposure to LPS impairs ROS production by mitochondria due to damage to mitochondrial DNA (mtDNA) and interruption of mitochondrial transcription and oxidative phosphorylation (OXPHOS). Moreover, LPS-induced apoptosis was shown to be dependent upon mitochondrial dysfunction in human cell lines (13). LPS-induced damage is associated with reversible oxidative stress, which can be used to model or as a target for the development of novel therapeutics for severe sepsis (14, 15).

Erythropoietin (EPO) is a hemopoietic hormone produced by kidney and liver, which stimulates erythropoiesis in the bone marrow (16, 17). The protective effect of EPO on brain and vasculature has been demonstrated in patients with acute stroke (17). Additionally, recombinant human EPO (rHuEpo) has been widely used to treat renal anemia in clinical settings (18). Exposure to EPO was shown to enhance mitochondrial biogenesis and mitochondrial function in human muscle tissues (19-21). EPO-induced reversal of mitochondrial dysfunction prompted us to hypothesize a potential preventive and therapeutic role of rHuEpo in the management of sepsis. In the present study, we investigated the protective effect of EPO against mitochondrial dysfunction in an LPS-induced sepsis model, and studied the underlying signaling mechanisms.

MATERIALS AND METHODS

Thirty-two adult male C57BL/6J mice (weight: 26-38 g) were purchased from Jilin University animal core and housed at 22-24°C with free access to food and water. The study was approved by the Jilin University Institutional Animal Care and Use Committee.

rHuEpo (20071102V, 100000 IU/tube) was purchased from Shenyang Sansheng Pharmaceutical Co. Ltd. LPS (Sigma-L2880) was purchased from Sigma. Interleukin (IL)-1β Elisa kit was purchased from Shanghai Meixuan Biological Science and Technology Ltd. ROS analysis kit and the antibodies against IL-1β, caspase-1, and NLRP3 were purchased from Nanjin Jiancheng Bioengineering Institute.

Mice (8 mice per group) were administered intraperitoneal injection of LPS (15 mg/kg) and/or human recombinant EPO (5000 U/kg) or an equal volume of 0.9% NaCl and tissues removed under general anesthesia 24 h after administration.

Enzyme-linked immunosorbent assay for interleukin 1β

Twenty-four hours after LPS injection, blood samples were obtained from rat eyeballs under inhalational anesthesia. Blood was allowed to solidify at room temperature and then centrifuged at 1000 *g* for 15 min. The supernatant was measured according to the mouse interleukin (IL)-1β Elisa kit. The IL-1β concentration in blood was calculated from the standard curve.

Western blotting

The mice were anesthetized with carbon dioxide and decapitated. Liver tissue were removed and homogenized in RIPA lysis buffer (Sigma) for 5 min. Homogenates were centrifuged at 12,000 g at 4°C for 1 h and the supernatant collected. Proteins were analyzed using Bradford protein assay (Bio-Rad). Equal amounts of proteins (40 μg) were separated by 8% SDS-PAGE gel at 70V and 90 V for 2 h, transferred onto PVDF membranes at 210 mA for 50 min, and incubated overnight at 4°C with antibodies against IL-1β (1:1000, Nan Jing Jian Cheng Bioengineering

Institute), caspase-1 (1:1000, Nan Jing Jian Cheng Bioengineering Institute), NLRP3 (1:1000, Santa Cruz, USA), and tubulin (1:1000, Ruiying Biological) as a control. Next, the membranes were incubated with secondary antibody goat anti-rabbit (1:20000, Ruiying Biological) at room temperature for 1 h. Blots were developed using chemiluminescent substrate made by solution A and B in a 1:1 ratio. Chemiluminescent bands were detected on a scanner (Chemicopy series) and quantified using NIH Image J software.

Reactive oxygen species assay

Liver tissues were homogenized in phosphate buffered saline (PBS) (1:20) for 5 min, and then centrifuged at 1000 g for 10 min. Protein concentration in the supernatant was measured by the Bradford method, the standard curve for which was made according to the absorbance obtained from graded concentration of bovine serum albumin (BSA) (0.10 mg/mL, 0.08 mg/mL, 0.06 mg/mL, 0.04 mg/mL, 0.02 mg/mL, and 0 mg/mL, respectively). The protein concentration was calculated according to the standard curve. Supernatants were subjected to fluorescence spectrophotometry (SpectraMAX Gemini XS; MDS Analytical Technologies) at 485 nm excitation and 530 nm emission wavelengths. Fluorescent intensity of liver tissue samples was measured with the reactive oxygen species (ROS) test kit according to the manufacturer's instructions; the final results were expressed as fluorescence intensity/mg protein.

Liver histological imaging

The left lobe of the liver was fixed in 2% formaldehyde in PBS, embedded in paraffin in PBS, and then sectioned. Phosphate buffered saline (PBS) Hematoxylin and Eosin (HE)-stained sections were examined with OLYMPUS microscope BX51.

Liver tissues were pre-fixed with 2.5% glutaraldehyde, post-fixed with 1% osmium, and dehydrated by passage through a graded ethanol series. The tissues were embedded with epoxy resin and sectioned with ultra-thin slicer LKB III. Sections were stained with uranyl acetate and lead citrate, and the liver ultra-structure examined by transmission electron microscopy (JEM-1200EX).

Quantitative real time polymerase chain reaction

The genomic DNA was extracted from the liver using the Biospin reagent according to the manufacturer's instructions. One μg of DNA from each sample was used for the PCR reaction. The mixture was prepared with 5 μL SYBR green PCR Master Mix (Applied Biosystems) and 0.2 μL primers. Phosphate buffered saline (PBS) hematoxylin and eosin (H&E) DNA Cytochrome C oxidase 1 (mtCOI) gene expression was normalized with 18s ribosomal DNA content. The primers used were:

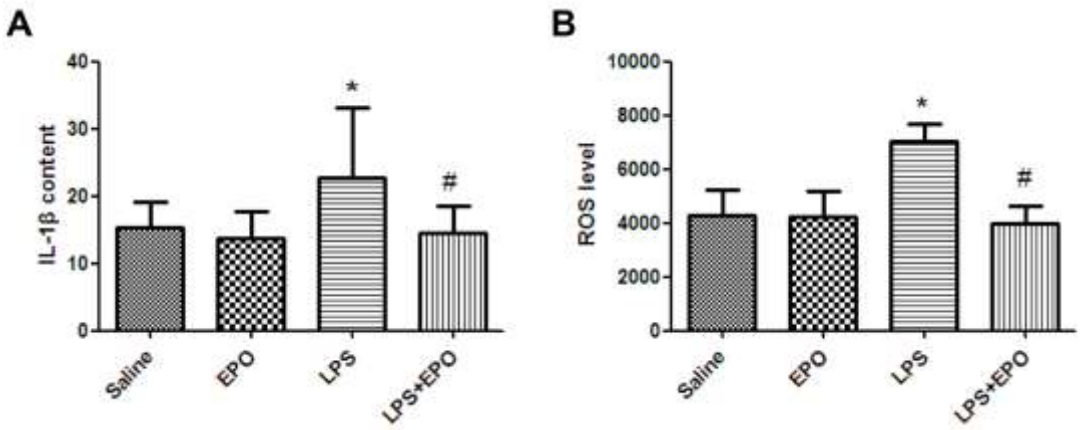

Fig. 1. *The IL-1β and ROS level in blood after LPS and EPO treatment.* ***A****) Results of ELISA assay showing IL-1β levels in blood in the saline, EPO, LPS, and LPS+EPO groups;* ***B****) Blood ROS level in the saline, EPO, LPS, and LPS+EPO groups. Data are presented as mean±standard error of the mean.* $^{*}P<0.05$ *or* $^{\#}<0.05$ *on one-way ANOVA*

18s forward primer: 5'-TAGAGGGACAAGTGGCGTTC-3';
18s reverse primer: 5'-CGCTGAGCCAGTCAGTGT-3';
COI forward: 5'-GCCCCAGATATAGCATTCCC-3';
COI reverse: 5'-GTTCATCCTGTTCCTGCTCC-3

Statistical analysis

Data are expressed as mean±standard deviation (SD). Group comparisons were performed using One-way ANOVA by SPSS 18.0. Differences were considered significant at $P < 0.05$.

RESULTS

EPO reversed the increased levels of IL-1β and ROS in blood induced by LPS

Since LPS treatment is known to stimulate the immune response, we utilized LPS to establish an animal model of sepsis and first detected the blood levels of IL-1β and ROS. Mice injected intraperitoneally with LPS (15 mg/kg) showed increased IL-1β level (22.64±10.54) as compared to that in mice injected with saline (13.64±4.07) or the EPO (14.31±3.11) control group, while a significant decrease in IL-1β level (14.44±4.14) was observed in mice which were administered human recombinant EPO (5000 U/kg) (Fig. 1A, $P<0.05$ *vs* LPS). Similarly, ROS level was significantly increased after LPS treatment (7029.73±664.51) as compared to that after administration of saline (4263.18±961.13) or EPO (4263.60±966.61), which was reversed by EPO administration (3979.91±676.76) (Fig. 1B, $P<0.05$ *vs* LPS). No significant difference was observed between the EPO and saline groups in respect to IL-1β and ROS levels, which suggested that EPO only had no effect on the IL-1β and ROS levels.

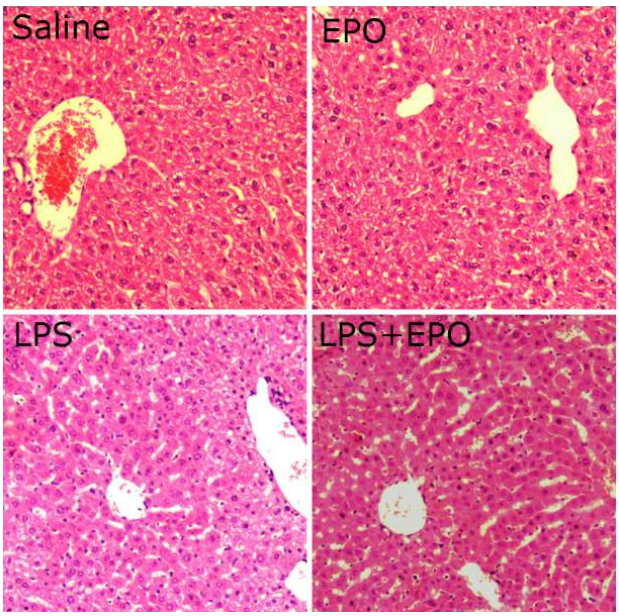

Fig. 3. *Histological changes induced by LPS and EPO treatments under light microscopy. Representative light microscopic histological images showing hepatic edema, lymphocytic infiltration, and hepatocellular necrosis caused by LPS (C), while normal liver histology was observed in the saline (A) and EPO (B) groups; the effect of EPO on LPS-induced hepatic edema (D).*

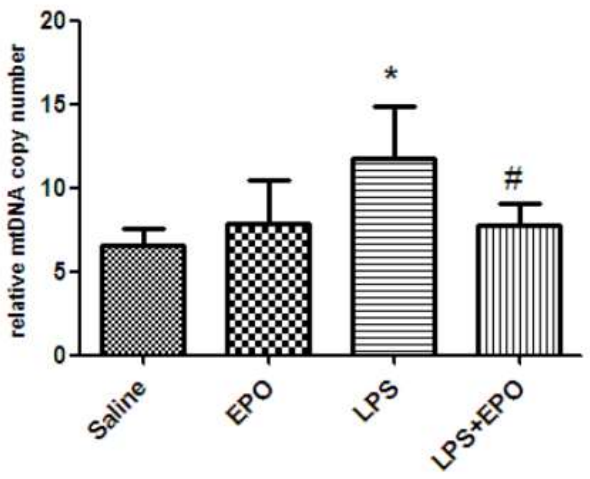

Fig. 2. *Mitochondrial (mt) DNA copy number in liver after LPS and EPO treatment. Results of quantitative real-time PCR showing the relative mtDNA copy numbers in liver in the saline, EPO, LPS, and LPS+EPO groups. Data are presented as mean±standard error of the mean. *P<0.05 or #<0.05 on one-way ANOVA*

Increased mtDNA copy number in liver induced by LPS was reversed by EPO

LPS is known to damage mitochondrial function in septic states. On qRT-PCR, we observed significant increase in mtDNA copy number in liver tissues of the LPS group (11.79±3.10) as compared to that of the saline (6.52±1.02) or EPO (7.43±2.85) groups; however, the LPS+EPO group showed a significant decrease in the mtDNA copy number (7.74±1.41), which was comparable to that in the LPS group

(Fig. 2, $P<0.05$). These findings demonstrated the protective effect of EPO against LPS-induced damage. EPO treatment had no effect on mtDNA copy number compared to the saline group.

EPO prevented the impaired histological alterations induced by LPS

We studied the LPS-induced histological changes in liver tissues, as well as the effect of EPO on these changes. Light microscopic images showed that LPS induced hepatic edema, lymphocytic infiltration, and hepatocellular necrosis, while normal liver histology was observed in the saline and EPO groups. However, histological changes in the LPS+EPO group were significantly attenuated as compared to those in the LPS group, which suggested that EPO attenuated the LPS-induced damage in liver cells (Fig. 3). On transmission electron microscopy, the ultra-structure of mitochondria in liver cells in the LPS group showed poor organization, while normal mitochondrial ultrastructure was observed in the control group; changes in mitochondrial ultrastructure in the LPS+EPO group were significantly attenuated as compared to those in the EPO group (Fig. 4). Liver histology in the EPO group was comparable to that in the saline group.

EPO attenuated the increased expressions of cell apoptosis-related proteins induced by LPS

To unravel the underlying mechanism of the beneficial effect of EPO in LPS-induced injury, we assessed the expressions of cell apoptosis-related proteins including IL-1β, caspase-1, and NLRP3 in liver after LPS exposure with and without EPO treatment. Results of Western blotting showed that LPS treatment induced a significant increase in protein expressions of IL-1β and NLRP3, a tendency that increased protein expressions of caspase-1 and cleaved caspase-1 as compared to that in the saline or EPO groups. However, the protein expressions of IL-1β and NLRP3 in the LPS+EPO group were significantly lower, a tendency that lowered the expressions of caspase-1 and cleaved caspase-1 as compared to those in the LPS group (Fig. 5). EPO treatment had no effect on protein levels as the protein expressions were comparable to those in the saline group. Collectively, Western blotting results showed that LPS treatment increased the protein

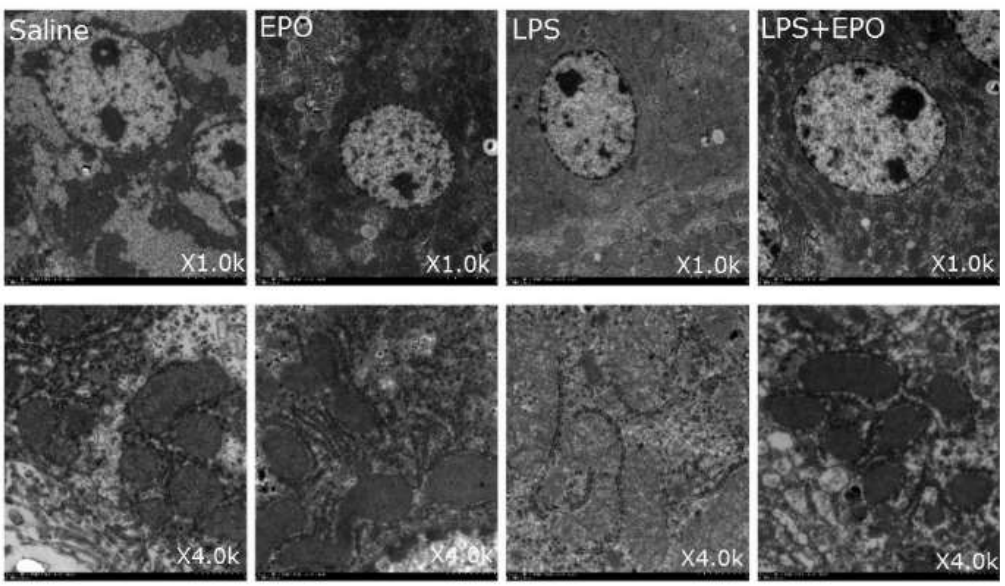

Fig. 4. *Transmission electron microscopy images showing ultra-structure of mitochondria after LPS and EPO treatment. Ultra-structural images obtained on transmission electron microscopy showing the structure of mitochondria in liver cells in the saline (**A**) and EPO (**B**) groups; Poor-organization of mitochondria in the LPS group (**C**); effect of EPO on LPS-induced mitochondrial structural changes (**D**).*

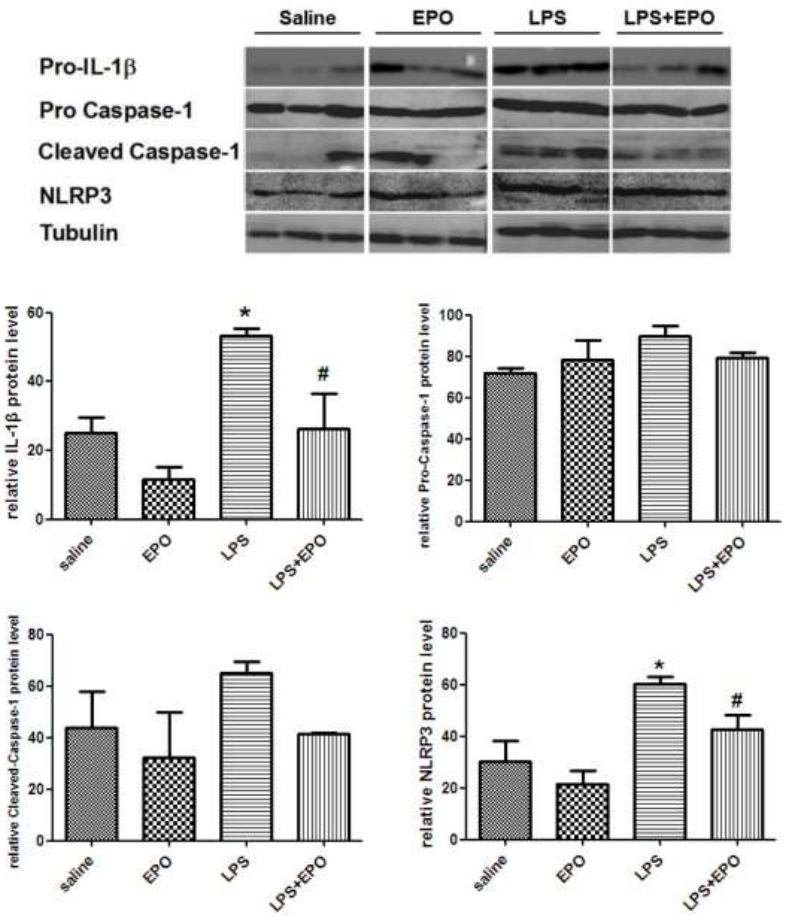

Fig. 5. *Results of Western blotting showing the protein expressions of IL-1β, cleaved caspase-1, and NLRP3 after LPS and EPO treatment. Western blot images showing the proteins expression of IL-1β, cleaved caspase-1, and NLRP3 of liver in the saline (**A**) and EPO (**B**) groups, and the effect of LPS on these protein expression, as well as the effect of EPO on LPS-induced changes. Tubulin served as the endogenous control. Data are presented as mean±standard error of the mean. $^{*}P<0.05$ or $^{\#}<0.05$ on one-way ANOVA.*

expressions of IL-1β, caspase-1, and NLRP3, which were suppressed by EPO+LPS; these findings suggest that EPO played a protective role against LPS-induced damage.

DISCUSSION

In the present study, we observed that LPS stimulated an immune response, increased the mtDNA copy number, and induced histological changes in liver. Moreover, our findings suggest that the LPS-induced damage was reversed by EPO administration. Our results provide new insights to investigate sepsis and unravel a novel therapeutic target for severe sepsis.

Severe sepsis is associated with a high mortality rate of up to 40%. Therapeutic research for management of sepsis is of great clinical import. Recent studies have shown sepsis to be related to mitochondrial functional apoptosis or loss. The beneficial effects of EPO on mitochondrial function have also been widely reported. Therefore, in this study, we intended to explore the mechanism by which EPO protects against organelle damage in sepsis.

Pathological hypoxia in liver cells during sepsis is believed to impair oxidative phosphorylation

in liver mitochondria. Mitochondrial dysfunction leads to production of a large number of ROS and mitochondrial DNA fragments, both of which induce activation of NLRP3 inflammasome including NLRP3, apoptosis-related speckle protein (ASC), and caspase-1 (22). Activation of NLRP3 recruits ASC and caspase-1 to accomplish self-oligomerization and self-cleavement, following which the functional NLRP3 cuts the precursor of IL-1β leading to its secretion in the extracellular space. Inflammatory reactions mediated by IL-1β further induces the release of a larger number of inflammatory factors (23). In the LPS-induced model of sepsis used in the present study, inflammatory reactions in liver were ostensibly induced by the LPS-induced increase in IL-1β and ROS levels. Likewise, the significant increase in the mtDNA copy numbers in liver cells after LPS treatment was indicative of mitochondrial dysfunction. Expressions of some other inflammatory factors such as NLRP3 and caspase-1 protein were also increased after exposure to LPS, which suggests that the mitochondrial dysfunction might be associated with NLRP3.

EPO treatment has been shown to alleviate renal injury and dysfunction in a mouse model of renal ischemia (24). A similar protective effect of EPO has also been demonstrated in a rat model of myocardial infarction (25). Likewise, several clinical studies have reported the beneficial effect of EPO against organelle damage in some diseases (17, 18), a subject which has evoked much research interest in recent years. In this study, administration of EPO alleviated LPS-induced changes. Our findings indicate a potential role of EPO in the treatment of sepsis. The beneficial effect is likely mediated via inhibition of NLRP3-mediated inflammatory reactions, as well as by mitochondrial rescue.

However, some limitations of the present study need to be acknowledged. The underlying mechanism of the effect of EPO against LPS-induced damage in liver is not clear. Although NLRP3 is a possible target of EPO, there is no definitive evidence in this regard. Therefore, manipulation of NLRP3 gene or protein expression with an agonist or antagonist in a future study will help clarify whether the increase or decrease in NLRP3 could alter the effects of EPO on inflammation and mitochondrial dysfunction. Moreover, use of transgenic technique to delete or overexpress NLRP3 to study its effect on sepsis is another area for future research. In addition, whether exogenous administration of EPO could reverse the effect of NLRP3 deletion or overexpression on sepsis will help elucidate the contribution of NLRP3 in inflammation, and mitochondrial dysfunction in sepsis. Furthermore, we did not determine cytochrome c, which was shown to be a marker of liver mitochondrial dysfunction in a previous study (26).

In conclusion, our study revealed a protective effect of EPO against inflammation and mitochondrial dysfunction in septic state. EPO is a potential candidate moiety for treatment of sepsis in clinical settings.

ACKNOWLEDGEMENTS

This study was supported by the Jilin Province Health Department Youth Fund.

REFERENCES

1. Mayr FB, Yende S, Angus DC. Epidemiology of severe sepsis. Virulence 2014; 5:4-11.
2. Martin-Loeches I, Levy MM, Artigas A. Management of severe sepsis: advances, challenges, and current status. Drug Des Devel Ther 2015; 9:2079-88.
3. Azevedo LC. Mitochondrial dysfunction during sepsis. Endocr Metab Immune Disord Drug Targets 2010; 10:214-23.
4. Wendel M, Heller AR. Mitochondrial function and dysfunction in sepsis. Wien Med Wochenschr 2010; 160:118-23.
5. Chan DC. Mitochondria: dynamic organelles in disease, aging, and development. Cell 2006; 125:1241-52.
6. Larsen FJ, Schiffer TA, Weitzberg E, Lundberg JO. Regulation of mitochondrial function and energetics by reactive nitrogen oxides. Free Radic Biol Med 2012; 53:1919-28.
7. Osellame LD, Blacker TS, Duchen MR. Cellular and molecular mechanisms of mitochondrial function. Best Pract Res Clin Endocrinol Metab

2012; 26:711-23.
8. Singer M. The role of mitochondrial dysfunction in sepsis-induced multi-organ failure. Virulence 2014; 5:66-72.
9. Brealey D, Singer M. Mitochondrial dysfunction in sepsis. Curr Infect Dis Rep 2003; 5:365-71.
10. Meng F, Lowell CA. Lipopolysaccharide (LPS)-induced macrophage activation and signal transduction in the absence of Src-family kinases Hck, Fgr, and Lyn. J Exp Med 1997; 185:1661-70.
11. Marshall JC. Lipopolysaccharide: an endotoxin or an exogenous hormone? Clin Infect Dis 2005; 41 Suppl 7:S470-80.
12. Rosenfeld Y, Shai Y. Lipopolysaccharide (Endotoxin)-host defense antibacterial peptides interactions: role in bacterial resistance and prevention of sepsis. Biochim Biophys Acta 2006; 1758:1513-22.
13. Kuwabara T, Imajoh-Ohmi S. LPS-induced apoptosis is dependent upon mitochondrial dysfunction. Apoptosis 2004; 9:467-74.
14. Suliman HB, Carraway MS, Welty-Wolf KE, Whorton AR, Piantadosi CA. Lipopolysaccharide stimulates mitochondrial biogenesis via activation of nuclear respiratory factor-1. J Biol Chem 2003; 278:41510-18.
15. Choumar A, Tarhuni A, Letteron P, et al. Lipopolysaccharide-induced mitochondrial DNA depletion. Antioxid Redox Signal 2011; 15:2837-54.
16. Peschle C, Marone G, Genovese A, Magli C, Condorelli M. Erythropoietin production in the rat: additive role of kidney and liver. Am J Physiol 1976; 230:845-48.
17. Jelkmann W, Wagner K. Beneficial and ominous aspects of the pleiotropic action of erythropoietin. Ann Hematol 2004; 83:673-86.
18. Francesco L, Pietro P, Del VL. Recombinant human epoetin beta in the treatment of renal anemia. Ther Clin Risk Manag 2007; 3:433-39.
19. Carraway MS, Suliman HB, Jones WS, Chen CW, Babiker A, Piantadosi CA. Erythropoietin activates mitochondrial biogenesis and couples red cell mass to mitochondrial mass in the heart. Circ Res 2010; 106:1722-30.
20. Plenge U, Belhage B, Guadalupe-Grau A, et al. Erythropoietin treatment enhances muscle mitochondrial capacity in humans. Front Physiol 2012; 3:50.
21. Qin C, Zhou S, Xiao Y, Chen L. Erythropoietin enhances mitochondrial biogenesis in cardiomyocytes exposed to chronic hypoxia through Akt/eNOS signalling pathway. Cell Biol Int 2014; 38:335-42.
22. Fink MP. Bench-to-bedside review: Cytopathic hypoxia. Crit Care 2002; 6:491-9.
23. Schroder K, Tschopp J. The inflammasomes. Cell 2010; 140:821-32.
24. Patel NS, Sharples EJ, Cuzzocrea S, Chatterjee PK, Britti D, Yaqoob MM, Thiemermann C. Pretreatment with EPO reduces the injury and dysfunction caused by ischemia/reperfusion in the mouse kidney in vivo. Kidney Int 2004; 66:983-9.
25. Li XJ, Wang XW, Du YJ. Protective effects of erythropoietin on myocardial infarction in rats: the role of AMP-activated protein kinase signaling pathway. Am J Med Sci 2011; 342:153-59.
26. Tarantino G, Colao A, Capone D, et al. Circulating levels of cytochrome C, gamma-glutamyl transferase, triglycerides and unconjugated bilirubin in overweight/obese patients with non-alcoholic fatty liver disease. J Biol Regul Homeost Agents 2011; 25:47-56.

EFFECTS OF TUMOR-ASSOCIATED MACROPHAGES ON THE PROLIFERATION AND MIGRATION OF ESOPHAGEAL CANCER-ASSOCIATED LYMPHATIC ENDOTHELIAL CELLS

JY. CHEN[1], LL. HE[2], HX. ZHANG[1], MM. SUN[3] and KS. CHEN[1]

[1]The First Affiliated Hospital of Zhengzhou University, Zhengzhou, China; [2]China-US (Henan) Hormel Cancer Institute, Zhengzhou, China; [3]Affiliated Tumor Hospital of Zhengzhou University, Zhengzhou, China

Received September 26, 2017 – Accepted February 8, 2018

The aim of this study was to explore whether M2 macrophages can be transformed into M1 macrophages, and to investigate the effect of different types of macrophages on the proliferation, migration and ring-forming ability of esophageal cancer-related lymphatic endothelial cell (LEC). Human monocytic leukemia cell line (THP-1 cell) was induced to differentiate to M1 macrophages (M1 group) and M2 macrophages (M2 group), and co-cultured with esophageal cancer-associated LEC. The individual esophageal cancer co-cultured with LEC was used as control. Different types of macrophages were observed by Cell counting kit-8 (CCK-8). Enzyme-linked immunosorbent assay (ELISA) was used to detect the VEGF-C concentration; the expression of VEGFR-3 protein and its mRNA was detected by Western blot and qRT-PCR, respectively. The positive rate of the M1 group induced by IFN-γ and LPS was significantly higher than that of M2 macrophages (48.57±5.98% *vs* 25.83±1.95%). The expression of VEGF-C in the supernatant of the M2 group was higher than that in the control group, but no significant differences regarding the expression of VEGF-C between M1 and control groups were found. In addition, the expression of VEGFR-3 on both mRNA and protein in esophageal cancer-related LEC of the M2 group was significantly higher than those in the control group; however, the M1 group had a significantly lower VEGFR-3 level on both mRNA and protein than the control group. Human M2 macrophages can be transformed into M1 macrophages, and can promote the proliferation, migration and ring-forming ability of esophageal cancer-associated LEC.

Esophageal cancer, as an aggressive gastrointestinal cancer, is one of the most threatening cancer types of the human digestive tract with a high rate of incidence and mortality; it is the eighth most common cancer worldwide, the five-year survival rate for esophageal cancer is only 15-25% (1). It has been disclosed that many factors contribute to its progression including local inflammation and esophagitis, in addition to several unhealthy eating habits such as poor diet, excessive drinking, and very hot drinks (2, 3).

The tumor microenvironment plays an important role for cancer development and metastasis (4). Tumor-associated macrophages (TAMs) are the main cellular components of the tumor microenvironment and plays a critical role in carcinogenesis and tumor progression (5, 6). Macrophages are derived from the differentiation of monocytes in the periphery. Being activated by lipopolysaccharides (LPS) or interferon-c, monocytes can become M1 (classically activated macrophage); when stimulated by interleukin

Key words: esophageal cancer associated with lymphoid endothelial cells, M1 macrophages, M2 macrophages, tumor-associated macrophages, vascular endothelial growth factor-C

Mailing address:
Dr Kuisheng Chen,
The First Affiliated Hospital
Zhengzhou University, No.1 of Eastern Jianshe Road,
Erqi District, Zhengzhou 450000, Henan Province, China
Tel.: 13837134366
e-mail: kuishengc@126.com

0393-974X (2018)

(IL)-4, IL-13, IL-10 and tumor growth factor-b1, monocytes can also become M2 (alternatively activated macrophage) (7). However, those two types of macrophages have a different tumor-regulating effect. M1 macrophages can kill tumor cells and inhibit the formation of tumor lymphatic vessels and blood vessels, while M2 macrophages mainly promote tumor lymphangiogenesis and angiogenesis, thereby promoting its metastasis (8, 9). The major regulatory factors that promote lymphangiogenesis are known as vascular endothelial growth factor-C (VEGF-C), which is capable of combining the specific receptor of vascular endothelial growth factor receptor-3 (VEGFR-3) on the surface of lymphatic endothelial cells (LEC) and induce tyrosine kinase phosphorylation, thus promoting the formation of new lymphatic vessels around the tumor and providing a pathway for the metastasis of lymphatic tubules. TAMs produce many proangiogenic factors and express high levels of VEGF-C, which promote cancer cell invasion, metastasis, angiogenesis and lymphangiogenesis (10). Previous study has addressed the relationship between pancreatic cancer cells and TAMs, suggesting that their interaction promotes the invasion of pancreatic cancer cell and the differentiation and migration of macrophages (11). Nevertheless, the precise role of TAMs in esophageal cancer has yet to be elucidated. This study aims to explore whether M2 macrophages can be transformed into M1 macrophages, and to investigate the effect of different types of macrophages on the proliferation, migration and ring-forming ability of esophageal cancer-related LEC.

MATERIALS AND METHODS

Cells and major reagents

THP-1 cell line was purchased from the cell bank of the Chinese Academy of Sciences (Shanghai, China); Human esophageal cancer associated lymphatic endothelial cells (LEC) were purchased from BioLeaf Biotech Co. Ltd (Shanghai, China); CD14 immunomagnetic bead antibody was bought from Miltenyi Biotec GmbH (Bergisch Gladbach, Germany); Cell Counting Kit-8 (CCK-8) proliferation detection reagents was bought form Jiangsu Baolai Biotechnology Co. Ltd (Yancheng City, Jiangsu, China); Matrix glue was purchased from Becton, Dickinson and Company (Franklin Lakes, New Jersey, USA); Anti-VEGFR-3 antibody was purchased from Abcam Trade Co., Ltd (Cambridge, Cambridgeshire, UK); Fluorescent quantitative PCR kit and q(RT) -PCR reverse transcription kit were all purchased in Dalian Takara company (Dalian, Liaoning, China). The target gene VEGFR-3 primer sequence and the internal reference gene (β-actin) were designed and synthesized by Shanghai Bioengineering Biotechnology Co., Ltd (Shanghai, China).

VEGFR-3 primer sequence: Forward Primer: 5'-GAGAGAGAGAAGGCAGCATAC -3'; Reverse Primer: 5'- GTGCTTCAGTGGTCACACTCC -3'.

β-actin primer sequence: Forward Primer: 5'-AGCGAGCATCCCCCAAAGTT -3'; Reverse Primer: 5'-GGGCACGAAGGCTCATCATT -3'.

Cell culture

The cells were cultured in an RPMI 1640 medium mixed with 10% fetal bovine serum (FBS), at 37°C in a 5% CO2 incubator. The cells were sub-cultured in the logarithmic growth phase. Parts of the cells were cryopreserved for later experiments.

Extraction of monocytes

Blood samples of 200 ml from healthy adults were extracted in EDTAK1 anticoagulant tubes and then diluted with an equal volume of phosphate buffer solution (PBS). The diluted blood sample was slowly added to the upper layer of lymphocyte separation with the ratio of 2:1. After centrifugation, the liquids were divided into three layers; the white layer between the upper layer and the intermediate layer was mononuclear cells, which were sucked out with a pipette and collected in a centrifuge tube. After centrifugation, the upper liquid were carefully poured out, the last mononuclear cells were washed twice with sterile PBS. Finally, Hanks solution was added to a cell suspension of peripheral blood mononuclear cell (PBMC). The human mononuclear cells were obtained by CD14 magnetic beads positive sorting according to the manufacturer's instructions. Flow cytometry was applied to detect the positive rate of mononuclear cells.

Transformation of human monocytes into M2 macrophages and the induction of M2 macrophages into M1 macrophages

Human mononuclear cells were cultured in 6-well

plates at 2 x 10^5/well. To change the solution after mononuclear cells adhered to the wall, recombinant human macrophage colony stimulating factor (M-CSF) was added to a new RM1640 complete medium with a concentration of 10 ng/ml. The solution was changed with a half amount per day, continuous induction for 6 days. The positive rates of CD163 cells in M2 macrophages and CD16 cells in M1 macrophages were detected by flow cytometry. Previously obtained M2 macrophages were cultured in complete medium without any inducer for 1 day. To change the solution, interferon-γ (IFN-R) 50ng/ml and LPS 10 ng/ml were added to the fresh complete medium, and the concentrations of IFN-R and LPS changed every day, continuous for 2-3 days. Flow cytometry was used to detect the positive rates of different types of macrophages.

Transformation and identification of THP-1 cells into M2 and M1 macrophages

Four 6-well plates were inoculated with mononuclear cells, with 2×10^5/well. The complete culture medium containing phorbol ester (10 ng/ml) was placed and cultured routinely in the incubator, and half amount of the fluid was changed every day for 2 continuous days. Cell morphology was observed and recorded under a microscope. 2 ml mixed medium containing IFN-γ (50ng/ml) and LPS (10ng/ml) were added to the no.1 and no.2 6-well plates, respectively. While 2 ml IL-4 with a concentration of 20 ng/ml was added to the no.3 and no.4 6-well plates, respectively. The fluid was changed in a half amount every day for 2 continuous days. Then the morphology of the cells was observed under inverted microscope. The positive expression rates of surface marker CD163 of M2 macrophages and CD16 of M1 macrophages were detected by flow cytometry. The supernatant of M1 and M2 macrophages were taken as the conditioned medium to co-culture with esophageal cancer-associated LEC, named M1 group and M2 group, respectively. The esophageal cance- associated LEC cultured in complete medium was taken as the control group.

Cell counting kit-8 (CCK-8) on the proliferation of esophageal cancer related LEC in different groups

Esophageal cancer-associated lymphoid cells in logarithmic phase were taken for digestion, suspension and counting, then the cell concentration adjusted. These cells were paved on five 96-well plates. Each plate was divided into three groups, M1 group, M2 group and control group, of independent experiments run in duplicate in each group. The OD values at 450 nm were measured at 12 h, 24 h, 36 h, 48 h and 60 h, respectively.

Transwell chamber observation on the effects of M1 and M2 macrophages on the migration of esophageal cancer associated LEC

Transwell chamber of 8 μm 24-well plates were selected and divided into three groups, M1 group, M2 group and control group. The upper chambers of the three groups were inoculated with 1×10^5/ml esophageal cancer-related LEC, the lower chambers were supplemented with M1 conditioned medium, M2 conditioned medium and RM1640 complete medium, with independent experiments run in duplicate in each group. Transwell chamber of the 24-well plate was placed in an incubator for 24 h and removed for the next step. Microscopic observation and statistical analysis were performed.

Effect of different culture mediums on the ring-forming ability of esophageal cancer-related LEC by matrix three-dimensional culture method

The experimental method was performed according to the manufacturer's instructions. After 48 h, the ring-forming situation in each group was observed. The number of ring formations in esophageal cancer-related LEC were collected and calculated under inverted phase contrast microscope, from 5 randomized visual fields of upper, lower, left, right and middle sites.

Detection of VEGF-C expression in supernatant of M1 macrophages and M2 macrophages by enzyme-linked immunosorbent assay

ELISSA was carried out according to the manufacturer's instructions. The absorption value of the sample was measured, and the concentration was calculated according to the formula.

Western blot Detection of VEGFR-3 protein expression in esophageal cancer-associated LEC after culture in different culture mediums

When the esophageal cancer-associated LEC was in the logarithmic phase, the cells were digested and counted, then the concentration adjusted to inoculate into in 24-well plate, according to different conditions of

culture medium (M1 group, M2 group and control group). After incubation for 24 h, the 24-well plate was taken out of the incubator; the medium was removed with a sterile pipette and washed twice with sterile PBS. High efficient RIPA cell lysate buffer was added into each well, and the samples were collected and centrifuged in a sterile-enzyme free centrifuge tube to obtain the supernatant. The protein concentration was measured by BCA protein concentration kit. A 10 µl loading buffer (4-fold dilution) was added to each 30 µl protein sample then was mixed and heated in a water bath for protein denaturation and then cooled to room temperature and centrifuged. The supernatant was directly taken out for the sample electrophoresis. Proteins were separated by sodium dodecylsulphate polyacrylamide gel electrophoresis (SDS-PAGE). Each well was filled with 20 µl loading buffer. Firstly, the voltage was set at 80 volt (V), when the sample (blue line) entered into the separation line between spacer gel and separation gel (about 30 min), the voltage was adjusted to 120 V. Once the blue band moved into the light green band of the marker strip (the light green band at the place of 10kDa), the electrophoresis was stopped. The requirement for strip was transferred to the PVDF membrane, then sealed with skimmed milk powder. The primary antibody was incubated overnight at 4°C. After washing the membrane, the second antibody was incubated for 2 h at room temperature and washed; chemiluminescence color and gray analysis were performed after exposure to the darkroom.

Detection of the expression of VEGFR-3 mRNA in esophageal cancer-associated LEC in different culture media by qRT-PCR assay

Esophageal cancer-associated LEC after culture with conditioned medium was collected. Trizol was used to separate the lymphocytes in each group, the total RNA concentration was extracted, reversed and transcribed into cDNA. The expression of VEGFR-3 mRNA was detected following the instructions of the qRT-PCR kit. The reaction conditions of RT-PCR amplification were: pre-denaturation 30 s 95°C, denaturation 3 s 95°C; 30 s 60°C; the above steps were repeated for 40 times, the melting curve was kept at 4°C. After reaction, the amplification curve, the melting curve and the standard curve were made by 7500 Software (version 2.3). The relative quantitative expression analysis was performed by Livak ($2^{-\Delta\Delta Ct}$) method.

Statistical analysis

SPSS17.0 software was used to process data. The *t*-test was used for the quantitative data of two samples. The comparison between the quantitative data of single factor

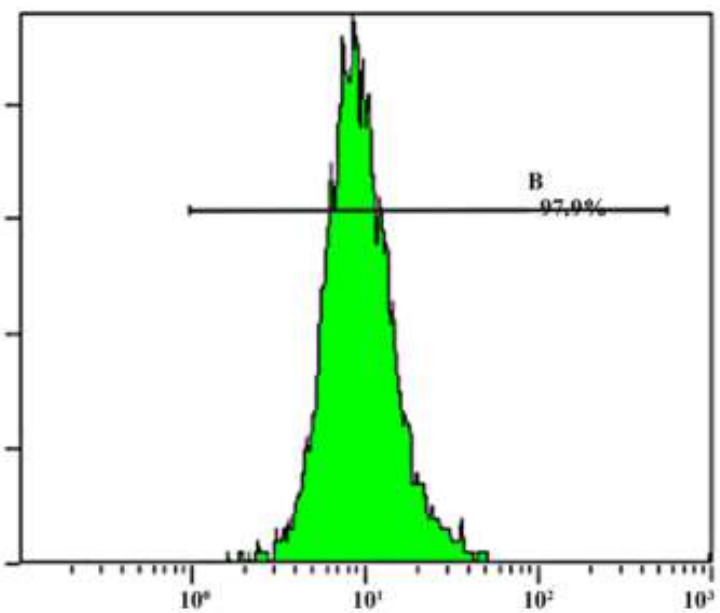

Fig. 1. *Expression rate of monocyte surface antigen CD14.*

and multi-sample was performed by one-way ANOVA, and LSD *t*-test was used for the pairwise comparison between multiple groups, with the inspection level as α=0.05.

RESULTS

Transformation of human monocytes to M2 macrophages and M2 macrophages into M1 macrophages

Positive expression of the surface markers of human monocytes

Mononuclear cells were obtained by magnetic bead screening. The positive rate of CD14, the monocyte surface marker, was 97.9±1.70% (Fig. 1).

Morphology of M1 and M2 macrophages

On the third day, the morphology of monocytes after induced by recombinant human M-CSF began to make some changes, which included increased cell volume, and stretched out pseudopodia in a small number of cells. At days 5-6, the volume of cells became larger than the volume at the third day, and the morphology of cells were seen as round or oval, and most of them had projections. After being induced by IFN-γ and LPS for 2-3 days, M2 macrophages had less projecting cells and more round cells, but there were no changes in the cell volume (Fig. 2).

Positive expression of M1 and M2 macrophage surface markers

After the monocytes induced by recombinant human M-CSF, the positive expression rate of CD163 in M2 macrophages was 66.37±2.67%, while the positive rate of CD16 in M1 macrophages was 13.37±4.41%. The results indicated that the majority of the monocytes were successfully induced as M2 macrophages.

When M2 macrophages were induced by IFN-γ and LPS, the positive expression rate of CD16 in M1 macrophages was 48.57±5.98%, while the positive rate of CD163 in M2 macrophages was 25.83±1.95%, which suggests the majority of the monocytes were changed to M2 macrophages, since not all of the cells were M1-like. Furthermore, the positive expression of M1 macrophages was significantly higher than that of monocytes after M-CSF induction ($P<0.05$) (Fig. 3 and Table I).

Correlation indexes of M1 and M2 macrophages after co-culture with esophageal cancer-associated lymphoid cells

Positive expression of surface markers of M1 and M2 macrophages

Monocytes were induced into M2 macrophages by stimulating PMA, IL-4 and IFN-γ; M2

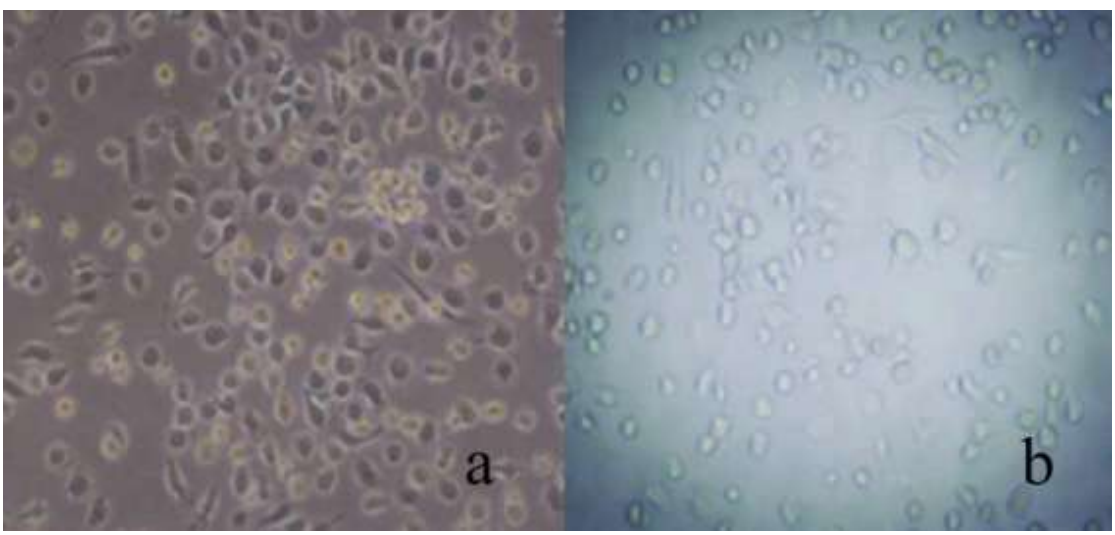

Fig. 2. ***a)*** *M2 macrophages after being induced by recombinant human M-CSF.* ***b)*** *M1 macrophages after being induced by IFN-γ and LPS.*

macrophages were induced by LPS into M1 macrophages. The positive expression rate of CD163 on M2 macrophages was 86.3±2.66%, and the positive expression rate of CD16 on M1 macrophages was 73.57±2.58%, suggesting that M1 and M2 macrophage model had been successfully established (Fig. 4).

Detection of proliferation of esophageal cancer associated with LEC by CCK-8 method

CCK-8, being nonradioactive, allows sensitive colorimetric assays for the determination of the number of viable cells in cell proliferation and cytotoxicity assays.

The conditioned medium of M2 macrophages promoted the proliferation of LEC, and the proliferation rate was significantly higher than that of the other two groups. While the proliferation rate of M1 macrophages was lower than that of the control group (M2 group > control group > M1 group). There was significant difference between the M2 group and M1 group (P<0.05), and the M2 group and control group (P<0.05), but there was no significant difference between the M1 group and control group (P>0.05) (Fig. 5; Table II).

Number of esophageal cancer-associated LEC by Transwell chamber

The number of cells in M2 group was significantly higher than in the other two groups (M2 group > control group > M1 group) (all P<0.05). As shown in Fig. 6a and Table III.

Number of rings of esophageal cancer associated LEC observed by matrix method

The number of rings in the M2 group was significantly higher than that in other two groups (M2 group > control group > M1 group). The pairwise comparison among the three groups were all statistically significant (P<0.05) (Fig. 6b; Table III).

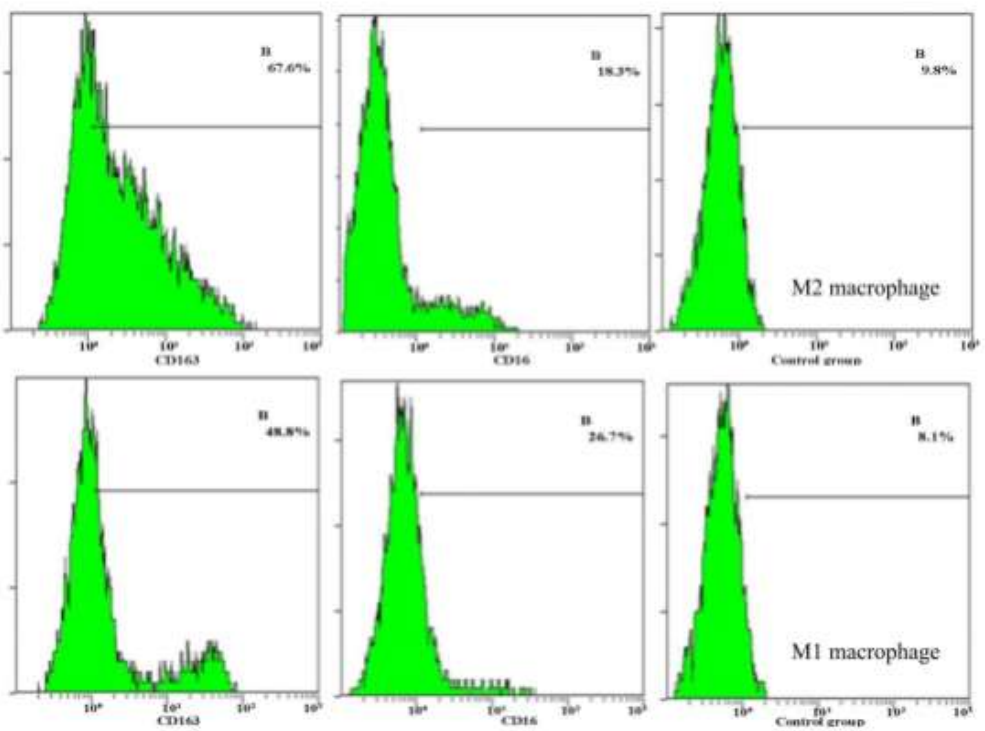

Fig. 3. *Expression of M2 macrophage surface antigen CD163 among three groups (M2 macrophage) (upper panel); expression of M1 macrophage surface antigen CD16 among three groups (M1 macrophage) (lower panel).*

Table I. *The positive expression rate of M1 and M2 macrophages (n=3, x±s)%.*

Macrophages classification	Positive expression rate of CD163	Positive expression rate of CD16	*t* value	*P* value
M2 macrophages	66.37±2.67	13.37±4.41	17.797	0.000
M1 macrophages	25.83±1.95	48.57±5.98	6.259	0.003
		t value = 8.203		
		P value = 0.001		

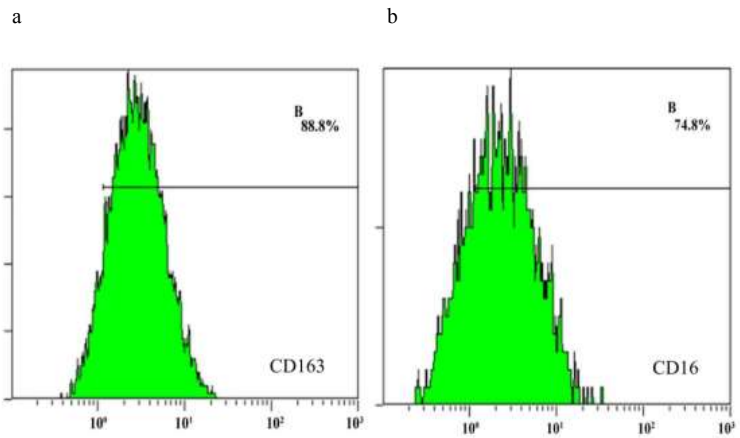

Fig. 4. ***a****) Expression rate of macrophage surface antigen CD163 (CD 163).* ***b****) Expression rate of macrophage surface antigen CD16 (CD 16).*

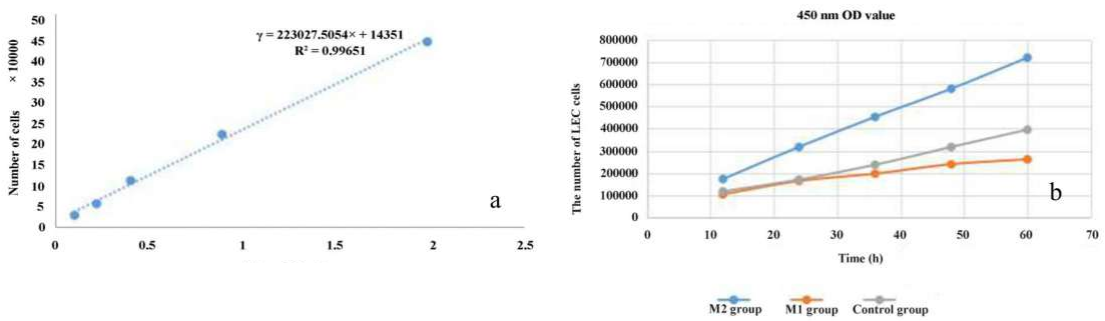

Fig. 5. ***a****) Standard growth curve of esophageal cancer-associated LEC.* ***b****) Growth curve of esophageal cancer-associated LEC cultured in different conditioned medium.*

Table II. *OD values of esophageal cancer-associated LEC among three groups.*

Groups	12 h	24 h	36 h	48 h	60 h	$\bar{x}$±s	*F* value	*P* value
M2 group (i=1)	0.71	1.36	1.97	2.54	3.17	1.95±0.43		
M1 group (i=2)	0.40	0.67	0.82	1.01	1.11	0.80±0.10	4.350	0.038
Control group (i=3)	0.46	0.70	1.00	1.36	1.71	1.05±0.22		

Table III. *Migration number of esophageal cancer associated LEC and ring number in esophageal cancer associated LEC of the three groups.*

Groups	M1 group (i=2)	M2 group (i=1)	Control group (i=3)	*F* value	*P* value
Number of stained cells	184	618	210	761.119	0.000
	190	647	248		
	176	650	236		
$\bar{x}$±s	183.3±7.02	638.3±17.67	231.3±19.43		
Number of rings	9	19	14	20.310	0.002
	8	15	10		
	7	18	13		
$\bar{x}$±s	8.0±1.0	17.3±2.1	12.3±2.1		

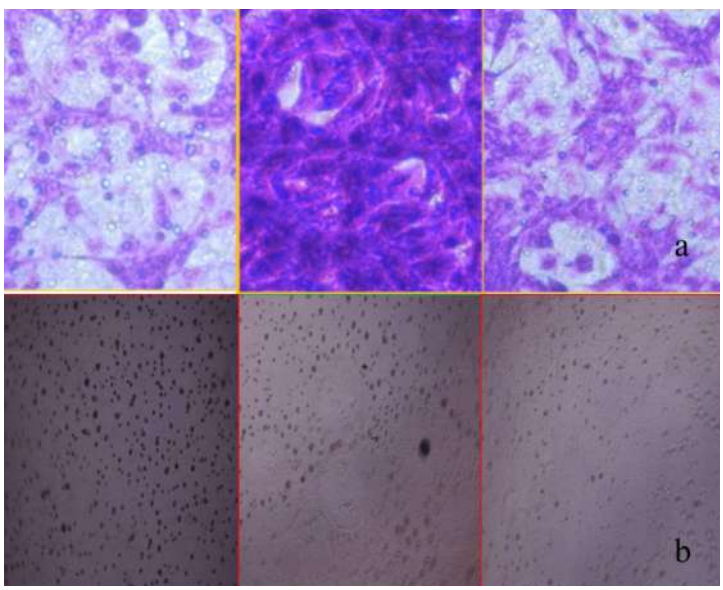

Fig. 6. ***a****) Migration situation of esophageal cancer-associated LEC in different groups (10×).* ***b****) Number of rings of esophageal cancer-associated LEC in different mediums observed by matrix method (6×)).*

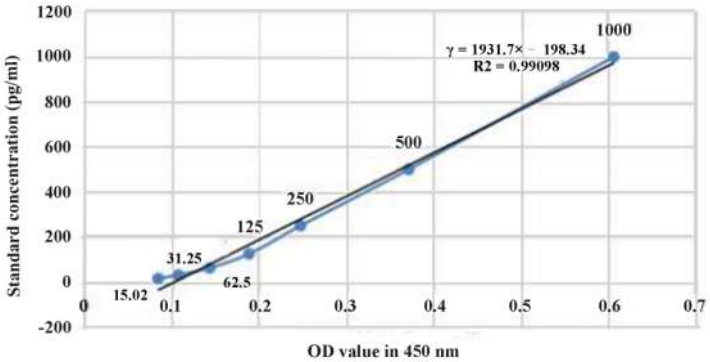

Fig. 7. *Standard curve of standard substance.*

Table IV. *VEGF-C protein levels in supernatant of the three groups.*

Groups	OD value			$\bar{x}$±S	*F* value	*P* value
M2 group (i=1)	0.201	0.195	0.212	0.2027±0.0086		
M1 group (i=2)	0.137	0.136	0.139	0.1373±0.0015	153.399	0.000
Control group (i=3)	0.140	0.141	0.137	0.1393±0.0021		

Detection of VEGF-C levels in supernatant detected by ELISA

The concentration of VEGF-C in the M2 group was significantly higher than that in the control group and M1 group (M2 group> M1 group> control group) (P<0.05). There was no significant difference regarding VEGF-C level between control group and M1 group (P>0.05), as shown in Fig. 7, Table IV. The concentration for VEGF-C in the M2 group was approximately 190pg/ml, while there was no VEGF-C secretion in M1 group.

Expression of VEGFR-3 protein in esophageal cancer-related LEC observed by Western blot

The expression of VEGFR-3 protein in the M2 group was significantly higher than that in the control group and M1 group (M2 group > control group > M1 group) (P<0.05). In addition, there was a significantly higher VEGFR-3 protein level in the control group than in the M1 group (P < 0.05) (Fig. 8, a and c).

Expression of VEGFR-3 mRNA in esophageal carcinoma-associated LEC observed by qRT-PCR

There were significant differences of VEGFR-3 mRNA expression among the three groups (P<0.05). The VEGFR-3 mRNA level in the M2 group was 3.01 times higher than in the control group, while the expression of VEGFR-3 mRNA in the M1 group was 0.90 times lower than that in the control group (Fig. 8b, Table V).

DISCUSSION

The tumor invades the lymphatic system mainly through the lymphatic network around the tumor tissue and its newly-formed lymphatic vessels (12). Tumor lymphangiogenesis is an extremely complex process, with many factors involved. TAMs are known to play an important role in tumor development and metastasis. In recent years, it has been demonstrated that TAMs not only play

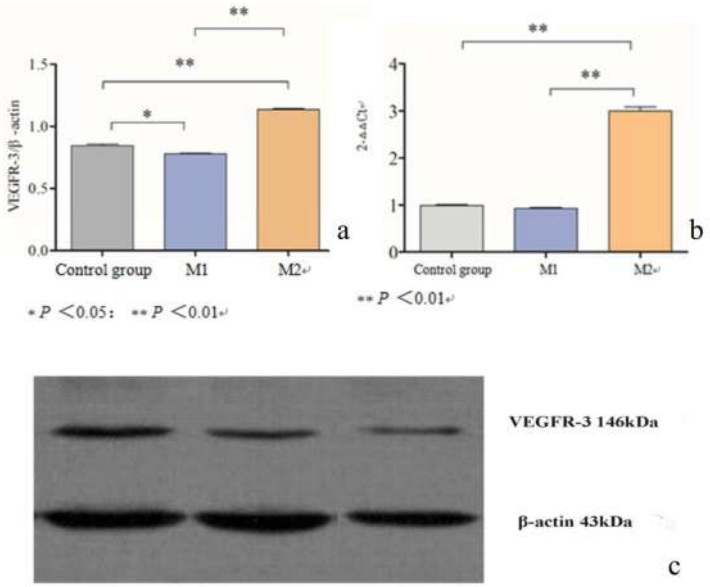

Fig. 8. ***a)*** *Expression of VEGFR-3 proteins in esophageal cancer-related LEC in different groups.* ***b)*** *Expression of VEGFR-3 mRNA in esophageal cancer-related LEC among the three groups.* ***c)*** *Relative expression of VEGFR-3 protein in esophageal carcinoma-associated LEC among the three groups.*

Table V. *Expression of VEGFR-3mRNA in esophageal carcinoma-associated LEC in three groups.*

Grouping	CT value of target gene			β-action CT value			*F* value	*P* value
M2 group	25.73	25.68	5.85	17.26	17.27	17.20		
M1 group	26.6	26.72	26.9	16.22	16.35	16.90	79.563	0.000
Control group	27.7	27.25	27.01	17.07	17.23	17.35		

an anti-tumor role, but are also involved in the process of tumor occurrence, development, growth and invasion, especially in tumor angiogenesis and lymphangiogenesis (13). VEGF-C, produced by TAMs, plays an important role in the generation of lymphatic vessels and in the lymphatic metastasis of cancer tissues (14). VEGF-C is one of the most important cytokines to promote lymphangiogenesis. Studies have shown that tumor cells can secrete VEGF-C and VEGF-D. Furthermore, an increase of M2 TAMs infiltration in tumor tissue is significantly correlated with tumor lymphatic metastasis (15, 16). Macrophages are cells with strong plasticity, and different active phenotypes. TAMs are more likely

to be M2 macrophages, and different phenotypes of TAMs could directly affect tumor development in the tumor microenvironment (17). In breast cancer tissue, TAMs can promote the increase of lymphatic microvessel density, the regeneration of lymphatic endothelial and the formation of lymphatic vessels through up-regulating the expression of VEGF-C (18). In pancreatic cancer, Kurahara et al. found that the increased number of M2 macrophages located in the stroma could promote the formation of lymphatic vessels and drive the process of lymph node metastasis (19). Some scholars have unveiled that cervical cancer cells can express VEGF-C; under the stimulation of VEGF-C and other inflammatory cytokines, mononuclear cells in the peripheral blood would enter into the interstitial tissue, transform into macrophages, and express VEGF-C and its receptor VEGFR-3, thus leading to a new lymphangiogenesis around the tumor and the occurrence of lymphatic metastasis (20). Therefore, it is of great significance to induce the polar transformation of macrophages, which may prevent the formation of lymphangiogenesis and tumor lymphatic metastasis. Kerjaschki et al. and other scholars believe that TAMs were involved in the lymphangiogenesis (21). TAMs firstly aggregated into clusters and fused with the germinated LEC, then gradually transformed into endothelial cells, participating in the formation of LEC and lymphatic vessels. Most scholars have found that VEGF-C secreted by TAMs can motivate the growth of LEC and promote the formation of lymphatic vessels. All of these methods provide the conditions for the lymphatic metastasis of tumor. Different types and functions of macrophage polarization options are used to promote the transformation of macrophages to M1 macrophages. For example, the application of colony-stimulating factor (CSF)-1 receptor inhibitors can activate macrophages to M1 macrophage polarization (22). As is well known, monocytes are precursors of macrophages. Under the induction of certain chemokines, monocytes could pass through the vascular endothelium and migrate into different tissues and differentiate into tissue-specific macrophages. Monocytes can be activated into M2 macrophages under the stimulation of macrophage CSF (23). An increasing number of studies have shown that the survival time of patients would be prolonged if there was an increased M1/M2 ratio (24). Our study revealed that human M2 macrophages could be transformed into M1 macrophages when induced by IFN-γ and LPS. M2 macrophages can promote the proliferation, migration and ring-forming ability of esophageal cancer-associated LEC by secreting VEGF-C, while M1 macrophages played an inhibitory effect on their migration and ring-forming ability. Macrophages can be induced to transform into M1 macrophages, and M2 macrophages can also be induced into M1 macrophages; these two processes would have an increased M1/M2 ratio tumor microenvironment, which is important to inhibit the development of tumor and lymphatic metastasis. It provides a theoretical basis for clinical prevention and treatment of lymphatic metastasis of esophageal cancer.

ACKNOWLEDGEMENTS

Project: The National Natural Science Fund (project number: 81570199); Henan Foundation and Frontier Technology Research Project (project number: 152300410026).

REFERENCES

1. Wu CC, Chen CJ. Esophageal carcinoma. N Engl J Med 2015; 372:1472.
2. Mitin T, Hunter JG, Thomas CR, Jr. Esophageal carcinoma. N Engl J Med 2015; 372:1471-72.
3. Adenis A, Robb WB, Mariette C. Esophageal carcinoma. N Engl J Med 2015; 372:1471.
4. Li H, Fan X, Houghton J. Tumor microenvironment: the role of the tumor stroma in cancer. J Cell Biochem 2007; 101:805-15.
5. Zheng X, Turkowski K, Mora J, Brune B, Seeger W, Weigert A, Savai R. Redirecting tumor-associated macrophages to become tumoricidal effectors as a novel strategy for cancer therapy. Oncotarget 2017; 8:48436-52.
6. Komohara Y, Fujiwara Y, Ohnishi K, Takeya M. Tumor-associated macrophages: Potential therapeutic targets for anti-cancer therapy. Adv Drug

Deliv Rev 2016; 99:180-85.
7. Germano G, Frapolli R, Belgiovine C, et al. Role of macrophage targeting in the antitumor activity of trabectedin. Cancer Cell 2013; 23:249-62.
8. Lewis CE, Pollard JW. Distinct role of macrophages in different tumor microenvironments. Cancer Res 2006; 66:605-12.
9. Yamaguchi T, Fushida S, Yamamoto Y, et al. Tumor-associated macrophages of the M2 phenotype contribute to progression in gastric cancer with peritoneal dissemination. Gastric Cancer 2016; 19:1052-65.
10. Schoppmann SF, Fenzl A, Nagy K, et al. VEGF-C expressing tumor-associated macrophages in lymph node positive breast cancer: impact on lymphangiogenesis and survival. Surgery 2006; 139:839-46.
11. Meng F, Li C, Li W, Gao Z, Guo K, Song S. Interaction between pancreatic cancer cells and tumor-associated macrophages promotes the invasion of pancreatic cancer cells and the differentiation and migration of macrophages. IUBMB Life 2014; 66:835-46.
12. Roszer T, Menendez-Gutierrez MP, Cedenilla M, Ricote M. Retinoid X receptors in macrophage biology. Trends Endocrinol Metab 2013; 24:460-68.
13. Gajewski TF, Schreiber H, Fu YX. Innate and adaptive immune cells in the tumor microenvironment. Nat Immunol 2013; 14:1014-22.
14. Lin EY, Li JF, Gnatovskiy L, et al. Macrophages regulate the angiogenic switch in a mouse model of breast cancer. Cancer Res 2006; 66:11238-46.
15. Chang WC, Chen JY, Lee CH, Yang AH. Expression of decoy receptor 3 in diffuse sclerosing variant of papillary thyroid carcinoma: correlation with M2 macrophage differentiation and lymphatic invasion. Thyroid 2013; 23:720-26.
16. Komohara Y, Hasita H, Ohnishi K, Fujiwara Y, Suzu S, Eto M, Takeya M. Macrophage infiltration and its prognostic relevance in clear cell renal cell carcinoma. Cancer Sci 2011; 102:1424-31.
17. Ostuni R, Kratochvill F, Murray PJ, Natoli G. Macrophages and cancer: from mechanisms to therapeutic implications. Trends Immunol 2015; 36:229-39.
18. Ding M, Fu X, Tan H, Wang R, Chen Z, Ding S. The effect of vascular endothelial growth factor C expression in tumor-associated macrophages on lymphangiogenesis and lymphatic metastasis in breast cancer. Mol Med Rep 2012; 6:1023-29.
19. Kurahara H, Takao S, Maemura K, et al. M2-polarized tumor-associated macrophage infiltration of regional lymph nodes is associated with nodal lymphangiogenesis and occult nodal involvement in pN0 pancreatic cancer. Pancreas 2013; 42:155-59.
20. Schoppmann SF, Birner P, Stockl J, et al. Tumor-associated macrophages express lymphatic endothelial growth factors and are related to peritumoral lymphangiogenesis. Am J Pathol 2002; 161:947-56.
21. Kerjaschki D. The crucial role of macrophages in lymphangiogenesis. J Clin Invest 2005; 115:2316-19.
22. Pyonteck SM, Akkari L, Schuhmacher AJ, et al. CSF-1R inhibition alters macrophage polarization and blocks glioma progression. Nat Med 2013; 19:1264-72.
23. Devaraj S, Jialal I. C-reactive protein polarizes human macrophages to an M1 phenotype and inhibits transformation to the M2 phenotype. Arterioscler Thromb Vasc Biol 2011; 31:1397-402.
24. Zhang M, He Y, Sun X, Li Q, Wang W, Zhao A, Di W. A high M1/M2 ratio of tumor-associated macrophages is associated with extended survival in ovarian cancer patients. J Ovarian Res 2014; 7:19.

EFFECT OF $CuSO_4$ AND NANO COPPER ON SERUM ANTIOXIDANT CAPACITY IN WEANED PIGLETS

Z. CHANG[1,2§], H. ZHANG[2§], H. DONG[1§], K. MEHMOOD[2,3], M. IJAZ[4], H.I. AHMAD[5], M.A. NAEEM[2], Q. WU[1], F. NABI[2] and H. ZHU[1]

[1]Key Laboratory of Clinical Veterinary Medicine in Tibet, Tibet Agriculture and Animal Husbandry College, Linzhi Tibet, China; [2]College of Veterinary Medicine, Huazhong Agricultural University, Wuhan, China; [3]University College of Veterinary and Animal Sciences, Islamia University of Bahawalpur, Bahawalpur, Pakistan; [4]Department of Clinical Medicine and Surgery, University of Veterinary and Animal Sciences, Lahore, Pakistan; [5]Key Laboratory of Agricultural Animal Genetics, Breeding, and Reproduction, Huazhong Agricultural University, Wuhan, P. R. China

Received December 2, 2017 – Accepted February 13, 2018

[§]These authors made equal contributions to this article

Copper is the most essential trace element in the animal body. Nano-sized copper particles have been widely used in a number of different animal species in modern medicinal practice. The present study was designed to examine the effect of dietary copper sulfate /($CuSO_4$) and nano copper supplementation on serum antioxidant capacity of weaning piglets. A total of 28 Duroc piglets (21 days, and weighing ~7 kg) were randomly divided into three equal groups. The control group (n=4) was administered with a normal standard diet; however the $CuSO_4$ (n=12) and nano copper (n=12) groups were treated with 50, 100 and 200 mg/kg/day body weight, respectively. After 28 days, blood serum copper-zinc superoxide dismutase (CuZn-SOD), ceruloplasmin (CP), malondialdehyde (MDA), myeloperoxidase (MPO), total antioxidant capacity (T-AOC), peroxidase (POD), nitric oxide (NO), nitric oxide synthase (NOS), hydrogen peroxide (H_2O_2) and inhibition of hydroxyl radical (CIHR) were analyzed from all groups. The results indicated that nano copper supplementation has significant ($P < 0.05$) effect on the serum antioxidant capability as compared to dietary $CuSO_4$ group in weaned piglets. Nano-size copper 100 mg/kg/day supplementation was confirmed to improve the immunity level by strengthening the antioxidant capacity of weaning piglets. Dietary supplementation with 100 mg/kg body weight nano copper could be a potential substitute for weaned piglets.

Copper is an essential and routinely added trace element of animals' diet (1, 2). It can effectively maintain the stability of the internal environment, additionally; it is closely related to hematopoiesis, metabolism, growth, reproduction and other important regular metabolic functions (2, 3). While copper is involved in comprising core components or cofactors of a variety of antioxidant enzymes of the important antioxidant system in the animal body. It can timely clean up the free radicals in the body to ensure the growth and decline of homeostasis of the body of free radicals and reduce peroxide damage (4, 5). Copper is normally added to swine diets in appropriate concentration to facilitate

Key words: $CuSO_4$, nano copper, antioxidant capacity, piglets

Mailing address:
Prof. Hongyun Zhu,
Key Laboratory of Clinical Veterinary Medicine in Tibet,
Tibet Agriculture and Animal Husbandry College,
Linzhi 860000 Tibet, China
Tel.: +86 13037168873
e-mail: zh0561@sina.com

0393-974X (2018)

normal growth performance (6). A large number of researchers showed that high copper supplemented-based diet had a significant role in promoting digestibility and growth performance, especially in the early growth period of pigs (2, 6). However, high quantity of copper has the advantage of sterilizing, promoting the secretion of growth hormone, and increasing feed intake and production performance in pigs. Furthermore, when feed exceeds in copper level, it leads to liver and kidney damage and poses environmental pollution (7).

At present, copper sulfate ($CuSO_4$) is the main feed additive on the market; however, excess $CuSO_4$ concentration becomes toxic with high feed intake over a long period of time in piglets (6). With the development of nanomaterial and nanotechnology with a higher bioavailability and bioactive function of nano copper, it gradually replaced the copper feed additives and became more widely used in animals (8). However, research regarding mechanism of action of nano copper in animal feed gives very scare information. The digestion, absorption, transport, metabolism and various biological functions require further study (9). Nano copper added in pig, livestock and poultry feed showed a good advantage with high absorption, and digestibility (7). Thus, this study was conducted to explore the effects of $CuSO_4$ and nano copper supplementation on serum antioxidant markers of weaned piglets (health dual hybrid D IV X large white pigs) to provide an experimental basis for the practical applications of nano copper as feed additive in weaned piglets.

MATERIALS AND METHODS

Animal treatment and experimental groups

All the experiments were conducted according to the institutional Animal Welfare and Research, Ethics Committee guideline of Huazhong Agricultural University, Wuhan, China.

A total of 28 Duroc piglets (21 days, and weighing ~7 kg) were provided by Hubei Academy of Agricultural Sciences, China. The piglets were randomly divided into three equal groups. The control group (n=4) administered with a standard normal diet; the $CuSO_4$ (n=12) and nano copper (n=12) groups were treated with basal diet supplemental with $CuSO_4$ and nano copper (50, 100 and 200 mg/kg), respectively. The nano copper of size 40 nm (99.5%; catalog: C112567) was purchased from Shanghai Aladdin Reagent Co., Ltd., China, and prepared as mentioned previously (10). The various concentrations of nano copper used during this study were prepared according to our previous study (11). After 28 days, blood samples were collected by anterior vena cava, and were centrifuged at 3000×g for 20 min for separation of serum and stored at -20°C, until subsequent use and further analysis. The content of serum antioxidant capacity markers containing copper-zinc superoxide dismutase (CuZn-SOD), ceruloplasmin (CP), malondialdehyde (MDA), myeloperoxidase (MPO), total antioxidant capacity (T-AOC), peroxidase (POD), nitric oxide (NO), nitric oxide synthase (NOS), hydrogen peroxide (H_2O_2) and inhibition of hydroxyl radical (CIHR) were analyzed using commercially available kits (Nanjing Jiancheng Bioengineering Institute, Nanjing, China) according to previous study (3). All the experiments were performed in triplicate.

Statistical analysis

Statistical analysis of the results was made with one way ANOVA by student's *t*-test to compare the differences between mean values of control and nano copper groups. The values of $P < 0.05$ were considered as statistically significant. All statistical analyses were performed using SPSS 19.0 software and the results are presented as means ± standard error of means (S.E.M).

RESULTS

Effect of $CuSO_4$ and nano copper on serum antioxidant

The antioxidant capability was examined with dietary supplementation of nano copper and $CuSO_4$ of different concentration on weaning piglets. Dietary supplementation with nano copper from days 1 to 28 post-weaning had a significant effect on the antioxidant capability in weaned piglets (Fig. 1-5). The results showed that following supplementary concentration with 50, 100 and 200 mg/kg/day of nano copper, SOD activity showed increasing trend compared to $CuSO_4$ and the control group (Fig. 1). Ceruloplasmin CP values also increased

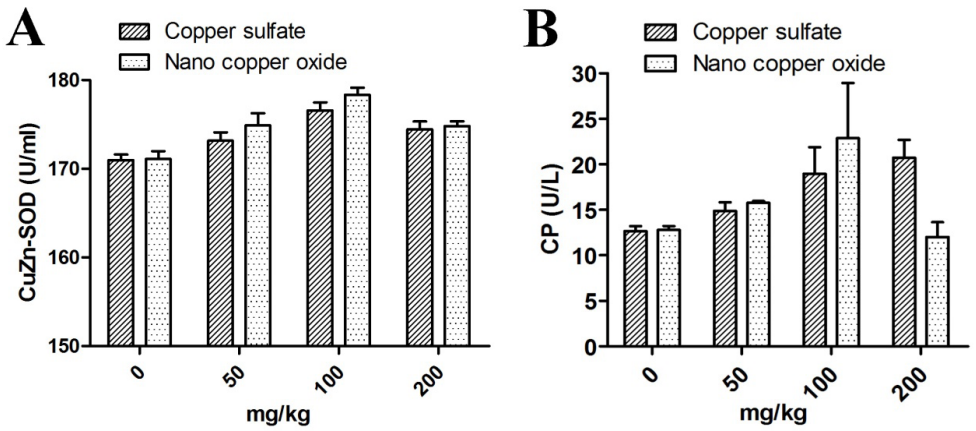

Fig. 1. *Comparison of different doses (0, 50, 100, 200 mg/kg) of copper sulfate ($CuSO_4$) and nano copper on serum antioxidant capacity in weaned piglets.* ***A****) Level of SOD activity;* ***B****) Level of CP activity.*

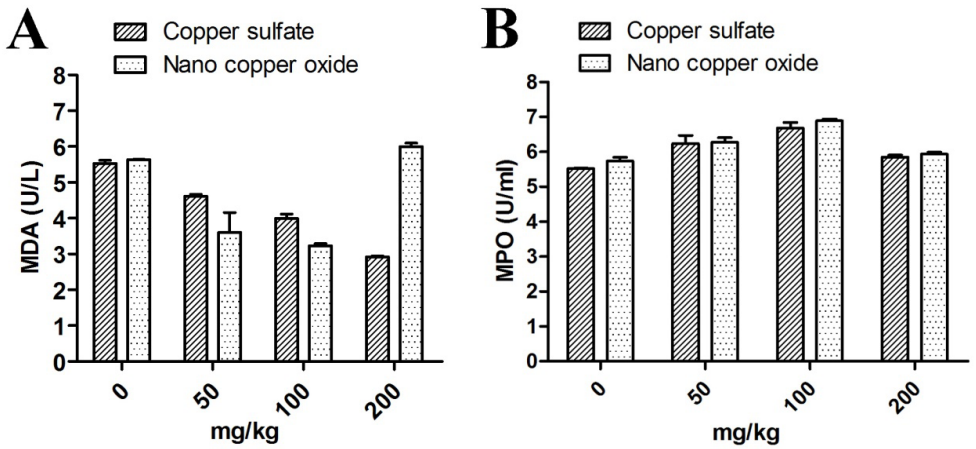

Fig. 2. *Comparison of different doses (0, 50, 100, 200 mg/kg) of copper sulfate ($CuSO_4$) and nano copper on serum antioxidant capacity in weaned piglets.* ***A****) Level of MDA contents;* ***B****) Level of MPO activity.*

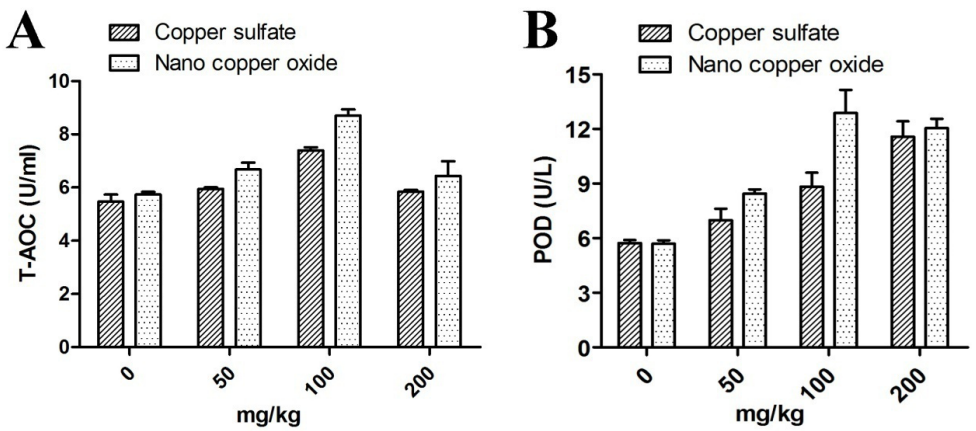

Fig. 3. *Comparison of different doses (0, 50, 100, 200 mg/kg) of copper sulfate ($CuSO_4$) and nano copper on serum antioxidant capacity in weaned piglets.* ***A****) Level of total antioxidant capacity;* ***B****) Level of POD activity.*

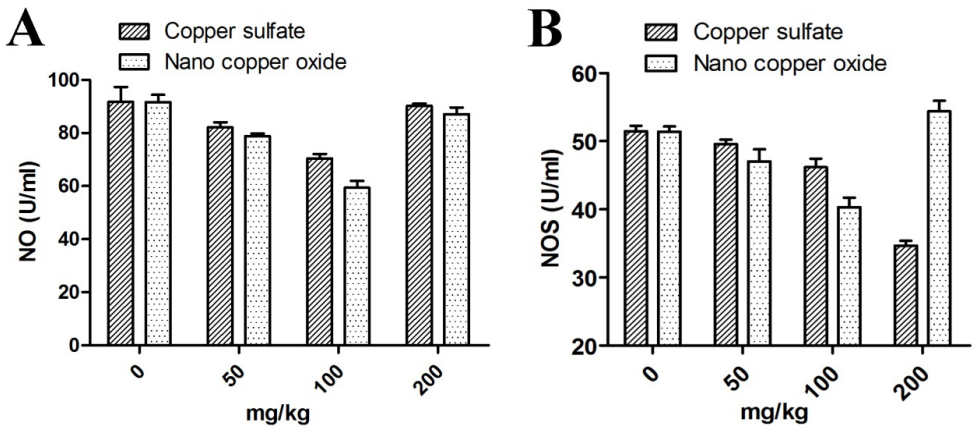

Fig. 4. *Comparison of different doses (0, 50, 100, 200 mg/kg) of copper sulfate ($CuSO_4$) and nano copper on serum antioxidant capacity in weaned piglets.* ***A****) Level of NO;* ***B****) Level of NOS activity.*

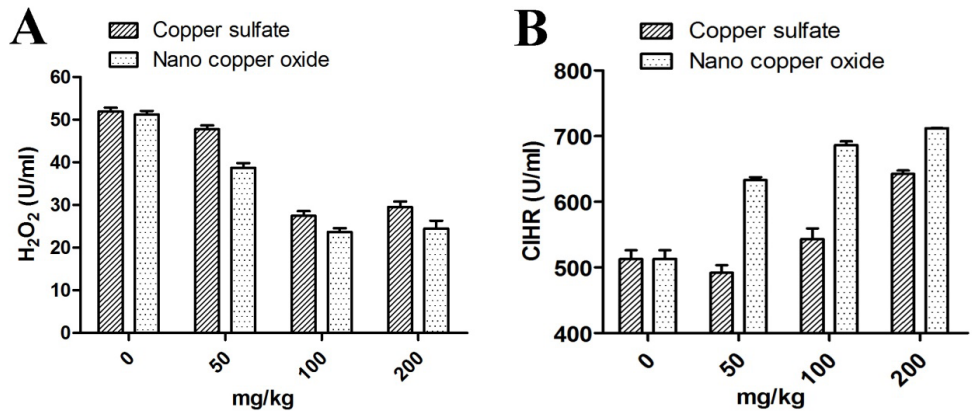

Fig. 5. *Comparison of different doses (0, 50, 100, 200 mg/kg) of copper sulfate ($CuSO_4$) and nano copper on serum antioxidant capacity in weaned piglets.* ***A****) Level of H_2O_2;* ***B****) Level of CIHR.*

significantly ($P<0.05$) especially with 100 mg/kg concentration as compared with control and $CuSO_4$ group. While with 200 mg/kg concentration CP value decreased significantly as compared to both groups (Fig. 1). The MDA content is an indicator of lipid peroxidation, and was significantly increased in the $CuSO_4$ group as compared with the nano copper group. MDA content decreased significantly with the dietary nano copper group as compared to the $CuSO_4$ and control groups, while MDA increased with 200 mg/kg/day body nano copper concentration as compared to the copper sulfate group (Fig. 2). The myeloperoxidase (MPO) content in CuSO4 and nano copper oxide groups had no significant effect in either group as compared to the control group. Therefore, it is presumed that the dietary different copper concentration has no direct effect on MPO activity (Fig. 2).

Total antioxidant capacity (T-AOC) was increased significantly in 50 and 100 mg/kg, while T-AOC decreased significantly in 200 mg/kg/day with dietary nano copper concentration as compared with CuSO4 and control groups (Fig. 3). Compared with the control and dietary CuSO4 groups, in the dietary supplementation

with nano copper group the peroxidase (POD) activity increased significantly (Fig. 3).

Nitric oxide (NO), and nitric oxide synthase (NOS) activity had lower content in serum of dietary nano copper supplemented group with different concentrations as compared with the control and dietary CuSO4 groups in 50 and 100 mg/kg. While NO and NOS increased in 200 mg/kg/day significantly with dietary nano copper concentration as compared with control group (Fig. 4).

In this experiment, hydrogen peroxide (H_2O_2) content gradually decreased with the increasing concentration of nano copper as compared to the control and CuSO4 groups (Fig. 5). The ability of serum-inhibited hydroxyl free radicals (CIHR) gradually increased in the nano copper oxide group as compared to the control and CuSO4 groups ($P < 0.05$).

DISCUSSION

Copper is an essential micronutrient and the most important feed additive in all animal species. Researchers have found that copper exist in various organs, tissues and cells, especially in the liver and kidney (12). It is involved in the growth and development of bones, connective tissue and many other organs including brain and heart (6, 7), and has been identified as stimulating immunity, helping in repair of injured tissues and helping in the healing process (4, 5). Therefore, the utilization rate of supplemented copper is improved and the amount of adding feed copper is reduced by improving biological effects of this element.

In this study, the effect of $CuSO_4$ and nano copper were investigated on the antioxidant capacity of weaning piglets. Experimental results demonstrated that the addition of nano copper to the weaned pigs' diet improved growth rate, especially 100 mg/kg body weight nano copper supplementation were significantly higher in SOD, CP, T-AOC, POD, NO, NOS and CIHR than the $CuSO_4$ supplemented group, indicating significant improvement in antioxidant and immunity of weaning pigs. Our results suggested that the effect of nanometer copper was positive on the absorption and utilization in weaning piglets. In addition, nano copper indicated an increase in the CP, T-AOC and POD indexes with the increasing concentration of nano copper, especially at the rate of 100 mg/kg body weight. Our results suggested that supplementary nano copper should not exceed 100 mg/kg/day body weight, because @200 mg/kg body weight it may cause damage and toxic effects in weaning piglets. Nanotechnology is a practical development of nano particles that can be used in improving the health of livestock by progressing the digestion and absorption. It is reported that dietary supplementation with nano copper inhibited the growth of various intestinal bacteria, while increasing intestinal microflora (12, 13).

Nano particles have smaller diameter, can improve the absorption and digestion processes in animals. Smaller sized nano particles contain a high rate of absorption in GIT, easily pass through capillaries and are absorbed by cells (14). Various experiments suggested that nano copper supplementation has significant effects on daily feed intake and demonstrated the highest antioxidant capacity in weaned piglets (15).

In conclusion, results indicated that nano copper supplemented food improves performance and antioxidant capability of weaning piglets than $CuSO_4$ supplementation. Nano-size copper 100 mg/kg/day supplementation confirmed the immunity level by strengthening the antioxidant capacity of weaning piglets. Dietary supplementation with 100 mg/kg body weight nano copper could be a potential alternative for weaned piglets.

ACKNOWLEDGEMENTS

This study was supported by Supported by Hubei Provincial Natural Science Foundation of China (Grant No: 2014CFB244), Supported by the Fundamental Research Funds for the Central Universities (Program No: 2011PYO78)

REFERENCES

1. Kubalakukuś A, Banaś D, Braziewicz J, et al. Analysis of copper concentration in human serum by application of total reflection X-ray fluorescence method. Biol Trace Elem Res 2014; 158:22-28.

2. Ognik K, Stępniowska A, Cholewińska E, Kozłowski K. The effect of administration of copper nanoparticles to chickens in drinking water on estimated intestinal absorption of iron, zinc, and calcium. Poultry Sci 2016; 95:2045-51.
3. Zhao CY, Tan SX, Xiao XY, Qiu XS, Pan JQ, Tang ZX. Effects of dietary zinc oxide nanoparticles on growth performance and antioxidative status in broilers. Biol Trace Elem Res 2014; 160:361-67.
4. Rout JR, Ram SS, Das R Chakraborty A, Sudarshan M, Sahoo SL. Copper-stress induced alterations in protein profile and antioxidant enzymes activities in the in vitro grown Withania somnifera L. Physiol Mol Biol Pla 2013; 19:353-61.
5. Song S, Zhang X, Wu H, Han Y, Zhang J, Ma E, Guo Y. Molecular basis for antioxidant enzymes in mediating copper detoxification in the nematode caenorhabditis elegans. Plos One 2014; 9:e107685.
6. Shelton NW, Tokach MD, Nelssen JL, Goodband RD, Dritz SS, DeRouchey JM, Hill GM. Effects of copper sulfate, tri-basic copper chloride, and zinc oxide on weanling pig growth and plasma mineral concentrations. Kansas State University Swine Day Report of Progress 2008; pp. 62-73.
7. Park JK, Kim JW, Yoo YB, et al. Effects of different sources of dietary chromium and copper on growth performances, nutrients digestibility, fecal Cr, Cu and Zn excretion in growing pigs. J Anim Sci Technol 2008; 50:355-62.
8. Gonzaleseguia A, Fu CM, Lu FY, Lien TF. Effects of nanocopper on copper availability and nutrients digestibility, growth performance and serum traits of piglets. Livest Sci 2009; 126:122-29.
9. Xu P, Xu J, Liu S, Yang Z. Nano copper induced apoptosis in podocytes via increasing oxidative stress. J Hazard Mater 2012; 241:279-86.
10. Yoshimura N, Kida K, Usutani S, Nishimura M. Histochemical localization of copper in various organs of brindled mice after copper therapy. Pathol Int 1995; 45(1):10.
11. Zhang H, Chang Z, Mehmood K, et al. Nano copper induces apoptosis in PK-15 cells via a mitochondria-mediated pathway. Biol Trace Elem Res 2018; 181(1):62-70.
12. Chang Z, Zhang H, Mehmood K, et al. Effect of nano copper on visceral organs and the contents of trace elements in weanling pigs. Toxin Reviews 2018; DOI: 10.1080/15569543.2017.1421559
13. Xu J, Li Z, Xu P, Xiao L, Yang Z. Nanosized copper oxide induces apoptosis through oxidative stress in podocytes. Arch Toxicol 2013; 87:1067-73.
14. Sahoo SK, Labhasetwar V. Nanotech approaches to drug delivery and imaging. Drug Discovery Today 2003; 8:1112-20.
15. Henry Y, Sève B, Colléaux Y, Ganier P, Saligaut C, Jego P. Interactive effects of dietary levels of tryptophan and protein on voluntary feed intake and growth performance in pigs, in relation to plasma free amino acids and hypothalamic serotonin. J Anim Sci 1992; 70(6):1873-87.

THYMOQUINONE PROTECTS AGAINST CEREBRAL SMALL VESSEL DISEASE: ROLE OF ANTIOXIDANT AND ANTI-INFLAMMATORY ACTIVITIES

D. GUAN[1], Y. LI[2], X. PENG[2], H. ZHAO[1], Y. MAO[1] and Y. CUI[1]

[1]Department of The Second Clinical Medical College, Henan University of Traditional Chinese Medicine, Zhengzhou, Henan, China; [2]Henan University of Traditional Chinese Medicine, Zhengzhou, Henan, China

Received January 9, 2018 – Accepted February 5, 2018

Cerebral small vessel disease (CSVD) is a leading cause of progressive decline of cognition and a major risk factor for stroke. Thymoquinone (TQ) is the major biological component of *Nigella sativa* (*N. sativa*) and its extracts. We explored the possible protective effect of TQ against CSVD in stroke-prone spontaneously hypertensive SHRsp rats. Morris water maze and novel object recognition tests were conducted to evaluate memory and cognitive function. mRNA expression of inflammatory factors were determined and oxidative stress was evaluated. We showed that TQ markedly decreased the level of systolic blood pressure in SHRsp rats. TQ reduced the escape latency time and the time spent in the target quadrant in the Morris water maze test in SHRsp rats. TQ also decreased the time spent with the novel object in SHRsp rats in both short- and long-term memory tests. TQ markedly increased the capacity to distinguish between familiar objects and novel objects in the SHRsp rats in the short- and long-term memory tests. The mRNA expression of IL-1β, IL-6, monocyte chemoattractant protein-1 and cyclooxygenase-2 in the brain of SHRsp rats was remarkably decreased by TQ, indicating the reduction of inflammation. Moreover, TQ increased the activities of superoxide dismutase and catalase, decreased the malondialdehyde level and increased glutathione level in the brain of SHRsp rats, indicating the attenuation of oxidative stress. In summary, we found that TQ could effectively attenuate the blood pressure and the injury of memory and cognition under the condition of CSVD. The anti-inflammatory and antioxidant activities of TQ may be responsible for its protective effect. We demonstrate that TQ is a novel candidate for the treatment of CSVD and its neurological outcome.

Cerebral small vessel disease (CSVD) is a leading cause of progressive decline of cognition and a major risk factor for stroke that causes a great burden on the individual and the healthcare system. Although CSVD contributes to only 20-30% of all strokes, it dramatically increases the risk of future strokes (1) and causes about 45% of dementia cases (2). As the population ages, the prevalence of CSVD is increasing. CSVD is a group of diseases involving a series of pathological processes in the brain, including small arteries, arterioles, capillaries and small veins. Injury of small penetrations supplying subcortical structure vessels results in blood–brain barrier (BBB) disruption, neuroinflammation, lacunar infarcts, microbleeds, and cognitive dysfunction. The major imaging features of CSVD are lacunar infarctions and white matter lesions, resulting in cognitive impairment, depression, gait disturbance

Key words: cerebral small vessel disease, thymoquinone, memory and cognition, inflammation, oxidative stress

Mailing address:
Dr Yinglin Cui,
School of Basic Medicine,
The Second Clinical Medical College,
Henan University of Traditional Chinese Medicine,
No.1 Jinshui Road, Zhengzhou, Henan 450046, China
Tel.: +86 13838069221
e-mail: yinglin_cui15@163.com

0393-974X (2018)

and increased stroke incidence. Therefore, efforts should be intensified to elucidate the mechanism of CSVD and develop novel effective treatments. Although the accurate mechanism of CSVD is not clear, oxidative stress is believed to play an important role. Oxidative stress is implicated in the arteriopathy of both non-amyloid and amyloid (cerebral amyloid angiopathy) forms of CSVD and its most important risk factors (hypertension and aging) (3). Oxidative stress also contributes to CSVD-related brain injury and cognitive impairment (3).

Previous studies have shown that *Nigella sativa* (*N. sativa*) possesses a variety of therapeutic activities, including anti-tumor cells, anti-inflammatory and analgesic, anti-epileptic, anti-histaminic, and diuretic and hypotensive effects. It has been proved that thymoquinone (2- isopropyl-5-methyl-1, 4-benzoquinone, TQ), one of the monoterpenoid hydrocarbon compounds of *N. sativa* volatile oil, is the major biological component of *N. sativa* and its extracts, which contributes to most of the activities. TQ possesses an antioxidant activity which is dependent on GSH, NADPH or NADH. TQ has been shown to attenuate brain injury via an anti-oxidative pathway in status epilepticus rats and attenuate seizure activity and lower hippocampal neuronal loss in an epilepsy model and in children with refractory seizures. TQ also exhibits neuroprotective effects against traumatic and ischemia-reperfusion brain injury (4, 5). In a study of subchronic oral administration, the administration of 90 mg/kg/day TQ showed no signs of toxicity or mortality.

In the current study, we explored the possible protective effect of TQ against CSVD in rats and searched for probable mechanisms. We demonstrated that TQ could effectively protect against CSVD in rats and the antioxidant and anti-inflammatory activities of TQ may play an important role.

MATERIALS AND METHODS

Animals and treatment

Sprague-Dawley (SD) rats (male, 15 weeks old), stroke-prone spontaneously hypertensive rats (male, 15 weeks old) were purchased from SLK (Shanghai, China) and then maintained in at controlled temperature (21±2°C), humidity (60±10%), and a 12 h light/dark cycle (exposed to artificial light from 7:00 am to 7:00 pm) and air ventilation (15 min/h). The rats were fed with a standard rodent laboratory diet and water *ad libitum*. All procedures were carried out in accordance with the conventional guidelines for experimentation with animals (National Institute of Health, Publication no. 85-23, revised 1996). All animal procedures were approved by the Review Board of Henan University of Traditional Chinese Medicine.

The rats were maintained under basal conditions for 10 days and then subdivided into four groups,10 rats in each group, as follows: Control: SD rats received vehicle (Normal saline, 10ml/kg, intraperitoneal injection); SHRsp: SHRsp rats received vehicle; 25 mg/kg TQ: SHRsp rats received oral gavage of 25 mg/kg TQ (Sigma-Aldrich, St. Louis, MO, USA) for 4 weeks; 50 mg/kg TQ: SHRsp rats received oral gavage of 50 mg/kg TQ for 4 weeks.

The systolic blood pressure of the rats in each group was measured using the tail cuff method (BP-98A; Softron Co, Tokyo, Japan).

Morris water maze test

At the end of the treatment, the Morris water maze test was conducted to evaluate the memory and cognitive function in rats. The Morris water maze test was performed as previously. In brief, a circular pool (1.3 m in diameter, 50 cm in depth) was filled with room-temperature water. One cm below the surface of the water, a transparent platform was placed in the southeastern quadrant. On the first day, the rats were put into the pool without the platform for 2 min to get used to the experimental environment. Over the next 4 days, the platform acquisition test was conducted 4 times per day. The rats were released from different starting points and allowed to swim for 60 s to search for the platform. The escape latency time was defined by the time spent to find the hidden platform by the rats and times longer than 60 s were recorded as 60 s. Twenty-four hours later, the rats were released from a new start position in the pool without the platform, which was termed the probe trial. The amount of time spent in the southeastern quadrant was recorded.

Novel object recognition test

The rats were individually placed in a plastic box with two objects with different forms. The rats were allowed to

freely move in the box for 5 min. This adaptive training was conducted again after 180 min. In the short-term memory test, we replaced one of the objects 180 min after the second training. The time spent by each animal with the novel object and the familiar object was recorded during a 10 min test period. In the long-term memory test, one of the objects was replaced by a novel object 24 h after the second training. The time spent by each rat with the novel object and the familiar object was again recorded during a 10 min test period. In the tests, exploration was defined as sniffing or touching the object with the nose or foreleg. The objects were washed after each test to avoid olfactory perception by the next rat.

Quantitative real-time PCR

Total RNA was extracted from livers using Trizol reagent (Invitrogen, CA, USA). The cDNA was synthesized using an miScript II RT Kit (Thermo Fisher Scientific Inc., Waltham, MA, USA), per the manufacturer's instructions. After reverse transcription of the RNA, cDNA was used as a template in PCR reactions using gene-specific primer pairs. Real-time PCR was performed on an Applied Biosystems 7500 cycler (Applied Biosystems, CA, USA) using a miScript SYBR Green PCR Kit (Thermo Fisher Scientific Inc.). β-actin was used as endogenous control for mRNA expression. The fold changes of target gene expression were determined with the ΔΔCt method, and the relative expression of these genes was calculated by the $2^{-\Delta CT}$ method and normalized to β-actin. The PCR conditions were as follows: 95°C for 5 min, 40 cycles of 30 s at 95°C, 30 s at 52–60°C (based on the target), and 60 s at 72°C. Primers used in the current study:

IL-1β:F:5'-ACCTGCTAGTGTGTGATGTTCCCA-3'; R: 5'-AGGTGGAGAGCTTTCAGCTCACAT-3'. IL-6: F: 5'-AATCTGCTCTGGTCTTCTTGGAG-3';R: 5'-GTTGGATGGTCTTGGTCCTTAG-3';MCP-1: F: 5'-ATGCAGGTCTCTGTCACGCT-3'; R: 5'-GGTGCTGAAGTCCTTAGGGT-3'. COX-2: F: 5'-GCATTCTTTGCCCAGCACTTCACT-3'; R: 5'-TTTAAGTCCACTCCATGGCCCAGT-3'. β-actin: F: 5'-CCACCCGCGAGTACAACCTTCTT -3'; R:5'-GAAGCCGGCCTTGCACATGCC -3'.

Oxidative stress

SOD and CAT activities, and GSH and MDA levels were measured using commercial assay kits (Nanjing Jiancheng Company, Jiangsu, China) according to the manufacturer's protocols.

Statistical analysis

Data were expressed as mean ± SEM. Statistical analysis was performed by one-way analysis of variance followed by an SNK-q test for multiple comparisons using Graph Pad Prism. $P < 0.05$ was considered as statistically significant.

RESULTS

TQ attenuates blood pressure in SHRsp rats

The systolic blood pressure in SHRsp rats was significantly higher than that in SD rats (Fig. 1A). Four-week administration of TQ markedly decreased the level of systolic blood pressure in SHRsp rats, which was in a dose-dependent manner (Fig. 1A). We showed that TQ exhibited an inhibitory effect on the increase of blood pressure in the stroke-prone spontaneously hypertensive rats.

TQ improves memory and cognitive performance in SHRsp rats

The memory and cognitive performance of the rats was assessed using the Morris water maze test and novel object recognition test. There was no significant difference between the rats in different groups on the hidden platform acquisition test on the first day. On days 2-5, the escape latency time in SHRsp rats was remarkably longer than that in SD rats (Fig. 1B). The escape latency time in SHRsp rats treated by TQ was significantly shorter on the hidden platform acquisition test on days 2-5, compared with SHRsp rats (Fig. 1B). Moreover, the time spent in the target quadrant in SHRsp rats was lower than that in SD rats during the probe trial? (Fig. 1C). The administration of TQ significantly increased the time spent in the target quadrant in SHRsp rats, which was in a dose-dependent manner (Fig. 1C).

In the novel object recognition tests, the time spent with the novel object in SHRsp rats were increased in both short and long term memory tests from the first to the fourth week (Tables I and II). The administration of TQ significantly decreased the time spent with the novel object in SHRsp rats in both short and long term memory tests (Tables I

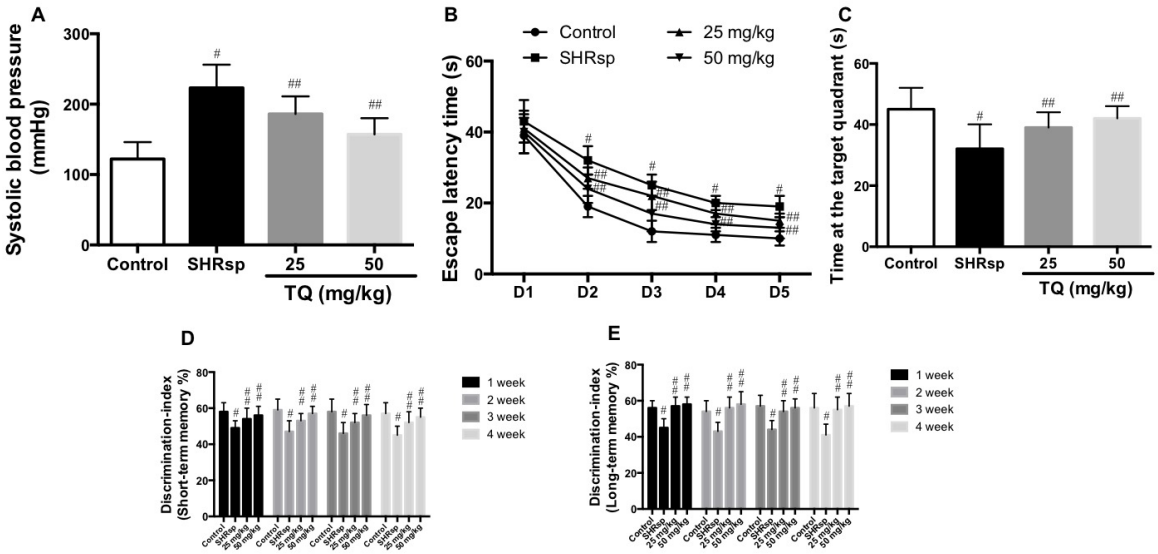

Fig. 1. *The effect of TQ on systolic blood pressure in SHRsp rats. SHRsp rats were administered 25 or 50 mg TQ for 4 weeks. SD rats were given equal volume of vehicle.* ***A)*** *The systolic blood pressure of the rats in each group was measured using the tail cuff method. Morris water maze test was performed to evaluate memory and cognitive function.* ***B)*** *The escape latency time.* ***C)*** *Time spent at the target quadrant. Novel object recognition test was performed to evaluate memory and cognitive function.* ***D)*** *Discrimination-index in the short term memory test.* ***E)*** *Discrimination-index in the long term memory test. *p<0.05, compared with Control. *p<0.05, compared with SHRsp rats.*

Table I. *Novel object recognition test: short-term memory.*

	Time spent with the novel object			
Groups	1 week	2 weeks	3 weeks	4 weeks
Control	8.12±2.21	7.98±2.17	7.93±1.97	7.74±2.03
SHRsp	3.72±1.36*	3.53±1.51*	3.42±1.48*	3.12±1.46*
25 mg/kg	5.13±1.25#	5.37±1.39#	5.29±1.66#	4.85±1.33#
50 mg/kg	6.89±2.21#	7.21±1.62#	6.75±1.92#	6.57±1.84#

**p<0.05, compared with Control. #p<0.05, compared with SHRsp.*

Table II. *Novel object recognition test: long-term memory.*

	Time spent with the novel object			
Groups	1 week	2 weeks	3 weeks	4 weeks
Control	7.21±2.24	6.96±2.02	6.92±1.87	6.87±2.22
SHRsp	3.21±1.48*	3.14±1.68*	2.89±1.58*	2.76±1.55*
25 mg/kg	5.17±1.68#	4.78±1.59#	4.61±1.72#	4.42±1.67#
50 mg/kg	6.41±2.01#	6.22±1.51#	6.16±1.48#	5.82±1.74#

**p<0.05, compared with Control. #p<0.05, compared with SHRsp.*

and II). Moreover, the discrimination index for the short- and long-term memory tests showed a marked decrease in the capacity to distinguish between familiar objects and novel objects in the SHRsp rats (Fig. 1D and E). The administration of TQ markedly increased the capacity to distinguish between familiar objects and novel objects in the SHRsp rats in the short- and long-term memory tests (Fig. 1D and E). Based on the results, we showed that TQ exhibited a protective effect against the injury of memory and cognitive performance in SHRsp rats.

TQ attenuates inflammation in the brain of SHRsp rats

We detected the effect of TQ on inflammation in the brain of SHRsp rats and the mRNA expression of several proinflammatory cytokines and regulators were examined. The mRNA expression of IL-1β (Fig. 2A), IL-6 (Fig. 2B), monocyte chemoattractant protein-1 (MCP-1) (Fig. 2C) and cyclooxygenase-2 (COX-2) (Fig. 2D) was significantly higher in the brain of SHRsp rats compared with that of SD rats. The administration of TQ dose-dependently decreased the levels of those proinflammatory markers in SHRsp rats. We suggest that TQ exhibited an anti-inflammatory effect in SHRsp rats.

TQ attenuates oxidative stress in the brain of SHRsp rats

The effect of TQ on oxidative stress in the brain of SHRsp rats was assessed by the determination of oxidative stress markers. As shown in Fig. 3A and B, the activities of antioxidant enzymes, including superoxide dismutase (SOD) and catalase (CAT), in the brain of SHRsp rats were increased compared with those in SD rats. TQ administration notably increased the activities of SOD and CAT in the brain of SHRsp rats. The level of malondialdehyde (MDA), the oxidant product of lipids, was higher in the brain of SHRsp rats than that in SD rats (Fig. 3C). This increase of MDA level was inhibited by TQ administration (Fig. 3C). The level of glutathione (GSH), an important antioxidant protein, was lower in the brain of SHRsp rats than that in SD rats (Fig. 3D). This decrease of GSH level was attenuated by TQ administration (Fig. 3D). The results suggested that TQ exhibited a potent antioxidant role in the brain of SHRsp rats.

DISCUSSION

In the present study, we tested the protective effect of TQ against hypertension-induced CSVD injury in SHRsp rats. SHRsp animals are the most commonly used model of CSVD. In SHRsp rats, blood pressure begins to increase at the age of 4 weeks and increases to more than 220 mm Hg at approximately 20 weeks. The pathological changes of small vessels in SHRsp rats are similar to those found in human CSVD (6). TQ exhibited a dose-dependent inhibitory effect against the increase of blood pressure in SHRsp rats at the age 17-20 weeks. TQ-induced decrease of blood pressure resulted in improvement of memory and cognitive performance. TQ markedly decreased the escape latency time and the time spent in the target quadrant in SHRsp rats. Moreover, TQ increased the time spent with the novel object and the capacity to distinguish between familiar objects and novel objects in the SHRsp rats.

Inflammation is an important pathological course in the pathogenesis of CSVD (7). Activated monocytes/macrophages are involved in the increase of permeability of the blood-brain barrier and subsequent injury (8). Abnormal levels of inflammatory cytokines are associated with the outcome of CSVD. Inhibition of COX-2 by an inhibitor reduces vascular wall thickness and ameliorates cognitive impairment in a cerebral small vessel disease rat model (9). TQ significantly decreased the expression of inflammatory markers in the brain of SHRsp rats, indicating that the anti-inflammatory activity of TQ may be involved in the protective effects against CSVD.

Oxidative stress plays critical roles in a variety of brain and neurological diseases, including CSVD and its associated neurological injuries. It is believed that oxidative stress participates in the arteriopathy of both non-amyloid and amyloid (cerebral amyloid angiopathy) forms of CSVD and its most important risk factors (hypertension and aging) (3). Oxidative stress is also considered to result in CSVD-related brain injury and cognitive impairment (3).

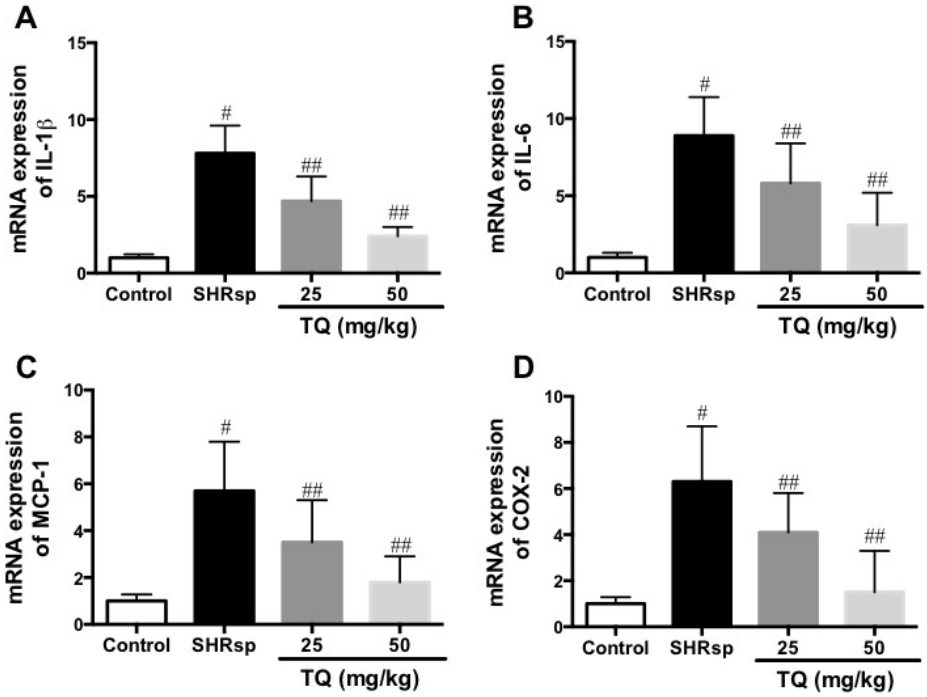

Fig. 2. *The effect of TQ on inflammation in the brain in SHRsp rats. SHRsp rats were administered 25 or 50 mg TQ for 4 weeks. SD rats were given equal volume of vehicle. mRNA expression of IL-1β (**A**), IL-6 (**B**), MCP-1 (**C**) and COX-2 (**D**) in the brain in SHRsp rats was determined by real-time PCR. *p<0.05, compared with Control. *p<0.05, compared with SHRsp rats.*

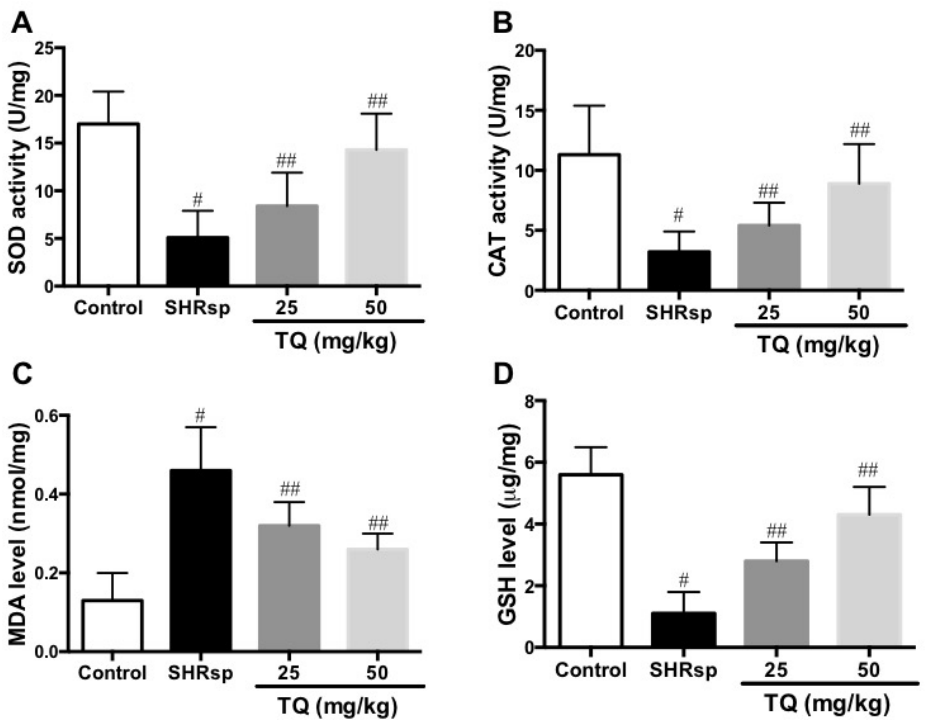

Fig. 3. *The effect of TQ on oxidative stress in the brain in SHRsp rats. SHRsp rats were administered 25 or 50 mg TQ for 4 weeks. SD rats were given equal volume of vehicle. The activities of SOD and CAT, and levels of MDA and GSH were detected using commercial kits. *p<0.05, compared with Control. *p<0.05, compared with SHRsp rats.*

Antioxidant intervention has been proposed to be a novel strategy for the treatment of CSVD (3). In the current study, we found that oxidative stress in SHRsp rats was attenuated by TQ.

In summary, we found that TQ could effectively attenuate the blood pressure and the injury of memory and cognition under the condition of CSVD. The anti-inflammatory and antioxidant activities of TQ may be responsible for the protective effect of TQ. However, more studies are needed to explore the target of TQ action and the molecular mechanism. Overall, we demonstrate that TQ is a novel candidate for the treatment of CSVD and its neurological outcome.

ACKNOWLEDGEMENTS

This study was supported by the National Natural Science Foundation of China (No. 81673943 and 81573919) and the Leading Talents Development Project of Traditional Chinese Medicine Clinical Disciplines, Administration of Traditional Chinese Medicine, Henan (201301006).

REFERENCES

1. Debette S, Markus HS. The clinical importance of white matter hyperintensities on brain magnetic resonance imaging: systematic review and meta-analysis. BMJ (Clinical research ed) 2010; 341:c3666.
2. Madigan JB, Wilcock DM, Hainsworth AH. Vascular contributions to cognitive impairment and dementia: topical review of animal models. Stroke 2016; 47(7):1953-9.
3. De Silva TM, Miller AA. Cerebral small vessel disease: targeting oxidative stress as a novel therapeutic strategy? Front Pharmacol 2016; 7:61.
4. Gulsen I, Ak H, Colcimen N, et al. Neuroprotective effects of thymoquinone on the hippocampus in a rat model of traumatic brain injury. World Neurosurg 2016; 86:243-49.
5. Xiao XY, Zhu YX, Bu JY, Li GW, Zhou JH, Zhou SP. Evaluation of neuroprotective effect of thymoquinone nanoformulation in the rodent cerebral ischemia-reperfusion model. BioMed Res Int 2016; 2016:2571060.
6. Hainsworth AH, Markus HS. Do in vivo experimental models reflect human cerebral small vessel disease? A systematic review. J Cereb Blood Flow Metab : official journal of the International Society of Cerebral Blood Flow and Metabolism 2008; 28(12):1877-91.
7. Wiseman SJ, Doubal FN, Chappell FM, et al. Plasma biomarkers of inflammation, endothelial function and hemostasis in cerebral small vessel disease. Cereb Dis (Basel, Switzerland). 2015; 40(3-4):157-64.
8. Rouhl RP, Damoiseaux JG, Lodder J, et al. Vascular inflammation in cerebral small vessel disease. Neurobiol Aging 2012; 33(8):1800-6.
9. Tang J, Xiao W, Li Q, et al. A Cyclooxygenase-2 inhibitor reduces vascular wall thickness and ameliorates cognitive impairment in a cerebral small vessel diseases rat model. Curr Alzheimer Res 2015; 12(7):704-10.

CYSTEINYL LEUKOTRIENES C_4 AND D_4 DOWNREGULATE HUMAN MAST CELL EXPRESSION OF TOLL-LIKE RECEPTORS 1 THROUGH 7

V. KARPOV[1], R. ILARRAZA[2], A. CATALLI[1] and M. KULKA[1,2]

[1]National Research Council Canada, Edmonton, Alberta, Canada; [2]Department of Medical Microbiology and Immunology, Faculty of Medicine, University of Alberta, Edmonton, Alberta, Canada

Received July 17,2017 – Accepted January 12, 2018

Cysteinyl leukotrienes (CysLT) are potent inflammatory lipid molecules that mediate some of the pathophysiological responses associated with asthma such as bronchoconstriction, vasodilation and increased microvascular permeability. As a result, CysLT receptor antagonists (LRA), such as montelukast, have been used to effectively treat patients with asthma. We have recently shown that mast cells are necessary modulators of innate immune responses to bacterial infection and an important component of this innate immune response may involve the production of CysLT. However, the effect of LRA on innate immune receptors, particularly on allergic effector cells, is unknown. This study determined the effect of CysLT on toll-like receptor (TLR) expression by the human mast cell line LAD2. Real-time PCR analysis determined that LTC_4, LTD_4 and LTE_4 downregulated mRNA expression of several TLR. Specifically in human CD34+-derived human mast cells (HuMC), LTC_4 inhibited expression of TLR1, 2, 4, 5, 6 and 7 while LTD4 inhibited expression of TLR1-7. Montelukast blocked LTC_4-mediated downregulation of all TLR, suggesting that these effects were mediated by activation of the CysLT1 receptor (CysLT1R). Flow cytometry analysis confirmed that LTC_4 downregulated surface expression of TLR2 which was blocked by montelukast. These data show that CysLT can modulate human mast cell expression of TLR and that montelukast may be beneficial for innate immune responses mediated by mast cells.

Activated mast cells (MC) release pro-inflammatory molecules such as histamine and leukotrienes (LT)(1). In asthma, LT mediate or modulate production of hematopoietic progenitor cells, eosinophil survival and recruitment, activity of cytokines and chemokines, exhaled nitric oxide production, smooth-muscle contraction, and proliferation of fibroblasts (2), among other processes. As a result, LT receptor antagonists (LRA) have been used to effectively treat patients with asthma and allergic airway inflammation (3). We recently showed that MC are necessary modulators of innate immune responses to bacterial infection and may involve cysteinyl LT (CysLT) production (4-6). Respiratory viral infections induce CysLT production and can lead to asthma exacerbations (7), prevented by LRA such as montelukast. Evidence therefore suggests that LRA may have direct effects on innate immune triggers mediated, at least in part, by pattern recognition receptors such as toll-like receptors (TLR).

The role of TLR and LT in the development of acute illness and long term chronic allergic disease of the airways is still poorly understood. Pathogen-

Key words: mast cells, cysteinyl leukotrienes, toll-like receptors (TLR)

Mailing address:
Marianna Kulka, PhD
National Institute of Nanotechnology,
National Research Council Canada,
11421 Saskatchewan Drive, Edmonton, AB T6G 2M9, Canada
Tel.: +1 780 641 1687
e-mail: marianna.kulka@nrc-cnrc.gc.ca

0393-974X (2018)

DISCLOSURE: ALL AUTHORS REPORT NO CONFLICTS OF INTEREST RELEVANT TO THIS ARTICLE.

associated molecular patterns (PAMPs) that activate TLR2 and TLR4 induce rodent MC to produce nanomolar quantities of CysLT (8) while TLR7 ligands decrease airway hyperresponsiveness and bronchoalveolar lavage LTB_4 production in an ovalbumin-induced allergic inflammation mouse model (9). Similarly, heat shock and acetylsalicylic acid induce the production and release of heat shock proteins from MC, and the heat shock proteins, such as Hsp70, stimulate leukotriene synthesis through activation of TLR4 (10). We hypothesized that CysLT in inflammatory microenvironments may modulate the expression of TLRs on MC.

MATERIALS AND METHODS

Reagents and human mast cell (HuMC) culture

All reagents were obtained from Sigma Aldrich (Oakville, Canada), unless otherwise stated. LAD2 MC were cultured in serum free media (StemPro-34 SFM, Invitrogen, Burlington, Canada) supplemented with 2 mM L-glutamine, 100U/ml penicillin, 50µg/ml streptomycin and 100ng/ml stem cell factor (SCF). The cell suspensions were seeded at a density of 10^5cells/ml and maintained at 37°C and 5% CO_2. Cells were fed by hemi-depletion of medium once per week.

Human peripheral blood derived $CD34^+$ mast cells (HuMC) were cultured in StemPro-34 SFM supplemented with 2 mM L-glutamine, 50µg/ml streptomycin, 100IU/ml penicillin, 100ng/ml SCF, and 100ng/ml recombinant human IL-6 (PeproTech, Inc., Rocky Hill, USA). Recombinant human IL-3 (30ng/ml) was added for the first week. Half of the culture medium was replaced every 7 days. Cultures at 8 to 10 weeks consisted of greater than 99% HuMC. Unless otherwise stated, all experiments were performed in StemPro-34 SFM complete with 10ng/mL SCF.

CysLT treatment

Cells (HuMC and LAD2) were treated with CysLTs (LTC_4, LTD_4, LTE_4, Cayman Chemical, Ann Arbor, USA) at 1.0 µM (unless otherwise shown) for 3 days (72 h) with fresh media containing CysLTs replenished every day.

Quantitative PCR analysis

Total RNA was isolated from each preparation using the RNeasy Mini Kit (Qiagen Inc. Valencia, USA).

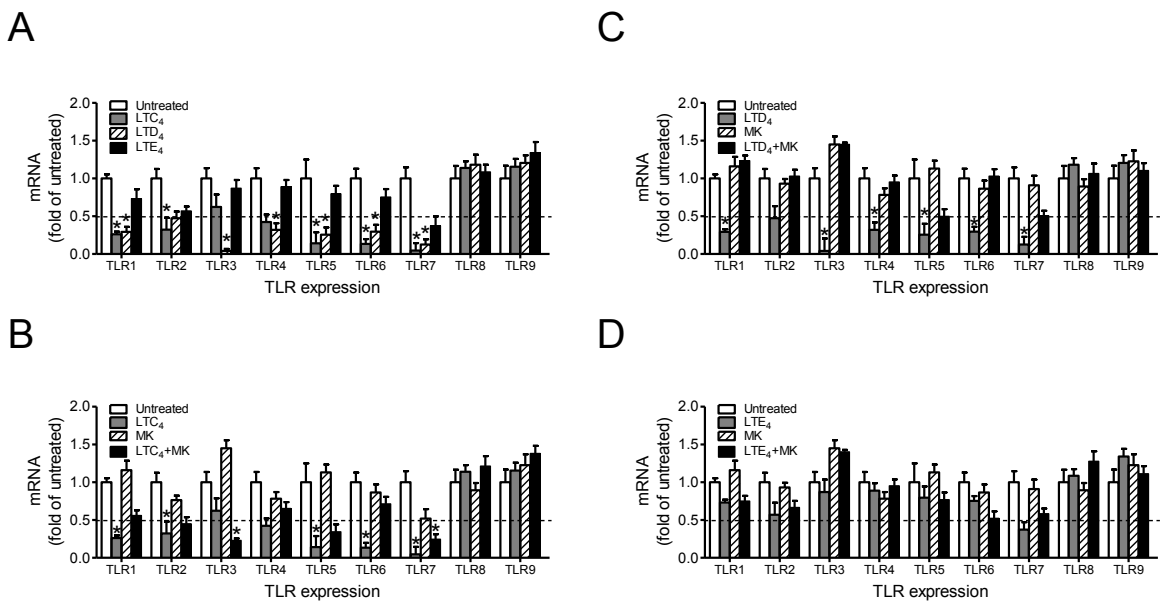

Fig. 1. *CysLTs downregulate TLR gene expression by cultured $CD34^+$-derived human mast cells (HuMC). HuMC were pretreated with LTC_4, LTD_4 or LTE_4 (1.0 uM) alone (**A**), or in presence or absence of MK (100 nM) (**B-D**), for 3 h and TLR expression was measured by qPCR (n=3, *p>0.01). Values below 0.5 (2-fold downregulation) were considered significant.*

Five micrograms of total cellular RNA was reverse transcribed using the Taqman Reverse Transcription reagents and Random Hexamer primer (Perkin–Elmer Applied Biosystems, Foster City, USA). Gene expression was analyzed using quantitative polymerase chain reaction (qPCR) on an StepOnePlus system (Invitrogen, Burlington, Canada). Fifty ng of cDNA was used in each quantitative PCR assay. Primer sets for PCR amplifications were designed using the Primer Express software (Perkin–Elmer Applied Biosystems, Guelph, Canada). All reactions were performed in triplicate for 40 cycles as per the manufacturer's recommendation. Results are expressed as relative mRNA corrected with reference to GAPDH mRNA as an internal control.

Flow cytometric analysis

Cells were washed and resuspended at 5 x 10^5 cells/mL in PBS/0.1% BSA and incubated with anti-CysLT1R [raised against human CysLT1 receptor C-terminal amino acids 318-337 (YVPRKKASLPEKGEEICKV)] or anti-CyLT2R (human CysLT2 receptor N-terminal amino acids 1-18 (MERKFMSLQPSISVSEME); both from Cayman Chemical, Ann Arbor, USA) or appropriate isotype control antibody (BD Biosciences, Mississauga, Canada) for 30 min at 4°C. Cells were washed twice and in the cases where the primary antibody was unconjugated, anti-rabbit-PE (BD Biosciences, Mississauga, Canada) or anti-mouse-PE (BD Biosciences, Mississauga, Canada) was added for 30 min at 4°C. Cells were washed twice, resuspended in PBS/0.1% BSA and analyzed on a FACSArray or FACSAria (BD Biosciences, Mississauga, Canada).

Cytokine enzyme-linked immunosorbent assays (ELISAs)

LAD2 were washed with media and suspended at 0.2 x 10^6 cells per well, preincubated with 1.0 µM LTC_4 (Cayman Chemical, Ann Arbor, USA) or untreated and stimulated with peptidoglycan (PGN), polyinosinic–polycytidylic acid sodium salt (polyI:C), lipopolysaccharide (LPS), lipoteichoic acid (LTA), all from Sigma-Aldrich, or Pam3CysSerLys4 (Pam3CSK4; InvivoGen, San Diego, USA) for 4 h and cell-free supernatants were analyzed for TNF release by ELISA (eBioscience, San Diego, USA).

DNA-binding activity of nuclear transcription factor proteins

Nuclear protein was extracted from LTC_4-treated LAD2 cells after TLR activation using a nuclear extract kit (Active Motif, Carlsbad, USA), according to the

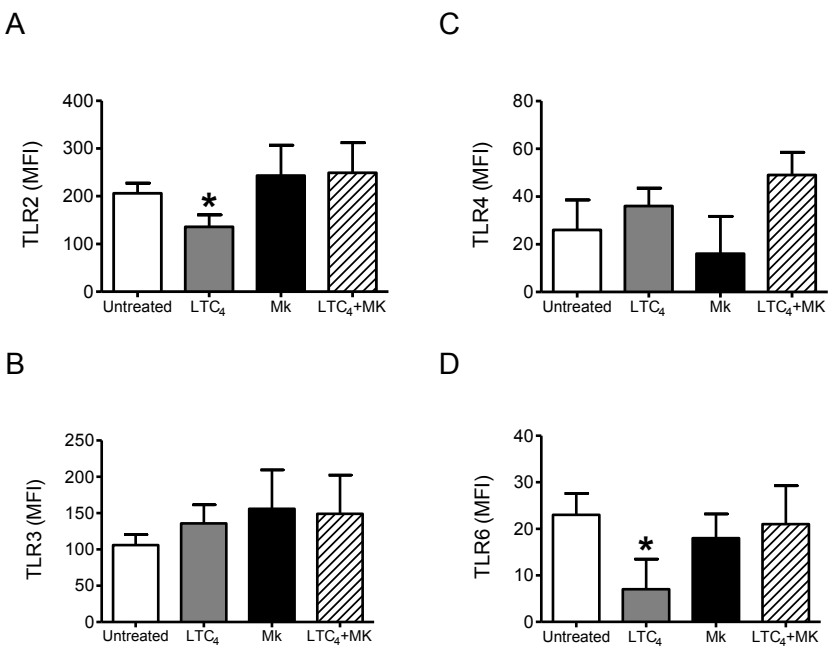

Fig. 2. *CysLTs downregulate TLR protein expression by cultured CD34+-derived human mast cells (HuMC). HuMC were pretreated with LTC_4, LTD_4 or LTE_4 (1.0 uM) or montelukast (MK; 100 nM) for 3 days (according to described methods) and TLR 2, 3, 4 and 6 (**A-D**, respectively) expression was measured by flow cytometry (n=5, *p>0.01). Values below 0.5 (2-fold downregulation) were considered significant.*

supplier's instructions. The nuclear extracts (10 μg of protein/aliquot) were assayed by ELISA (TransAM kits; Active Motif, Carlsbad, USA) for DNA-binding activity of IRF-3, IRF-7 and NF-κB p50. The transcription factor proteins, bound to immobilized oligonucleotides corresponding to appropriate consensus gene response elements, were detected with specific Abs, followed by HRP-conjugated anti-Ig, according to the supplier's instructions. DNA-binding activity was expressed as a percentage of the maximum response.

Statistical analysis

Each experiment was performed at least 3 separate times and in quadruplicate and values displayed represent mean +/- standard error of the mean. P values were determined by Student's *t*-test (between groups) or one-way ANOVA (comparing more than two groups).

RESULTS

CysLT downregulates expression of TLR

It was hypothesized that CysLT modified TLR expression and TLR ligand-mediated mast cell responses. As reported by our group and others, $CD34^+$-derived primary human mast cells (HuMC) express variable levels of CysLT1R and CysLT2R surface expression, with some donor $CD34^+$ cells giving rise to HuMC with high levels of CysLTR expression. Using HuMC cultured from a donor that consistently produced cells that expressed high levels of CysLT, we determined the effect of CysLT on TLR expression. HuMC were treated with LTC_4, LTD_4 and LTE_4 (1 μM) for 3 h and TLR mRNA expression was measured by qPCR (Fig. 1A). Overall, CysLTs downregulated TLR expression

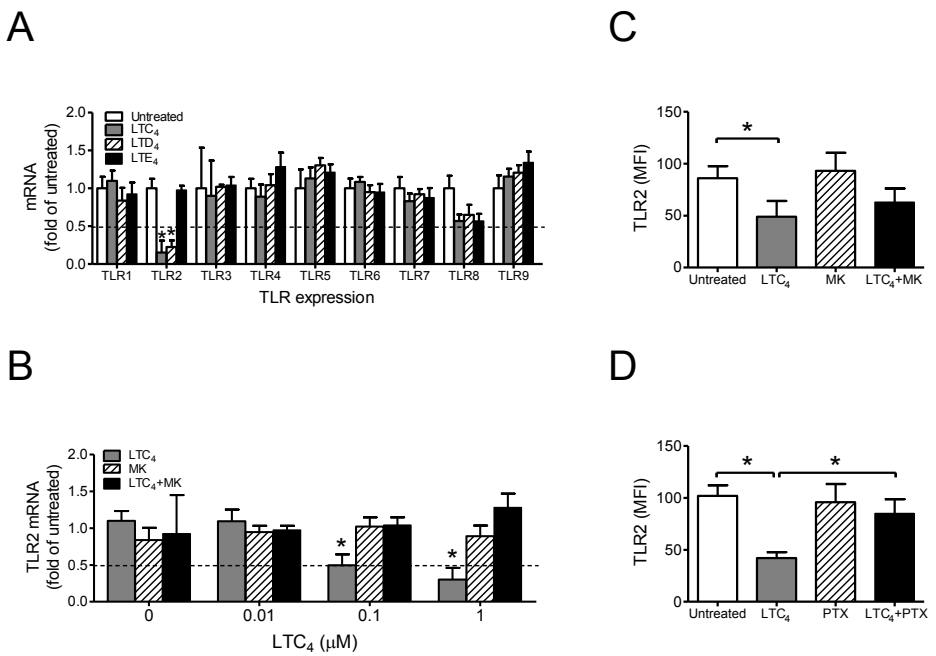

Fig. 3. *CysLTs downregulate TLR2 expression by a human mast cell line (LAD2). **A**) LAD2 were pretreated with LTC_4, LTD_4 or LTE_4 (1.0 uM) for 3 h and TLR expression was measured by qPCR (n=3, *p>0.01). Values below 0.5 (2-fold downregulation) were considered to be significant. **B**) LAD2 were pretreated with LTC_4 or montelukast (MK; 100 nM) for 3 days (according to described methods) and TLR expression was measured by qPCR (n=5, *p>0.01). **C**) LAD2 were pretreated with LTC_4 (1.0 uM) or MK (100 nM) for 3 days (according to described methods) and TLR expression was measured by flow cytometry (n=5, *p<0.05). Values below 0.5 (2-fold downregulation) were considered to be significant. **D**) LAD were pretreated with LTC_4 (1.0 uM) or Pertussis toxin (PTX; 30 nM) for 3 days and TLR expression was measured by flow cytometry (n=7, *p<0.05).*

by at least 2-fold (0.5-fold expression compared to untreated control). LTC_4 downregulated expression of TLR1, TLR2, TLR4, TLR5, TLR6 and TLR7; LTD_4 downregulated expression of TLR1, TLR2, TLR3, TLR4, TLR5, TLR6 and TLR7; and LTE_4 downregulated expression of TLR7 but had no significant expression on any of the other TLRs. None of the CysLTs tested significantly modulated expression of TLR8 or TLR9.

In general, montelukast inhibited LTC_4 and LTD_4-induced changes in expression of these TLRs (Fig. 1, B and C) but had no significant effect on LTE_4-mediated downregulation of TLR7 (Fig. 1D). Montelukast alone had no significant effect on TLR expression by HuMC.

Analysis of TLR protein expression using flow cytometry confirmed that LTC_4 treatment downregulated expression of TLR2 and TLR6 (Fig. 2). However, changes in expression of TLR3 and TLR4 were not detectable.

The effect was then examined of CysLT on TLR expression in the LAD2 mast cell line. Unlike the primary cultured HuMC, LTC_4 significantly downregulated TLR2 but had no effect on any of the other TLRs (Fig. 3A). LTD_4 and LTE_4 also had no detectable effect on TLR expression. Follow-up analysis by qPCR showed that LTC_4 dose-dependently downregulated TLR2 expression and that this decrease was blocked by montelukast (Fig. 3B). Similarly, flow cytometry analysis of TLR2 expression by LAD2 showed that LTC_4 downregulated expression of TLR2 and that this was also sensitive to montelukast treatment (Fig 3C). LTC_4-mediated downregulation of TLR2 was sensitive to pertussis toxin (PTX) (Fig. 3D), suggesting that these effects were mediated via a G protein-coupled receptor.

CysLT inhibit TLR-mediated responses by HuMC

To determine whether CysLT-mediated changes in TLR expression could alter mast cell activation by TLR ligands, we pre-incubated HuMC with LTC_4,

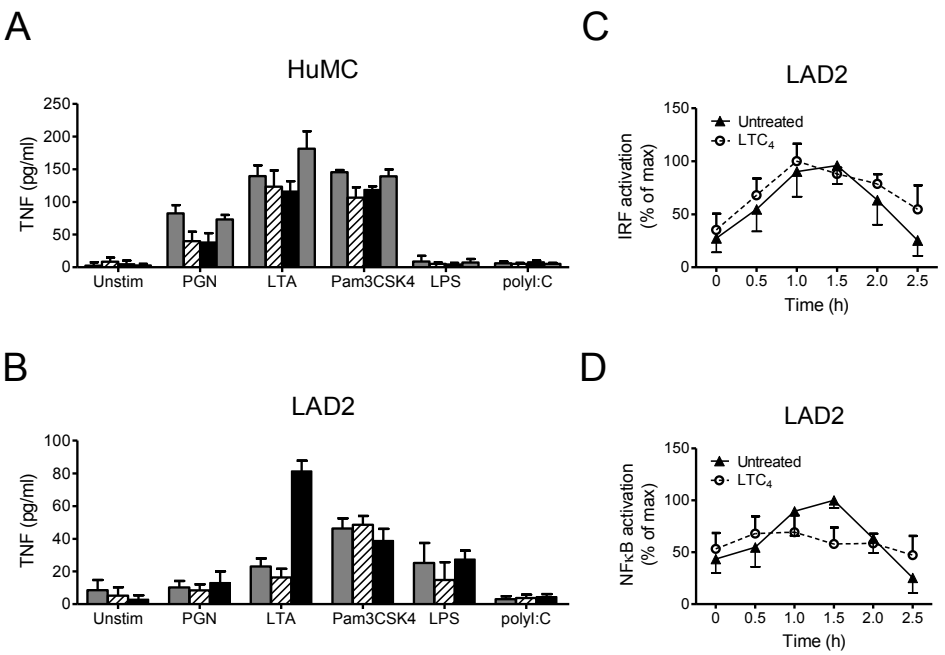

Fig. 4. *CysLTs inhibit TLR function. HuMC (**A**) and LAD2 (**B**) were pre-treated with LTE_4, LTD_4 and LTE_4, stimulated with TLR ligands (PGN, LTA, Pam3CSK, LPS and poly I:C) and TNF production was measured by ELISA (n=5, *p<0.01). **C**) LAD2 cells were pretreated with LTC_4 and activated with LPS/poly I:C and IRF3 translocation was measured as described. **D**) LAD2 cells were pretreated with LTC_4 and activated with LTA and NF-kB translocation was measured as described. Data are presented as percentage of maximum response in each experiment (n=3, *p<0.01).*

LTD_4 and LTE_4 and measured their release of TNF in response to established TLR ligands. The results show that LTC_4 pre-treatment renders HuMC less responsive to LTA and LPS but not Pam3CSK4, PGN or polyI:C (Fig. 4A). Similarly, LTD_4 pretreatment renders HuMC less responsive to LTA and LPS but not Pam3CSK4, PGN or polyI:C.

Since LTC_4 pre-treatment resulted in TLR2 downregulation by LAD2 cells, we performed a similar experiment with LAD2 cells. LTC_4 pre-treatment rendered LAD2 cells less responsive to LTA-induced TNF production but had no effect on PGN, Pam3CSK, LPS or polyI:C-mediated activation (Fig. 4B).

LTC4 does not alter IRF-3 or IRF-7 activation upon stimulation with LTA

It has been shown that all of the TLR receptors signal through NF-kB to activate the production of mediators such as TNF. However, IRF family members such as IRF-3 and IRF-7 are involved in TLR3 and TLR4 but not TLR2 signaling (11). To test the hypothesis that LTC4 reduced responsiveness via TLR2 but not TLR3 or TLR4 receptors in LAD2, LAD2 was pretreated with LTC_4, activated then with either LPS/polyI:C or LTA and measured IRF-3, IRF-7 and NF-κB activation/translocation (Fig. 4, C and D). As expected, LPS/polyI:C activated IRF-3 (Fig. 4C) and IRF-7 (data not shown) but LTC_4 pretreatment had no effect on these responses. Conversely, LTC_4 inhibited LTA-induced NK-κB activation (Fig. 4D) but had no effect on LPS/polyI:C induced activation of NF-κB (data not shown).

DISCUSSION

We evaluated the effect of CysLT on expression and activity of TLR in MC. CysLTs, particularly LTC_4, downregulated several TLRs in HuMC in a PTX- and montelukast-sensitive manner. This suggests an involvement of G proteins and CysLT1R, a finding we corroborated since cells deficient in CysLT1R, but not CysLT2R, did not downregulate TLR2 after LTC_4 treatment, and HuMC cultured with LTC_4 show reduced TLR2 responses.

G protein-coupled (GPCRs) signaling via CysLTR may ultimately block activation of the pro-inflammatory transcription factor nuclear factor kappa B (NF-κB). Indeed, LTC_4 treatment made MC less responsive to LTA and LPS (TLR2 and TLR4 ligands) but not Pam3CSK4, PGN and polyI:C (TLR2 and TLR3 ligands). Abnormal TLR expression may contribute to the progression of some inflammatory diseases.

Other groups have also found that GPCR signaling modifies TLR-mediated *in vivo* immune responses: direct activation of heterotrimeric Gαq, Gα13 and Gαi proteins suppresses LPS-stimulated IL-12p40 production and impairs the T cell-activating ability of LPS-treated monocytes; CysLT1R stimulation can elicit responses through both PTX-sensitive (Gαi) and -insensitive G-proteins (Gαq, Gα11/12/13); in alveolar macrophages, LTD_4 activates CysLT1R through Gαq to enhance FcγR-mediated phagocytosis and microbicidal activity (12), whereas LTD_4-induced stress fiber formation in intestinal epithelial cells is mediated by Gαi and PTX-insensitive Gα12 proteins (13).

We reported that HuMC activation by substance P upregulates TLR2 expression and activity (14). Substance P signals partially through a GPCR, the neurokinin receptor (NK1R), but our data suggest it may also be NK1R-independent (15), which may explain why CysLT and substance P have divergent effects on TLR expression in HuMC.

ACKNOWLEDGEMENTS

We wish to thank Clayton MacDonald for his technical support with some of the assays described. This work was funded by an unrestricted investigator-initiated grant from Merck Frosst Canada, the Canadian Institutes of Health Research (grant number 125679) and the National Research Council of Canada.

REFERENCES

1. Boyce JA, Broide D, Matsumoto K, Bochner BS. Advances in mechanisms of asthma, allergy, and immunology in 2008. J Allergy Clin Immunol 2009; 123(3):569-74.

2. Mehrotra AK, Henderson WR, Jr. The role of leukotrienes in airway remodeling. Curr Molecr Med 2009; 9(3):383-91.
3. Nayak A, Langdon RB. Montelukast in the treatment of allergic rhinitis: an evidence-based review. Drugs 2007; 67(6):887-901.
4. Kulka M, Alexopoulou L, Flavell RA, Metcalfe DD. Activation of mast cells by double-stranded RNA: Evidence for activation through Toll-like receptor 3. J Allergy Clin Immunol 2004; 114(1):174-82.
5. Kulka M, Fukuishi N, Rottem M, Mekori YA, Metcalf D. Mast cells which interact with Escherichia coli upregulate genes associated with innate immunity and become less responsive to FcεRI-mediated activation. J Leukoc Biol 2006; 79(2):339-50.
6. Kirshenbaum AS, Swindle E, Kulka M, Wu Y, Metcalfe DD. Effect of Lipopolysaccharide (LPS) and Peptidoglycan (PGN) on human mast cell numbers, cytokine production, and protease composition. BMC Immunol 2008; 9(1):45.
7. Kim CK, Koh JY, Han TH, Kim do K, Kim BI, Koh YY. Increased levels of BAL cysteinyl leukotrienes in acute RSV bronchiolitis. Acta Paediatr 2006; 95(4):479-85.
8. Babolewska E, Witczak P, Pietrzak A, Brzezinska-Blaszczyk E. Different potency of bacterial antigens TLR2 and TLR4 ligands in stimulating mature mast cells to cysteinyl leukotriene synthesis. Microbiol Immunol 2012; 56(3):183-90.
9. Adner M, Starkhammar M, Georen SK, Dahlen SE, Cardell LO. Toll-like receptor (TLR) 7 decreases and TLR9 increases the airway responses in mice with established allergic inflammation. Eur J Pharmacol 2013; 718(1-3):544-51.
10. Mortaz E, Redegeld FA, Dunsmore K, Odoms K, Wong HR, Nijkamp FP, Engels F. Stimulation of cysteinyl leukotriene production in mast cells by heat shock and acetylsalicylic acid. Eur J Pharmacol 2007; 561(1-3):214-19.
11. Hildebrand D, Sahr A, Wolfle SJ, Heeg K, Kubatzky KF. Regulation of Toll-like receptor 4-mediated immune responses through Pasteurella multocida toxin-induced G protein signalling. Cell Comm Signal 2012; 10(1):22.
12. Peres CM, Aronoff DM, Serezani CH, Flamand N, Faccioli LH, Peters-Golden M. Specific leukotriene receptors couple to distinct G proteins to effect stimulation of alveolar macrophage host defense functions. J Immunol 2007; 179(8):5454-61.
13. Nielsen CK, Massoumi R, Sonnerlind M, Sjolander A. Leukotriene D4 activates distinct G-proteins in intestinal epithelial cells to regulate stress fibre formation and to generate intracellular Ca2+ mobilisation and ERK1/2 activation. Exp Cell Res 2005; 302(1):31-39.
14. Tancowny BP, Karpov V, Schleimer RP, Kulka M. Substance P primes lipoteichoic acid- and Pam3CysSerLys4-mediated activation of human mast cells by up-regulating Toll-like receptor 2. Immunology 2010; 131(2):220-30.
15. Kulka M, Sheen CH, Tancowny BP, Grammer LC, Schleimer RP. Neuropeptides activate human mast cell degranulation and chemokine production. Immunology 2008; 123(3):398-410.

STUDY ON PHYSIOLOGICAL AND PSYCHOLOGICAL COMPREHENSIVE NURSING OF ELDERLY TUMOR PATIENTS AFTER SURGERY

LM. ZHANG[1], HY. LI[2], B. LIU[3], MY. LI[3], XL. YAO[4] and YH. CHANG[3]

[1]Thyroid Surgery Department, Harbin Medical University Cancer Hospital, Harbin, China; [2]Nursing Department, Harbin Medical University Cancer Hospital, Harbin, China; [3]The First Department of Medical Oncology, Harbin Medical University Cancer Hospital, Harbin, China; [4]Endoscope Room, Harbin Medical University Cancer Hospital, Harbin, China

Received December 21, 2017 – Accepted March 12, 2013

The aim of this study is to formulate nursing schemes for elderly tumor patients after surgery according to their clinical characteristics, and give effective guidance for alleviating the patients' psychological anxiety. One hundred elderly tumor patients admitted to the oncology department of the Affiliated Cancer Hospital of Harbin Medical University were included and divided into an intervention group (50) and a control group (50). Nursing intervention was performed on the intervention group, and routine nursing was performed in the control group. One day before surgery, all the patients were asked to fill in a self-rating anxiety scale (SAS) and a self-rating depression scale (SDS), and their blood pressure and heart rate data were measured. After surgery, the patients were asked to fill in a form which investigated their pain degree, recovery situation and satisfaction degree. The heart rate and blood pressure of the patients in the intervention group recovered faster than those of the control group, with lower SAS and SDS scores and shorter recovery time. In conclusion, effective nursing intervention played a crucial role in the postoperative recovery of elderly tumor patients by reducing pain and anxiety degrees, which improved the patients' satisfaction with the nursing.

In recent years, the incidence of malignant tumors has been rising due to the unhealthy living means of modern people (1). With high mortality rates, malignant tumors have been taken as strong sources of stress by many (2). Once diagnosed with malignant tumors, people will show fear and anxiety, suffering a great physical and psychological blow. Berger et al. (3) found that cancer-related fatigue (CRF) was a painful symptom after surgery and chronic renal failure also affected the quality of life, and requires physical activity and psychosocial intervention. Zhu et al. (4) found that long-duration surgery could lead to hypoxemia, electrolyte imbalance and perioperative pain in elderly patients, and methods which could reduce the surgical harm to elderly patients should be sought. In recent decades, with the change of medical modes, modern nursing has established the "people-oriented" central idea (5). At present, nursing intervention has not yet been popularized in China and for elderly tumor patients after surgery this is particularly important. The general means of nursing intervention is psychological counseling, health education, music therapy, etc. (6).

Key words: elderly, malignant tumor, nursing intervention

Mailing address:
Yonghong Chang,
No.150 Ha Ping Road,
Nangang District, The First Department of Medical Oncology, Harbin Medical University Cancer Hospital,
Harbin,150040,China
e-mail: yonghchang@yeah.net

0393-974X (2018)

Scientific and reasonable nursing intervention can help reduce unhealthy emotions of patients. Through observing elderly subjects who had undergone gynecologic malignant tumor chemotherapy, Yuan et al. (7) found that positive mental intervention could reduce anxiety and maintain a stable psychological status. Luo et al. (8) also found that nursing intervention could significantly stabilize the emotion of elderly patients with acute coronary syndrome. Relying on the advanced medical technology of Harbin Medical University, Heilongjiang, China, 100 cases of elderly tumor patients were included in this study and divided into a nursing intervention group and a control group to compare the clinical indicators after surgery. This work aims to provide suggestions and guidance for clinical medical nursing in the future.

Patients with tumors all have negative performance physiologically and psychologically. Tumor and various treatment means will brings physiological discomfort which can cause pain, loss of appetite, sleep disorders and complications and psychological problems such as anxiety disorder and depression. Substantial evidence has shown that physiological discomfort can aggravate the physiological burden of patients and shorten the lifespan; depression can shorten 10~20% of the lifespan of tumor patients (9). Moreover, elderly patients have more severe physiological pain and mental discomfort compared to younger patients because of the weakened physical function and emotional state. Through investigation, Li et al. (10) found that elderly patients with rectal carcinoma had poorer quality of life (QOL), more complications and severe insomnia and inappetence compared to young patients. Elderly patients feel more anxious and upset regarding the disease and surgery because of their weaker understanding capability. Moreover, their postoperative recovery is also poor, which can aggravate their fear and anxiety. Multiple factors result in the decline of QOL of elderly patients. Scientific nursing intervention is greatly beneficial to the relief of negative emotion and improvement of QOL of these subjects.

MATERIALS AND METHODS

Study subjects

One hundred elderly tumor patients accepted by the oncology department of the First Affiliated Hospital of Harbin Medical University in 2017 were included. The inclusive criteria included patients aged 60-80 years who needed to undergo surgery, without any long-term chronic medical history or psychiatric history, with certain cognitive ability and understanding ability (Mini-mental State Examination (MMSE) scale result between 27 and 30), and signing the consent after being informed of the experimental procedures.

Preoperative preparation stage

Prior to surgery, all the patients were asked to fill in a self-rating anxiety scale (SAS) (11) and a self-rating depression scale (SDS) (12), including their blood pressure, blood sugar and heart rate measurements. The control group received conventional nursing (13) and were prepared for surgery by being given information of the operation. The intervention group received nursing described below.

Psychological aspect: The nursing staff communicated with the patients, listened patiently to the description of their feelings, and increased their recognition of diseases to make them believe in modern medical technologies in scientific ways. For patients with different degrees of cultural, different language patterns were used to illustrate the necessity, method and safety of the operation to reduce the stress reaction during surgery. As the operating room was unfamiliar to the patients, they could go into the operation room for visiting if available. If not, pictures of the operating room were shown to the patients to reduce their fear.

Physiological aspect: The patients were trained to control emotions by means of deep breathing and distraction.

Surgery stage

For the patients in the control group, the nursing staff greeted them at the door of the operating room, and after entering anesthesia and postural care were carried out. For the patients in the intervention group, the nursing staffs carried out the following actions.

Psychological aspect: The nursing staff explained the equipment in the operation room to the patients and smiled at them to relax and warm their hearts and make them feel safe and friendly. Moreover, they gave serious and scientific answers to the patients' questions to promote the

patients acceptance of the surgery in an optimistic manner. Before anesthesia, the nursing staffs talked about some topics which were of interest to the patients to distract their attention. Furthermore, the adverse reaction of anesthesia was explained to the patients in advance.

Physiological aspect: Sponge pads and other soft objects were used for position control to reduce skin contact surface and nerve damage and prevent the convex part to be compressed, to ensure the maximum comfort degree of the patients. Moreover, heat preservation and shielding measures were offered to relieve the discomfort and anxiety of the patients. The patients might experience cold or chills during the operation, in which case the nursing staff took heat preservation measures to relieve discomfort, such as adjusting the room temperature and providing a heating blanket.

Postoperative rehabilitation stage

For the patients in the control group, the nursing staff and the anesthetist accompanied them to the recovery room and informed them of the surgical instruments. For the patients in the intervention group, the nursing staff carried out the following actions the following work.

Psychological aspect: the patients were informed that

Table I. *Comparison of general data between the two groups.*

Group		Control group (n=50)		Interventional group (n=50)	
		Number of cases	%	Number of cases	%
Job	Cadre	16	32	15	30
	Worker	14	28	14	28
	Farmer	11	22	11	22
	Other	9	18	10	20
Educational level	Senior high school or higher	28	56	27	54
	Junior high school or higher	22	44	23	46
Economic condition	Good	13	26	12	24
	General	32	64	33	66
	Poor	5	10	5	10
Medical payment form	Public	32	64	29	58
	Self	18	36	21	42

the operation was successful to relieve feelings of panic. If the patients felt dizzy or sick, they were told that these are normal reactions after surgery. Frequent conversions were carried out with the patients on their topics of interest to ensure their rehabilitation in a happy atmosphere (14).

Physiological aspect: Nursing staff should pay attention to the patients' warmth to avoid symptoms such as cold and fever. The patients were encouraged to do stretching exercises within their scope. They cooperated with family members to carry out postoperative nursing and rehabilitation training of the patients, observed the rehabilitation status of the patients at all times, and gave corresponding guidance. The patients were provided with comfort rest environment and guided to take a comfortable

Table II. *Comparison of blood pressure and heart rate between the two groups.*

Heart rate ($\bar{x} \pm s$, times/min)			Blood pressure ($\bar{x} \pm s$, mmHg)			
			systolic pressure		diastolic pressure	
	Before intervention	After intervention	Before intervention	After intervention	Before intervention	After intervention
Intervention group	80.2±10.7	77.3±10.6 (*)	130.2±10.4	125.7±9.3 (*)	78.4±10.7	70.6±10.2 (*)
Control group	80.5±10.2	83.4±10.2 (*)	131.5±11.1	135.9±10.3 (*)	78.9±10.1	81.3±10.1 (*)

** statistically significant, P <0.05.*

Table III. *Comparison of the SAS and SDS scores between the two groups.*

SAS ($\bar{x} \pm s$, point)			SDS ($\bar{x} \pm s$, point)		
	Before intervention	After intervention		Before intervention	After intervention
Intervention group	43.1±5.3	33.5±5.1(*)	Intervention group	47.9±5.2	36.3±5.3(*)
Control group	43.2±4.8	45.2±4.8(*)	Control group	47.6±4.9	48.2±5.1(*)

** statistically significant, P <0.05.*

Table IV. *Comparison of the infection rate between the two groups.*

	Cases of infection	Infection rate	χ^2 value	P value
Intervention group (n=50)	1	2%	14.242	0.005
Control group (n=50)	2	4%		

position. Moreover, the nursing staff made the effort to distract the attentions of patients with pain.

Observation indicators

SAS and SDS forms were used to test the mental state of the patients in both groups, for analysis. Living quality evaluation forms were used to evaluate the QOL of the patients according to their cognitive ability, mental function and health status. Sleeping quality, QOL and social support were compared between the two groups.

In order to ensure the authenticity and reliability of the data, the contents of the questionnaires were kept strictly confidential, and the patients completed the questionnaire within the prescribed time without being instructed. According to the above criteria, 100 questionnaires were issued and 100 questionnaires were recovered. The recovery rate was 100%. But within the 100 questionnaires recovered, some were with incomplete answers or substandard answers, which were ineffective and excluded. Hence, the total effective questionnaire number was 92, with 46 for each group and an effective rate of 92%.

Statistical analysis

The Excel database of the SPSS13.0 system software was used to analyze data. The collected general data of the patients was compared between the two groups. The χ^2 test was used for postoperative data, while independent-samples *t*-test was used for other data.

RESULTS

Among the included 100 elderly tumor patients, the oldest was 76 years old while the youngest was 62 years old. The average age of the intervention group was 71.25 years while that of the control group was 70.3 years and there were no significant differences between the two groups.

No apparent difference was observed in the general data of the two groups such as job, educational level, economic condition and medical payment form, as shown in Table I.

Blood pressure and heart rate

Before intervention, the blood pressure and heart rate of the two groups showed no statistically remarkable differences. After intervention, there were significant differences in the blood pressure and heart rate between the two groups, as shown in Table II.

The heart rate, systolic blood pressure and diastolic blood pressure of the intervention group declined to 77.3±10.6, 125.7±9.3 and 125.7±9.3, respectively, after nursing intervention, which was more beneficial for surgery and postoperative recovery. The heart rate and blood pressure of patients who were not given nursing intervention were increased, indicating high mental pressure of those patients. Thus, it could be concluded that nursing intervention could effectively control stable preoperative blood pressure and heart rate before surgery and restore normal body condition more rapidly after surgery.

Besides the heart rate and blood pressure, other vital signs of the intervention group, such as breathing, body temperature and pulse, were also more stable than those of the control group, indicating that nursing intervention could stabilize vital signs of patients and facilitate postoperative recovery.

Depression and anxiety degree

Before intervention, there were no statistical differences in the SAS and SDS scores between the two groups. After intervention, the SAS and SDS scores of the intervention group were significantly lower than those of the control group, as shown in Table III.

Table III shows that the depression and anxiety conditions of the two groups were similar before intervention, but in the intervention group were relieved after intervention, and the difference between the two groups were significant ($P < 0.05$). It can therefore be concluded that nursing intervention could effectively relieve the anxious and depressive emotions of the patients.

Infection rate between the two groups

The observation of the postoperative incision infection suggested that the incision infection rate of the intervention group was 2%, much lower than that of the control group ($\chi^2=14.242$, $P < 0.05$).

Postoperative recovery conditions

After surgery, the time period before the patients could sit, stand up and do activities were recorded, as shown in Fig. 1.

As shown in Fig. 1, there was statistical significance in each item between the two groups. Nursing intervention was helpful to the incision healing of the patients and could shorten hospital stay. The patients who received comprehensive nursing intervention could sit up less than 2 days after nursing, stand up less than 3 days after nursing, and do activity less than 4 days after nursing, indicating better outcomes than patients in the control group.

Comparison of sleeping quality between the two groups

The sleeping quality of patients in the two groups was evaluated using the Pittsburgh Sleep Quality Index (PSQI), and the statistical results are shown in Fig. 2. There was a remarkable difference between the two groups ($P < 0.05$).

The value of PSQI was between 0 and 21. Higher score indicated poorer sleeping quality. It was found that the value of PSQI of the intervention group was lower than that of the control group (5.1 *vs* 7.8), and the difference was significant ($p < 0.05$). It revealed that nursing intervention could improve sleeping quality and promote postoperative recovery.

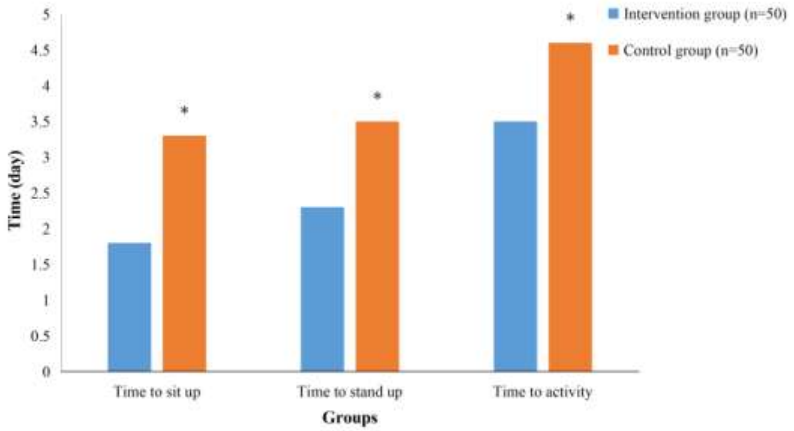

Fig. 1. *Comparison of postoperative recovery time between the two groups.*

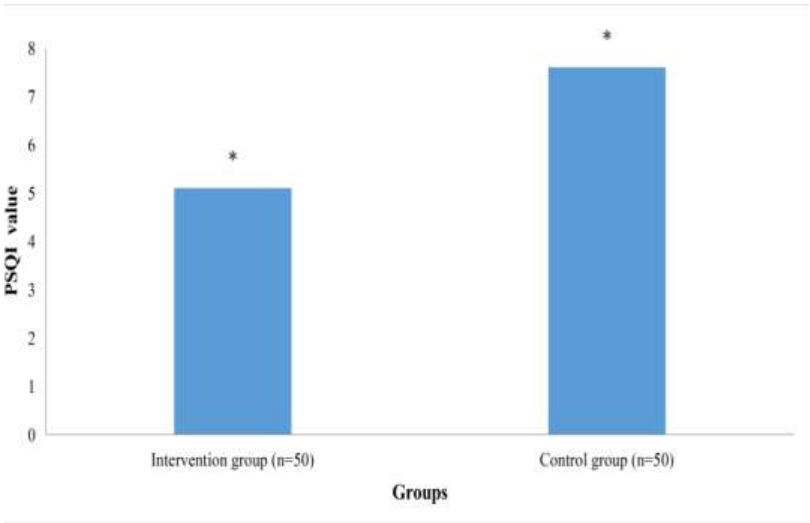

Fig. 2. *Comparison of sleeping quality between the two groups*

Comparison of QOL between the two groups

EORTC QOL-C30 (European Organization for Research and Treatment of Cancer, Quality of Life Questionnaire-Core 30) suggested that the two groups had significant differences in scores for emotional function (EF), cognitive function (CF), social function (SF) and quality of life 2 (QOL 2) (Fig. 3).

As shown n Fig. 3, all the scores of the intervention group were higher than those of the control group, indicating that nursing intervention relieved negative emotions such as anxiety and depression, improved sleeping quality, and significantly enhanced QOL.

Comparison of social support between the two groups

Social support rating scale was used to evaluate the social support quality of patients in the two groups. It was found that the scores of social support, subjective support and social availability of the intervention group were higher than those of the control group, and the total score of the intervention group was also higher than that of the control group (45 *vs* 39) (Fig. 4).

DISCUSSION

As the physiological functions of the organs

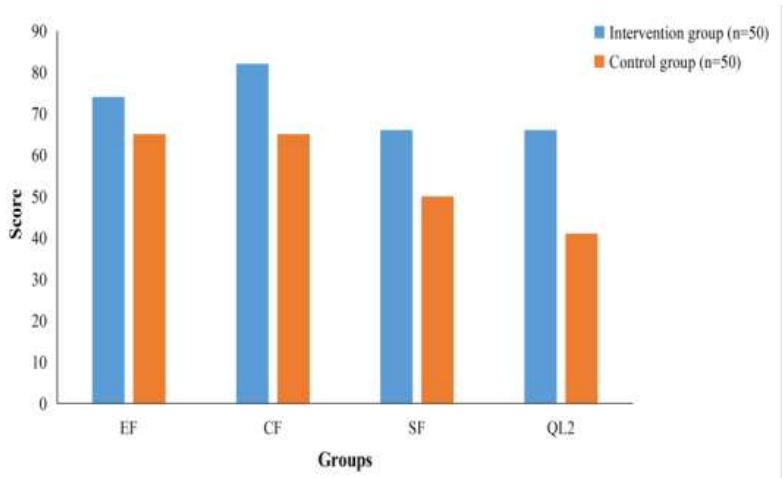

Fig. 3. *Comparison of QOL between the two groups*

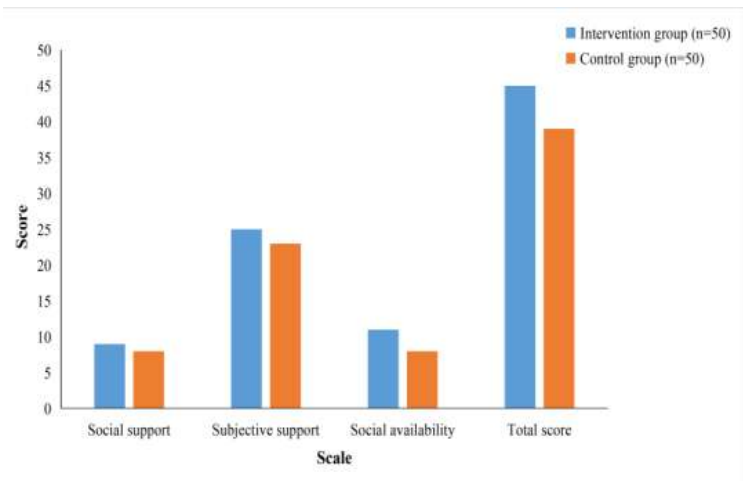

Fig. 4. *Comparison of social support between the two groups.*

of elderly patients are degenerated, they tire more easily during surgery and are more intolerable to the operation, which increases the risks of surgery. Nevertheless, the biggest safety hazards in elderly subjects undergoing surgery are some chronic geriatric diseases such as hypertension and diabetes (16). Though the surgical safety rate of elderly patients increases with the improvement of medical technologies, it is still lower than that of young patients (17).

As elderly patients were not familiar with the disease-related knowledge, they suffered mental changes after hospitalization, with their SAS and SDS scores obviously higher than the normal level. It was found that the anxiety and depression degrees of the patients in the intervention group decreased significantly after intervention nursing was given. Patients in the intervention group had a good understanding of their own condition, disease and surgery, which relieved anxiety. Moreover, the comfort and care during surgery also established a good trust relationship between the patients and hospitals; as a result, the patients showed high acceptance to the surgery. In the postoperative nursing, the patients had positive expectation for recovery and less anxiety and depression, which was beneficial to recovery. However, patients in the control group had insufficient understanding of the disease, intense fear and were severely upset before and during surgery and, moreover, were not positive after surgery.

Social support is considered to be a buffer factor of social psychological stimulation (18), which can maintain the good mood of people and is particularly effective in the treatment of cancer patients. Social support is divided into three categories: objective, subjective and utilization. Through the study, it was found that both the groups obtained social support after surgery, but the social support of the intervention group was larger than the control group because they were informed of their disease condition, the hospital condition and surgical schemes before the operation which enabled them to actively cooperate with the treatment.

In conclusion, nursing intervention could relieve the anxiety and depression of elderly patients and recover their blood pressure and heart rate to normal levels. Also, nursing intervention promoted the postoperative recovery of the patients and increased their satisfaction degree on the nursing carried out. Nevertheless, there are drawbacks in this study, for example, the small sample size, which may lead to the deviation of the experimental results, which should be improved in future studies.

ACKNOWLEDGEMENTS

This work was supported by the Health Department Foundation of Heilongjiang Province (2016-090).

REFERENCES

1. Liu P, Zhang SY, Chen XF. Analysis on the incidence of malignant tumors in Zhangjiagang city, during 2006~2009. Jiangsu J Preventive Med 2011; 1358(260):33-36.
2. Mulligan EA, Schuster Wachen J, Naik AD, Gosian J, Moye J. Cancer as a criterion a traumatic stressor for veterans: Prevalence and correlates. Psychol Trauma-US 2014; 6(Suppl 1):S73.
3. Berger AM, Gerber LH, Mayer DK. Cancer-related fatigue: implications for breast cancer survivors. Cancer 2012; 118(8 Suppl):2261.
4. Zhu L, Liu YS, Shen Y, Xia B. The risk factors of postoperative delirium in elderly tumor surgical patients after general anesthesia. J Clinic Anesthesiol 2013; 29(10):948-50.
5. Rushton CA, Satchithananda DK, Kadam UT. Comorbidity in modern nursing: a closer look at heart failure. Br J Nurs 2011; 20(5):280.
6. Lamet AR, Sonshine R, Walsh SM, Molnar D, Rafalko S. A pilot study of a creative bonding intervention to promote nursing students' attitudes towards taking care of older people. Nurs Res Pract 2011; (1):537634.
7. Yuan X, Cui M. Effect of psychological intervention and health instruction on negative emotions of senile patients with gynecological malignant tumor chemotherapy. Chin J Pract Nerv Dis 2014; 8:34-36.
8. Luo T, Liu L Y, Zhang JM. Clinical effect of nursing intervention for senile acute coronary syndrome

patient. Chin J Mod Drug Appl 2015; 8:177-78.
9. Montgomery K L, Kim J S, Franklin C. Acceptance and commitment therapy for psychological and physiological illnesses: a systematic review for social workers. Health Soc Work 2011; 36(3):169-81.
10. Li K, Li JP, Huang MJ, Zhang R, Hu YJ. Quality of life of elderly Chinese rectal cancer patients after preventative anal surgery: a cohort study. Hepato-gastroenterol 2013; 60(126):1376-82.
11. Samakouri M, Bouhos G, Kadoglou M, Giantzelidou A, Tsolaki K, Livaditis M. Standardization of the Greek version of Zung's Self-rating Anxiety Scale (SAS). Psychiatrike 2012; 23(3):212.
12. Chagas MH, Tumas V, Loureiro SR, et al. Validity of a Brazilian version of the Zung self-rating depression scale for screening of depression in patients with Parkinson's disease. Parkinsonism Relat D 2010; 16(1):42-45.
13. Saleh BS, Nusair H, Al ZN, AJ SS, Saleh U. The nursing rounds system: effect of patient's call light use, bed sores, fall and satisfaction level. Int J Nurs Pract 2013; 19(1):299.
14. Söderström L, Thors AE, Rosenblad A, Frid H, Saletti A, Bergkvist L. Mealtime habits and meal provision are associated with malnutrition among elderly patients admitted to hospital. Clin Nutr 2013; 32(2):281-88.
15. Schuemie MJ, Ryan PB, Dumouchel W, Suchard MA, Madign D. Interpreting observational studies: why empirical calibration is needed to correct p-values. Stat Med 2014; 33(2):209-18.
16. Tolone S, Docimo G, Del GG, et al. Long term quality of life after laparoscopic antireflux surgery for the elderly. Bmc Surg 2013; 13(S2):S10.
17. Martén E, Langevin C J, Kaswan S, et al. The safety of rhytidectomy in the elderly. Plast Reconstr Surg 2011; 127(6):2455.
18. Bender IB, Seltzer S, Soltanoff W. Rapid heartbeat, but dry palms: reactions of heart rate and skin conductance levels to social rejection. Front Psychol 2014; 5(3):956.

LONG NON-CODING RNA SNHG16 CONTRIBUTES TO GLIOMA MALIGNANCY BY COMPETITIVELY BINDING miR-20a-5p WITH E2F1

B-Y. YANG[1], Q. MENG[2], Y. SUN[2], L. GAO[2] and J-X. YANG[3]

[1]Department of Neurosurgery, 999 Brain Hospital of Guang Dong, Guang Zhou, China;
[2]Department of Neurosurgery, Tangdu Hospital, Fourth Military Medical University, Xi'an, China;
[3]Department of Neurosurgery, The Second People Hospital of Xin Xiang, Xin Xiang, China

Received August 1, 2017 – Accepted December 20, 2017

The first three Authors contributed equally to this work

Glioma is among the most fatal and highly aggressive primary malignant tumors in the central nervous system. Small nucleolar RNA host gene 16 (SNHG16) is identified to play an oncogenic role in several cancers. However, the exact mechanism of SNHG16 action in the regulation of glioma development remains unknown. LncRNA SNHG16 was increased in glioma tissues and cells compared with normal brain tissues and cells. SNHG16 expression was correlated with the malignancy and poor prognosis of glioma patients. SNHG16 and E2F1 contained a binding site of miR-20a-5p. miR-20a-5p was decreased in glioma tissues and cells compared with normal brain tissues and cells. Downregulation of miR-20a-5p was correlated with the malignancy and poor prognosis of glioma patients. In glioma tissues, the expression of SNHG16 was negatively correlated with miR-20a-5p. Downregulation of SNHG16 increased miR-20a-5p expression. miR-20a-5p mimic reduced the luciferase activity of SNHG16 and E2F1; miR-20a-5p mimic enhanced the inhibition of cell proliferation, invasion, migration, and EMT, and increase of apoptosis induced by SNHG16 knockdown. Anti-miR-20a-5p reversed the effects of shSNHG16. We also found that SNHG16 may act as a ceRNA for miR-20a-5p, enhancing the expression of E2F1. Additionally, knockdown of SNHG16 remarkably reduced the increase of tumor volumes in xenograft mouse models. In tumor tissues, knockdown of SNHG16 increased the expression of miR-20a-5p, reduced EMT and increased apoptosis. In conclusion, SNHG16 promotes glioma tumorigenesis by sponging miR-20a-5p, leading to the enhancement of its endogenous targets E2F1. The data provides a new clue for the role of SNHG16/miR-20a-5p/E2F1 in the development of glioma.

Glioma is among the most fatal and highly aggressive primary malignant tumors in the central nervous system (1). Even with advancement in treatment with surgical resection in combination with radiation therapy and chemotherapy, the prognosis for patients with malignant glioma remains poor. Because of the extremely high proliferation and invasiveness, the cumulative 1-year survival rate of glioma patients is less than 30%, and glioma patients usually have a median survival of approximately 12-15 months (2). The molecular determinants of glioma development and aggressiveness are not adequately defined. A better understanding of the molecular pathogenesis of glioma may identify new

Key words: glioma, LncRNA SNHG16, miR-20a-5p, proliferation, invasion, migration

Mailing address:
Dr Ji-Xue Yang,
Department of Neurosurgery,
The Second People Hospital of Xin Xiang,
Xin Xiang 453003, China
Tel.: +86 13837322427

0393-974X (2018)

biomarkers of prognosis and targets for treatment.

In recent years, the development of techniques in RNA sequencing and high-throughput transcriptome identified a large amount of noncoding RNAs (ncRNAs) (3, 4). Several studies have proved that these ncRNAs are not junk in the cell and play a variety of biological roles, including regulation of cancer development (3, 4). Long non-coding RNAs (LncRNAs), greater than 200 nt in length, are a category of noncoding RNAs without protein-coding capability (5). The role of LncRNAs in cancer regulation has been confirmed to be in prevalent cancer types (6). Small nucleolar RNA host gene 16 (SNHG16) is an LncRNA that has been identified to play an oncogenic role in colorectal cancer (7), neuroblastoma (8), breast cancer (9), lung adenocarcinoma (10) and bladder cancer (11). However, the role of LncRNA SNHG16 in glioma still remains elusive.

In the current study, we investigated how SNHG16 contributed to the progression of glioma and explored the underlying mechanisms. We found that SNHG16 functioned as an oncogenic molecule in glioma and microRNA-20a-5p was the target of SNHG16 that mediated its oncogenic function. SNHG16 completely competitively bound miR-20a-5p with E2F transcription factor 1 (E2F1). These findings indicate that the SNHG16/miR-20a-5p/E2F1 interaction is important for the development and progression of glioma and provides new candidates for glioma treatment.

MATERIALS AND METHODS

Patients and tissue specimens

This study was approved by the Ethics Committee of Tangdu Hospital, Fourth Military Medical University. A total of 76 glioma specimens were obtained from astrocytoma patients (WHO grade I tumours, 15; grade II, 20; grade III, 19; and grade IV, 22) from Tangdu Hospital, Fourth Military Medical University between November 2015 and March 2017. Twelve normal brain tissues from age- and gender-matched patients with cerebral trauma or cerebral hemorrhage were used as normal controls. Before the surgical resection, the patients had undergone no chemotherapy or radiation therapy. Informed consent was given by all the patients. Immediately after surgery, we collected the glioma tissues and tissue samples were stored in liquid nitrogen for the examination of RNA expression. Two independent experienced clinical pathologists performed the pathological diagnosis according to the WHO classification. From the date of surgical resection, all the patients were followed-up for 60 months. Overall survival (OS) was defined as the length of time between surgery and death or the last follow-up examination (if death did not occur).

Cell culture and transfection

The cell lines, including human glioma cell lines (U87, U251, LN229 and T98G) and human brain astrocytes (HEB cell) were purchased from the American Type Culture Collection (ATCC, Rockville, MD, USA). Cells were cultured in Dulbecco's Modified Eagle's Medium (DMEM; Gibco, Rockville, MD, USA) supplemented with 10% fetal bovine serum (FBS; Gibco, Rockville, MD, USA), 100 U/ml penicillin and 100 mg/ml streptomycin in a humidified incubator at 37°C with 5% CO_2. The shNC, shSNHG16, miR-20a-5p mimic and inhibitor and their respective negative control RNAs were provided by Ribobio Biotechnology (Guangzhou, China). U87 and LN229 cells were transfected with shNC, shSNHG16, miR-20a-5p mimic, NC-mimic, anti-miR-20a-5p, and anti-NC using lipofectamine 2000 reagent (Invitrogen, Carlsbad, CA, USA).

Cell proliferation

Cell proliferation was determined using Cell Counting Kit-8 kit (CCK-8; Beyotime, Shanghai, China). Briefly, after the treatment, a volume of 10 µl CCK-8 solution in 100 µl serum-free medium was added into each well. Cells were then incubated at 37°C for 2 h and the absorbance at 450 nM was detected using a microplate reader (Synergy 4; BioTek, Winooski, VT, USA). The experiment was performed repeatedly and individually thrice.

Apoptosis

Apoptosis was determined by TUNEL staining using TUNEL fluorescence FITC kit (Roche, Basel, Switzerland). Briefly, after the treatment, cells were fixed with 4% paraformaldehyde and permeabilized with 0.1% Triton X-100. After that, samples were incubated with TUNEL reaction mixture at 37°C for 1 h. After

washing with PBS, cells were analyzed using FACScan flow cytometer (Becton-Dickinson Biosciences, USA) and percentage of TUNEL-stained apoptotic cells was recorded. The experiment was performed repeatedly and individually thrice.

Invasion and migration assays

Transwell assay was used to evaluate invasion ability by the use of a 24-well plate with Transwell chamber inserts (8 mm pore size, Corning, USA) precoated with Matrigel (BD Biosciences, USA). In brief, 700 µl media supplemented with 20% FBS was added to the lower chamber. 1×10^5 cells in 100 µl serum-free DMEM medium were seeded in the upper chamber. After 24 h of incubation, cells remaining in the upper surface of the membranes were removed with cotton buds. Cells migrated to the underside of the chamber were fixed with 4% paraformaldehyde for 0.5 h and stained with crystal violet. The cells adhering to the lower surface of the membrane were counted under a light microscope (Olympus, Japan) in six random fields. The experiment was performed repeatedly and individually thrice.

The wounding healing assay was conducted to evaluate migration ability. In brief, cells were cultured in a 24-well chamber and grown to confluence. Then, the confluent cell monolayer was scraped with a pipette tip. Washing was conducted to remove detached and damaged cells. After 24 h of incubation, cell migration was observed using a light microscope (Olympus, Japan). The experiment was performed repeatedly and individually thrice.

Quantitative real-time PCR

Total RNA was extracted using miRNeasy mini kit (Qiagen, Hilden, Germany). cDNA was synthesized from total RNA using High-Capacity cDNA Reverse Transcription Kit (Applied Biosystems, Foster City, CA, USA). Quantitative real-time polymerase chain reaction (PCR) was performed using SYBR green Premix Ex Taq II (Takara) on an ABI PRISM 7500 real-time PCR system (Applied Biosystems, Foster City, CA, USA). GAPDH was used as the endogenous control for detection of mRNA expression level, while U6 was used as endogenous control for miRNA expression analysis. Data were collected and analyzed using $2^{-\Delta\Delta Ct}$ method for quantification of the relative mRNA expression levels. The experiment was performed repeatedly and individually thrice. Relative expression of target gene was expressed as fold change with control set to 1.

Luciferase reporter assay

pGL3-SNHG16 (SNHG16-WT) and pGL3-E2F1 (E2F1-WT) were generated by insertion of the SNHG16 or E2F1 cDNA fragment containing the predicted potential miR-20a-5p binding sites into the pGL3-Basic luciferase reporter vector (Promega, Madison, WI, USA). pGL3-SNHG16 MUT (SNHG16-MUT) and pGL3-E2F1 MUT (E2F1- MUT) were generated by mutation of the potential miR-20a-5p binding sites. Luciferase activity was determined using the Dual-luciferase reporter assay system (Promega, Madison, WI, USA). Briefly, cells were co-transfected with 100 ng of the constructs (SNHG16-WT, or SNHG16-MUT; E2F1-WT, or E2F1-MUT) and 30 ng miR-20a-5p mimic or NC-mimic lipofectamine 2000 reagent (Invitrogen, Carlsbad, CA, USA). After 48 h of incubation, the relative luciferase activity was normalized to the Renilla luciferase activity according to the manufacturer's instructions. The experiment was performed repeatedly and individually thrice.

RNA immunoprecipitation (RIP) assay

RIP was conducted to evaluate the interaction between SNHG16 and E2F1 mRNA using an EZ-Magna RIP RNA-Binding Protein Immunoprecipitation Kit (Millipore, Billerica, MA, USA). Briefly, cells stably transfected with shSNHG16 or shNC were lysed by RIP lysis buffer. Then, cell lysates were incubated with RIP buffer containing human anti-Ago2 antibody (Millipore)-conjugated magnetic beads. Normal mouse IgG (Millipore) was used as a negative control. Protein from samples was digested by proteinase K buffer and then immunoprecipitated RNA was isolated. Purified RNA was analyzed by real-time PCR to detect the expression of SNHG16 and E2F1. The experiment was performed repeatedly and individually thrice.

In vivo nude mouse models

Animal experiments were approved by the animal experimental committee of Tangdu Hospital, Fourth Military Medical University. Male 5-6-week-old BALB/C nude mice (16-18g) were purchased from the Animal Center of Fourth Military Medical University. Briefly, the nude mice were subcutaneously transplanted with 4×10^6

U87 cells which were stably transfected with shSNHG16 and shNC. Mice were allowed to carry the tumor for 40 days and tumor growth in mice was monitored using a vernier caliper. Tumor volume (mm^3) was determined by the equation: length×width^2/2. At the end of the experiment, mice were sacrificed and tumor tissues were collected for further examination.

Statistical analysis

Data were expressed as mean ± SD of three independent experiments and statistical analyses were performed using GraphPad Prism (version 5.0). Student's *t*-test and one-way analysis of variance (ANOVA) were conducted for either two or multiple group statistical analysis. Correlations were analyzed using Pearson correlation coefficient. OS was analyzed using Kaplan-Meier method. $P < 0.05$ was considered to be statistically significant.

RESULTS

Upregulation of LncRNA SNHG16 is associated with poor prognosis of glioma patients

The expression level of LncRNA SNHG16 in normal brain tissues and glioma tissues was examined. SNHG16 expression level was significantly increased in glioma tissues, compared with that in normal brain tissues (Fig. 1A). Moreover, differential expression of SNHG16 in low-grade (I–II) and high-grade (III–IV) glioma tissues was examined. We found that the expression of SNHG16 in samples of high-grade glioma was markedly increased compared with that in low-grade samples (Fig. 1B). SNHG16 expression in glioma cell lines, including T98G, U87, U251 and LN229 cells, was notably higher than that in human brain astrocyte, HEB cells (Fig. 1C). Furthermore, high SNHG16 expression resulted in a shorter OS time than those with low SNHG16 expression (Fig. 1D).

SNHG16 is a target of miR-20a-5p

Bioinformatics analysis was performed using Starbase v2.0 to predict a binding site in SNHG16 by miR-20a-5p (Fig. 2A). U87 and LN229 cells were transfected with shRNAs of SNHG16 to knock down the expression of SNHG16 (Fig. 2, B and C). Downregualtion of SNHG16 resulted in a significant increase of miR-20a-5p expression in U87 and LN229 cells (Fig. 2, D and E). miR-20a-5p mimic markedly decreased the luciferase activity of SNHG16-WT (Fig. 2, F and G), whereas miR-20a-5p mimic did not affect the luciferase activity of SNHG16-MUT (Fig. 2, F and G). The results indicate that SNHG16 acted as a molecular sponge for miR-20a-5p.

Downregulation of miR-20a-5p is associated with poor prognosis of glioma patients

The expression level of miR-20a-5p in normal brain tissues and glioma tissues was examined. miR-20a-5p expression level was significantly decreased in glioma tissues, compared with that in normal brain tissues (Fig. 3A). Moreover, differential expression of miR-20a-5p in low-grade (I–II) and high-grade (III–IV) glioma tissues was examined. We found that the expression of miR-20a-5p in samples of high-grade glioma was markedly decreased compared with that in samples of low-grade (Fig. 3B). miR-20a-5p expression in glioma cell lines, including T98G, U87, U251 and LN229 cells, was notably lower than that in HEB cells (Fig. 3C). Furthermore, low miR-20a-5p expression contributed to a shorter OS time than those with high miR-20a-5p expression (Fig. 3D). Furthermore, the expression of SNHG16 and miR-20a-5p in glioma tissues was negatively correlated (Fig. 3E).

SNHG16 enhances glioma malignancy through regulation of miR-20a-5p

There is a possible role of SNHG16 and miR-20a-5p in glioma cell proliferation, apoptosis, invasion, migration and epithelial-mesenchymal transition (EMT) in U87 and LN229 cells. Cells were co-transfected with shSNHG16 and miR-20a-5p mimics or inhibitors or their negative controls. Downregulation of SNHG16 markedly decreased cell proliferation (Fig. 4, A and B) and increased apoptosis in U87 and LN229 cells (Fig. 4, C and D). Moreover, downregulation of SNHG16 resulted in a significant increase of caspase 3 activity in U87 and LN229 cells (Fig. 4, E and F). Furthermore, Transwell and wound healing assays were conducted to evaluate the invasion and migration capability. As shown in Fig. 5, A

and B, downregulation of SNHG16 resulted in a significant decrease of the number of invaded cells. In addition, downregulation of SNHG16 reduced the distance of cell migration in wound healing assay (Fig. 5, C and D). Moreover, downregulation of SNHG16 decreased the expression of N-cadherin (Fig. 5, E and F) and Vimentin (Fig. 5, G and H). miR-20a-5p mimic promoted the effect of SNHG16 on cell proliferation, apoptosis, invasion, migration and EMT in U87 and LN229 cells (Figs. 4 and 5). In contrast, miR-20a-5p inhibitor inhibited the effect of SNHG16 on cell proliferation, apoptosis, invasion, migration and EMT in U87 and LN229 cells (Figs. 4 and 5). Moreover, treatment of miR-20a-5p alone decreased cell proliferation (Fig. 6, A and B), increased apoptosis (Fig. 6, C and D), and decreased invasion (Fig. 6, E and F) and migration (Fig. 6, G and H) ability in U87 and LN229 cells. These results indicated that SNHG16 regulated the glioma cell malignancy by modulating miR-20a-5p expression.

SNHG16 is predicted to be ceRNA of E2F1 by directly binding miR-20a-5p

Using bioinformatics analysis, we found predicted binding site of miR-20a-5p in E2F1 (Fig. 7A). miR-20a-5p mimic significantly reduced the expression of E2F1 in U87 and LN229 cells (Fig. 7, B and C). miR-20a-5p mimic markedly decreased the luciferase activity of E2F1-WT (Fig. 7, D and E), whereas miR-20a-5p mimic did not affect the luciferase activity of E2F1-MUT (Fig. 7, D and E). To investigate whether SNHG16 can act as a ceRNA for E2F1 by mediating miR-20a-5p in glioma, we performed a RIP assay on Ago2. Downregulation of SNHG16 in U87 and LN229 cells decreased the enrichment of Ago2 on SNHG16 but remarkably increased the enrichment on E2F1 (Fig. 7, F and G). Furthermore, knockdown of SNHG16 decreased the mRNA expression of E2F1, which could be further suppressed by co-transfection with miR-20a-5p mimic, but abolished by co-transfection with anti-miR-20a-5p (Fig. 7, H and I). In general, these data indicate that SNHG16 functions as a ceRNA to regulate E2F1 expression by sponging miR-20a-5p.

SNHG16 facilitates glioma tumor growth in xenograft mice

In order to evaluate the role of SNHG16 in glioma *in vivo*, xenograft mouse model was established. As shown in Fig. 8A, downregulation of SNHG16 resulted in a significant reduction of tumor growth in nude mice. In addition, downregulation of SNHG16 increased miR-20a-5p expression (Fig. 8B), decreased the expression of E2F1 (Fig. 8C), N-cadherin (Fig. 8D), Vimentin (Fig. 8E), Cyclin D1 (Fig. 8F), and Ki67 (Fig. 8G) in tumor tissues in mice. Moreover, downregulation of SNHG16 increased Bax expression (Fig. 8H) and reduced Bcl-2 expression (Fig. 8I) in transplanted tumors. The findings indicated that SNHG16 was required for glioma tumor growth in xenograft mice.

DISCUSSION

Emerging evidence has suggested that dysregulation of LncRNAs is believed to be associated with cancer development and progression, including metastasis, radio- and chemo-therapy resistance, apoptosis, and epigenetic regulation of tumor biology (12-15). LncRNAs could function as biomarkers for the early diagnosis and prediction of prognosis, and key targets for early treatment. SNHG16 has been identified to play an oncogenic role in colorectal cancer (7), neuroblastoma (8), breast cancer (9), lung adenocarcinoma (10) and bladder cancer (11). In this study, we detected the SNHG16 transcripts in human glioma tissues and revealed higher expression levels in glioma tissues compared with the normal controls. The findings also revealed that SNHG16 was correlated with the increase of pathological degree and poor prognosis in glioma. Furthermore, knockdown of SNHG16 resulted in a significant decrease of glioma cell proliferation, increase of apoptosis, reduction of invasion and migration, and decrease of EMT. These data suggested an oncogenic role of SNHG16 in glioma.

In this study, bioinformatics analysis showed that SNHG16 contains one conserved target site for miR-20a-5p, and downregulation of SNHG16 led to the increase of miR-20a-5p expression. Numerous studies have reported the regulatory role of miR-

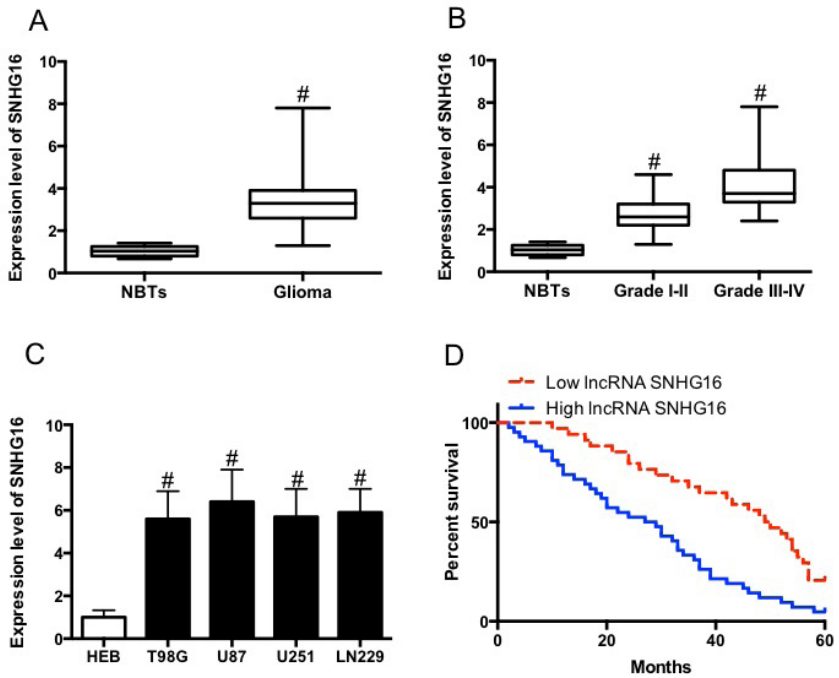

Fig. 1. *Upregulation of LncRNA SNHG16 expression is correlated with poor prognosis in glioma patients. **A**) SNHG16 expression in 12 normal brain tissues and 76 human glioma tissues were measured by qRT-PCR. **B**) SNHG16 expression in low-grade (I–II) (35) and high-grade (III–IV) (41) glioma tissues. **C**) SNHG16 expression in normal brain and four glioma cell lines as determined by qRT-PCR. Relative expression of target gene was expressed as fold change with control set to 1. **D**) The patients with glioma were divided into SNHG16 high-expression and low-expression groups, and Kaplan–Meier analysis was performed to evaluate the relationship of SNHG16 expression level with prognosis of glioma patients. #p<0.05, compared with control.*

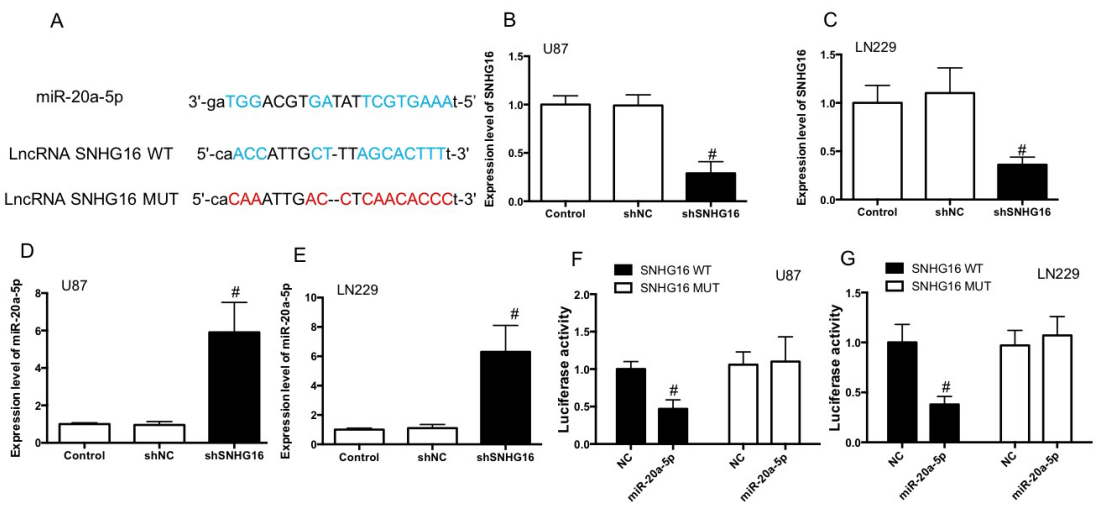

Fig. 2. *SNHG16 is a target of miR-20a-5p. **A**) The predicted binding sites of miR-20a-5p in SNHG16 (SNHG16-WT) and SNHG16 mutant (SNHG16-MUT) sequences. **B, C**) SNHG16 expression was analyzed by real-time PCR after knockdown of SNHG16 in U87 and LN229 cells. **D**, **E**) miR-20a-5p expression was detected in U87 and LN229 cells after the transfection of shSNHG16. Relative expression of target gene was expressed as fold change with control set to 1. **F**, **G**) Luciferase activity was determined in U87 and LN229 cells co-transfected with miR-20a-5p mimic or NC-mimic and pGL3 luciferase reporters containing SNHG16-WT or SNHG16-MUT sequences. #p<0.05, compared with control.*

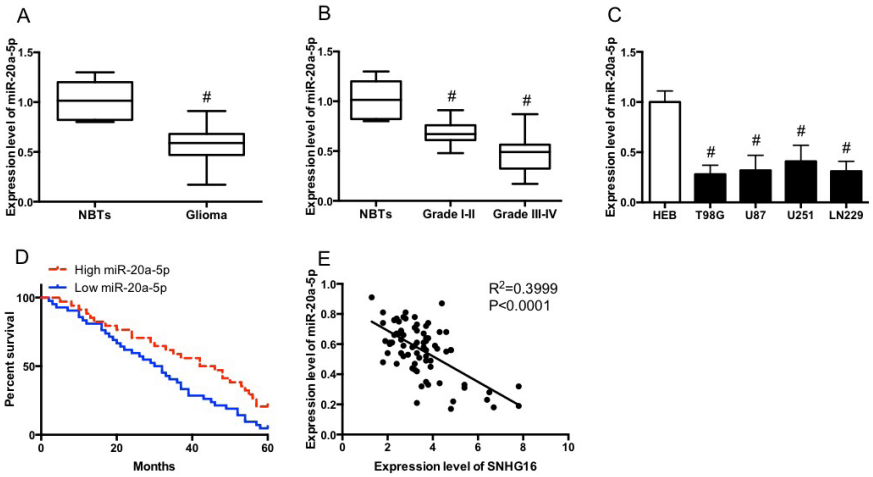

Fig. 3. *Downregulation of miR-20a-5p expression is correlated with poor prognosis in glioma patients.* ***A****) miR-20a-5p expression in 12 normal brain tissues and 76 human glioma tissues was measured by qRT-PCR.* ***B****) miR-20a-5p expression in low-grade (I–II) (35) and high-grade (III–IV) (41) glioma tissues.* ***C****) miR-20a-5p expression in normal brain and four glioma cell lines as determined by qRT-PCR. Relative expression of target gene was expressed as fold change with control set to 1.* ***D****) The patients with glioma were divided into miR-20a-5p high-expression and low-expression groups and Kaplan–Meier analysis was performed to evaluate the relationship of miR-20a-5p expression level with prognosis of glioma patients.* ***E****) Pearson's correlation analysis of the relationship between SNHG16 and miR-20a-5p. #p<0.05, compared with control.*

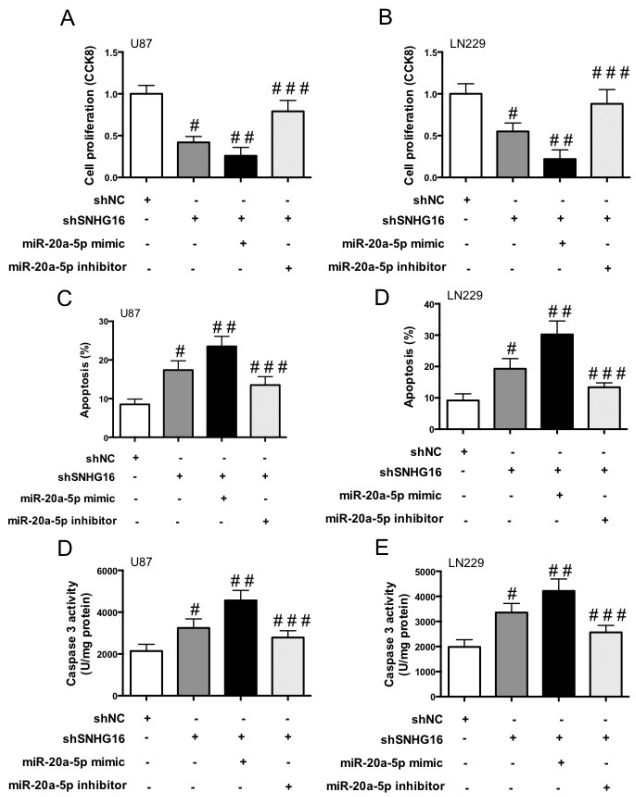

Fig. 4. *shSNHG16 decreases proliferation and increases apoptosis by negative regulation of miR-20a-5p.* ***A****,* ***B****) U87 and LN229 cells were co-transfected with shSNHG16 and miR-20a-5p mimic or anti- miR-20a-5p and cell viability was detected by CCK-8 analysis.* ***C****,* ***D****) Flow cytometry was used to explore the apoptosis. Caspase 3 activity was measured (****E*** *and* ***F****). #p<0.05, compared with shNC. ##p<0.05, compared with shSNHG16. ###p<0.05, compared with shSNHG16 and miR-20a-5p.*

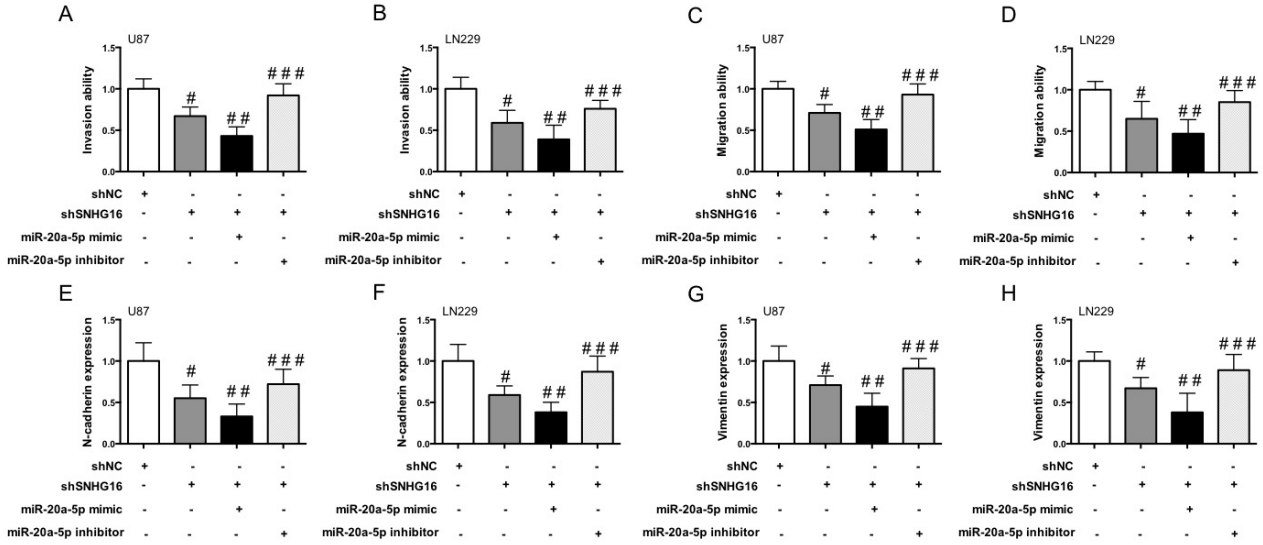

Fig. 5. *shSNHG16 decreases malignancy in glioma by negative regulation of miR-20a-5p.U87 and LN229 cells were co-transfected with shSNHG16 and miR-20a-5p mimic or anti- miR-20a-5p. **A**, **B**) The invasion of transfected cells was determined by Transwell assay. **C**, **D**) The migration of transfected cells was determined by wounding healing assay. mRNA expression of N-cadherin (**E**, **F**) and Vimentin (**G**, **H**) was determined. Relative expression of target gene was expressed as fold change with control set to 1. #p<0.05, compared with shNC. ##p<0.05, compared with shSNHG16. ###p<0.05, compared with shSNHG16 and miR-20a-5p.*

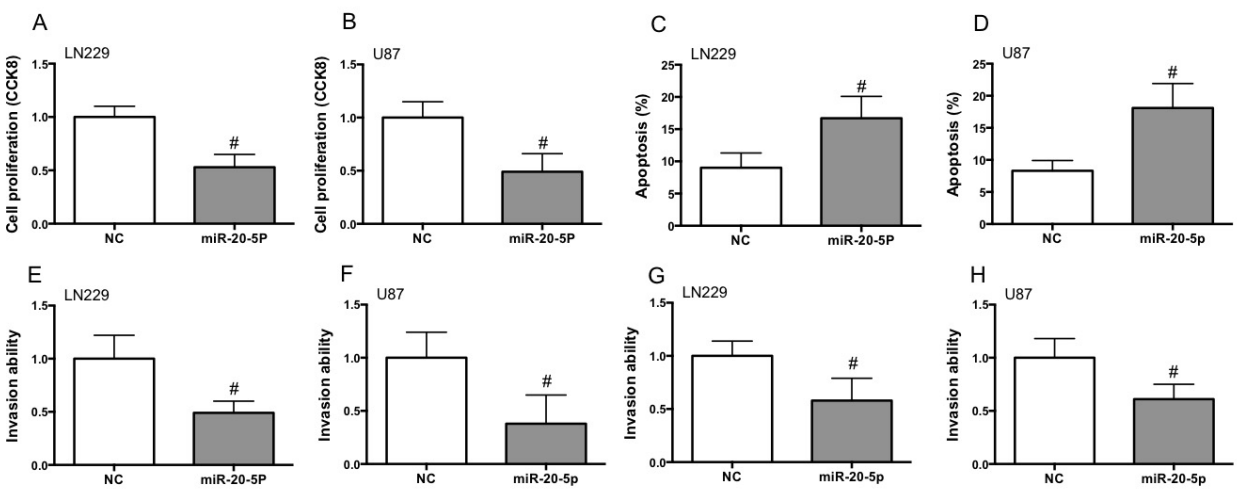

Fig. 6. *miR-20a-5p mimic decreases malignancy in glioma cells. **A**, **B**) U87 and LN229 cells were transfected with miR-20a-5p mimic and cell viability was detected by CCK-8 analysis. **C**, **D**) Flow cytometry was used to explore the apoptosis. **E**, **F**) The invasion of transfected cells was determined by Transwell assay. **G**, **H**) The migration of transfected cells was determined by wounding healing assay. #p<0.05, compared with NC.*

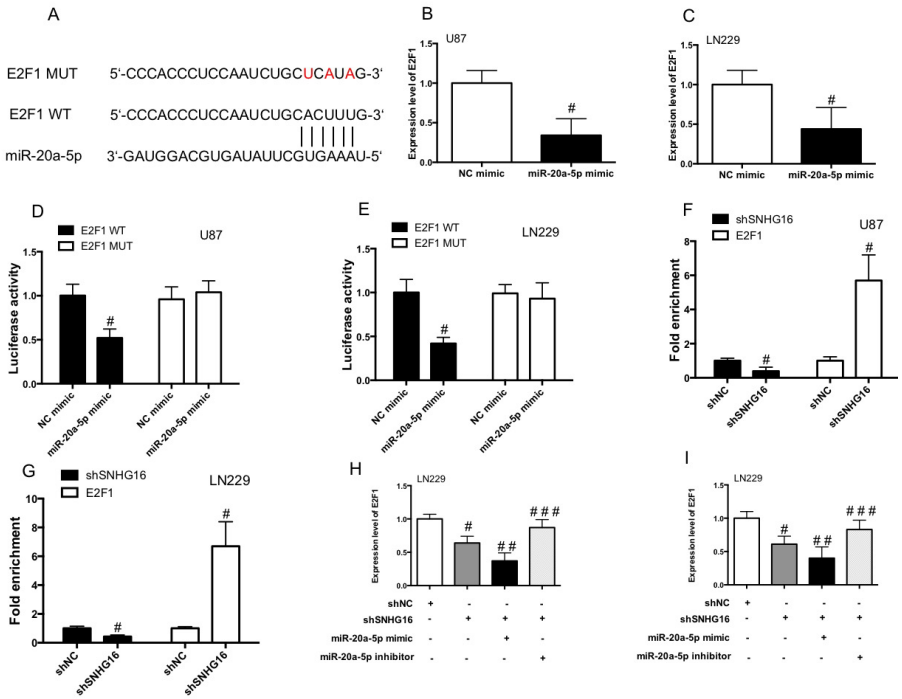

Fig. 7. *SNHG16 acts as a ceRNA for miR-20a-5p to enhance E2F1 expression.* ***A)*** *Bioinformatics analysis revealed the putative binding sequences of miR-20a-5p on E2F1 and the mutant sequences.* ***B***, ***C)*** *miR-20a-5p mimic reduced the mRNA expression of E2F1 in U87 and LN229 cells.* ***D***, ***E)*** *Luciferase activity was determined in U87 and LN229 cells co-transfected with miR-20a-5p mimic or NC-mimic and pGL3 luciferase reporters containing E2F1-WT or E2F1-MUT sequences.* ***F***, ***G)*** *RIP assay of the enrichment of Ago2 on SNHG16 and E2F1 transcripts relative to IgG in stable shSNHG16 U87 and LN229 cells.* ***H***, ***I)*** *The mRNA expression of E2F1 was assayed in stable shSNHG16 U87 and LN229 cells co-transfected with miR-20a-5p mimic or anti-miR-20a-5p. Relative expression of target gene was expressed as fold change with control set to 1. #p<0.05, compared with shNC. ##p<0.05, compared with shSNHG16. ###p<0.05, compared with shSNHG16 and miR-20a-5p.*

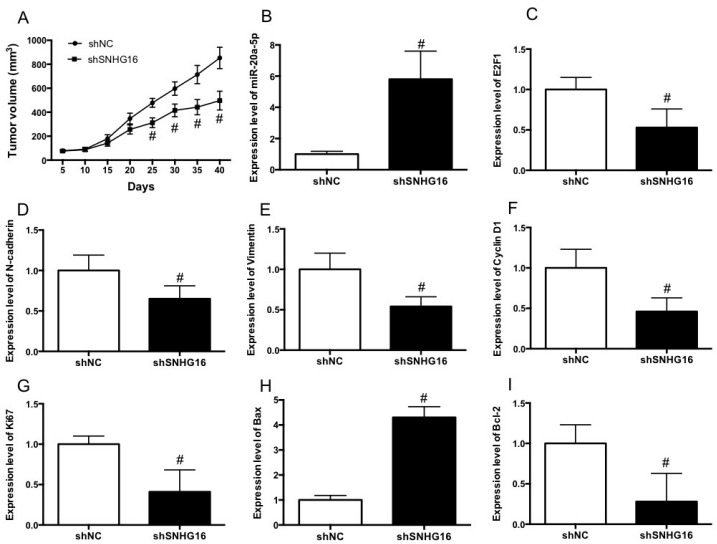

Fig. 8. *SNHG16 promotes glioma tumor growth in a xenograft mouse model.* ***A)*** *U87 cells stably transfected with shSNHG16 and shNC were subcutaneously injected into nude mice and tumor volumes were measured. mRNA expression of miR-20a-5p (**B**), E2F1 (**C**), N-cadherin (**D**), Vimentin (**E**), Cyclin D1 (**F**), Ki67 (**G**), Bax (**H**), and Bcl-2 (**I**). #p<0.05, compared with shNC.*

20a-5p in cancer. Chen et al. reported that miR-20a-5p targets RUNX3 to regulate proliferation and migration of human hepatocellular cancer cells (16). miR-20a-5p could promote colorectal cancer invasion and metastasis by downregulating Smad4 (17). miR-20a-5p repressed multi-drug resistance in osteosarcoma by targeting the KIF26B gene (18). However, evidence also showed that upregulation of miR-20a-5p, was associated with advanced clinical stages of astrocytoma (19). To further investigate the relationship between SNHG16 and miR-20a-5p, we conducted a dual-luciferase reporter assay and found that miR-20a-5p mimic decreased the luciferase activity of SNHG16-WT but not SNHG16-MUT. miR-20a-5p mimic could enhance the effects of shSNHG16 on proliferation, apoptosis, invasion, migration, and EMT process. In parallel, miR-20a-5p inhibitor abolished the effects of shSNHG16 on cell proliferation, apoptosis, invasion, migration, and EMT process. Therefore, SNHG16 modulates glioma tumorigenesis by negatively regulating miR-20a-5p expression.

E2F1 belongs to the E2F transcription factor family (20). Previous studies have found that abnormal E2F1 expression is associated with cell proliferation (21) and cisplatin chemoresistance (22). Bioinformatics analysis was performed and showed that E2F1 was a potential target of miR-20a-5p. We showed that transfection with miR-20a-5p mimic significantly decreased the mRNA expression of E2F1 in glioma cells. Moreover, miR-20a-5p notably reduced the luciferase activity of wild-type E2F1, but did not affect the luciferase activity of mutant E2F1. These data indicate that miR-20a-5p inhibits E2F1 expression in glioma cells. A previous study reported an auto-regulatory feedback loop between E2F1 and miR-20a-5p/20b-5p, and indicated that miR-20a-5p, miR-20b-5p and E2F1 are involved in myoblast proliferation and differentiation through the auto-regulation between E2F1 and miR-20a-5p/20b-5p (23). In combination with these findings, it is demonstrated that the interaction between miR-20a-5p and E2F1 may be a common mechanism.

In order to further examine whether SNHG16 regulates the tumorigenesis of glioma by regulating E2F1 expression, we used the RIP assay on Ago2 in U87 and LN229 cells with stable downregulation of SNHG16. Our results demonstrated that downregulation of SNHG16 remarkably decreased the enrichment of SNHG16, but enhanced the enrichment of E2F1. Moreover, knockdown of SNHG16 resulted in a suppression of E2F1 mRNA expression, which could be abrogated by anti-miR-20a-5p, but enhanced by miR-20a-5p mimic. These results suggest that SNHG16 acts as a ceRNA of E2F1 by sponging miR-20a-5p. Substantial studies have shown that LncRNA functions as ceRNA (24). ceRNAs are RNA transcripts which can communicate with each other at post-transcription level by competing for shared miRNAs (25, 26). ceRNA networks link the function of protein-coding mRNAs with that of non-coding RNAs such as microRNA, lncRNA, pseudogenic RNA and circular RNA (25, 26). Since Pandol PP. and his group presented a ceRNA hypothesis in 2011 (27), increasing evidence has been provided that lncRNAs as ceRNAs were involved in cancer onset and progression (28). In addition, the role and mechanism of SNHG16 were confirmed in a xenograft mouse model. shSNHG16 significantly inhibited the increase of tumor volumes, decreased proliferation and EMT biomarkers, and promoted apoptosis. These results indicate that SNHG16 promotes glioma development by regulating the expression of E2F1.

In conclusion, our results showed that SNHG16 functioned as an oncogene in gliomas. SNHG16 acted as a ceRNA for miR-20a-5p to promote glioma progression through regulation of E2F1 expression. The data provide a new clue for the role of SNHG16/miR-20a-5p/E2F1 in the development of glioma. This new regulatory network may be a novel therapeutic target in the future.

REFERENCES

1. Reifenberger G, Wirsching HG, Knobbe-Thomsen CB, Weller M. Advances in the molecular genetics of gliomas - implications for classification and therapy. Nat Rev Clin Oncol 2017; 14(7):434-52.
2. Meyer MA. Malignant gliomas in adults. N Engl J Med 2008; 359(17):1850.
3. Li X, Shen JK, Hornicek FJ, Xiao T, Duan Z. Noncoding RNA in drug resistant sarcoma. Oncotarget 2017; 8(40):69086-104.
4. Bhan A, Soleimani M, Mandal SS. Long noncoding RNA and cancer: A new paradigm. Cancer Res 2017;

77(15):3965-81.
5. Khalil AM, Guttman M, Huarte M, et al. Many human large intergenic noncoding RNAs associate with chromatin-modifying complexes and affect gene expression. Proc Natl Acad Sci U S A 2009; 106(28):11667-72.
6. Prensner JR, Chinnaiyan AM. The emergence of lncRNAs in cancer biology. Cancer Discov 2011; 1(5):391-407.
7. Christensen LL, True K, Hamilton MP, et al. Snhg16 is regulated by the Wnt pathway in colorectal cancer and affects genes involved in lipid metabolism. Mol Oncol 2016; 10(8):1266-82.
8. Yu M, Ohira M, Li Y, et al. High expression of ncRAN, a novel non-coding RNA mapped to chromosome 17q25.1, is associated with poor prognosis in neuroblastoma. Int J Oncol 2009; 34(4):931-38.
9. Cai C, Huo Q, Wang X, Chen B, Yang Q. Snhg16 contributes to breast cancer cell migration by competitively binding mir-98 with e2f5. Biochem Biophys Res Commun 2017; 485(2):272-78.
10. Yan L, Jiao D, Hu H, Wang J, Tang X, Chen J, Chen Q. Identification of lymph node metastasis-related microRNAs in lung adenocarcinoma and analysis of the underlying mechanisms using a bioinformatics approach. Exp Biol Med (Maywood) 2017; 242(7):709-17.
11. Zhu Y, Yu M, Li Z, et al. NcRAN, a newly identified long noncoding rna, enhances human bladder tumor growth, invasion, and survival. Urology 2011; 77(2):e511-15.
12. Liu B, Sun L, Liu Q, et al. A cytoplasmic nf-kappab interacting long noncoding RNA blocks ikappab phosphorylation and suppresses breast cancer metastasis. Cancer Cell 2015; 27(3):370-81.
13. Li T, Xie J, Shen C, et al. Amplification of long noncoding RNA ZFAS1 promotes metastasis in hepatocellular carcinoma. Cancer Res 2015; 75(15):3181-91.
14. Poliseno L, Salmena L, Zhang J, Carver B, Haveman WJ, Pandolfi PP. A coding-independent function of gene and pseudogene mRNAs regulates tumour biology. Nature 2010; 465(7301):1033-38.
15. Mattick JS, Makunin IV. Non-coding RNA. Hum Mol Genet 2006; 15 Spec No 1:R17-29.
16. Chen Y, Wang X, Cheng J, Wang Z, Jiang T, Hou N, Liu N, Song T, Huang C. MicroRNA-20a-5p targets RUNX3 to regulate proliferation and migration of human hepatocellular cancer cells. Oncol Rep 2016; 36(6):3379-86.
17. Cheng D, Zhao S, Tang H, et al. MicroRNA-20a-5p promotes colorectal cancer invasion and metastasis by downregulating SMAD4. Oncotarget 2016; 7(29):45199-213.
18. Pu Y, Yi Q, Zhao F, Wang H, Cai W, Cai S. Mir-20a-5p represses multi-drug resistance in osteosarcoma by targeting the kif26b gene. Cancer Cell Int 2016; 16:64.
19. Zhi F, Shao N, Wang R, et al. Identification of 9 serum microRNAs as potential noninvasive biomarkers of human astrocytoma. Neuro Oncol 2015; 17(3):383-91.
20. Teplyuk NM, Uhlmann EJ, Wong AH, et al. MicroRNA-10b inhibition reduces E2F1-mediated transcription and mir-15/16 activity in glioblastoma. Oncotarget 2015; 6(6):3770-83.
21. Sun JY, Xiao WZ, Wang F, et al. MicroRNA-320 inhibits cell proliferation in glioma by targeting E2F1. Mol Med Rep 2015; 12(2):2355-59.
22. Chen W, Yang Y, Chen B, Lu P, Zhan L, Yu Q, Cao K, Li Q. Mir-136 targets E2F1 to reverse cisplatin chemosensitivity in glioma cells. J Neurooncol 2014; 120(1):43-53.
23. Luo W, Li G, Yi Z, Nie Q, Zhang X. E2f1-miR-20a-5p/20b-5p auto-regulatory feedback loop involved in myoblast proliferation and differentiation. Sci Rep 2016; 6:27904.
24. Thomson DW, Dinger ME. Endogenous microRNA sponges: Evidence and controversy. Nat Rev Genet 2016; 17(5):272-83.
25. Qi X, Zhang DH, Wu N, Xiao JH, Wang X, Ma W. CeRNA in cancer: Possible functions and clinical implications. J Med Genet 2015; 52(10):710-18.
26. Ergun S, Oztuzcu S. Oncocers: CeRNA-mediated cross-talk by sponging miRNAs in oncogenic pathways. Tumour Biol 2015; 36(5):3129-36.
27. Salmena L, Poliseno L, Tay Y, Kats L, Pandolfi PP. A ceRNA hypothesis: The rosetta stone of a hidden rna language? Cell 2011; 146(3):353-58.
28. Liu D, Yu X, Wang S, et al. The gain and loss of long noncoding RNA associated-competing endogenous RNAs in prostate cancer. Oncotarget 2016; 7(35):57228-38.

LETTER TO THE EDITOR

CLINICAL VALUE OF COMBINED TESTS FOR TUMOR MARKERS FOR GASTRIC CANCER

MX. XU[1], HJ. CUI[2], TL. YAO[3] and YF. GUI[1]

[1]Inspection Department, Affiliated HongQi Hospital of MuDanJiang Medical University, Mudanjiang City, China; [2]Oncology Department, Affiliated HongQi Hospital of MuDanJiang Medical University, Mudanjiang City, China; [3]Emergency Department, Affiliated HongQi Hospital of MuDanJiang Medical University, Mudanjiang City, China

Received December1, 2017 – Accepted January 31, 2018

To study the clinical diagnostic value of treating gastric cancer (GC) with combined tests for tumor markers (CEA, CA199, CA242 and CA724), fifty healthy subjects, 50 patients with GC at different stages and 50 patients with benign GC were randomly selected from our hospital. These subjects were divided into a normal group A, an experimental group B and a control group C. Venous blood was drawn and tested for four serum tumor markers. The SPSS 18.0 analytic system was then used to analyze the data. Tumor markers for GC at different stages, different pathological patterns and tumor incidence are discussed. The difference in expression levels of tumor markers between group C and group A was not statistically significant (P>0.05). The differences in expression levels between group B in stage I and stage II and those of groups A and C was statistically significant (P<0.05). At the same time, the differences in expression levels of group B in stage III and stage IV and those of groups A and C were also statistically significant (P<0.01). For different sizes of tumors, taking 5 cm as a maximum, normal expression and abnormal expression of the four tumor markers was different (P<0.05). The tumor incidence of the combined test for the four tumor markers was conspicuously higher than that of single tests. Moreover, the difference between the tumor incidence of the combined test in stages I, II and III and that of single tests in the same stages was of statistical significance (P<0.05); however, the difference was not statistically significant in stage IV (P>0.05). The combined testing for tumor markers is useful for clinical diagnosis of GC.

To the Editor,

Gastric cancer (GC) is a common malignant tumor of the digestive system, which starts from the top portion of the gastrointestinal tract (1). There are no obvious symptoms in the early stage. Research has shown that there is a higher survival rate if a patient with is treated in the early stages (2). Thus, diagnosing GC at an early stage is essential for its treatment and prognosis. It is well-known that substances produced by GC cells, referred to as tumor markers, can be tested for in gastric fluids and other tissues (3). In other words, tumor markers are produced by and exist alongside a tumor, and are closely related to tumor genesis and development. Thus, tumor marker testing is important for diagnosing GC in its early stages, assessing treatment effectiveness and monitoring recurrence (4). In China, malignant whole body tumors are the

Key words: GC, tumor marker, combined test, proliferation, clinical diagnosis

Mailing address:
Dr Yifang Gui,
TongXiang Road No. 5
Affiliated HongQi Hospital,
MuDanJiang Medical University,
MuDanJing City,
HeiLongJiang Province, China
e-mail: yifanggui001@163.com

0393-974X (2018)

third most deadly type of cancer. Clinically, tumor markers have played an increasingly important role in recent years (5-6), as they can be used to determine whether neoplastic tissue exists. With an increasing number of patients with GC, a greater number of researchers are focusing their studies on diagnosing GC in its early stages. Matsuo et al. (7) studied the value of Narrow Band Imaging (NBI) and acetic acid in the early diagnosis of GC. Furina et al. (8) separated organic compounds from urine specimens of patients with GC, considering them as biomarkers. After they were isolated and identified by gas-liquid chromatography, the organic compounds were considered to be good for diagnosing GC in its early stages. Four tumor markers, carcinoembryonic antigen (CEA), salivary acidified pentose (CA199), gastrointestinal cancer antigen (CA242) and GC and ovarian cancer antigen (CA724), were selected here. Through a combined test for these four tumor markers, pathological patterns, tumor sizes and tumor incidences were compared, and it was concluded that a combined test is more accurate and valuable for diagnosis.

MATERIALS AND METHODS

Study subjects

Fifty patients with GC, including 16 cases in stage I, 15 cases in stage II, 10 cases in stage III and 9 cases in stage IV, treated at the Affiliated HongQi Hospital of MuDanJiang Medical University from Dec 2015 to Dec 2016 were enrolled in the study. All of these patients, having not received any related chemotherapy treatment previously, were included in the experimental group B. Another 50 patients with benign GC were selected and set as control group C. In addition, 50 healthy persons were chosen and set as a normal group A. The ratio of males to females in group A was 30:20, and the average age was 40.1±5.7. The ratio of males to females in group B was 30:20, and the average age was 41.7±5.9. The ratio of males to females in group C was 30:20, and the average age was 42.2±5.4. Patients in group B and C did not have other diseases. Differences in patients' sex and ages among these three groups was not statistically significant ($P>0.05$). The study was approved by the Ethics Committee of the Affiliated HongQi Hospital of MuDanJiang Medical University, and all the patients signed an informed consent to participate in the study.

Materials and instruments

A Roche Electrochemiluminescence (ECL) immunity analyzer, constant-temperature centrifuge machine and antibody-labeled ELISA Kit were provided by the Affiliated HongQi Hospital of MuDanJiang Medical University.

Venous blood sampling

Five mL of fasting venous blood of patients in the

Table I. *Basic information of patients in experimental group B.*

Pathological pattern	Ulcerative type	33
	Infiltrating type	8
	Protrude type	4
	Others	5
Invasion location	Tunica serosa	23
	Placenta percreta	13
	Muscular layer	8
	Submucosa	4
	Mucous layer	2

three groups were taken and placed in an EP tube. The tube was then placed at room temperature and centrifuged for 10 min at 3000r/min, after which serum was collected for future testing.

Combined test for markers

Four tumor markers, CEA, CA199, CA242 and CA724, were tested using the Roche Electrochemiluminescence (ECL) immunity analyzer by means of enzyme-labeled immunoassay.

Statistical analysis

The SPSS 18.0 analytical system was used to analyze the data and the standard difference was set as P=0.05. When P<0.05, it was a statistically significant difference.

RESULTS

Basic information

Most of the 50 patients with GC in group B were diagnosed with the ulcerative type, which accounted for 66%, followed by the infiltrating, protruding and other types. There were five locations of invasion, including tunica serosa (main invasion location), placenta percreta, muscularis, submucosa and mucosa (Table I). The percentages of occurrence within the group were 46%, 26%, 20%, 8% and 4%, respectively.

Comparison of testing results of tumor markers

Table II shows that the difference between group C and group A was not statistically significant. Comparisons of tumor markers between group B in stage I and stage II and groups A and C were statistically significant (P<0.05). In addition, comparisons of tumor markers between group B in stage III and stage IV and groups A and C were of significant statistical difference (P<0.01). Thus, the four tumor markers had distinguishing features in malignant tumors, and tumor marker levels were related to clinical analysis of the tumor.

Relationship between tumor marker and pathological pattern and tumor size

In the combined test for the four tumor markers, there was statistical significance between the different pathological patterns and the different tumor sizes (P<0.05) (Table III). For the three pathological patterns, abnormal expression and normal expression were significantly different. For different tumor sizes, taking 5 cm as a maximum, normal expression and abnormal expression of the four tumor markers were different (P<0.05), which entails that the four tumor markers were meaningful for testing pathological pattern and tumor size.

Table II. *Testing results of the four tumor markers of the three groups.*

	CEA	CA199	CA242	CA724
Group A	1.79±0.15	29.54±1.79	4.27±0.32	3.55±1.23
Group B in stage I	3.83±0.53*	47.32±0.62*	21.31±1.28*	12.01±0.55
Group B in stage II	6.91±1.69*	53.07±1.34*	27.41±1.33*	15.70±0.04*
Group B in stage III	12.49±1.07*#	109.47±4.98*#	47.38±2.35*#	37.02±0.86*#
Group B in stage IV	16.57±10.09*#	179.29±15.97*#	67.01±13.24*#	100.31±21.22*#
Group C	1.87±0.47	32.14±1.34	4.21±0.17	3.66±0.54

*Note: * denotes comparison with experimental group A and control group C, P<0.05.*

 # denotes comparison with experimental group A and control group C, P<0.01.

Table III. *Relation between tumor markers, pathological patterns and tumor sizes.*

		Ulcerative Type (13± 10.09mg/ml)	Infiltrating Type (7.87±5.36mg/ml)	Protruding Type (20.54± 17.05mg/ml)	P	Tumor Size (5 cm)	P
CEA	Normal	6	2	1	<0.05	3	<0.05
	Abnormal	27	6	3		19	
CA199	Normal	4	1	0	<0.05	4	<0.05
	Abnormal	29	7	4		15	
CA242	Normal	8	3	2	<0.05	6	<0.05
	Abnormal	25	5	2		20	
CA724	Normal	7	1	0	<0.05	2	<0.05
	Abnormal	26	7	4		22	

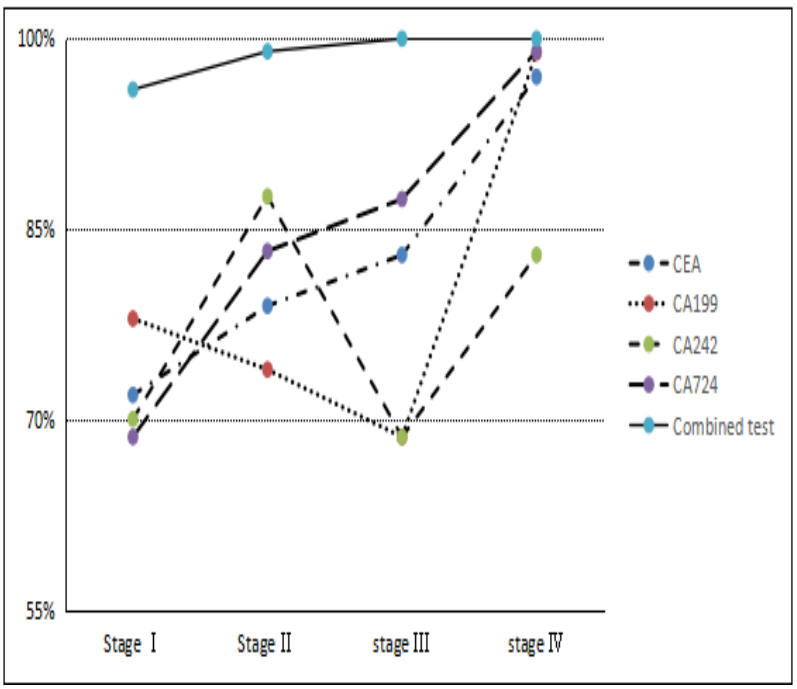

Fig. 1. *Tumor incidence comparison between combined test and single test.*

Tumor incidence comparison between combined test and single test

As shown in Fig. 1, the tumor incidence of the combined tested of all four tumor markers was apparently higher than that of the single test. Differences between tumor incidences of combined test in stages I, II and III and that of the single test in the same stages were statistically significant (P<0.05), while that of stage IV was not statistically significant (P>0.05).

DISCUSSION

With the popularization of testing techniques for GC, techniques involving tumor markers are being continuously developed, including combined

tests for multiple tumor markers. At present, there are more than ten types of tumor markers for clinical testing, but diagnostic indicators with strong specificity are still lacking (9). Four tumor markers were chosen here. CEA, a glycoprotein that is widely present in archenteric cancer, can be used as an antigen to provoke an immune reaction, and is used to identify many kinds of tumors. It has thus been identified as a universal tumor marker. It is remarkable for monitoring the development of and judging treatment effectiveness in colorectal cancer and GC (10). CA199 is an antigen reflecting the existence of a tumor, and whose presence in tumors is larger than in normal tissue. Thus, tumor type, genesis and differentiation can be identified if this marker is tested for in tissue (11). CA242 is a sialyl carbohydrate antigen produced by colon cancer cell lines that can be identified using monoclonal antibodies with hybridoma technology (12). CA724 is a mucin molecule of high molecular weight (HMW), and can be used for evaluating and monitoring cancer (13). Fan B (14) introduced a biochip marking system, finding that markers were related to clinical pathological. Glucose-regulated protein (GRP78), glutathione S transferase (GSTP1), apolipoprotein AI(ApoAI), α-1 antitrypsin (α1AT) and gastrokine-1 (gkn-1) were regarded as tumor markers by Wu et al. (15) in their study, which found that the presence of glutathione S transferase (GSTP1) in GC cases was conspicuously increased.

Four tumor markers, CEA, CA199, CA242 and CA724, were selected to conduct a combined test. The results of pathological patterns, tumor sizes and tumor incidences indicate that combined tests for tumor markers are very helpful for the clinical diagnosis of GC. With the promotion of molecular biology theory and technology, partial molecular level detection can be used to detect the presence of malignant tumors, thereby it can promote production of more tumor markers and needs to be further explored.

REFERENCES

1. Wang HM, Huang CM, Zheng CH, et al. Tumor size as a prognostic factor in patients with advanced GC in the lower third of the stomach. World J Gastroenterol 2012; 18(38):5470-75.
2. Zare A, Mahmoodi M, Mohammad K, Zeraati H, Hosseini M, Holakouie Naieni K. Factors affecting the survival of patients with GC undergone surgery at Iran cancer institute: univariate and multivariate analyses. Iran J Public Health 014; 43(6):800-8.
3. Kurygin AA, Maĭstrenko NA, Khrykov GN, Beliak NP. The role of tumor markers in diagnosing metastases of GC: preoperative diagnostics (part I). Vestn Khir Im I I Grek 2009 [Article in Russian]; 168(4):16-19.
4. Jing JX, Wang Y, Xu XQ, et alTumor markers for diagnosis, monitoring of recurrence and prognosis in patients with upper gastrointestinal tract cancer. Asian Pac J Cancer Prev 2014; 15(23):10267-72.
5. Wang HP, Wu HY, Wang Y, Wang L. Combined detection of tumor markers and serum inflammatory factors in the diagnosis and treatment of gynecologic oncology. J Biol Regul Homeost Agents 2017; 31(3):691-95.
6. Polanska H, Heger Z, Gumulec J, et al. Effect of HPV on tumor expression levels of the most commonly used markers in HNSCC. Tumour Biol 2016; 37(6):7193-201.
7. Matsuo K, Takedatsu H, Mukasa M, et al. Diagnosis of early GC using narrow band imaging and acetic acid. World J Gastroenterol 2015; 21(4):1268-74.
8. Furina RR, Ryzhkov VL, Mitrakova NN, Koptina AV, Safiullin IK, Lychagin KA, Eroshkin PR. The method for early diagnosis of the GC based metabolomics research. Eksp Klin Gastroenterol 2014; 10:14-7.
9. Farlow EC, Patel K, Basu S, et al. Development of a multiplexed tumor-associated autoantibody-based blood test for the detection of non-small cell lung cancer. Clin Cancer Res 2010; 16(13):3452-62.
10. Nakatsura T, Kageshita T, Ito S, et al. Identification of Glypican-3 as a novel tumor marker for melanoma. Clin Cancer Res 2004; 10(19):6612-21.
11. Zhao S, Mei Y, Wang Y, Zhu J, Zheng G, Ma R. Levels of CEA, CA153, CA199, CA724 and AFP in nipple discharge of breast cancer patients. Int J Clin Exp Med 2015; 8(11):20837-44.
12. Lei XF, Jia SZ, Ye J, Qiao YL, Zhao GM, Li XH, Chang H. Application values of detection of serum CA199, CA242 and CA50 in the diagnosis

of pancreatic cancer. J Biol Regul Homeost Agents 2017; 31(2):383-88.
13. Zhu Z, Chen Z, Chen C, et al. Opposite variation tendencies of serum CA724 levels in patients with colon and rectal carcinoma. Mol Clin Oncol 2014; 2(1):139-45.
14. Fan B, Xiong B. Investigation of serum tumor markers in the diagnosis of GC. Hepatogastroenterology 2011; 58(105):239-45.
15. Wu JY, Cheng CC, Wang JY, Wu DC, Hsieh JS, Lee SC, Wang WM. Discovery of Tumor Markers for GC by Proteomics. PLoS One 2014; 9(1):e84158.

LETTER TO THE EDITOR

PREVALENCE OF DEGNALA DISEASE IN BOVINE ALONG WITH SCREENING OF TOXIGENIC FUNGI ISOLATED FROM CONTAMINATED RICE STRAW

M. NAZAR[1,2], M.S. KHAN[1], M. IJAZ[1], A.A. ANJUM[1], S. SANA[1], E.M.N. SETYAWAN[3], M.I. SALEEM[4] and I. AHMAD[5]

[1]University of Veterinary and Animal Sciences, Lahore, Pakistan; [2]University of Agriculture Faisalabad, Sub Campus Burewala, Pakistan; [3]Department of Theriogenology and Biotechnology, College of Veterinary Medicine, Seoul National University, Seoul, Korea; [4]CMS Department, University of Agriculture, Faisalabad, Pakistan; [5]Faculty of Veterinary and Animal Sciences, University of the Poonch, Rawalakot Azad Jammu and Kashmir, Pakistan

Received November 3, 2017 – Accepted January 31, 2018

Toxigenic potential of different candidate fungi, isolated from rice straw feed of Degnala disease-affected bovines was analyzed along with species, age, gender and seasonal prevalence. Of 1,536 cases, 104 (6.77%) showed positive signs with a significant association ($p<0.05$) between this disease and rice straw feeding, in buffaloes, and bovine aged over 1 year in the winter season. Complete blood count showed a marked increase in erythrocyte sedimentation rate and all white blood cells numbers, except lymphocytes in positive cases. There was a significant increase ($p<0.05$) in alanine amino transferase, aspirate amino transferase and alkaline phosphatase in the liver function test. At the same time, an increased value of creatinine was noted in the renal function test. For isolation and screening of toxigenic fungi, rice straw samples (n=40) being fed to the positive cases were processed further, and 85 fungal isolates were found, mainly of *Aspergillus* (57), *Penicillium* (10), *Fusarium* (04), *Zygomycetes* (03), *Curvularia* (01) and unidentified (10). All isolated fungi were subjected for mycotoxin production and only 11 showed mycotoxin-producing capability (including *Aspergillus, Penicillium* and *Fusarium* isolates) analyzed by thin layer chromatography and quantified through high performance liquid chromatography. It is concluded that all the fungi contaminating rice straw feed of Degnala affected animals were not toxigenic. This work will help in establishing major mycotoxin-producing fungi leading to the probable cause of Degnala disease in bovine.

Fodder shortage all over the world is a problem which is increasing day by day due to agriculture land being utilized for residential purpose and cultivation of cash crops as major agricultural shareholders. Animals are facing severe deficiency both in energy and protein by 26% and 38%, respectively (1).

In scarcity seasons farmers have to move towards the utilization of valuable cash crops or the by-products of cereal crops (1) to fulfill the appetite of large ruminants. Among these by-products are wheat straw and rice straw. Especially during the windy months of winter, feeding of rice straw is commonly practiced in the rice producing areas of Punjab, Pakistan.

Rice crops need more water as compared to most of the other cereal crops for its normal production.

Key words: buffalo, Degnala disease, isolation, mycotoxin, toxigenic fungi

Mailing address:
Dr. Mudassar Nazar,
University of Agriculture,
Faisalabad,
Sub Campus Burewala- 61010, Pakistan
Tel.: +92-321-4051772
e-mail: m.nazar@uaf.edu.pk

0393-974X (2018)

If humidity is increased, due to rainfall during the period of wind and low temperature i.e. winter season, storage of rice straw near water-logged areas, flooded conditions or its storage immediately after harvesting may lead to the production of fungal colonies (2). These fungal colonies which are the suspected cause of a specific, un-clear and non-descriptive problem known as Degnala disease, which is dry gangrene or mycotoxicosis (3).

Dairy animals become infected by mycotoxins when they consume the affected feed which may lead to many physiological problems. Degnala disease, which is suspected to have a mycotoxin origin, exists in the Indo-Pak sub-continent, causing necrosis and gangrenous lesions on the hoof, ears and tails of bovines fed on rice straw (4). Initially, there is necrosis and later the affected areas of animal shed off (2). A widespread occurrence of the disease has been reported from rice growing areas of Indo-Pak which causes considerable economic losses. Some fungi are capable of generating more than one type of mycotoxins while some mycotoxins are created by more than one kind of fungi (3, 5, 6).

In this study, we have tried to converge the diagnosis of Degnala disease by screening the mycotoxin-producing fungi after isolation and identification on the basis of micro/macroscopic characteristics, thin layer chromatography and high performance chromatography along with prevalence analysis related to this disease in Sheikhupura and Gujranwala, two rice growing districts of Punjab, Pakistan.

MATERIALS AND METHODS

Sampling strategy and prevalence

The study was carried out on clinically suspected cattle and buffaloes having a history of rice straw feeding located in two rice growing districts of Punjab, viz Gujranwala and Sheikhupura. Clinical signs were taken as an inclusion criteria. Blood samples from positive (n=10) and negative cases (n=10) for hemato-biochemical analysis were taken along with rice straw samples being fed to the positive cases (n=40) for the isolation and identification of fungal growth.

The total sample size of 1,536 numbers of animals was calculated based on formula (7) with 95% confidence interval at 5% desired absolute precision by assuming the expected prevalence of 50%.

$$n = \frac{P \times (1 - P) \times \left(Z_{1-\frac{\alpha}{2}}\right)^2}{d^2}$$

Where, n= required sample size; P= prevalence of diseased animals in population (0.5); $Z_{1-\frac{\alpha}{2}}^2$ = square of standard normal Z value corresponding to cumulative probability of $1 - \frac{\alpha}{2}$ $(1.96)^2$; α= 1 – confidence interval (0.05); d= desired level of absolute precision (0.05). The Prevalence of the disease was calculated according to Thrusfield (7).

Isolation and identification of fungus

Rice straw samples (n=40) from the feedings of positive cases were collected. Then 2 g of each sample of rice straw was rinsed by 10 mL of normal saline (NS) and then this NS was poured onto sterilized Sabouraud's Dextrose Agar (SDA) containing petri plates and incubated at 28°C for 5 days. Spores from each single colony were picked by sterile needle loop and transferred to other SDA plates repeatedly till a single purified colony of an individual fungus was obtained. Individual primary fungus was identified by macroscopic and microscopic characters according to www.drfungi.com.

Mycotoxin production and extraction

Mycotoxins were produced and extracted by following the Official methods of analysis of AOAC International Baltimore, MD USA (8) by culturing individual fungal isolate on Sabouraud's Dextrose Broth containing flasks plugged with cotton for 45 days in the dark. Shaking was carried out regularly 2-3 times every day to avoid sporulation.

Thin layer chromatography

Commercially available TLC plates were spotted with known positive as well as negative controls along with fungal extracts with the help of a glass syringe, spotting was carried out by placing the plates on a hot-plate for limiting the sample on a small area. Mobile phase was prepared by adding 95 mL chloroform and 5 mL acetone in a developing glass tank. Plates were observed under UV light (366

nm) in Wood's chamber.

HPLC for toxigenicity confirmation

Mycotoxin-producing fungal species analyzed by TLC were confirmed and comparatively quantified by HPLC by taking standards of Aflatoxins B1 and B2 (20ppb each) at the Quality Operation Laboratory of the University of Veterinary and Animal Sciences, Lahore, by using a modified method of the Association of Official Analytical Chemist (9).

Statistical analysis

Data on prevalence and associated risk factors of the disease were estimated by Pearson's *chi*-squared test while data on blood profile was analyzed applying *t*-test using GraphPad Prism 5 software (GraphPad Software, Inc., USA) and probability (p) value <0.05 was considered significant (10).

RESULTS

Prevalence

The overall prevalence was 6.77% in the two districts. The difference in the prevalence was found significant ($p<0.05$) in buffaloes as compared to cattle. However gender-related prevalence was not significantly different ($p>0.05$). The data revealed a significant difference ($p<0.05$) among age groups, with a higher number of cases in the older group (animals with an age of more than one year). Most of the cases were seen at the end of winter season

Table I. *Univariate analysis of risk factors associated with the Degnala disease in cattle and buffaloes in Punjab.*

Variable	Parameter	Total	Positive	Percentage	Univariate Analysis		
					Odd ratio	Confidence Interval	*P-Value*
Species	Cattle	768	12	1.56	8.574	4.656-15.790	<0.0001
	Buffalo	768	92	11.97			
Gender	Male	332	25	7.53	1.025	0.540-1.376	0.5340
	Female	1204	79	6.56			
Age	< 1Year	441	16	3.63	2.316	1.343-3.993	0.0019
	Over 1Year	1095	88	8.04			
Feeding	Rice straw	1536	104	6.77	0.004461	0.0002767-0.07191	<0.0001
	Wheat straw	1536	0	0.00			
Area	Sheikhupura	768	63	8.20	0.6508	0.4337-0.9766	0.0368
	Gujranwala	768	41	5.34			
Season	Winter	1536	90	5.86	0.1478	0.08376-0.2608	<0.0001
	Spring	1536	14	0.91			
	Summer	1536	00	00			
	Autumn	1536	00	00			

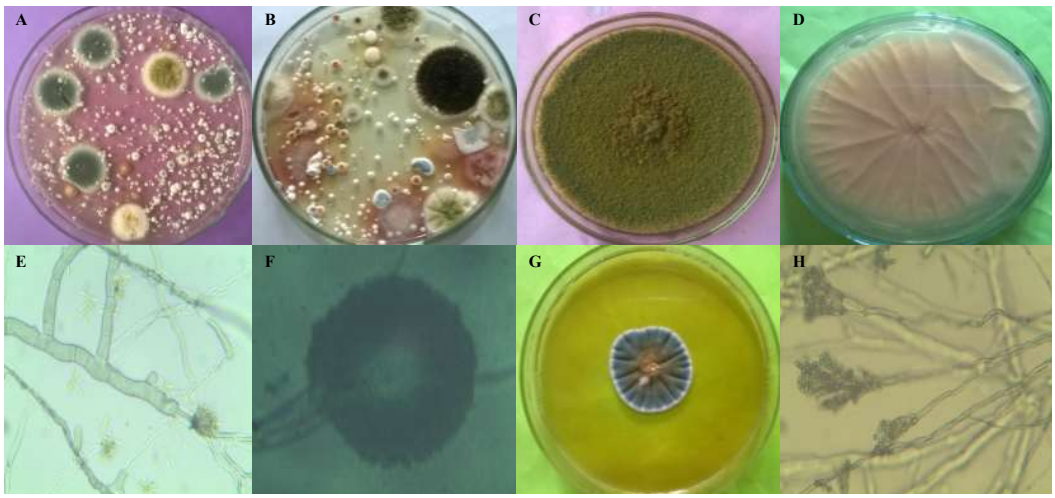

Fig. 1. ***A, B)*** *(primary culture) showing pattern of multiple growths.* ***C-F)*** *(Aspergillus) C showing Obverse and D showing reverse sided view of petri plate while E and F are the microscopic views (400X) showing septate-hyaline hyphae and spore forming pattern respectively;* ***(G-H)*** *(Penicillium) G showing obverse view and H is the spore forming pattern in Penicillium.*

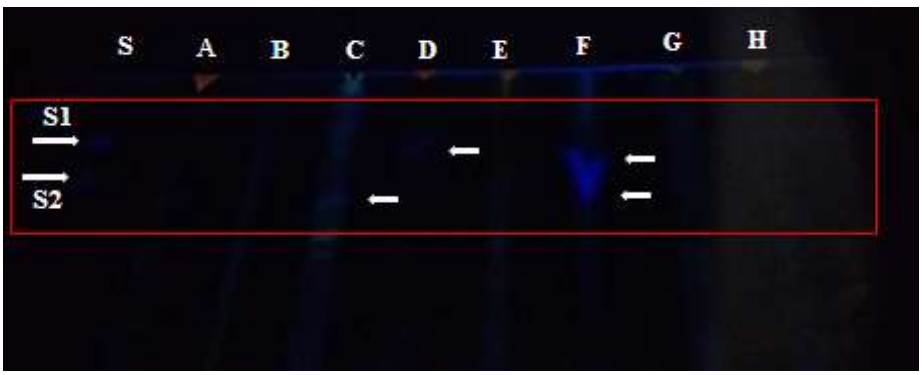

Fig. 2. *Thin layer chromatography for qualitative analysis of different fungal samples observed under UV lamp (366 nM). S indicates movement line for standard mycotoxins.S1 arrow indicating standard B1 (20ppb) spot, S2 arrow indicating standard B2 (20ppb) spot. AH showing movement line for different fungal samples, arrow showing fungal isolates (C, D, F) positive for toxigenic property.*

after a rainfall in these areas and there was a strong association between rice straw feeding and Degnala disease in cattle and buffaloes (Table I).

Hematobiochemical analysis

Comparison of CBC of affected with healthy animals showed basophilia, monocytophilia and neutrophilia with lymphocytopenia while eosinophils were found within normal range. Haemoglobin contents (Hb), ESR, basophils, monocytes, lymphocytes and neutrophils were found significantly affected ($p<0.05$) while PCV, TEC, TLC and eosinophils were not found significant ($p>0.05$). Liver function tests showed values of alanine amino transferase (ALT), aspirate amino transferase (AST) and alkaline phosphatase (ALP) were significantly ($p<0.05$) increased while bilirubin was within normal range. Data related to creatinine showed an increased value but not statistically significant while blood urea nitrogen was within normal range in the renal function test.

Isolation of toxigenic fungi

Macroscopic characters were included as obverse and reverse colony characteristics of individual fungal isolate. Obverse colony characters of each fungus (immature and mature) were recorded including whether the colony was granular, fluffy, cottony, sticky, folded or mucoid and whether folds or rings were present in colonies or not. While in the case of reverse colony characters, color present on the reverse side of the petri plates having pure fungal growth, number and pattern of folds and rings were also observed (Fig. 1).There were 85 isolates of fungal growth (Fig. 1) which were mainly *Aspergillus* (n=57), *Penecillium* (n=10), *Fusarium* (n=04), *Zygomycetes* (n=03), *Curvularia* (n=01) and some unidentified (n=10).

There were 11 fungal isolates with toxigenic ability among which *A. niger* (n=01 isolate of blue fluorescence), *A. flavus* (n=06 isolates of blue fluorescence), *A.terrus* (n=02 isolates of blue fluorescence), *Penicillium* and *Fusarium* (n=01 isolate each, of green fluorescence) were identified (Fig. 2). Quantification of mycotoxins was made through HPLC by comparing with the standard curves of B1 and B2 aflatoxins (Fig. 3).

DISCUSSION

Prevalence of Degnala disease has been reported by many researchers in all the rice growing areas of Pakistan, Nepal and India (5, 6). The prevalence of Degnala was significantly high in buffaloes as compared to that of cattle in the present investigations. These results were in agreement with the findings of different Researchers (5, 11-13).

A significant difference was reported regarding gender-related prevalence. In the present study, seasonality was observed in the appearance of

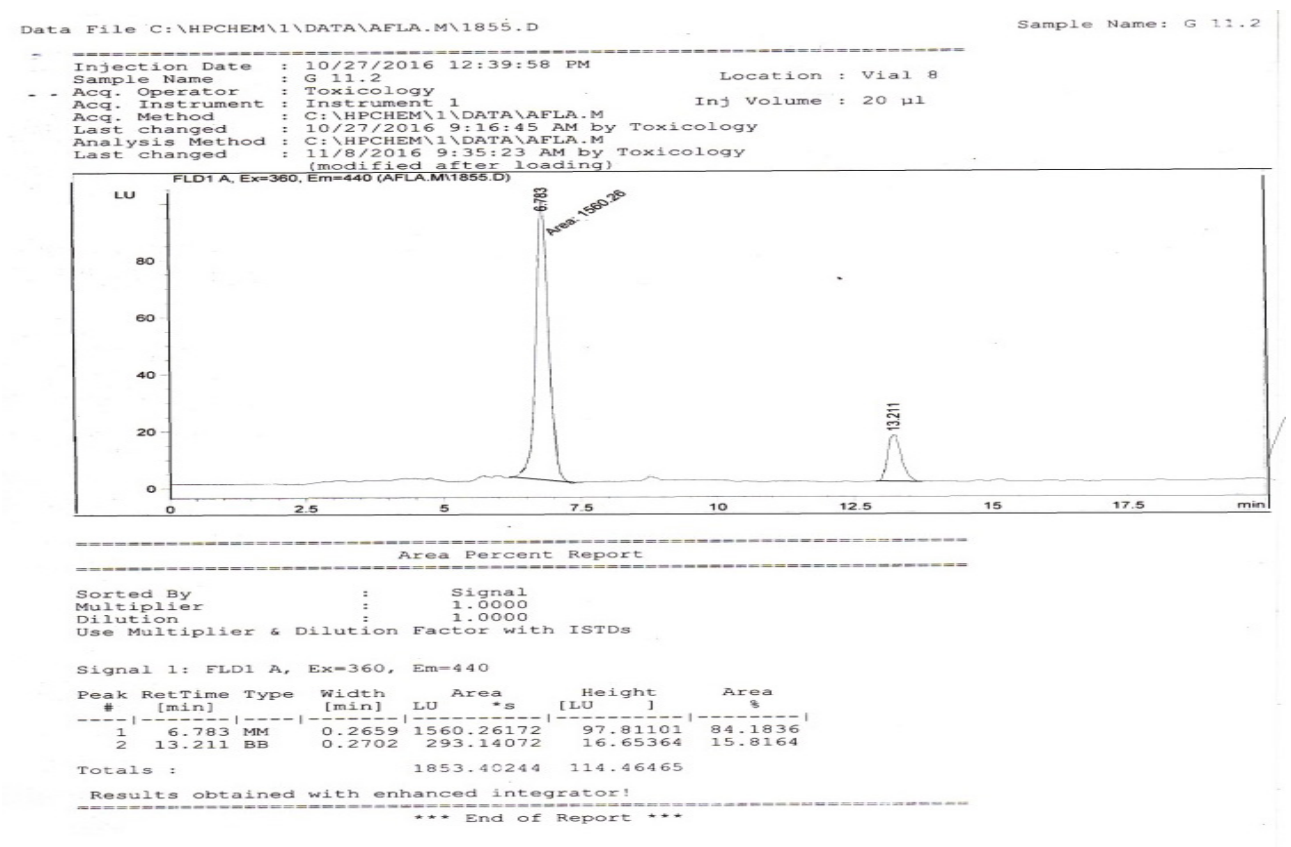

Fig. 3. *Time verses concentration curves (1st B1 and 2nd B2 aflatoxin) compared with the standard curves in Aspergillus terrus, (G 11.2 = Sample I.D) isolate.*

clinical signs which were seen during or at the end of winter. These results were in line with the findings of other Authors (12-14). Hemato-biochemical analysis showed fluctuations compared to the healthy bovine samples. The results were in agreement with the findings of Karki et al. (15) who reported an increase in TEC, decrease in PCV and Hb. This might be due to an inflammatory reaction along with secondary reactions which causes increase in TEC with neutrophilia.

Data on liver and kidney function tests showed an involvement of hyper-detoxification process which is an indication of the involvement of toxins in the body after being affected by the disease. Involvement of mycotoxins has been assumed by many authors (6, 12). Through blood circulation, the toxins distribute to peripheral tissues where they causes vasoconstriction due to collagen and elastin dissolution, leading to the development of skin lesions (5). Histopathological examination showed necrosis, eosinophilic infiltration in the subcutaneous connective tissues and loss of architectural details of the affected parts of the body, but there was no growth of any fungal isolate from tissue scrapings from gangrene affected areas which strengthens this assumption that pathogenesis in Degnala disease involves mycotoxins instead of a local involvement of some saprophytic fungi (3, 4).

This was the first study of its kind and there is no report indicating toxigenic strains in the diet of Degnala disease-infected animals. It was concluded that only a few number of fungal isolates extracted from rice straw feedings of the affected animals have the ability to produce mycotoxins.

REFERENCES

1. Riaz M, Ahmad M, Sarwar M, Raza S. Nutritional evaluation of sugarcane tops in conventional feeding management system during fodder scarcity season of Pakistan. Int J Agricul Biol 2008; 10(6):665-68.
2. Jadhav K, Patel J, Gajbhiye P. A note on impact of Degnala disease on milk production in Kankrej cattle. Indian J Anim Res 2003; 37(1):73-74.
3. Kumar M. Therapeutic management of degnala disease in a buffalo calf: a case report. Int J Agricol Sci Vet Med 2016; 4:6-7.
4. Kathiriya J, Savaliya K, Ahlawat A, Godasara S, Patel J. A unique case of Deg Nala disease in Gir cow and its therapeutic management. Int J Curr Microbiol App Sci 2017; 6(5):190-92.
5. Irfan M. The clinical picture and pathology of" Deg Nala disease" in buffaloes and cattle in West Pakistan. Vet Rec 1971; 88(16):422-24.
6. Karki K, Manandhar P, Koirala P, Manandhar S. Moldy rice straw poisoning in dairy cattle in Kathmandu Valley Nepal. Bull Enviro Pharmacol Life Sci 2012; 1(2):18-20.
7. M T. Veterinary Epidemiology. 2nd ed. UK: Black Well Science; 2005. 182-9 p.
8. AOAC. Official methods of analysis of AOAC International Baltimore, MD USA Association of Official Analytical Chemists Method No 99408 2000(17th Ed.).
9. AOAC. Association of Official Analytical Chemists. Inc, Maryland, USA Method number 99033. 1995(16th Edition).
10. Steel RG, Torrie JH, Dickey DA. Principles and procedures of statistics: A biological approach: McGraw-Hill; 1997.
11. Dandapat P, Nanda PK, Bandyopadhyay S, Kaushal A, Sikdar A. Prevalence of Deg Nala disease in eastern India and its reproduction in buffaloes by feeding Fusarium oxysporum infested rice straw. Asian Pac J Trop Med 2011; 4(1):54-57.
12. Maqbool A, Khan MA, Yaqoob M, Khan IA, Badar N, Mahamood F. Prevalence, etiology, chemotherapy and control of Deg Nala disease in buffaloes and cattle in Pakistan. Veterinarski Arhiv 1998; 68(6):213-17.
13. Sikdar A, Chakraborty G, Bhattacharya D, et al. An outbreak of gangrenous syndrome among buffaloes and cattle in West Bengal: clinicopathological studies. Trop Anim Health Prod 2000; 32(3):165-71.
14. Kalra D, Bhatia K. Degnala disease in buffaloes and cattle: epidemiological investigations. J Environl Pathol, Toxicol Oncol: official organ of the International Society for Environmental Toxicology and Cancer. 1990; 10(3):132-5.
15. Karki K, Manandhar P, Koirala P. A Laboratory outbreak investigation of post-monsoon endemic moist eczematous syndrome in cattle in Jhapa District of Nepal. Vet World 2008; 1(8):233-6.

LETTER TO THE EDITOR

SPOLIGOTYPING ANALYSIS OF *MYCOBACTERIUM TUBERCULOSIS* WITH TB-SPRINT TECHNOLOGY

S. ALI[1], C. SOLA[2], M. HARRISON[3], M. TAHIR[4], A. SHEED KHAN[5], M. MUMTAZ[6], E. CHIMARA[7] and F. HASSAN[1]

[1]Microbiology Department, Quaid-e-Azam University Islamabad, Pakistan; [2]Institut de Biologie Intégrative de la Cellule, France; [3]Laboratório de Biologia Molecula, Instituto Oswaldo Cruz, Brasil; [4]Capital University of Science and Technology, Islamabad, Pakistan; [5]Provincial TB Reference Laboratory, Khyber Pakhtunkhwa, Pakistan; [6]Department of Microbiology, Haripur University, Haripur, Pakistan; [7]Institute Adolfo Lutz, São Paulo, Brazil

Received November 4, 2017 – Accepted February 6, 2018

Spoligotyping is a highly reproducible, fast polymerase chain reaction (PCR)-based approach for identification of different strains of *Mycobacterium tuberculosis* through genotyping of *Mycobacterium tuberculosis* complex (MTB). Molecular typing of MTB is helpful for understanding and controlling TB epidemics. Spoligotyping was performed on 166 strains of MTB collected from 25 districts of Khyber Pakhtunkhwa, Pakistan. Results were analyzed using online database, SITVIT2, developed by the Institute Pasteur de Guadeloupe, France and SPSS software V.15 (IMB Inc). Drug susceptibility test (DST) was performed on all strains using commercial liquid media in BACTECMGIT 960 instrument. Spoligotyping results showed that 145 (88%) strains displayed known patterns while 21 (12%) were new. Central Asian strain (CAS) was the predominant family (73%, x2=19.9, P=0.001) followed by Beijing (5.4%) and T1 (4.2%). CAS1-Dehli was the major sub-family (82%) among the CAS family (x2=664, P=0.0001). Furthermore, new spoligotyping patterns were clustered using the maximum parsimony (MP) test to find any evolutionary relationship with pre-published genotypes. Analysis showed that the majority of the strains with unknown pattern have an evolutionary link with CAS strain, and 9 (5.4%) of the unknown strains were epidemiologically linked and named CAS-KPK (Khyber Pakhtunkhwa). The present study demonstrated that CAS is a predominant strain of MTB prevailing in different areas of the Khyber Pakhtunkhwa province of Pakistan. Spoligotyping pattern of some strains could not match other reported pattern in the international database. Other tools, like MIRU/ VNTR, can be helpful to perform investigation of its epidemiological characteristics in future.

To the Editor,

Tuberculosis (TB) has been a major public health problem in Pakistan for the last few decades and was declared by World Health Organization (WHO) as a global emergency in 1993. Various national as well as international authorities are highly concerned and are contributing their efforts to abolish TB. Pakistan is among 22 countries identified by WHO for its high burden of TB cases reported annually. Millions of Afghan refugees have seasonal traffic between the two countries that demonstrates epidemiological linkage and evolutionary genomic characteristic

Key words: spoligotyping, VNTR, DST, CAS, TB-SPRINT

Mailing address:
Dr Fariha Hassan,
Microbiology Department,
Quaid-E-Azam University,
Islamabad, Pakistan
Tel.: +92 051 9064 3065
e-mail: farihahasan@yahoo.com

0393-974X (2018)

of *Mycobacterium tuberculosis* (MTB) strains in Pakistan. Genome of the MTB contains variable copies of 36bp direct repeats (DR) in a specific locus. These DR loci are interspersed with 34 bp to 41 bp conserved sequence called spacer. More than 94 spacers has been identified to date, however, only 43 are in use for genotyping while others contribute to only a slight increase in information (1). This set of 43 unique spacer sequences has been used to classify MTB strains based on the pattern of the presence or absence of DR (2). Variation in the number of spacer is attributed to combinational or individual effect of the genomic process like homologous recombination, DNA replication or transposition of the IS6110 element in the DR locus. DR loci is a family of clustered regularly interspaced short palindromic repeats (CRISPR) and its function in bacterial metabolism or its relationship with spacers has not been well defined (3), however, it is evident from the literature that certain patterns of DR are linked to the evolutionary process (1).

Spoligotyping is the most highly adopted PCR-based method for genotyping analysis and has been considered as the most reliable and cost-effective approach. Various new techniques have been proposed for spoligotyping analysis, such as DNA microarray (4), PixSysn QUAD 4500 Microarrayer (5), TB-SPRINT, hydrogel microarray (6) and spoligotyping (7). TB-SPRINT is based on microbead assay that provides spoligotyping profile and simultaneous detection of common mutation in the hot spot region of *rpo*B, *kat*G and *Inh*A genes to evaluate drug resistance to rifampicin and isoniazid in MTB. TB-SPRINT is a useful tool for epidemiology studies of tuberculosis in poor resource countries because of its high-throughput and lower cost (7). The aim of the current study was to investigate the epidemiological link between MTB strains and their genotypic families found in Pakistan based on spoligotyping the TB-SPRINT method.

MATERIALS AND METHODS

This study was approved by the research and ethics committee of the Provincial TB Control Program Khyber Pakhtunkhwa (TB/KP/R&D-25-17). Samples for the current study were collected from the Provincial TB Reference Laboratory, Peshawar; equipped with biosafety level-III facility (BSLIII). Samples were digested and decontaminated using the standard N-acetyl-L-cysteine sodium hydroxide (NALC-NaOH) method. Decontaminated samples were inoculated on Lowenstein-Jensen medium (LJ) and mycobacterium growth indicator tube (MGIT). Positive growth in the tubes was confirmed by Tbc ID device (Ref: 245159, Becton, Dickinson). All confirmed mycobacterial isolates were subsequently processed for genotyping analysis targeting DR locus in MTB as described by Kamerbeek et al. DNA was extracted from the culture using the Cetyl-trimethyl-ammonium-bromide (CTAB) method (2).

TB-SPRINT assay was performed on all samples using a Luminex 200 (Luminex Corp, Austin, TX) instrument (7). Spoligotypes patterns in binary format were entered into the SITVIT2, a proprietary database of the Institute Pasteur de la Guadeloupe, which is an updated version of SpolDB4 and SITVIT-WEB databases (8, 9). Discriminatory index in the original SITVIT database is measured with Hunter–Gaston Diversity Index system (HGDI). Based on the HGDI index system, strains were initially grouped in one of the 9 precursor lineages(clades), include Beijing, CAS, S,T, X, LAM, Haarlem, EAI and AFRI (9). The selected strain matched with pre-publish SIT were assigned as sub-family name, while strains with unknown pattern were declared as orphan. All the strains whose pattern could not fall within the 9 precursor lineages and having a low HGDI index were declared as new-pattern. Furthermore, patterns of all the strains originating from Pakistan were collected from the database and were compared with new-spoligotyping patterns using Bionumerics software (version 6.6; Applied Maths, Sint-MartensLatem, Belgium) to find any evolutionary relationship to the pre-published genotypes.

The genetic diversity was laid out as maximum parsimony tree construct (MP) using default settings in MEGA7. Phylogenic tree was obtained using the Subtree-Pruning-Regrafting (SPR) algorithm taking 43 direct repeat pattern as sequence (10).

RESULTS

A total of 200 isolates of MTB were analyzed by spoligotyping TB-SPRINT method. Among these

isolates 166 produced valid and interpretable results. Patterns of 145 isolates were found in international database (SITVIT2) and 21 (13%) unique patterns were declared as new types (Table I). Results showed that the Central Asian Strain (CAS) was the predominant genotype lineage 72.8% (n=121), followed by Beijing 5.4% (n=9), T1 4.2% (n=7), and 4.8% (n=8) were other types (Fig.1).

Cluster analysis of high prevalent lineages

Detailed analysis of CAS strains resulted in 11 different clusters or sub-families. Among the sub-families CAS1-Dehli (SIT26) was the predominant genotype (n=78) followed by SIT 1401 (n=5) and SIT 794 (n=4). Pattern of one member of CAS family did not match in the SITVIT database and thus was declared as CAS-Orphan. All strains belonging to the Beijing family were grouped in two clusters SIT1 (n=8) and SIT941 (n=1). Members of the T1 family were grouped in five different clusters (SIT51, SIT53, SIT273, SIT732, SIT189) and one T1 orphan. It was also found that EAI1-SOM, EAI5, EAI6-BGD1, H1, LAM9-ZWE, Manu, EAI3-IND and X1 are rarely distributed in this region.

All 21 strains with unique spoligotyping patterns were grouped in 13 clusters based on similarity index of maximum parsimony (MP) test.

New cluster was further analyzed through different methods to find any evolutionary relationship to the pre-published genotypes. Results indicated that the majority of the unique patterns are sub lineage of the CAS family except for orphan KP1 that is more closely related to T1 (SIT189). Similarly, orphan-KP2 is closely linked to orphan Pak6. A detailed tree is represented in Fig. 2. These spoligotyping patterns are not only unique to Pakistan but also to the international database and have not been reported elsewhere, thus no SIT had been assigned to date (Table I).

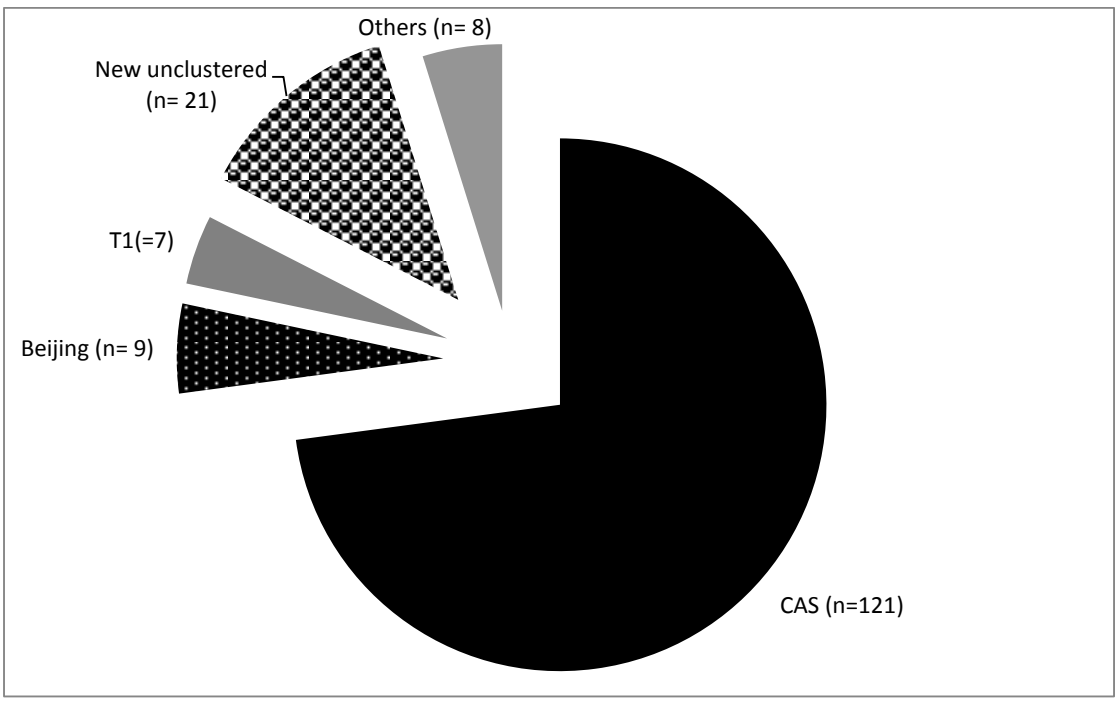

Fig. 1. *Graphical analysis of 166 MTB isolated collected from different areas of Pakistan. CAS shown in the black area is the dominant spoligotype. New un-clustered strains are shown in the black dotted graph. Less frequent spoligotypes are grouped in the other categories in the gray area.*

Table I. *Each Spoligotype pattern is a combination of 43 spacers denoted by white and black boxes. A black box represents the presence of a specific spacer at that location while a white box represents the absence of spacer. Series 1-42 shows different spoligo patterns of MTB genotypes while series 43 to 55 represents new patterns that were not matched in SITVIT database.*

S.No	Spoligotype pattern	Lineage (Sub-Family)	SIT	Frequency
1	□□□□□□□□□□■□■□□□□□□□□□□□□□□□□□□□□□■■■■■■■■■	**Beijing**	1	1
2	□□□□□□□□□□□□□□□□□□□□□□□□□□□□□□□□□□□■■■■■■■■■	**Beijing**	1	7
3	□□□□□□□□□□□□□□□□□□□□□□□□□□□□□□□□□□□■■■■■■□■■	**Beijing**	941	1
4	■■■□□□□■■■■■■□■■■■■■■□□□□□□□□□□□□□□□■■■■■■	**CAS Orphan**	0	1
5	■■■□□□□■■■■■■■■■■■■■■□□□□□□□□□□□□□□■■■■■■■■■	**CAS**	142	3
6	■■■□□□□■■■■■■■■■■■■■■□□□□□□□□□□□□□□■■■■■■■■■	**CAS**	356	1
7	■■■□□□□■■■■■■■■■■■■■■□□□□□□□□□□□□□□■■■■■■■■■	**CAS**	485	1
8	■■■□□□□■■■■■■■■■■■■■■■□□□□□□□□□□□□□□■■■■■■■	**CAS**	486	1
9	■■■□□□□■■■■■■■■■■■■■■■□□□□□□□□□□□□□□■■■■■■■	**CAS**	486	1
10	■■■□□□□■■■■■■■■■■■■■■□□□□□□□□□□□□□□■■■■■■■■■	**CAS**	1093	1
11	■■■□□□□■■■■■■■□□□□□□□□□□□□□□□□□□□□□□■■□■■■	**CAS**	1120	1
12	■■■□□□□■■■■■■■■■■■■■■■□□□□□□□□□□□□□□□□□□□□	**CAS**	1151	1
13	■■■□□□□□□□■■■■■■■■■■■■■□□□□□□□□□□□□□■■■■■■■■	**CAS**	1151	2
14	■■■□□□□■■■■■■■■■■■■■■■□□□□□□□□□□□□□□□■■■■■	**CAS**	1789	1
15	■■■□□□□■■■■■■■■■■■■■■□□□□□□□□□□□□□□□■■■■■■■	**CAS**	1949	2
16	■■■□□□□■■■■■■■■■■■■■■□□■■■■■■■■■□□□□■■■■■■■	**CAS (CAS_New)**	27	2
17	■■■□□□□■■■■■■■■■■■■■■□□□□□□□□□□□□■■□□■■■■■	**CAS (CAS1-Delhi)**	25	5
18	■■■□□□□■■■■■■■■■■■■■■□□□□□□□□□□□□□■■■■■■■■■	**CAS (CAS1-Delhi)**	26	78
19	■■■□□□□■■■■■■■□■■■■■■■□□□□□□□□□□□□□■■■■■■■■■	**CAS (CAS1-Delhi)**	141	2
20	■■■□□□□■■■■■■■■■■■■■■□□□□□□□□□□□□■■□■■■■■■	**CAS (CAS1-Delhi)**	428	2
21	■■■□□□□■■■■■■■■■■■■■■□□□□□□□□□□□□■■■■■□■■■	**CAS (CAS1-Delhi)**	429	1
22	■■■□□□□■■■■■■□■■■■■■■■□□□□□□□□□□□□■■■■■■■■■	**CAS (CAS1-Delhi)**	794	4
23	■■■□□□□■□■■■■■■■■■■■■■□□□□□□□□□□□□■■■■■■■■■	**CAS (CAS1-Delhi)**	1092	1
24	■■■□□□□■■■■■■■■■■■■■■□□□□□□□□□□□□■■■■□■■■■	**CAS (CAS1-Delhi)**	1401	5
25	■■■□□□□■■■■■■■■■■■■■■□□□□□□□□□□□□■□□□■■■■■	**CAS (CAS1-Delhi)**	1787	1
26	■■■□□□□■■■■■■■■■■■■□■□□□□□□□□□□□□■■■■■■■■■	**CAS (CAS1-Delhi)**	2145	1
27	■■■□□□□■□□■■■■■■■■■■■■□□□□□□□□□□□□■■■■■■■■■	**CAS (CAS1-Delhi)**	2237	1
28	■■■□□□□□□□■■■■■■■■■■■■□□□□□□□□□□□□■■■■■■■■■	**CAS (CAS2)**	288	2
29	■■■■■■■■■■■■■■■■■■■■■■■■■■■□□□□■□■■■■■□■■■	**EAI1-SOM**	48	1
30	■□□■■■■■■■■■■■■■■■■■■■■■■■■■□□□□■□■■□□□■■■■	EAI3-IND	11	1
31	■■■□□□□□□■■■■■■■■■■■■□□■■□□□□□□■□■■■■■■■■■	EAI5	1473	1
32	■■■□□□□□□■■■■■■■■■■■■□□■■■■□□□□□■□■■■■■■■■■	EAI6-BGD1	129	1
33	■■■■■■■■■■■■■■■■■■■■■■■■■■□□□□□□■□□□□■■■□■■■	**H1**	62	1
34	■■■■■■■■■■■■■■■■■■■■■■□□□□■■□□□□■■□□□□■■■■■■■	**LAM9-ZWE**	59	1
35	■■■■■■■■■■■■■■■■■■■■■■■■■■■■■□□■■■■■■■■■■■	**Manu**	54	1
36	■■■■■□■■■■■■■■■■□□□□□■■■■■■■■■■□□□□■■■■■■■	**T1 (Orphan)**	0	1
37	■■■■■■■■■■■■■■■■■■■■■■■■■■■■■■■□□□□■■■□□□□	**T1**	51	1
38	■■■■■■■■■■■■■■■■■■■■■■■■■■■■■■■□□□□■■■■■■■	**T1**	53	2
39	■■■■■■■■■■■■■□□□□■■■■■■■■■■■■■■□□□□■■■■■■■	**T1**	189	1
40	■■■■■■■■■■■■■■■■■■■□■■□□■■■□■■■□□□□■■■■■■■	**T1**	573	1
41	■■■■■■■■■■■■■■□□■■■■■■■■■■■■■■□□□□■■■■■■■	**T1**	732	1
42	■■■■■■■■■■■■■■■■■□■■■■■■■■■■■■■□□□□■■□□□□■	**X2**	137	1
43	■■■■■■■■■■■□□□□■■■■■■■■■■■■■■■□□□□■■■■■■■	**Orpan_KP1**	0	1
44	■■■□□□□■■■■■■■■■■■■■■■■■■■■■■■□□■■■■■■■■■	**Orpan_KP2**	0	1
45	■■■□□□□■■■■■■■□□□□□□□□□□□□□□□□□□□□□□■□■■■■■	**Orpan_KP3 (CAS-KPK)**	0	9
46	■■■□□□□■■■■■■■□□□■■■■■□□□□□□□□□□□□■■■■■■■■■	**Orpan_KP4**	0	1
47	■■■□□□□■■■■■■■□□□□□□□□□□□□□□□□□□□□□□■□■■■■■	**Orpan_KP5**	0	1
48	■■■□□□□■■■■■■□□■■■■■■■□□□□□□□□□□□□□■■■■■■■■■	**Orpan_KP6**	0	1
49	■■■□□□□■■■■■■□□□□□□□□□□□□□□□□□□□□□□□■■■■□□	**Orpan_KP7**	0	1
50	■■■□□□□■■■■■□■■■■■■■■□□□□□□□□□□□□□■■■■■■■■■	**Orpan_KP8**	0	1
51	■■■□□□□■■■■□□□□□□□□■■■□□□□□□□□□□□□■■■■■■■■■	**Orpan_KP9**	0	1
52	■■■□□□□■■■■□□□□□□□□■□□□□□□□□□□□□□□□■■■■■■■	**Orpan_KP10**	0	1
53	■■■□□□□□□□■■■■■■■■■■■■□□□□□□□□□□□□■■■■■■■□■	**Orpan_KP11**	0	1
54	■■■□□□□□□□□□□■■■■■■■■□□□□□□□□□□□□□■■■■■■■■■	**Orpan_KP12**	0	1
55	■■■■■■■■■■■■■■■■■■□□□□□□□□□□□□□□□□□□■■■■■■	**Orpan_KP13**	54	1

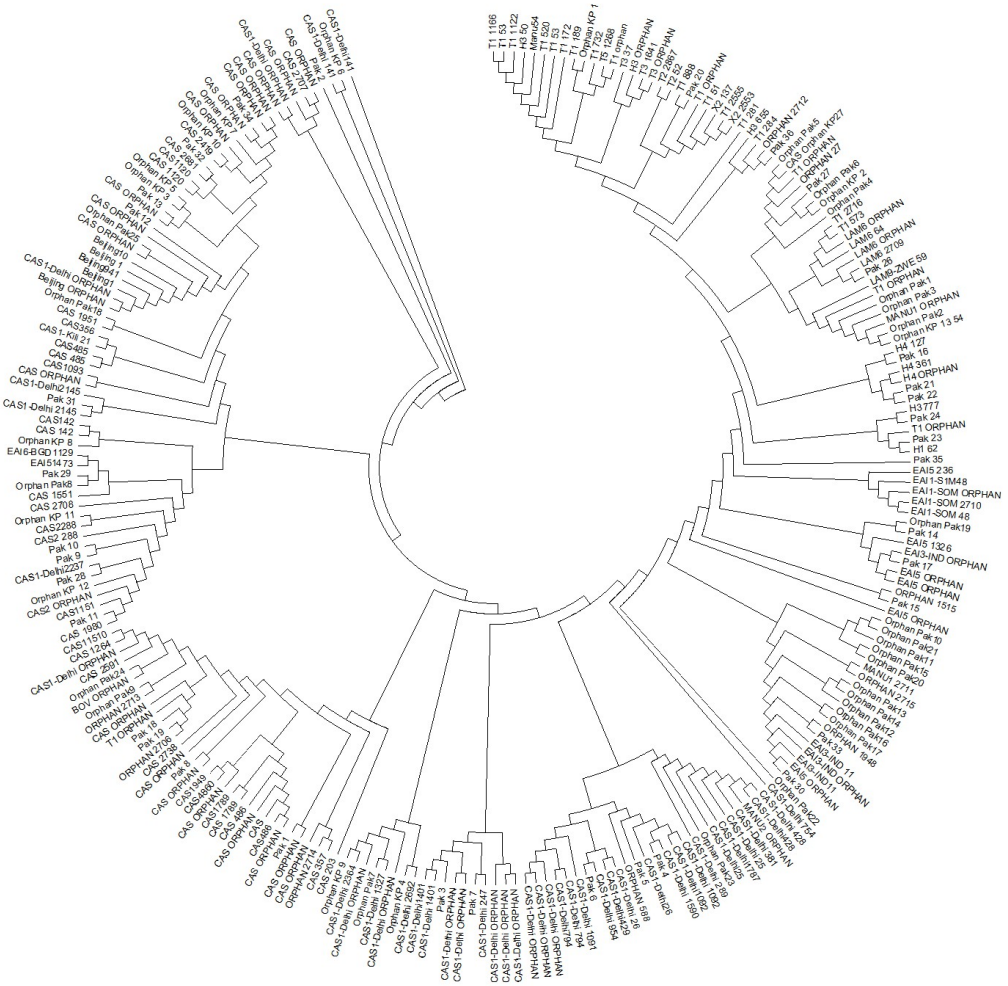

Fig. 2. *Maximum Parsimony analysis of new unclustered spoligotypes. The tree shows relationship of new unclustered spoligotyes in this study to the previously published spoligotype pattern from Pakistan. New spoligotype pattern in this study is numbered as Orphan KP 1 to Orphan KP 13.*

DISCUSSION

Many techniques have been used for MTB genotyping like RFLP, AFLP, MIRU VNTR and spoligotyping. The spoligotyping technique has been used worldwide for genotyping and epidemiological studies of MTB and was originally developed by Kamerbeek based on repeating identical direct repeats interspersed by short spacers of variable length (2). A public database SITVITWEB is available for the analysis of spoligotyping pattern that consist of 86,000 isolates collected from 160 countries. This database constitutes 7105 shared and 4364 orphan pattern and a total of 67 prototypes of lineages (clades) including AFR, BOV, Beijing, CAS, H1, LAM and Manu (9). Distribution of these spoligotypes was analyzed within and among the eight studied continental regions: Africa, East Asia, Europe, Oceania, Central America, South America, North America, Middle East and Central Asia. It is evident from literature that these genotypes are specific to certain geographical regions like in South America LAM is more prevalent followed by T and Haarlem lineage 49.3%, 26.7%, 15.7%, respectively. Similarly, CAS is more prevalent in South East Asia (9, 11). Our study represents the first in-depth

analysis of molecular epidemiology of tuberculosis in the study area. Considering spoligotyping patterns of majority of the strains the current study confirmed a more diverse population structure with a total of 12 different genotypes, grouped in 55 different clusters. However, by far the most dominant strain was CAS-1 Delhi belonging to CAS lineage. Overall distribution of genotypes in Khyber Pakhtunkhwa was in line with other spoligotyping analysis in Pakistan (11–13). A rather large population of 12% of strains could not be matched to the internationally defined genotypes in the database and was declared "new". Interestingly, spoligotyping pattern of new genotypes in the previous investigations were underestimated and left unstudied (12, 13). In-depth analysis revealed clear identification of CAS by presence of first three spacers followed by a set of 4 absent (4–7) and two more spacers (33-340). We confirmed that the majority of the new spoligotypes in this study are evolved from CAS characterized by the absence of spacers 4–7 and 23–34 as changes in the DR locus are most likely to occur via consecutive irreversible deletions of either single or contiguous blocks (1, 14).

The current study provides basic information of prevailing strains of MTB in KPK Pakistan. We found that CAS is the pre-dominant strain which is epidemiologically linked and the majority of the un-clustered strains are evolved from the pre-existing CAS strains. Other tools, like MIRU/VNTR in combination with TB-SPRINT, will further explore diversity patterns of un-clustered MTB.

ACKNOWLEDGEMENTS

TB Control Program Khyber Pakhtunkhwa, manager BSL-III laboratory facility for ethical support.

REFERENCES

1. Van Embden JD, van Gorkom T, Kremer K, Jansen R, van Der Zeijst BA, Schouls LM. Genetic variation and evolutionary origin of the direct repeat locus of Mycobacterium tuberculosis complex bacteria. J Bacteriol 2000; 182:2393-401.
2. Kamerbeek J, Schouls L, Kolk A, et al. Simultaneous detection and strain differentiation of Mycobacterium tuberculosis for diagnosis and epidemiology. J Clin Microbiol 1997; 35:907-14.
3. Jansen R, van Embden JDA, Gaastra W, Schouls LM. Identification of a novel family of sequence repeats among prokaryotes. Omics J Integr Biol 2002; 6:23-33.
4. Ruettger A, Nieter J, Skrypnyk A, et al. Rapid spoligotyping of Mycobacterium tuberculosis complex bacteria by use of a microarray system with automatic data processing and assignment. J Clin Microbiol 2012; 50:2492-95.
5. Song EJ, Jeong HJ, Lee SM, et al. A DNA chip-based spoligotyping method for the strain identification of Mycobacterium tuberculosis isolates. J Microbiol Methods 2007; 68:430-33.
6. Bespyatykh JA, Zimenkov DV, Shitikov EA, et al. Spoligotyping of Mycobacterium tuberculosis complex isolates using hydrogel oligonucleotide microarrays. Infect Genet Evol J Mol Epidemiol Evol Genet Infect Dis 2014; 26:41-46.
7. Gomgnimbou MK, Hernández-Neuta I, Panaiotov S, et al. Tuberculosis-spoligo-rifampin-isoniazid typing: an all-in-one assay technique for surveillance and control of multidrug-resistant tuberculosis on luminex devices. J Clin Microbiol 2013; 51:3527-34.
8. Brudey K, Driscoll JR, Rigouts L, et al. Mycobacterium tuberculosis complex genetic diversity: mining the fourth international spoligotyping database (SpolDB4) for classification, population genetics and epidemiology. BMC Microbiol 2006; 6:23.
9. Demay C, Liens B, Burguière T, et al. SITVITWEB – A publicly available international multimarker database for studying Mycobacterium tuberculosis genetic diversity and molecular epidemiology. Infect Genet Evol 2012; 12:755-66.
10. Kumar S, Stecher G, Tamura K. MEGA7: Molecular evolutionary genetics analysis version 7.0 for bigger datasets. Mol Biol Evol 2016; msw054.
11. Tanveer M, Hasan Z, Siddiqui AR, Ali A, Kanji A, Ghebremicheal S, Hasan R. Genotyping and drug resistance patterns of M. tuberculosis strains in Pakistan. BMC Infect Dis 2008; 8:171.
12. Yasmin M, Gomgnimbou MK, Siddiqui RT, Refrégier G, Sola C. Multi-drug resistant Mycobacterium tuberculosis complex genetic diversity and clues on

recent transmission in Punjab, Pakistan. Infect Genet Evol 2014; 27:6-14.

13. Hasan Z, Tanveer M, Kanji A, Hasan Q, Ghebremichael S, Hasan R. Spoligotyping of Mycobacterium tuberculosis isolates from Pakistan reveals predominance of central Asian strain 1 and Beijing isolates. J Clin Microbiol 2006; 44:1763-68.
14. Sola C, Filliol I, Gutierrez MC, Mokrousov I, Vincent V, Rastogi N. Spoligotype database of Mycobacterium tuberculosis: biogeographic distribution of shared types and epidemiologic and phylogenetic perspectives. Emerg Infect Dis 2001; 7:390.

LETTER TO THE EDITOR

NEUROPROTECTION OF ULINASTATIN ON TRANSIENT CEREBRAL ISCHEMIA VIA ANTIOXIDATIVE MECHANISMS

HX. HU[1], DH. XU[1], WN. JU[2], C. MA[3], X. WANG[2] and XL. LIU[1]

[1]Department of Emergency Medicine, The First Hospital of Jilin University, Changchun, Jilin, China; [2]Department of Neurology and Neuroscience Center, The First Hospital of Jilin University, Changchun, Jilin, China; [3]Department of Brain Tumor Surgery, The First Hospital of Jilin University, Changchun, Jilin, China

Received December 11, 2017 – Accepted February 9, 2018

Ulinastatin [also called urinary trypsin inhibitor (UTI)] has beneficial effects on cerebral ischemic injury evoked by cardiac arrest (CA). However, the underlying mechanisms are unknown. The purpose of this report was to determine the involvement of antioxidative signal pathway of the hippocampus in effects of UTI in the process of neurological functions after transient cerebral ischemia. CA was induced by asphyxia followed by cardiopulmonary resuscitation in rats. Western blot analysis and ELISA were used to examine expression of Nrf2-antioxidant response element (ARE) and superoxide dismutases (SOD), and the levels of products of oxidative stress. In addition, the modified neurological severity score (mNSS) and spatial working memory performance were employed to assess neurological deficiencies in CA rats. Our results show that CA impaired Nrf2-ARE and SOD in the hippocampus CA1 region and amplified products of oxidative stress, namely 8-isoprostaglandin F2α (8-iso PGF2α) and 8-hydroxy-2'-deoxyguanosine (8-OHdG). Systemic administration of UTI largely restored Nrf2-ARE and SOD, and this also attenuated amplification of 8-iso PGF2α and 8-OHdG induced by cerebral ischemia and thereby alleviated neurological deficits with increasing survival of CA rats. Our data suggest that UTI improves Nrf2-ARE signals and inhibits products of oxidative stress in the hippocampus, which is linked to improvement of neurological deficiencies in transient cerebral ischemia. UTI plays a beneficial role in modulating cerebral ischemic injury via antioxidative mechanisms.

To the Editor,

During cardiac arrest (CA), blood flow and oxygen delivery are abruptly halted which leads to systemic ischemic injury in various organs including the brain (1). Although cardiopulmonary resuscitation (CPR) is applied inadequate blood flow and tissue oxygen delivery still persist due to myocardial dysfunction, hemodynamic instability and microvascular dysfunction. Thus, it is important to study signal pathways involved in neuroprotective effects and further determine biological agents that can attenuate the damage evoked by cerebral ischemia.

Ulinastatin, also called urinary trypsin inhibitor (UTI), is a glycoprotein acting as a trypsin inhibitor (2). It can be derived from urine or synthetically produced and is conventionally effective to treat pancreatitis, toxic shock and sepsis, etc. (2-4).

Key words: ulinastatin, cardiac arrest, cerebral ischemia, oxidative stress, cardiopulmonary resuscitation

Mailing address:
Dr Xu Wang,
Department of Neurology and Neuroscience Center,
Department of Emergency Medicine,
The First Hospital of Jilin University, 71 Xinmin Street,
Changchun, Jilin 130021, China
Tel.: +86 431 88782593
e-mail: wangxxu2016@163.com

0393-974X (2018)

UTI has also been reported to suppress neutrophil accumulation and activity. The genes and proteins regulated by UTI are implicated in the inflammatory process (5). Previous studies indicate the protective effects of UTI against ischemia/reperfusion injury in numerous diseases (2). Our recent study further showed that UTI can attenuate amplification of central pro-inflammatory cytokine (PIC) signal in rats with transient cerebral ischemia induced by CA, thereby leading to improvement of neurological functions, brain tissue edema and survival (6). UTI has also been reported to attenuate neuronal nuclear factor (NF)-κB and PICs and inhibit PIC apoptotic signals (7-9).

Nuclear factor (erythroid-derived 2)-like 2 (Nrf2) is a transcription factor and as a basic leucine zipper protein it regulates the expression of antioxidant proteins protecting against oxidative damage triggered by injury and inflammation (10). Numerous drugs that stimulate the Nrf2 pathway have been used for treatment of diseases caused by oxidative stress (11). Thus, in this study, in order to determine the engagement of oxidative stress, we first examined Nrf2-antioxidant response element (ARE) pathway in the hippocampus following CA. We further examined superoxide dismutases (SOD), a class of enzymes to catalyze the dismutation of superoxide; 8-isoprostaglandin F2α (8-iso PGF2α, a product of oxidative stress), and 8-hydroxy-2'-deoxyguanosine (8-OHdG, a key biomarker of protein oxidation). We hypothesized that UTI restores Nrf2 and Nrf2-regulated NADPH quinone oxidoreductase-1 (NQO1), improves the levels of SOD, and decreases oxidative production in hippocampus CA1 of ischemic animals. Our overall hypothesis was that UTI has a beneficial role in modulating neurological deficits and survival evoked by CA-induced cerebral ischemia via antioxidative mechanisms.

MATERIALS AND METHODS

All the animal procedures were approved by the Institutional Animal Care and Use Committee of Jilin University, which are in compliance with the Guideline for the Care and Use of laboratory Animals of the U.S. NIH. Seventy-two male Sprague–Dawley rats (200–300g) were used in our research.

The ischemia was produced in the CA model induced by asphyxia. Briefly, the rats were anesthetized with an isoflurane-oxygen mixture (2-5% isoflurane in 100% oxygen). An endotracheal tube was first inserted and attached to a ventilator. The ventral tail artery was cannulated to monitor systemic arterial pressure. The right jugular vein was cannulated for a continuous infusion of saline (at a rate of 0.1 ml/hour) to maintain baseline blood pressure and fluid balance. Body temperature was continuously monitored and maintained at 37°C with a heating pad and external heating lamps. Asphyxia was induced by stopping mechanical ventilation and clamping the tracheal tubes at the end of expiration. Resuscitation efforts began 6 min following induced CA. For this purpose, rats were orotracheally intubated for mechanical ventilation accompanied by chest compression delivered by a mechanical compressor at a rate of 200/min for 5 min. Once spontaneous heartbeat returned, epinephrine (2 μg) was administered to achieve a mean arterial blood pressure of >80 mmHg. Ventilation was adjusted for animals to regain spontaneous respiration and achieve normoxia. In the sham operated animals, the same surgical procedures were performed without cardiac arrest and resuscitation.

The rats were randomly divided into three groups. Group 1 (n=12): the rats received the same surgical procedures and endotracheal intubation was performed with no asphyxia and CPR. Group 2 (n=30): CA and CPR were performed and 0.5 ml of saline (i.p., every 12 hours for 7 days) was given after CA. Group 3 (n=30): CA and CPR were carried out and 20000 units/kg body weight of UTI (i.p., every 12 hours for 7 days) was injected after CA. At the end of each experiment, the rats were sacrificed and then the hippocampus was taken out for biochemical measurements. Seven days after the rats had received all the treatments, the modified method of Neurological Severity Score (mNSS) was used to examine neurological functions, as described previously (6). Note that mNSS was generally used to assess a combination of motor, sensory, and balance functions. Neurological function was graded on a scale of 0–18 (normal score, 0; maximal deficit score, 18). If we found that mNSS score of rats was > 0 before CA, this indicated that the rats were abnormal and they were excluded from the experiment. It is noted that the experiments were performed in a blind manner.

Spatial working memory performance was assessed by recording spontaneous alternation performance in a Y-maze. The maze was made of grey-painted vinyl-chloride. Each arm was 50 cm long, 30 cm high and 10 cm wide and converged at an equal angle. Each rat was placed at the center of the maze and allowed to move freely through it during an 8-minute period. The numbers of arm entries were recorded. An alternation was defined as entries into all arms. The percentage of alternation was calculated as (actual alternations /total entered-2) x100.

Brain edema (brain water content) was determined after CA. The brain slices (2 mm thick) of the hemispheres and cerebellum were cut. The whole brain water content was calculated from all slices. The brain slices were weighed to obtain the wet weight immediately and dried in an oven at 100 C° for 24 h to obtain the dry weight. The cerebellum was used as the internal control. The water content was expressed as the following formula: [(wet weight) − (dry weight)]/(wet weight) × 100%.

The tissues from each rat were sampled for the analysis. In brief, the hippocampus CA1 region of the rats was removed under an anatomical microscopy. Total protein was extracted by homogenizing the hippocampus sample in ice-cold immunoprecipitation assay buffer with protease inhibitor cocktail kit. The lysates were centrifuged and the supernatants were collected for measurements of protein concentrations using a bicinchoninic acid assay reagent kit.

After being denatured by heating at 95°C in an SDS sample buffer, the supernatant samples were loaded onto Mini-Protean TGX Precast gels and electrically transferred to a polyvinylidene fluoride membrane. The membrane was then incubated overnight with primary antibodies: rabbit anti-Nrf2, anti-NQO1 and anti-SOD. After being fully washed, the membrane was incubated with horseradish peroxidase-linked anti-rabbit secondary antibody and visualized for immunoreactivity. All antibodies were obtained from Abcam Co. and Santa Cruz Biotech, USA. The membrane was stripped and incubated with mouse anti-β-actin to show equal loading of the protein. The bands recognized by the primary antibody were visualized by exposure of the membrane onto an X-ray film. Then, the film was scanned and the optical densities of primary antibodies and β-actin bands were determined using the Scion Software. Values for densities of immunoreactive bands/β-actin band from the same lane were determined. Each of the values was then normalized to a control sample.

The levels of 8-iso PGF2α and 8-hydroxy-2'-deoxyguanosine (8-OHdG) were examined using ELISA (Promega Co. and Abcam Co., USA) according to the provided description and modification. Briefly, polystyrene 96-well microtitel immunoplates were coated with affinity-purified rabbit primary antibodies. Parallel wells were coated with purified rabbit IgG for evaluation of nonspecific signal. After overnight incubation, plates were washed. Then, the diluted samples and 8-iso PGF2α/8-OHdG standard solutions were distributed in each plate. The plates were washed and incubated with anti-8-iso PGF2α/8-OHdG galactosidase. Then, the plates were washed and incubated with substrate solution. After incubation, the optical density was measured using an ELISA reader. Using the same method, the levels of PICs including IL-1β, IL-6 and TNF-α were examined usingby ELISA (Promega Co.).

Experimental data were analyzed using ANOVA. As appropriate, Tukey's *post hoc* tests were used. All values were presented as mean ± standard deviation. For all analyses, differences were considered significant at $P < 0.05$. All statistical analyses were performed using SPSS for Windows version 20.0.

RESULTS

Effects of UTI on survival and neurological functions

The survival rate of seven days was 100% (12/12 rats) in sham control rats; 60% (18/30 rats) in CA rats; 83% (25/30 rats) in CA rats injected with UTI. It is noted that the survival rate was increased when CA rats received UTI treatment as compared to CA ratS without treatment (Fig. 1A). Data obtained from those survival rats were included for the analysis in this report.

Also, water content of brain tissues was demonstrated (Fig. 1B), indicating that CA amplified water content of brain tissues in rats and administration of UTI significantly attenuated increases of water content.

Fig. 1C shows that CA increased the mNSS in rats ($P<0.05$, control rats *vs* CA rats; n=12 in control and n=18 in CA group). Fig. 1c further demonstrates that UTI significantly attenuated the impaired mNSS

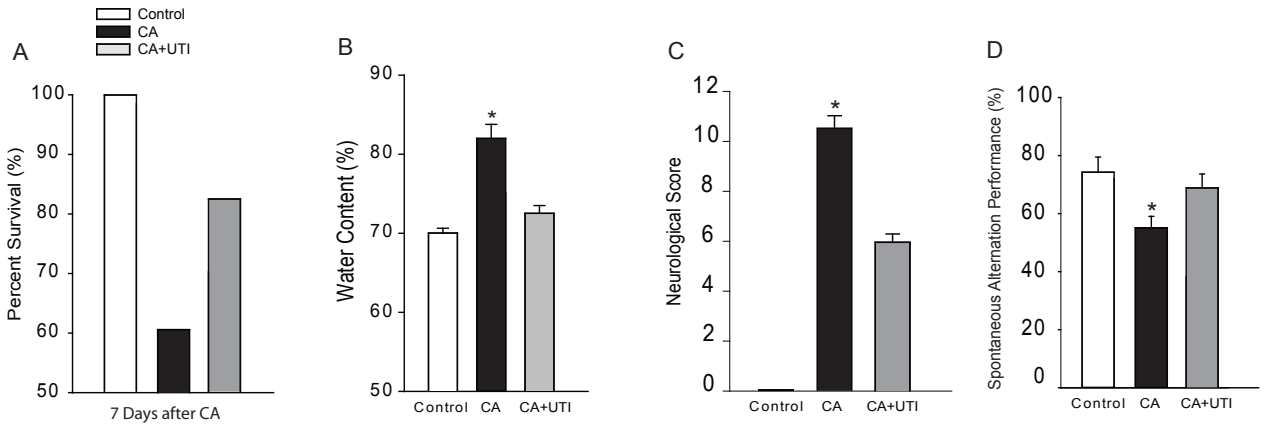

Fig. 1. ***A, B****) The survival rate of 7 days and water content of brain tissues were increased in rats after CA and they were improved by administration of UTI.* ***C****) Neurological functions. The mNSS was increased in rats after CA and it was significantly improved by systemic administration of UTI.* ***D****). Spatial working memory performance was decreased in CA rats and this was greatly restored by UTI. *P<0.05 vs control rats and CA rats injected with UTI. The number of rats=12 in control; =18 in CA group; and =25 in CA group with UTI.*

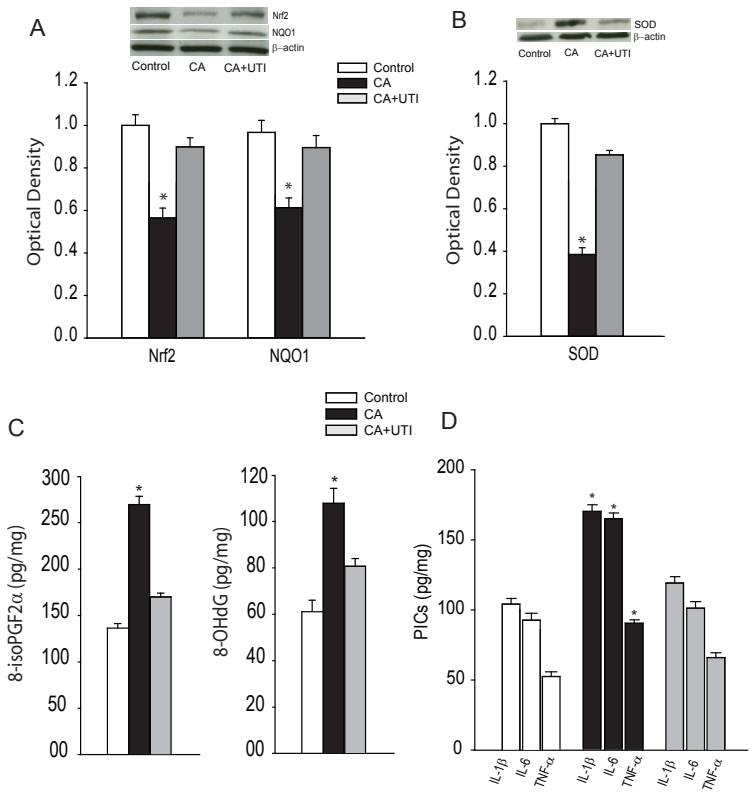

Fig. 2. *Effects of UTI on signal pathways of oxidative stress.* ***A, B****). Protein expression levels of Nrf2-ARE and SOD. Top panel and bottom panel are representative bands and averaged data: Nrf2/NQO1 and SOD were decreased in the hippocampus of CA rats and UTI can restore impaired Nrf2/NQO1 and downregulated SOD. *P<0.05, CA rats vs control rats and CA rats injected with UTI. n=6 in each of control and CA groups; n=8 in CA rats with UTI.* ***C, D****). Induction of CA amplified the levels of oxidative product 8-iso PGF2α and 8-OHdG, and PICs in the hippocampus CA1 region. Systemic administration of UTI attenuated increases of 8-iso PGF2α and 8-OHdG, and PICs in CA rats. *P < 0.05 vs control rats and CA rats injected with UTI. n=12 in control; =18 in CA group; and =25 in CA group with UTI.*

in animals following CA (P<0.05, CA rats with no treatment *vs* CA rats with UTI; n=25 in CA group with UTI).

Spatial working memory performance was also assessed by recording spontaneous alternation performance. Likewise, Fig. 1D shows that the percentage of spontaneous alternation was impaired in CA rats as compared with control rats. A decrease of spontaneous alternation was largely recovered in CA rats with injection of UTI. In addition, the number of arm entries was determined by counting the number of arms each animal entered in the maze during the test as a measure of activity level. No significant differences in the number of arm entries were observed among the three groups.

Engagement of antioxidative mechanisms

Fig. 2A shows that the protein expression levels of Nrf2 and Nrf2-regulated NQO1 were decreased in CA rats and UTI can restore impaired Nrf2 signal expression (P<0.05, CA rats *vs* controls and CA rats with UTI; n=6-8). Similarly, Fig. 2B further shows UTI can improve downregulation of SOD expression (P<0.05, CA rats *vs* controls and CA rats with UTI; n=6-8). Note that expression of Nrf2, NQO1 and SOD was not significantly changed by UTI in the control group.

Fig. 2C shows that 8-iso PGF 2α was increased in the hippocampus of CA rats (P <0.05 *vs* control rats, n=12 in control and n=18 in CA rats). It is noted that administration of UTI significantly attenuated increases of 8-iso PGF2α (P <0.05 *vs* CA rats without treatment; n=25 in CA rats plus UTI). There were no significant differences observed in the levels of 8-iso PGF2α between the control group and CA group with UTI (P >0.05). In addition, Fig. 2C further illustrates that induction of CA significantly increased the levels of 8-OHdG in the hippocampus (P <0.05 *vs* control rats, n=12 in control and n=18 in CA rats) and UTI attenuated increases of 8-OHdG (P <0.05 *vs* CA rats without treatment; n=25 in CA rats plus UTI).

In order to confirm the effectiveness of UTI, PICs in the hippocampus were examined (Fig. 2D). IL-1β, IL-6 and TNF-α were increased in the hippocampus seven days after CA (P <0.05 *vs* control, n=12 in the control group and n=18 in the CA group). Administration of UTI significantly attenuated the amplified levels of IL-1β, IL-6 and TNF-α (P <0.05 *vs* no treatment; n=25 in group: CA plus UTI).

DISCUSSION

Under normal or unstressed conditions, Nrf2 is kept in the cytoplasm by a cluster of proteins that degrade it quickly (12-14). Under oxidative stress, Nrf2 is not degraded, but it travels to the nucleus where Nrf2 binds to a DNA promoter and initiates transcription of anti-oxidative genes and their proteins (12-14). In the nucleus, Nrf2 combines (forms a heterodimer) with a small Maf protein and binds to the ARE in the upstream promoter region of many anti-oxidative genes, and initiates their transcription (14). Our data show that CA impairs the protein expression levels of Nrf2-ARE pathway in the hippocampus. We also observed that downregulation of Nrf2 and NQO1 were accompanied with decreases of SOD. Moreover, we observed that products of oxidative stress 8-iso PGF2α and 8-OHdG were increased in the hippocampus of CA rats. Notably, UTI can significantly recover impairment of Nrf2-ARE and SOD following CA. UTI can also attenuate amplification of 8-iso PGF2α and 8-OHdG levels as well as PICs. Thus, activation of Nrf2-ARE pathway is implicated for benefits to ischemic brain diseases associated with oxidative stress and inflammation (11).

A recent study suggested that CA increases PICs, including IL-1β, IL-6 and TNF-α, and upregulates their receptors IL-1R, IL-6R and TNFR1 in the hippocampus (9). Hypoxia inducible factor-1α (HIF-1α) stimulator or blocking HIF-1α breakdown attenuates the exaggerated PIC signals in the hippocampus induced by CA (9), and as a result neuronal apoptosis and neurological deficits are attenuated (7). This study also indicated that stabilizing HIF-1α attenuates increases of Caspase-3 and TUNEL evoked by CA, and thus improves neurological deficits and neuronal edema (7). In particular, recent studies suggest that administration of UTI plays a protective role in regulating neurological deficits observed in CA rats via central PIC mechanisms (6, 8). Our current study showed that UTI attenuated increases of IL-1β, IL-6 and

TNF-α in the hippocampus induced by CA whereas it decreased products of oxidative stress.

In conclusion, transient global ischemia induced by CA impairs the protein levels of Nrf2-ARE signal and SOD in the hippocampus, thereby leading to increases of products of oxidative stress. Systemic administration of UTI can recover deficiency of Nrf2-ARE and SOD in ischemic animals. As a result, this improves water content of brain tissues, neurological Severity Score, memory performance and survival in CA rats. Our data indicate the beneficial role played by UTI in alleviating cerebral ischemia reperfusion injury via antioxidative mechanisms.

ACKNOWLEDGEMENTS

This study was supported by grants from the First Hospital of Jilin University (JDYY52015016), Norman Bethune Program of Jilin University (No.2015335), Science and Technology Development Program of Jilin Province (20160520160JH), and grants from Health Department of Jilin Province (2012Z005) as well as from the National Natural Science Foundation of China (No.81471830).

REFERENCES

1. Nolan JP, Neumar RW, Adrie C, Aibiki M, Berg RA, Böttiger BW et al. Post-cardiac arrest syndrome: Epidemiology, pathophysiology, treatment, and prognostication: A Scientific Statement from the International Liaison Committee on Resuscitation; the American Heart Association Emergency Cardiovascular Care Committee; the Council on Cardiovascular Surgery and Anesthesia; the Council on Cardiopulmonary, Perioperative, and Critical Care; the Council on Clinical Cardiology; the Council on Stroke. Resuscitation 2008; 79:350-79.
2. Inoue K, Takano H. Urinary trypsin inhibitor as a therapeutic option for endotoxin-related inflammatory disorders. Expert Opin Investig Drugs 2010; 19:513-20.
3. Karnad DR, Bhadade R, Verma PK, Moulick ND, Daga MK, Chafekar ND, Iyer S. Intravenous administration of ulinastatin (human urinary trypsin inhibitor) in severe sepsis: a multicenter randomized controlled study. Intensive Care Med 2014; 40:830-38.
4. Wang G, Wen J, Wilbur RR, Wen P, Zhou SF, Xiao X. The effect of somatostatin, ulinastatin and Salvia miltiorrhiza on severe acute pancreatitis treatment. Am J Med Sci 2013; 346:371-76.
5. Inoue K, Takano H, Yanagisawa R, Yoshikawa T. Protective effects of urinary trypsin inhibitor on systemic inflammatory response induced by lipopolysaccharide. J Clin Biochem Nutri 2008; 43:139-42.
6. Jiang XM, Hu JH, Wang LL, Ma C, Wang X, Liu XL. Effects of ulinastatin on global ischemia via brain pro-inflammation signal. Translational Neurosci 2016; 7:158-63.
7. Liu X, Lu J, Xing J. Stabilization of HIF-1α modulates VEGF and Caspase-3 in hippocampus of rats following transient global ischemia induced by asphyxial cardiac arrest. Life Sci 2016; 151:243-49.
8. Sui B, Li Y, Ma L. Postconditioning improvement effects of ulinastatin on brain injury following cardiopulmonary resuscitation. Exp Ther Med 2014; 8:1301-7.
9. Xing J, Lu J. HIF-1alpha activation attenuates IL-6 and TNF-alpha pathways in hippocampus of rats following transient global ischemia. Cell Physiol Biochem 2016; 39:511-20.
10. Moi P, Chan K, Asunis I, Cao A, Kan YW. Isolation of NF-E2-related factor 2 (Nrf2), a NF-E2-like basic leucine zipper transcriptional activator that binds to the tandem NF-E2/AP1 repeat of the beta-globin locus control region. PNAS 1994; 91:9926-30.
11. Gold R, Kappos L, Arnold DL, et al. Placebo-controlled phase 3 study of oral BG-12 for relapsing multiple sclerosis. New Eng J Med 2012; 367:1098-107.
12. Itoh K, Chiba T, Takahashi S, et al. An Nrf2/small Maf heterodimer mediates the induction of phase II detoxifying enzyme genes through antioxidant response elements. Biochem Biophy Res Comm 1997; 236:313-22.
13. Sekhar KR, Rachakonda G, Freeman ML. Cysteine-based regulation of the CUL3 adaptor protein Keap1. Toxicol Appl Pharmacol 2010; 244:21-26.
14. Yamamoto T, Suzuki T, Kobayashi A, Wakabayashi J, Maher J, Motohashi H, Yamamoto M. Physiological significance of reactive cysteine residues of Keap1 in determining Nrf2 activity. Mol Cell Biol 2008; 28:2758-70.

JOURNAL OF BIOLOGICAL REGULATORS & HOMEOSTATIC AGENTS Vol. 32, no. 2, 289-293 (2018)

LETTER TO THE EDITOR

MEDICAMENTOUS THROMBOLYSIS DISGUISES PULMONARY THROMBOEMBOLISM AS A CAUSE OF DEATH

I. ŠOŠA[1], A. FERENCIC[1], V. STEMBERGA[1], G. ZAMOLO[2], S. ARBANAS[1], I. DASEK[2], M. PERKOVIC[3] and D. CUCULIC[1]

[1]Department of Forensic Medicine and Criminalistics, Rijeka University School of Medicine, Rijeka, Croatia; [2]Department of Pathology, Faculty of Medicine, Rijeka University School of Medicine, Rijeka, Croatia; [3]Odjel za patologiju – Opca bolnica Pula, Pula, Croatia

Received November 22, 2017 – Accepted February 15, 2018

The first two Authors contributed equally to this paper

We report the case of a 31-year-old female who was admitted to the emergency department with symptoms of cardiac arrest and ultimately died in spite of enormous resuscitation efforts. During resuscitation, pulmonary embolism was considered as a possible non-cardiac cause of cardiac arrest, and following its extremely unfavorable prognosis, the fatal outcome was not so surprising. However, since acute pulmonary emboli obstructing blood flow to a lobe or multiple lung segments was suspected, alteplase was indicated and administered. At the autopsy, no venous thrombosis in the vena cava, pelvic veins, or any of the lower extremity veins was documented; conversely, nor were specific signs of pulmonary thromboembolism (PTE) found macroscopically, until this was confirmed by histopathological staining which is not used as a routine diagnostic tool in forensic medicine. In this study, we conclude that PTE is generally overlooked as the principal diagnosis and the cause of death. Rightful postmortem diagnosis could lead to increased vigilance and a change in management in many of such cases, which could result in improved survival. Motivated by providing better awareness of PTE, this study aimed to illustrate unrecognized PTE and pathological findings that were masked by thrombolytic drugs.

To the Editor,

A recent literature review reveals a relative lack of studies on pulmonary embolism found at (1, 2). In the present case, any common symptoms such as chest pain, dyspnoea and hemoptysis were absent. Nor were even some of the classical precursors, such as phlebitis, malignancy, and recent surgery, present (3).

Aside from the capacity of the lungs to remove the thromboemboli, endogenous thrombolysis in which the fibrin networks within a clot are dissolved by enzymatic activity (4), thromboemboli may become fragmentized by exogenous thrombolysis where medicamentous thrombolysis also falls (5). Endogenous thrombolysis is probably how a considerable percentage of emboli (large and small) disappear before morphologic investigation. One form of exogenous thrombolysis involves medicamentous treatment, and it classically involves intravenous administration of thrombolytic agents (e.g., alteplase) that convert native plasminogen to plasmin which, in turn, hydrolyzes the fibrin of thromboemboli, resulting in clot lysis (6-8). Finding microembolism

Key words: alteplase, autopsy, pulmonary thromboembolism

Mailing address:
Dr. Ivan SOSA, PhD, M.D.
Department of Forensic Medicine and Criminalistics,
Rijeka University School of Medicine,
Braće Branchetta 20, 51 000 Rijeka, Croatia
e-mail: ivan.sosa@medri.uniri.hr

0393-974X (2018)

DISCLOSURE: ALL AUTHORS REPORT NO CONFLICTS OF INTEREST RELEVANT TO THIS ARTICLE.

in small arteries suggests fragmentation of large thromboemboli (4) and, without a proper staining technique, the pathologist can hardly provide a reliable opinion on the pulmonary thromboembolism (PTE).

Taking into account that cardiovascular diseases present the most common cause of death in Croatia (9), we present the case of 31-year-old female who suffered a cardiopulmonary arrest and ultimately died. Since the precision of collecting antecedent factors involved before death are lacking, we intend to contribute to a better understanding of PTE, which turned out to be the underlying pathology after all.

Briefly, the objective of this study is to describe immediately unrecognized PTE and pathological findings in the autopsy that are hidden by medicamentous thrombolytic agents (8). It has been often seen that when gross pathology could not evaluate the cause of death, a conclusive opinion could be given by histopathological techniques (10).

Case report

A 31-year-old female suffered a cardiopulmonary arrest and was brought by the ambulance to the Centre for Emergency Medicine of the Clinical Hospital in Rijeka. After corresponding clinical assessment and the ultrasound exclusion of the presence of free liquid in the pericardial, pleural and abdominal cavity, PTE was assessed as a possible cause of the cardiac arrest. This decision resulted in the application of systematic fibrinolytic therapy with 50 mg of alteplase and continuation of the external cardiac massage (5, 6, 8). After one hour in resuscitation there was a return of the spontaneous circulation, which was confirmed clinically and by echocardiography. With all the appropriate measures taken in the post-reanimation care of the patient, in preparation for an emergency multislice computed tomography (MSCT) of the brain and MSCT pulmonary angiography, she re-entered cardiac arrest (10). Alongside all the resuscitation procedures she was administered another 50 mg of alteplase (6, 7). However, despite all the actions undertaken, she succumbed one hour and thirty minutes after admission.

The family of the patient gave informed, signed consent to participate in the study, and consented voluntarily to have samples stored in the manner and for the purpose indicated above.

Postmortem findings

On gross examination, no visible thrombotic formations were present (11). Among nonspecific findings, we recorded cerebral edema, mild cardiac

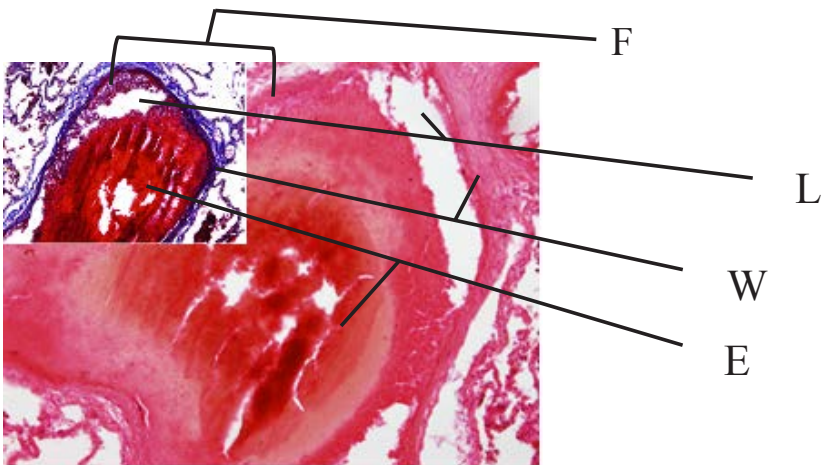

Fig. 1. *Embolus observed in the pulmonary circulation. Lesser microphotography (insert) represents pulmonary tissue stained with Masson's trichrome staining, whilst larger microphotography (x10) represents adjacent section of pulmonary tissue stained with (standard) hematoxylin-eosin (H&E) staining technique.*
L: blood vessel lumen; W: blood vessel wall; E: embolus; F:fibrin mesh

hypertrophy without visible lesions, pulmonary edema and congestion (2, 11).

At the autopsy, the lungs were cut coronally into 1-cm thick slices, and carefully inspected for emboli and other pathological lesions. Blocks of all such lesions were taken for histological examination. The blocks were fixed for a further 24 h in formaldehyde, dehydrated in alcohol, cleared in xylol, and embedded in paraffin wax. Sections (5 microns) were stained with hematoxylin and eosin (H&E) and by the Masson's trichrome method. Microscopic examination showed the peripheral pulmonary arteries to be occluded by thromboembolic masses with the same internal structure. The pulmonary parenchyma was intensely congested with intra-alveolar edema (2).

Histological slices of basal parts taken from both lungs indicated fibrin mesh still visible with Masson's trichrome staining (Fig. 1) which is not a standard staining method in day to day forensic medicine practice. Except for the peripheral rim containing erythrocytes and fibrin visible in H&E stained sections, the rest of the thrombus consisted of acellular, eosinophilic granules with enclosed fibrin and thrombocytes. However, sections stained with Masson's trichrome clearly demonstrated fibrin accumulations combined with erythrocytes and blood remnants located near the blood vessel wall, indicating the existence of thrombotic lesions, and slightly granular emboli in proximal pulmonary arteries (11). These clusters were mainly positioned adjacent to the arterial intima, occluding approximately 70% of the lumen.

DISCUSSION

This presented case highlights how the diagnosis of PTE continues to be challenging to recognize even when it is considered antemortem; thrombolytics can disguise postmortem findings of PTE.

Morphological effects of PTE depend on the size and general condition of the circulation. This case is interesting because the patient died of massive PTE that was disguised due to thrombolytic treatment.

We present a patient admitted to the emergency department after suffering a cardiopulmonary arrest. After clinical assessment and the ultrasound exclusion of the presence of free liquid in the body cavities, we considered PTE as a possible cause of the cardiac arrest (2, 12).

Widespread primary thrombosis in the pulmonary artery, though rare, does occur, particularly with primary pulmonary hypertension. Morphologically, it is difficult to distinguish emboli from primary thrombi in the small vessels of the lung (4). When diagnosed on time and treated properly, PTE rarely causes death. However, despite advances in diagnostic methods, treatment, and prophylaxis, the incidence and mortality rates of acute PTE seem to have changed little in past decades. It has been seen many times that when the cause of death was impossible to determine by gross pathology, the histology came across – like "turned the trumps"; and we could give a conclusive opinion on the involved cardiac pathology (13).

Morphology of PTE depends on the size and general condition of the circulation. Large emboli are usually caught in the main pulmonary artery or its principal branches, or they can settle on the bifurcation as a riding embolus. PTE is, in epidemiological and clinical sense, an exceedingly puzzling condition, especially bearing in mind that it is hard to obtain postmortem data on the disease. Moreover, most fatal episodes can only be identified through autopsy, and this was exactly the scenario of our case (1-3).

Since we could not visualize thrombotic emboli in small pulmonary arteries by standard H&E, we resorted to Masson's trichrome staining (Fig. 1). This staining protocol usually used for collagen fibers was chosen in our case to detect the collagen fibers in tissues such as skin, heart, etc. on formalin-fixed, paraffin-embedded sections, and may also be used for frozen sections (2, 14). The collagen fibers will be stained blue, the nuclei will be stained black and the background is stained red.

None of the pathoanatomic diagnoses found at the autopsy can be taken into consideration as a cause of death by themselves without further tests being made. Generally, PTE is easily overlooked as the major diagnosis and the cause of death. Premortem diagnosis could have led to a change in management in many of these cases, which could have resulted in improved survival.

Whenever the embolic blockage is located distally, there is a greater likelihood of the occurrence of infarction (15). When hemorrhage and lung necrosis are associated, pulmonary infarction is present (7, 16). Disturbed cardiovascular conditions precipitate pulmonary infarction. About three-quarters of pulmonary infarctions occur in the lower lobes, and more than half are multiple. There are different sizes, from barely visible to those occupying larger parts of the lobes. Pulmonary infarcts are typically hemorrhagic and in earlier stages look like arched red, blue areas. Pleura covering the infarcted region is usually roofed by fibrous exudate (15).

Our report emphasizes the importance of autopsies to the medical community. In fact, postmortem examinations allow for the comparison of different clinical techniques, devices, and drugs. Such a multidisciplinary approach to everyday medical issues serves to the betterment of science and positively influences the development of the public health network. Despite whether an autopsy is performed for forensic or pathological purposes, quality informative resources are crucial for a correct pathoanatomical diagnosis. Usually, such information is obtained from clinically managed repositories and consultation meetings. Mainly, due to the fear of medical negligence lawsuits, legal considerations in relation to the autopsy should be a part of any post-autopsy discussion. Since our patient died before the MSCT scan was made, we relied only on the clinical assessment. This knowledge pointed us in a direction where we used a staining method that is not performed regularly, therefore we were able to visualize something that was not apparent. In this way, we confirmed the clinical diagnosis and the correct approach of the physician. No matter that the accent this work gives and its scientific value, it is also proof of the mutual benefits all parties receive in cases where interdisciplinary cooperation is present.

There are, inasmuch, inherited thrombophilic states where defects of coagulation, inherited defects of fibrinolysis, inherited defects of platelets in relation to PTE or inherited defects of enzymatic pathway in relation to development are overviewed. However, it is far beyond the scope of this discussion to follow all inherited factors related to PTE (17).

REFERENCES

1. Dada MA, Ansar NA. Origins of .... the postmortem examination in diagnosis. J Clin Pathol 1996; 49:965-66.
2. Morrell MT, Dunnill MS. The post-mortem incidence of pulmonary embolism in a hospital population. Br J Surg 1968; 55(5):347-52.
3. Roy S, Laerum F, Brosstad F, Kvernebo K, Sakariassen KS. Selective venous thrombolysis with the nipple-balloon catheter: comparative evaluation in vivo. J Vasc Interv Radiol 1999; 10(6):817-24.
4. Wagenvoort CA. Pathology of pulmonary thromboembolism. Chest 1995; 107(1):10S-7S.
5. Subramanian R, White CJ. Mechanical interventions and thrombolytic therapy in venous thrombosis and pulmonary embolism. Ochsner J 2002; 4(1):30-36.
6. Martin C, Sobolewski K, Bridgeman P, Boutsikaris D. Systemic thrombolysis for pulmonary embolism: a review. P T 2016; 41(12):770-75.
7. Goldhaber SZ, Haire WD, Feldstein ML, et al. Alteplase versus heparin in acute pulmonary embolism: randomised trial assessing right-ventricular function and pulmonary perfusion. Lancet 1993; 341(8844):507-11.
8. Vedantham S, Piazza G, Sista AK, Goldenberg NA. Guidance for the use of thrombolytic therapy for the treatment of venous thromboembolism. J Thromb Thrombolysis 2016; 41(1):68-80.
9. Ostroški L. Statistical yearbook of the Republic of Croatia 2012. Zagreb: Croatian Bureau of Statistics; 2012.
10. Henzler T, Barraza JM, Jr, Nance JW, Jr et al. CT imaging of acute pulmonary embolism. J Cardiovasc Comput Tomogr 2011; 5(1):3-11.
11. Gill JR. The medicolegal evaluation of fatal pulmonary thromboembolism. Forensic pathology reviews. Springer; 2005. p. 285-302.
12. Kurkciyan I, Meron G, Sterz F, et al. Pulmonary embolism as a cause of cardiac arrest: presentation and outcome. Arch Intern Med 2000; 160(10):1529-35.
13. Tabib A, Loire R, Chalabreysse L, et al. Circumstances of death and gross and microscopic observations in a series of 200 cases of sudden death associated with arrhythmogenic right ventricular cardiomyopathy and/or dysplasia. Circulation. 2003; 108(24):3000-5.

14. Garvey W. Modified elastic tissue-Masson trichrome stain. Stain Technol 1984; 59(4):213-16.
15. Wacker WE, Rosenthal M, Snodgrass PJ, Amador E. A triad for the diagnosis of pulmonary embolism and infarction. Jama 1961; 178(1):8-13.
16. Babyn PS, Gahunia HK, Massicotte P. Pulmonary thromboembolism in children. Pediatr Radiol 2005; 35(3):258-74. doi:10.1007/s00247-004-1353-y.
17. Konecny F. Inherited trombophilic states and pulmonary embolism. J Res Med Sci 2009; 14:43-56.

LETTER TO THE EDITOR

SUDDEN-ONSET UNILATERAL PTOSIS INDUCED BY PITUITARY MACROADENOMA, WITH FALSE-POSITIVE JOLLY AND NEOSTIGMINE TESTS

G-X. SHEN[1], K-J. WU[1], Z. CHEN[2], Y-F. GAO[2] and G-X. NAN[1]

[1]Department of Neurology, China-Japan Union Hospital of Jilin University, Changchun, Jilin Province, China; [2]Department of Neurosurgery, China-Japan Union Hospital of Jilin University, Changchun, Jilin Province, China

Received January 24, 2018 – Accepted February 15, 2018

The development of ptosis as a consequence of pituitary tumor is an exceptionally rare occurrence. Here, we describe the case of sudden-onset unilateral ptosis induced by pituitary macroadenoma. The condition was characterized by false-positive Jolly and neostigmine tests. These findings mimic oculomotor nerve palsy and make the correct diagnostics rather challenging. The case points to the fact that patients with acquired ptosis need detailed neuroophthalmological examination.

To the Editor,

The development of ptosis (drooping or falling of the upper eyelid) is linked to the dysfunction of the muscles that raise the upper eyelid or problems with innervation of these muscles. Acquired unilateral ptosis can be manifested in a number of conditions including ocular myasthenia gravis (OMG), posterior communicating artery (PCA) aneurysm, trauma, diabetes mellitus, inflammation, or lesions of the lid or orbit. However, ptosis is rarely seen in pituitary tumors. With the growth of pituitary tumor, loss of vision and visual field defects due to compression of the optic nerve and optic chiasm develop as common neurological symptoms. Ptosis as a symptom of oculomotor nerve palsies may occur alone or combined with diplopia or/and dilated pupil.

In regards to oculomotor nerve palsies following pituitary tumor, we searched in article titles and abstracts in the Pubmed database using the term "pituitary ptosis" up until Dec 31, 2017. Almost all reported cases presented as ptosis combined with diluted pupil or/and limited extraocular muscle function. However, isolated ptosis as the sole symptom of oculomotor nerve palsy with pupil-sparing is extremely rare, as only two cases were previously reported (1, 2). Herein, we describe a rare case of unilateral ptosis followed by pituitary macroadenoma mimicking OMG.

Case report

A 41-year-old man developed a sudden-onset prominent right eyelid ptosis as the main complaint for 7 days without diurnal fluctuation. The patient had no history of trauma, diabetes mellitus, drug use, inflammation or lesions of the lid or orbit. On neurological examination, he showed right eyelid ptosis with limited extraocular muscles function, spared bilateral pupil and no other manifestations (Fig. 1A). Jolly test (rapid eye blinking test) (3) showed dramatic aggravation of ptosis covering the right eye (Fig. 1B). Furthermore, 30 min after intramuscular administration of neostigmine (1.5 mg), significant recovery of ptosis was observed, thus indicating positive test finding (Fig. 1C). The

Key words: pituitary adenoma, oculomotor nerve palsy, myasthenia gravis, rapid eye blinking test, neostigmine test

Mailing address:
Guangxian Nan, MD, PhD
Department of Neurology, China-Japan Union Hospital
Jilin University, No. 126 Xiantai Avenue,
Changchun, Jilin Province, 130033, China
Tel.: +86 0431 84995606 - Fax: +86 0431 84995606
e-mail: guanx_n90@163.com

0393-974X (2018)

chest CT showed no significant findings in thymus. Taking into account the positive neostigmine tests, the patient was diagnosed with OMG, and pyridostigmine bromide (60 mg orally 3 times daily) was administered. However, the treatment had no significant therapeutic effects. The subsequent tests for acetycholine receptor antibodies (AChR-Abs) and muscle-specific receptor tyrosine kinase antibodies (MuSK-Abs) were negative. The brain magnetic resonance angiography (MRA) did not reveal intracerebral aneurysm. The magnetic resonance imaging (MRI) demonstrated a giant mass (2.3 x 2.8 x 4.3 cm) in the pituitary fossa. This mass caused the compression of the right optic nerve and optic chiasm, with extension towards right cavernous sinus (Fig. 2). The serum prolactin level was significantly increased, exceeding the level of 4200.0 mIU/L. Ophthalmological examination showed decreased visual acuity (0.02) with optic atrophy on the right eye and mild visual field defects. Pituitary tumor was decompressed by endoscopic transsphenoidal surgery after intravenous steroid administration. Pathological analysis confirmed the diagnosis of pituitary prolactinoma. At one-month follow-up, the ptosis and vision-related symptoms improved. The follow-up MRI demonstrated that the mass had shrunk to a malacic lesion with reduced involvement of the optic nerve and the invasion of cavernous sinus.

The patient signed the informed consent form for publication of this case report.

DISCUSSION

Our patient presented with sudden-onset prominent right eyelid ptosis with a spared pupil as the main complaint. Clinical examination found that pituitary macroadenoma was responsible for the development of this case of isolated ptosis with pupil-sparing. This conclusion was based on the fact that patient's history, brain MRA and lab tests excluded the diagnosis of OMG, PCA aneurysm, trauma, inflammation, or lesions of the lid or orbit. The lesion in pituitary gland was visible on the brain MRI. The pituitary macroadenoma had extension toward right cavernous sinus where oculomotor nerve located in the uppermost coincided with ptosis on the right side. The clinical symptoms progressively improved with decompression of pituitary macroadenoma.

However, we initially misdiagnosed the ptosis as OMG due to specific manifestations observed in this case. Firstly, the isolated ptosis rather than vision loss and visual field defects, the most common symptoms in a pituitary tumor, was the main complaint. As ptosis was a notable manifestation with the right eye covered, the vision loss may have been overwhelmed by ptosis and received less attention. Secondly, the positive result of non-invasive bedside rapid eye blinking test and more convincing neostigmine test are suggestive of possible OMG. To our knowledge, false-positive results of neostigmine test have never been reported, but an alternative edrophonium test was reported to produce false-positive results in patients with intracranial mass and various neuromuscular diseases, such as amyotrophic lateral sclerosis (ALS), botulism, Guillain-Barre syndrome, as well as in patients with drug-induced symptoms (4, 5). Of all the muscles supplied by the oculomotor nerve, *levator palpebrae superioris* was the most commonly affected one in the cases of oculomotor palsies following pituitary tumors (1, 6). Regardless of the stage of tumor growth, ptosis occurred and manifested with loss of vision or visual field defects in varying degrees (7). The topographic arrangement of the fibers within the oculomotor nerve in the cavernous sinus and the corresponding neuromuscular mechanisms remain to be elucidated. Oculomotor palsy in the late stage of tumor growth is likely to arise from progressive mechanical compression, but in the sudden-onset cases it may be attributed to insufficient extraneural blood supply originating from branches of the meningohypophyseal trunk to the intracranial oculomotor nerve (7, 8).

In conclusion, unilateral ptosis as the sole symptom of partial oculomotor nerve palsy can occur in patients with pituitary adenoma mimicking OMG, and positive Jolly and neostigmine test are not always suggestive of OMG. In addition, our case is a reminder that patients with acquired ptosis need detailed neuroophthalmological examination.

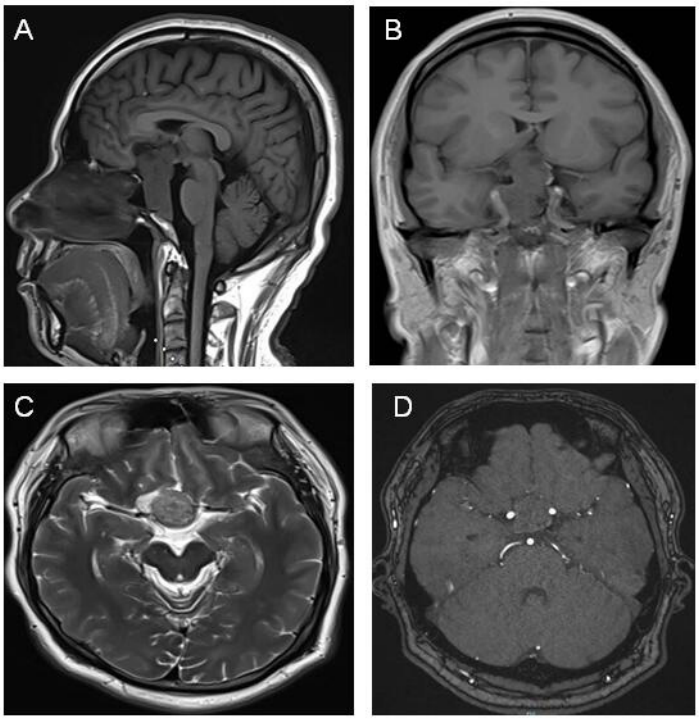

Fig. 1. *The changes of ptosis during auxiliary tests. Right eyelid ptosis was shown at rest (**A**). Dramatic aggravation of ptosis covering the right eye during Jolly test with repetitive blink for 30 times (**B**). Neostigmine test revealed significant recovery of ptosis approximately 30 minutes after intramuscular injection (**C**).*

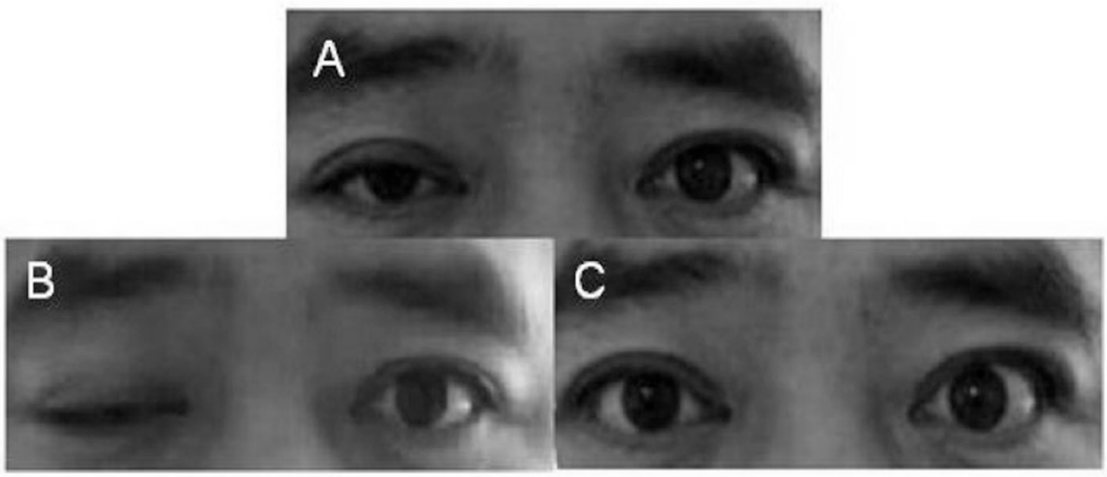

Fig. 2. *Pituitary macroadenoma. Sagittal T1-weighted (**A**), coronal T1-weighted (**B**) and axial T2-weighted images (**C**) reveal a 2.3 x 2.8 x 4.3 cm-sized giant mass in the pituitary fossa with the compression of the right optic nerves and extension toward right cavernous sinus.*

REFERENCES

1. Yen MY, Liu JH, Jaw SJ. Ptosis as the early manifestation of pituitary tumour. Br J Ophthalmol 1990; 74:188-91.
2. Robert CM Jr, Feigenbaum JA, Stern EW. Ocular palsy occurring with pituitary tumors. J Neurosurg 1973; 38:17-19.
3. Ahmed SV. Innovative bedside 'screening' test for myasthenia gravis. BMJ Case Rep 2010; doi:10.1136/bcr.08.2008.0724
4. Dirr LY, Donofrio PD, Patton JF, Troost BT. A false-positive edrophonium test in a patient with a brainstem glioma. Neurology 1989; 39:865-67.
5. Oh SJ, Cho HK. Edrophonium responsiveness not necessarily diagnostic of myasthenia gravis. Muscle Nerve 1990; 13:187-91.
6. Chuang CC, Chen E, Huang YC, Tu PH, Chen YL, Pai PC. Surgical outcome of oculomotor nerve palsy in pituitary adenoma. J Clin Neurosci 2011; 18:1463-68.
7. Cho WJ, Joo SP, Kim TS, Seo BR. Pituitary apoplexy presenting as isolated third cranial nerve palsy with ptosis: two case reports. J Korean Neurosurg Soc 2009; 45:118-21.
8. Cahill M, Bannigan J, Eustace P. Anatomy of the extraneural blood supply to the intracranial oculomotor nerve. Br J Ophthalmol 1996; 80:177-81.

JOURNAL OF BIOLOGICAL REGULATORS & HOMEOSTATIC AGENTS Vol. 32, no. 2, 299-305 (2018)

LETTER TO THE EDITOR

EXPRESSIONS AND CLINICAL SIGNIFICANCE OF FACTORS RELATED TO ACUTE CORONARY SYNDROME

H. SUN, J. ZHANG, Y. ZHENG and S. SHANG

Department of Cardiology, Traditional Chinese Medicine Hospital of Zhengzhou, Zhengzhou, Henan, China

Received December 21, 2017 – Accepted February 8, 2018

The first two Authors contributed equally to this work

Acute coronary syndrome (ACS) is the acute stage of coronary artery disease, which remains a major cause of mortality and morbidity. It is essential to explore the role of matrix metalloproteinase -2 (MMP-2) and interleukin (IL)-18 and their association with disease in patients with severe ACS. Circulating MMP-2 and IL-18 levels were measured using enzyme linked immunosorbent assay (ELISA) in 94 subjects with acute coronary syndrome (ACS, n=38), stable angina pectoris (SAP, n=27) and healthy individuals (control group, n=29). We examined the correlations between the levels of MMP-2 and IL-18 and cardiac risk factors in ACS. Logistic regression analysis was performed to screen for factors that predict ACS. Both MMP-2 and IL-18 concentrations were increased in the ACS group compared to the SAP group or control group (*P*<0.01). Especially, MMP-2 and IL-18 were highly expressed in the patients with ST elevated myocardial infarction (STEMI). Both serum levels of MMP-2 and IL-18 in the single-, double- and triple-vessel lesion group were higher compared to the control group (*P*<0.01). MMP-2 levels were positively correlated with IL-18 (r=0.639, *P*<0.01), CK-MB (r=0.47, *P*=0.003) and hs-CRP levels (r=0.583, *P*<0.01). The logistic regression analysis showed that increases in MMP-2 levels may be a powerful predictor of ACS. Thus, the changes in levels of serum MMP-2 and IL-18 may be useful in the diagnosis of ACS and prediction of its prognosis.

To the Editor,

Acute coronary syndrome (ACS), the acute stage of coronary artery disease, remains a major cause of mortality and morbidity. Much attention has been focused on the potential role of inflammatory mediators as prognostic or diagnostic markers or therapeutic targets of atherosclerotic cardiovascular disease (1).

MMP-2 Matrix metalloproteases (MMPs) are critical for vascular remodeling by regulating degradation of the extracellular matrix (ECM) (2). Increasing evidence shows that MMP-2 act specially on the basement membranes and practically degraded collagen, which play a pathogenic role in the development of the atherosclerotic plaques (3-4). Interleukin (IL)-18, a family member of IL-1 family cytokines, exhibits characteristics of other pro-inflammatory cytokines including increase in cell adhesion molecules, nitric oxide synthesis, and chemokine production (5). IL-18 is known as a

Key words: matrix metalloproteinase -2, interleukin-18, acute coronary syndrome

Mailing address:
Dr Shuzhong Shang,
Department of Cardiology,
Traditional Chinese Medicine Hospital of Zhengzhou,
No.65 Wenhuagong Road,
Zhengzhou 450052, Henan, China
e-mail: 634161707@qq.com

0393-974X (2018)

DISCLOSURE: ALL AUTHORS REPORT NO CONFLICTS OF INTEREST RELEVANT TO THIS ARTICLE.

predictor of cardiovascular death in cardiovascular disease (CVD) patients and is involved in atherosclerotic plaque destabilization (6).

However, clinical data regarding the correlation between serum concentrations of MMP-2 and IL-18 and the severity of ACS are limited. Hence, serum concentrations of these biomarkers and their relationship with disease severity in patients with ACS were investigated in the present study.

MATERIALS AND METHODS

Patients

A total of 94 subjects were enrolled in the study, including 65 patients with CAD from the Traditional Chinese Medicine Hospital of Zhengzhou in China and 29 healthy individuals (13 men, mean age 58.07±9.12 years) as the control group from the year of 2015 to the year of 2017. All the patients were divided into two groups: one group with acute coronary syndrome including ST-elevation acute myocardial infarction (STEMI) or unstable angina pectoris (UAP), another group with stable angina pectoris (SAP). We performed coronary angiography (CAG) on each patient. This study was approved by the ethics committee of Traditional Chinese Medicine Hospital of Zhengzhou and was in accordance with the Helsinki Declaration. Written informed consent was obtained from all participants.

Clinical definition

CAD was defined as the angiographic evidence of stenosis in any epicardial coronary artery presence of a 50% or greater decrease in internal diameter (7). The definition of STEMI was according to criteria stated by the consensus document of the Joint European Society of Cardiology/American College of Cardiology Committee for the redefinition of myocardial infarction: a typical increase and gradual decrease (troponin) or more rapid rise and fall (CK-MB) of biochemical markers of myocardial necrosis and at least one of the following: ischemic symptoms, electrocardiogram (ECG) changes indicative of new ischemia (ST segment elevation), development of pathologic Q waves on ECG, and imaging evidence of a new loss of viable myocardium or new regional wall motion abnormality (8). In case of UAP, the diagnostic criteria constituted chest pain at rest with either an ST segment depression of at least 0.1 mV or a T-wave inversion in 2 or more continuous electrocardiographic leads and no biomarkers of myocardial necrosis (based on two or more blood samples collected at least 6 h apart, with a reference limit of the 99th percentile of the normal population). NSTEMI is distinguished from UAP by elevated levels of cardiac enzymes and biomarkers of myocyte necrosis (9). The criteria of SAP included chest pain for at least 6 months accompanied by evidence of severe coronary artery disease on coronary angiography, with no clinically evident ischemic episodes during the week preceding arteriography (10). CAD patients with a history of cardiomyopathy, valvular heart disease, severe renal failure, respiratory insufficiency, severe hepatic disease, malignant neoplasia or terminal cachexia, active infective diseases, peripheral angiopathy, or cerebral vessel diseases were excluded. Individuals with a history of CVD (myocardial infarction, unstable angina, stroke, or cardiovascular revascularization), type 2 diabetes, stage 2 hypertension (resting blood pressure ≥160/100 mmHg), malignancy, or severe renal or hepatic disease were excluded from the healthy control groups.

Data collection

Trained doctoral research assistants retrospectively reviewed all individual medical records. Demographic characteristics (age, sex) and data regarding the presence of cardiac risk factors (body mass index, hypertension, family history of CAD and smoking status were collected. In addition, biochemical factors such as total cholesterol (TC), triglyceride (TG), low-density lipoprotein cholesterol (LDL-C), high-density lipoprotein cholesterol (HDL-C), and high-sensitivity C-reactive protein (hs-CRP) were measured by the clinical laboratory of the hospital. Our hospital used two-dimensional echocardiography combining a digital imaging system (Vivid-7; GE Medical System, Willoughby, Ohio, USA) assessed the left-ventricular ejection fraction (LVEF, %).

Coronary angiography

All subjects enrolled in the protocol underwent diagnostic CAG using standard techniques. The angiographic analysis was conducted by two experienced interventional cardiologists who were unaware of the subjects' clinical information. The number of involved coronary branches were used to assess the extent and severity of CAD. According to the results of CAG, patients with CAD were grouped into single-vessel, double-vessel, and triple-vessel disease groups.

Enzyme linked immunosorbent assay detection of MMP-2 and IL-18

Peripheral blood samples were collected from all subjects upon admission and allowed to clot by leaving undisturbed at room temperature for 15-30 min. The clot was removed by centrifuging at 2000 rcf for 10 min at 4°C, then subsequently stored at -80°C. Serum levels of IL-18 and MMP-2 were analyzed with Enzyme linked immunosorbent assay (ELISA) kit (Nanjing Jiancheng Technology Industry Co. Ltd., Nanjing, China).

Statistical analysis

SPSS version 20.0 (IBM SPSS Inc, Chicago, USA) was used for data analysis. Continuous variables with normal distribution were presented as mean ± standard deviation (SD), otherwise as median (interquartile range). The Shapiro-Wilk test evaluated normality. Categorical variables were presented as absolute and relative frequencies. Mean values in groups were compared by parametric statistics (Student's *t*-test and ANOVA) or non-parametric statistics (Mann–Whitney and Kruskal–Wallis tests), depending on the distribution of the variable of interest. Pearson's regression analysis (normal distribution) or Spearman's test (non-normal distribution) were used for the correlation studies. Multiple logistic regression analysis with

Table I. *Baseline characteristics of the study participants.*

Clinical variables	ACS group	SAP group	Control group
Number of patients	38	27	29
Sex(Male/Female)	16/22	17/10	13/16
Age(years)	59.34±10.24	59.26±11.93	58.07±9.12
BMI(kg/m^2)	23.25±0.88 $^{\#}$	22.69±1.26	22.51±1.10
Medical History			
Hypertension (%)	24(63.1)$^{\#}$	21(77.8)$^{\#}$	9(31.0)
Family history of CAD (%)	6(15.8)	3(11.1)	1(3.4)
Smoking history (%)	4(10.5)	8(29.6)	4(13.8)
Diagnostic tests			
TC(mmol/L)	4.34±1.14	4.43±1.15	3.79±0.85
TG(mmol/L)	1.60(1.00,2.15)	1.49(0.88,2.53)	1.34(0.97,2.14)
LDL-C(mmol/L)	2.63±0.90$^{\#}$	2.75±0.86$^{\#}$	2.11±0.63
HDL-C(mmol/L)	1.03(0.92,1.21)$^{\#}$	1.09(0.83,1.20)$^{\#}$	1.20(1.06,1.46)

Data are expressed as mean ± standard deviation or median (inter-quartile range).
ACS: acute coronary syndrome; SAP: stable angina pectoris; BMI: body mass index;
CAD: coronary artery disease; TC: total cholesterol; TG: triglyceride; LDL-C: low-density lipoprotein cholesterol; HDL-C: high-density lipoprotein cholesterol.
** $P<0.05$ in comparison with SAP group; $^{\#}P<0.05$ in comparison with control group.*

enter method was carried out to identify risk factors that contributed to occurrence of ACS. P<0.05 was considered as statistically significant.

RESULTS

Basic characteristics of the subjects

Thirty-eight patients with ACS, 27 with SAP, and 29 healthy individuals were enrolled in this study. The basic clinical characteristics of the study participants are presented in Table I. There was no significant difference in gender, age, history of smoking, or family history of CAD in these three groups. The expression of TC and TG had no differences in statistical levels, however, compared with the healthy group, more patients with ACS had

Table II. *Comparisons of cardiac biomarkers and plasma levels of MMP-2 and IL-18 in each group.*

	ACS group	SAP group	Control group
Number of patients	38	27	29
MMP-2(ng/L)	623.2±166.5*#	182.5±74.45	109.3±46.91
IL-18(ng/L)	37.04±10.64*#	10.27±4.29	7.08±5.23
hs-CRP(mg/L)	8.88(3.59,11.83)*#	1.56(0.68,3.33)	1.05(0.54,2.69)
CK-MB(U/L)	23.00(15.00,41.00)*#	12.00(10.00,16.00)	11.00(9.00,14.50)
LVEF (%)	60.00(49.75,63.00)*#	63.00(61.00,64.00)	63.00(61.00,65.00)

Data are expressed as mean ± standard deviation or median (inter-quartile range).
*ACS: acute coronary syndrome; SAP: stable angina pectoris; MMP-2: matrix metalloproteinase-2; IL-18: interleukin-18; hs-CRP: high-sensitivity C-reactive protein; LVEF: left ventricular ejection fraction. * P<0.05 in comparison with SAP group; #P<0.05 in comparison with control group.*

Table III. *Logistic regression analysis for the detection of independent relationship with the occurrence of ACS.*

Variables	*b*	*SE*	Wald X^2	*OR*	95%CI	*P* value
Constant	-3.44	1.68	4.19	0.03	-	0.041
MMP-2	0.02	0.01	7.29	1.02	1.01-1.05	0.016
IL-18	-0.06	0.09	0.36	0.95	0.79-1.13	0.547
HDL	-2.30	1.48	2.41	0.10	0.05-1.82	0.12
LDL-C	1.22	0.58	4.47	3.39	1.09-10.534	0.034
hs-CRP	-0.09	0.09	1.04	0.91	0.77-1.09	0.31

ACS: acute coronary syndrome; SE: standard Error; OR: odds ratio; CI: confidence interval; MMP-2: matrix metalloproteinase-2; IL-18: interleukin-18; HDL-C: high-density lipoprotein cholesterol; LDL-C: low-density lipoprotein cholesterol; hs-CRP: high-sensitivity C-reactive protein.

a history of hypertension, higher LDL-C levels and lower HDL-C levels (P<0.05).

Comparison of cardiac biomarkers and serum levels of MMP-2 and IL-18 in each group

The comparisons of serum levels of MMP-2 and IL-18 as well as related cardiac biomarkers in the three groups are shown in Table II,. A higher expression of MMP-2 and IL-18 in patients with ACS compared to the SAP group or control group (P<0.01) was shown; hs-CRP, CK-MB and LVEF were much higher in the ACS group compared to the SAP group or control group (P<0.01). Patients with SAP had a higher expression of IL-18, MMP-2, hs-CRP, and CK-MB, but there was no difference when compared to the control group (P>0.05). Especially, expressions of MMP-2 and IL-18 were much higher in the patients with STEMI when compared with those in patients with NSTEMI/UAP (Fig. 1).

Comparison of concentrations of MMP-2 and IL-18 in single, double and triple-vessel disease groups

The expressions of MMP-2 were (350.8±209.50) ng/L in the single-vessel group, (454.10±289.40) ng/L in the double-vessel group and (547.20±244.00) ng/L in the triple-vessel group. The expressions of MMP-2 in the vessel lesion groups were higher than in the control group (109.30±46.91) ng/L (P<0.01). The expressions of IL-18 were (18.78±12.77) ng/L in the single-vessel group, (29.10±16.98) ng/L in the double-vessel group and (31.93±15.07) ng/L in the triple-vessel group. The expressions of IL-18 in the vessel lesion groups were higher than the control group (7.08±5.23) ng/L (P<0.01). However, there was no significant difference in serum levels of MMP-2 and IL-18 between the double and triple-vessel disease groups. Meanwhile, the single-vessel disease group had much lower levels of MMP-2 and IL-18 compared to the double-vessel or triple-vessel lesions groups (P<0.01).

Correlation of MMP-2 and IL-18 among each other and with clinical parameters of ACS patients

The correlated results are presented of the serum biomarkers in patients with ACS. IL-18 was significantly positive correlated with MMP-2 (r=0.639, P<0.01). In addition, both MMP-2 and IL-18 positively correlated with hs-CRP (r=0.583, P<0.01; r=0.603, P<0.01). The positive correlation was observed in the analysis results of MMP-2 or IL-18 with CK-MB (r=0.470, P<0.01; r=0.514, P<0.01).

Logistic regression analysis for the detection of an independent predictor of ACS

To determine the association of possible risk factors for ACS and the occurrence of ACS, we performed logistic regression analysis with hs-CRP, LDL-C, HDL-C, IL-18 and MMP-2 as covariates and with or without ACS as dependent variables. With the enter method, Wald, the binary logistic

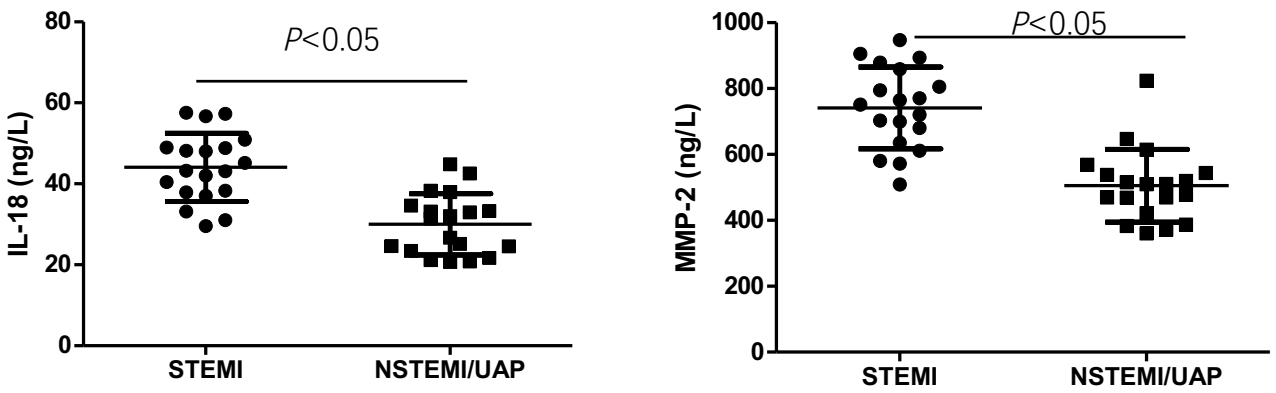

Fig. 1. *Expression of IL-18 and MMP-2 in patients with STEMI or NSTEMI/USP.*

regression analysis, showed that increases in MMP-2 and LDL-C were powerful predictive factors for the occurrence of ACS (Table III).

DISCUSSION

In the present study, MMP-2 and IL-18 concentrations were expressed differently in the groups with coronary vessel lesions, which may reflect the stenosis degree of coronary vessels to some extent. Also, MMP-2 and IL-18 expressions were much higher in the ACS group (Table II), especially in the patients with STEMI (Fig. 1), which provided more evidence that increased MMP-2 and IL-18 may promote atherosclerotic plaques prone to rupture. Thus, inhibiting IL-18 and MMP-2 biology activity may protect cardiac tissue from injury (11). In addition, IL-18 had positive correlation to MMP-2, and both IL-18 and MMP-2 were positively correlated with hs-CRP and CK-MB in patients with ACS, which further confirmed the interactive effect on the atherosclerosis-involved inflammation and reflected the severity of myocardial injury. MMP-2 has been considered to play a role in the process of atherosclerotic lesions by modulating the cell-to-cell communication with activated surrounding cells, such as inflammatory cells (2). These two factors interact with each other and thus enhance the process of atherosclerosis. Furthermore, MMP-2 and LDL-C played roles in predicting the development of ACS. Some limitations of our study must be considered. Troponin is a far more specific marker and it would be important to look at troponin in a further study. Larger clinical trials, longer follow-up and research to uncover underlying mechanisms are needed to validate the findings of this study. In conclusion, the results of our study indicated that the variation in serum MMP-2 and IL-18 concentrations may reflect the degree of inflammation in ACS and the severity of coronary arterial atherosclerosis. The determination of MMP-2 may aid in predicting the development of ACS.

ACKNOWLEDGEMENTS

This study was supported by the Technology Talents Team Construction Program of Zhengzhou City-Science and Technology Talents (121PLJRC538).

REFERENCES

1. Apostolakis S, Spandidos D. Chemokines and atherosclerosis: focus on the CX3CL1/CX3CR1 pathway. Acta Pharmacol Sin 2013; 34:1251-56.
2. Dollery CM, McEwan JR, Henney AM. Matrix metalloproteases and cardiovascular disease. Circ Res 1995; 77:863-68.
3. Galis ZS, Sukhova KG, Lark MAW, Libby P. Increased expression of matrix metalloproteases and matrix degrading activity in vulnerable regions of human atherosclerotic plaques. J Clin Invest 1994; 94:2493-503.
4. Brown DL, Hibbs MS, Kearney M, Loushin C, Isner JM. Identification of 92-kDa gelatinase in human coronary atherosclerotic lesions. Association of active enzyme synthesis with unstable angina. Circulation 1995; 91:2125-33.
5. Dinarello CA, Novick D, Kim S, Kaplanski G. Interleukin-18 and IL-18 binding protein. Front Immunol 2013; 4:289.
6. Trøseid M, Seljeflot I, Arnesen H. The role of interleukin-18 in the metabolic syndrome. Cardiovasc Diabetol 2010; 9:11.
7. Smith SC Jr, Dove JT, Jacobs AK, et al. ACC/AHA guidelines for percutaneous coronary intervention: a report of the American College of Cardiology/American Heart Association Task Force on Practice Guidelines (Committee to Revise the 1993 Guidelines for Percutaneous Transluminal Coronary Angioplasty). J Am Coll Cardiol 2001; 37:2215-39.
8. Alpert JS, Thygesen K, Antman E, Bassand JP. Myocardial infarction redefined--a consensus document of The Joint European Society of Cardiology/American College of Cardiology Committee for the redefinition of myocardial infarction. J Am Coll Cardiol 2000; 36:959-69.
9. Anderson JL, Adams CD, Antman EM, et al. 2011 ACCF/AHA Focused Update Incorporated Into the ACC/AHA 2007 Guidelines for the Management of Patients With Unstable Angina/Non-ST-Elevation Myocardial Infarction: a report of the American College of Cardiology Foundation/American Heart

Association Task Force on Practice Guidelines. Circulation 2011; 123:426-579.

10. Gibbons RJ, Abrams J, Chatterjee K, et al. ACC/AHA 2002 guideline update for the management of patients with chronic stable angina--summary article: a report of the American College of Cardiology/American Heart Association Task Force on practice guidelines (Committee on the Management of Patients With Chronic Stable Angina). J Am Coll Cardiol 2003; 41:159-68.
11. Wang M, Markel TA, Meldrum DR. Interleukin 18 in the heart. Shock 2008; 30:3-10.

LETTER TO THE EDITOR

GLUCOCORTICOIDS IN COMBINATION WITH URSODESOXYCHOLIC ACID IN THE TREATMENT OF AUTOIMMUNE HEPATITIS

WY. LI[1], XS. YANG[2] and YC. WANG[2]

[1]Department of Infectious Diseases, Binzhou People's Hospital, Shandong, China; [2]Department of Rheumatism, Binzhou People's Hospital, Shandong, China

Received August 19, 2017– Accepted February 16, 2018

Autoimmune hepatitis (AH) is usually manifested as chronic hepatitis in clinics; it mayl evolve to liver cirrhosis, hepatic failure, and even death if treatment is delayed. To investigate the clinical efficacy of glucocorticoids in combination with ursodesoxycholic acid in the treatment of glucocorticoids in combination with ursodesoxycholic acid, one hundred and twenty patients with AH who were admitted to the hospital from February 2014 and February 2016 were selected and randomly divided into an observation group and a control group using random number table. Patients in the control group were treated by glucocorticoids only, while patients in the observation group were treated by ursodesoxycholic acid and glucocorticoids. Patients in both groups were treated for six months. The clinical efficacy of the two groups was evaluated after treatment. The levels of alanine aminotransferase (ALT), aspartate aminotransferase (AST), direct bilirubin (DBIL) and total bilirubin (TBIL) of the two groups both decreased after treatment (P<0.05), the improvement of the level of liver function of the observation group was superior to that of the control group, and the difference was statistically significant (P<0.05); after treatment, the levels of serum immunoglobulin G (IgG) and immunoglobulin m (IgM) of both groups significantly reduced after treatment, and the difference within groups before and after treatment had no statistical significance (P<0.05). The reduction of the immunological indicators of the observation group was more remarkable after treatment, and the difference between the two groups had statistical significance (P>0.05). The complete remission rate of the observation group was significantly higher than that of the control group; the incidence of adverse reactions was lower than that of the control group, and the difference had statistical significance (P<0.05). Thus it can be concluded that glucocorticoids in combination with ursodesoxycholic acid has favorable efficacy in treating AH as it can promote the improvement of liver function and effectively reduce the dose of glucocorticoids and the incidence of adverse reactions. The therapy is of great clinical values.

To the Editor,

Autoimmune hepatitis (AH), a clinical chronic hepatitis syndrome, has a higher incidence among females than males. Autoimmune response is induced by unable to identify liver antigen components because of decreased immunotolerance (1, 2), however the fundamental cause has not yet been identified. It has been hypothesized to be correlated to some environmental or infection factors (3, 4). AH has many clinical manifestations, is usually occult at onset and

Key words: autoimmune hepatitis, glucocorticoids, ursodesoxycholic acid

Mailing address:
Dr Wenyu Li,
No.515 Huanghe 7th Road,
Department of Infectious Diseases,
Binzhou People's Hospital,
Binzhou, Shandong, 256610, China
e-mail: liweny0543@163.com

0393-974X (2018)

may also be acute. Immunosuppressors are frequently used as treatment, for example, prednisone which is the first choice in the treatment (5), however its long-term administration can result in severe side effects, hence some patients stop treatment because of intolerance.

In recent years, the efficacy of ursodesoxycholic acid as a nontoxic hydrophilic cholic acid in the treatment of AH has gradually been given attention. One study (6) suggested that glucocorticoids in combination with ursodesoxycholic acid could reduce the adverse reactions induced by glucocorticoids, which is more beneficial to the recovery of patients. In this study HA patients were treated with glucocorticoid monotherapy and glucocorticoids in combination with ursodesoxycholic acid to explore the values, and found that the combination therapy gave satisfactory results.

MATERIALS AND METHODS

Study subjects

One hundred and twenty patients with autoimmune hepatitis who were admitted to the Binzhou People's Hospital between February 2014 and February 2016 were selected for this study. All the patients were diagnosed referring to the simplified diagnostic criteria of AH formulated by international autoimmune hepatitis group (2008) (8). The biopsy results of liver tissues satisfied the diagnostic criteria. Patients who had other category of hepatitis, severe liver and kidney function deficiency, gastrointestinal bleeding or mental disturbance, refused to coordinate with treatment, or had recently taken drugs such as glucocorticoids and immunosuppressor, and pregnant and lactant women were excluded. The study was approved by the ethics committee of Binzhou People's Hospital, and all the patients signed informed consent.

They patients were randomly divided into an observation group and a control group. In the observation group, there were 17 males and 43 females aged from 34 to 49 years (average 43.15±5.17 years); they had had AHfor one to two years (average 1.23±0.21 years); four patients also suffered from liver cirrhosis. In the control group, there were 21 males and 39 females aged from 33 to 47 years (average 42.23±4.08 years); they had had AH for 0.5 to 2 years (average 1.15±0.25 years); six patients also suffered from liver cirrhosis. The difference of data between the two groups had no statistical significance ($P>0.05$).

Treatment

The patients in the control group were treated by prednison (Xinxiang Forgood Pharmaceutical Co., Ltd., China; batch no.: H41020210; specification: 5 mg). The primary dose was 60 mg/d. After seven days of administration, there was a reduction of 10 mg every seven days. After 35 days, the dose became 20 mg/d till the disease condition was relieved. The patients in the observation group were given ursodeoxycholic acid capsules (Dr. Falk Pharma GmbH; batch no.: H20100502; specification: 250 mg) and prednison. The dose of ursodeoxycholic acid capsules was 500 mg/d, twice one day. The dose of prednison of the observation group was half that of the control group. The treatment of both groups lasted for six months.

Detection of baseline parameters

Fasting venous blood was collected before treatment. Serum antinuclear antibody (ANA) was detected using indirect immunofluorescence and kits (Euroimmun Company, Germany). The sample buffer was diluted in a ratio of 1:100; the diluent was dropped on a antigen-coated microtiter plate, 25 μl each well. The plate was sealed after negative and positive comparison and incubated. Fluorescein isothiocyanate (FITC) labeled anti-human immunoglobulin G (IgG) was added, followed by washing. Titer ≥1:100 was determined as positive. Anti-liver cytosol antibody type 1 (LC-1) and anti-soluable liver antigen antibodies/anti-liver pancreas (SLA/LP) were detected using immunoblotting. Serum diluent was added to the antigen-coated microtiter plate, 50 μl each well. Whether the serum diluent was positive or negative was determined before plate sealing. Then the plate was incubated for 0.5 h, followed by washing. Enzyme labeled anti-human IgG was added. It was placed in a reaction zone after incubation, followed by 10 min of color development and washing. It was determined as positive if strongly stained band was clearly observed.

Detection of liver function and immune indexes

Four ml of fasting venous blood was collected from each patient before and after treatment, respectively, and centrifuged. The supernatant was taken and detected. Beckman-coulter instrument and the matched reagents were used to detect liver function indexes such as serum total bilirubin (TBil), direct bilirubin (DBIL), alanine

aminotransferase (ALT) and aspartate aminotransferase (AST). Immunological indexes such as IgG and IgM were detected using HITACHI 7600 biochemical analyzer.

Clinical efficacy

The determination criteria for the curative efficacy (7) were as follows. If the clinical symptoms basically disappeared and the levels of ALT and TBIL decreased to the levels which were two times that of the normal values, it was determined as complete response. If the clinical symptoms basically remitted and ALT and TBIL decreased to the levels which were higher than half of the levels before treatment, it was determined as effective. If the clinical symptoms had no remission, the disease condition aggravated, or the patient died, it was determined as ineffective. The formula of the overall effective rate was: overall effective rate=(number of cases with significant efficacy+number of cases with effective effect)/total number of cases×100%.

The occurrence of adverse reactions of the two groups were observed and recorded.

Statistical analysis

Data were statistically processed using SPSS ver. 21.0. Measurement data were expressed by mean ± standard deviation (SD). The comparison of data before and after treatment was performed using paired sample *t*-test; the comparison between groups was performed by independent sample *t*-test. Enumeration data were expressed by rate or constituent ratio; the comparison between groups was performed by *Chi*-squared test. Difference was considered as statistically significant if $P<0.05$.

RESULTS

Comparison of positive detection rates of serum ANA, LC-1 and SLA/LP between the two groups

In the observation group, the positive detection rates of ANA, LC-1 and SLA-LP were 86.67% (52/60), 8.33% (5/60) and 5% (3/60), respectively. In the control group, the positive detection rates of ANA, LC-1 and SLA-LP were 83.33% (50/60), 10% (6/60) and 3.33% (2/60), respectively. The differences of the positive detection rates of ANA, LC-1 and SLA-LP had no statistical significance ($P>0.05$).

Comparison of liver function between the two groups

After treatment, the levels of serum ALT, AST, DBIL and TBIL of the two groups significantly reduced, and the difference before and after treatment within the same group had statistical significance ($P<0.05$). Compared to the control group, the

Table I. *Comparison of liver function indicators.*

Group	Observation group		Control group	
	Before	After	Before	After
ALT/(U·L^{-1})	267.41±46.10	36.23±6.15$^{*\#}$	275.24±35.13	57.74±6.82*
AST/(U·L^{-1})	143.52±28.47	36.17±5.41$^{*\#}$	142.36±29.37	49.72±5.37*
DBIL/(μmol·L^{-1})	136.43±58.72	17.41±4.22$^{*\#}$	135.32±59.27	52.57±7.48*
TBIL/(μmol·L^{-1})	76.41±8.64	32.45±4.04$^{*\#}$	76.44±8.66	50.85±3.37*

$^{*}P<0.05$ compared to before treatment in the same group; $^{\#}P<0.05$ compared to the control group after treatment.

Table II. *Comparison of the immunological indicators.*

Group	Observation group		Control group	
	Before	After	Before	After
Ig G/(g·L^{-1})	31.52±9.43	14.72±6.46$^{*\#}$	30.58±10.14	22.31±6.76*
Ig M/(g·L^{-1})	5.49±2.35	1.51±1.22$^{*\#}$	5.47±2.32	3.15±1.32*

* *P<0.05 compared to before treatment in the same group;* $^{\#}$ *P<0.05 compared to the control group after treatment.*

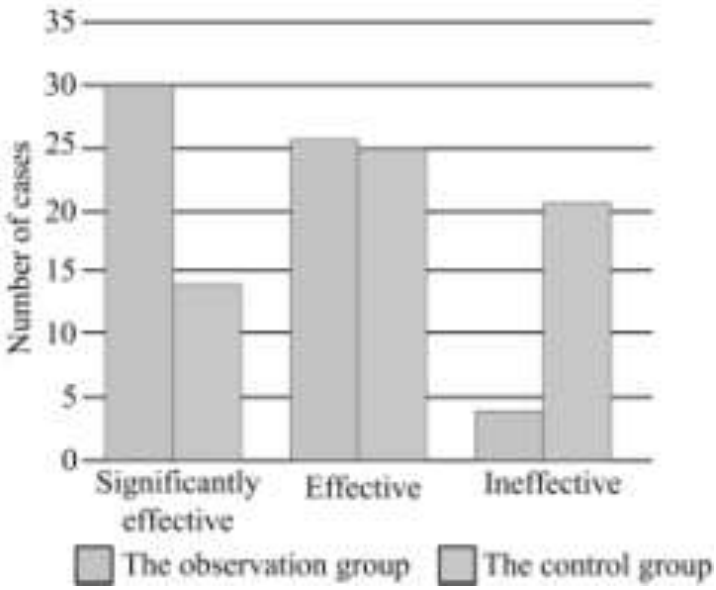

Fig. 1. *Comparison of clinical efficacy between the two groups.*

reduction of liver function indicators of the observation group was more remarkable (P<0.05; Table I).

Comparison of immunological indicators between the two groups

The levels of serum IgG and IgM of the two groups significantly decreased after treatment, and the differences were statistically significant (P<0.05); the decrease of values of the immunological indicators of the observation group was more remarkable after treatment, and the difference between the two groups had statistical significance (P<0.05; Table II).

Comparison of clinical efficacy between the two groups

The overall effective rate of the observation group was 93.33% (56/60), which was remarkably higher than the control group (65%, 39/60). The difference was statistically significant (χ^2=9.026; P<0.05; Fig. 1).

Comparison of incidence of adverse reactions between the two groups

All the patients persisted in the treatment till the end, and there was no missed dose of drugs during the treatment. During treatment, there were 7 cases of crinosity, 4 cases of moon-shaped face, 5 cases of

acne and 3 cases of osteoporosis in the control group; the incidence of adverse reactions was 31.7%. The corresponding number in the observation group was 3, 0, 2 and 1, respectively; the incidence of adverse reactions was 10%. The incidence of adverse reactions of the observation group was significantly lower than that of the control group (χ^2=5.107, P=0.023).

DISCUSSION

Currently, prednison is considered as the recognized treatment therapy for AH. One study (9) found that treatment with immunosuppressors could relieve the disease condition of 65% of patients with AH within two years, and the ten-year survival rate of patients without liver cirrhosis was 90%. This study also found that the values of the liver function associated immunological indicators of the prednisone-treated control group significantly decreased after treatment. However, long-term and indefinite application of glucocorticoids will increase the risks of peptic ulcer, diabetes, osteoporosis and infection. Moreover, most of patients with AH are females. Patients may abandon treatment due to the adverse reactions induced by glucocorticoids such as central obesity, moon-shaped face and crinosity. Ursodesoxycholic acid which is a non-toxic, hydrophilic cholic acid only induces mild side effects. Miyake et al. (10) treated 8 patients with type I AH with ursodesoxycholic acid for two years and found that it could effectively reduce the levels of serum ALT, AST, IgG and γ globulin. The results of this study demonstrated that the values of liver function-associated indicators and immunological indicators of the observation group were significantly decreased after treatment, and the improvement of the observation group was superior to that of the control group, suggesting ursodesoxycholic acid in combination with glucocorticoids had better efficacy in the treatment of AH. The dosage of prednison in the observation group was half that of the control group. The incidence of adverse reactions induced by glucocorticoids was significantly lower than that of the control group. The results obtained in this study were similar to that of the study of Tan et al. (11).

In conclusion, ursodesoxycholic acid in combination with glucocorticoids had favorable efficacy in the treatment of autoimmune hepatitis. It can apparently relieve the biochemical indexes of liver function, enhance immunity, and reduce adverse reactions. Hence the therapy is worth clinical promotion.

REFERENCES

1. Ilyas JA, O'Mahony CA, Vierling JM. Liver transplantation in autoimmune liver diseases. Best Pract Res Clin Gastroenterol 2011; 25(6):765-82.
2. Li XY, Shen J, Ran ZH. Crosstalk between the gut and the liver via susceptibility loci: Novel advances in inflammatory bowel disease and autoimmune liver disease. Clin Immunol 2017; 175:115-23.
3. Bian ZL, Miao Q, Zhong W, et al. Treatment of cholestatic fibrosis by altering gene expression of Cthrc1: Implications for autoimmune and non-autoimmune liver disease. J Autoimm 2015; 63:76-87.
4. Czaja AJ. The prevention and reversal of hepatic fibrosis in autoimmune hepatitis. Aliment Pharmacol Ther 2014; 39(4):385-406.
5. European Association for the Study of the Liver. EASL clinical practice guidelines: autoimmune hepatitis. J Hepatol 2015; 63(4):971-1004.
6. Levy C, Naik J, Giordano C, et al. Hispanics with primary biliary cirrhosis are more likely to have features of autoimmune hepatitis and reduced response to ursodeoxycholic acid than non-Hispanics. Clin Gastroenterol Hepatol 2014; 12(8):1398-405.
7. Ma X, Qiu DK. Chinese consensus on the diagnosis and management of autoimmune hepatitis (2015). Chin Hepatol 2015; 24(12):969-82.
8. Hennes EM, Zeniya M, Czaja AJ, et al. Simplified criteria for the diagnosis of autoimmune hepatitis. Hepatol 2008; 48(1):169-76.
9. Panayi V, Froud OJ, Vine L, et al. The natural history of autoimmune hepatitis presenting with jaundice. Eur J Gastroenterol Hepatol 2014; 26:640-45.
10. Miyake Y, Iwasaki Y, Kobashi H, et al. Efficacy of ursodeoxycholic acid for Japanese patients with autoimmune hepatitis. Hepatol Int 2009; 3(4):556-62.
11. Tan YW, Wu JC, Yu XJ. Efficacy of ursodeoxycholic acid in the treatment of type I autoimmune hepatitis. Chin J Clin Hepatol 2004; (5):27-28.

LETTER TO THE EDITOR

EVALUATING THE UTILITY OF AUTOANTIBODIES FOR DISEASE ACTIVITY AND RELAPSE IN GIANT CELL ARTERITIS

T. KURET[1], K. LAKOTA[1,2], A. HOČEVAR[1], B. BURJA[1], S. ČUČNIK[1,3] and S. SODIN-SEMRL[1,2]

[1]Department of Rheumatology, University Medical Centre Ljubljana, Ljubljana, Slovenia; [2]Faculty of Mathematics, Natural Science and Information Technologies, University of Primorska, Koper, Slovenia; [3]Faculty of Pharmacy, University of Ljubljana, Ljubljana, Slovenia

Received August 1, 2017 – Accepted February 13, 2018

In patients with giant cell arteritis (GCA), autoantibodies against cytoskeletal elements, cardiolipin, neutrophil cytoplasmic antigens, ferritin, endothelial and smooth muscle cells have been reported, however no updated reviews are available evaluating their clinical utility. Methodology of detection is important, especially for quantitative assays, e.g. enzyme-linked immunoassays and multiplex bead-based immunoassays, while semiquantitative assays contribute valuable data on isoforms, epitope mapping and cellular localization. Most studies to date reporting on antiphospholipid antibodies in GCA have focused on anti-cardiolipin antibodies (aCL), while the highest prevalence of autoantibodies in GCA patients was reported for the anti-N-terminal peptides of the ferritin heavy chain (92%). Anti-neutrophil cytoplasmic antibodies were shown to be present in only a small percentage of GCA patients, decreasing after therapy, however in combination with aCL and antibodies against peptides of N-terminal ferritin heavy chain, they could represent an added value in detecting relapse in GCA patients.

To the Editor,

Giant cell arteritis (GCA) is a systemic autoimmune large-vessel vasculitis affecting primarily the aorta and its major branches, especially extracranial branches of the carotid artery. It is the most common vasculitis in the elderly with incidence increasing progressively after 50 years and reaching a peak between 70 and 80 years. Most common signs and symptoms include headache, jaw claudication, visual disturbances, scalp or tongue necrosis and polymyalgia rheumatica (PMR). Due to possible occurrence of serious complications, such as permanent vision loss and cerebrovascular events, an appropriate and early diagnosis is crucial. However, the diagnosis of GCA is not always straightforward, with invasive temporal artery biopsy (TAB) representing the gold standard, emerging ultrasound methodology and no useful serological diagnostic or disease progression markers available to date. Key pathogenic drivers in GCA are components of innate, as well as adaptive immunity. Activated dendritic cells trigger the recruitment of $CD4^+$ T-cells, which polarize into Th1 and Th17 and produce IFN-γ and IL-17, respectively. Monocytes are also recruited and later differentiate into macrophages which can form giant cells, the histological hallmark of GCA. IL-17 can induce activation and migration of neutrophils, which have recently been reported to be involved in GCA pathogenesis. With the contribution of vascular smooth muscle cells, immune cells then

Key words: giant cell arteritis, autoantibodies, diagnosis, biomarkers, relapse

Mailing address:
Associate Professor Snezna Sodin-Semrl, PhD,
Department of Rheumatology,
University Medical Center Ljubljana,
Vodnikova 62, Ljubljana SI-1000, Slovenia
Tel.: +386 1 522 5596
e-mail: ssodin1@yahoo.com

0393-974X (2018)

DISCLOSURE: ALL AUTHORS REPORT NO CONFLICTS OF INTEREST RELEVANT TO THIS ARTICLE.

trigger the destruction and remodeling of the arterial wall. Although GCA is considered to be a T-cell driven disease, the humoral immune response seems to participate with B-cells detected in TABs (1). Moreover, the distribution of B lymphocytes was found to be highly disrupted in newly diagnosed GCA patients, returning to normal distribution during remission. B-effector cells (which returned to normal during remission) demonstrated an enhanced potential to produce pro-inflammatory IL-6, possibly showing an interplay between T and B cells in the pathogenesis of GCA (2).

Several types of autoantibodies can be detected in GCA, such as antiphospholipid (aPL) antibodies (3-5), anti-ferritin autoantibodies (6, 7), autoantibodies targeting the cytoskeleton (8), endothelial and vascular smooth muscle cells (VSMC) (9-11). Recently, newer methods of detection (e.g. recombinant cDNA expression cloning and proteomic approaches) renewed an interest in the potential of autoantibodies as markers of GCA. In particular, anti-neutrophil cytoplasmic (ANCA), anti-cardiolipin (aCL) and anti-ferritin antibodies (against heavy chain and peptides) have been reported to be associated with relapses (3, 6, 7, 12). The purpose of the current report was to evaluate autoantibodies in GCA, in terms of their prevalence, methods of detection and, especially, clinical utility (e.g. association with relapses). In the last two decades, multiple autoantibodies have been identified and measured in GCA using different methods (Table I).

Autoantibodies against cytoskeletal antigens

Using a testis-derived cDNA expression library incubated with sera of 3 untreated GCA patients, Schmits at al. identified 33 autoantibodies. Among

Table I. *Autoantibodies in GCA patients, their prevalence and method of detection in the last 20 years.*

Year	Autoantibodies detected in GCA patients	Prevalence % (n/total)	Method of detection	Reference
1997	AECA	33 (13/39)	ELISA	Navarro *et al*. (10)
1998	aCL	29 (30/105)	ELISA	Duhaut *et al*. (4)
2001	Anti-PT	36 (29/80)	ELISA	Espinosa *et al*. (5)
2001	Anti-β2GPI	11 (9/80)	ELISA	Espinosa *et al*. (5)
2001	Anti-VSMC	N/A	2D electrophoresis	Régent *et al.* (9)
2002	Mostly anti-cytoskeletal antibodies	N/A	SEREX	Schmits *et al*. (8)
2008	ANCA	30 (9/30)	IIF	Gil *et al*. (12)
2008	Anti-hHSP60	N/A	ELISA	López-Hoyos *et al*. (13)
2012	Anti-tissue transglutaminase	12 (3/26)	Multiplex bead-based immunoassay	Shor *et al*. (14)
2012	Anti-ferritin (27 AA of N-terminal heavy chain)	92 (131/142)	ELISA	Baerlecken *et al.* (6)
2017	Anti-14-3-3 protein	N/A	Multiplex bead-based immunoassay	Kistner *et al*. (15)

Abbreviations. AA: amino acid; aCL: anti-cardiolipin antibodies; AECA: anti-endothelial cells antibodies; ANCA: anti-neutrophil cytoplasmic antibodies; β2GPI: beta 2 glycoprotein 1; ELISA: enzyme-linked immunosorbent assay; GCA: giant cell arteritis; hHSP60: human heat shock protein 60; IIF: indirect immunofluorescence; N/A: not available; PT: prothrombin; SEREX: serological analysis of recombinant cDNA expression libraries; VSMC: vascular smooth muscle cells.

these, antibody reactivity towards five autoantigens was found in a higher proportion of patients compared to healthy blood donors (HBDs), representing mostly components of the cytoskeleton (e.g. myosin, cytokeratin, spectrin). Antibodies to lamin C and nuclear 14 kDa autoantigen were present in one-third of GCA/PMR patients (n=6/19) and none of HBDs (n=12). Antibodies to cytokeratin type 15 and mitochondrial cytochrome oxidase subunit II were present in 26% (5/19) GCA/PMR patients compared to only 8% (1/12) HBDs. Autoantibodies to human myosin heavy chain 7 were present in 21% (4/19) patients and 17% (2/12) controls. Sera of one GCA patient in remission under steroid therapy reacted with 14/33 antigens, compared to 26/33 before treatment, indicating higher autoantibody reactivity in the active phase of the disease (8).

Neutrophil antibodies

GCA patients, followed longitudinally, were reported to have ANCA detected by indirect immunofluorescence (IIF) in 30% (n=9/30) of the cases, 44% (4/9) of which exhibited a perinuclear (p-ANCA) and 22% (2/9) a cytoplasmic (c-ANCA) staining pattern. None of p-ANCA- or c-ANCA-positive patients showed reactivity towards myeloperoxidase (MPO) or proteinase 3 (PR3), when enzyme-linked immunosorbent assay (ELISA) was performed. Results of 22% (2/9) GCA patients on IIF could not be determined as either p-ANCA or c-ANCA, but rather showed reactivity towards both, MPO and PR3, following ELISA. There were no significant differences observed between ANCA-positive (c-ANCA, p-ANCA, MPO or PR3) and ANCA-negative patients in clinical features or number of relapses. Relapses occurred earlier in the presence of ANCA than in the absence (6 months *vs* 31.5 months), however, the results were obtained at the time when GCA patients had already received steroid therapy (12) (Table II).

Table II. *Association of autoantibodies with relapses in GCA patients.*

Number of patients	Antibody	Prevalence % (n/total)	Relapse *vs* remission % (n/total)	Conclusion	Reference
30 GCA	ANCA	30 (9/30)	55.6 (5/9) ANCA + *vs* 42.8 (9/21) ANCA -. Relapse occurred earlier in ANCA $^{+}$ (6 m *vs* 31.5 m)	Predictive of an early relapse	Gil *et al.*, 2008 (12)
58 GCA	aCL	46.6 (27/58)	74 (20/27) patients with relapse had significant rise in aCL levels *vs* 0 (0/31) patients in remission	Useful in the detection of flares and relapses (74% sensitivity and 100% specifity)	Liozon *et al.*, 2000 (3)
142 GCA/ PMR	Ferritin heavy chain (AA 19-45)	92 (131/142)	69 (22/32) patients with relapse were anti-ferritin heavy chain + *vs* 13 (4/30) patients in remission	Useful marker of disease activity	Baerlecken *et al.*, 2012 (6)
70 GCA/ PMR	Ferritin peptides (any of AA 19-45, 79-104, 105-143)	100 (11/11) before treatment; 66 (46/70) in treated and untreated patients	75 (24/32) patients with relapse were anti-ferritin peptides $^{+}$ *vs* 46 (6/13) patients in remission and 40 (10/25) patients in partial remission	Valuable markers of GCA/PMR with/ without disease flares	Grose *et al.*, 2013 (7)

Abbreviations. AA: amino acid; aCL: anti-cardiolipin antibodies; ANCA: anti-neutrophil cytoplasmic antibodies; GCA: giant cell arteritis; PMR: polymyalgia rheumatica.

Antiphospholipid antibodies

An early report in 1998, on a high number of newly diagnosed GCA/PMR patients (n=266) showed aCL prevalence of 29% in GCA (n=30/105), 5% in PMR (n=4/79), 21% in GCA/PMR (n=17/82) patients and only 2.9% in age- and sex-matched HBDs (n=6/210), as detected by ELISA. The percentage of aCL-positive individuals was higher in TAB^+ (31%) GCA patients compared to TAB^- (17%) (4).

Liozon et al. reported on 46.6% (27/58) aCL positive, steroid-naïve GCA patients. After steroid therapy, levels of aCL decreased in all GCA patients, except one. A significant increase in aCL levels was observed in 74.2% (20/27) of GCA patients with GCA-related inflammatory episodes, while in patients with controlled disease, no increase in aCL was observed. aCL was reported to be useful in detecting flares and relapses in GCA with fair sensitivity (74%) and 100% specificity (3) (Table II).

A year later, in 2001, aCL were found in 30% (24/80) GCA/PMR patients, compared to 1% (1/100) age- and sex-matched HBDs. Moreover, 11% (9/80) had antibodies against β2GPI glycoprotein I (β2GPI) and 36% (29/80) had antibodies against prothrombin (PT). However, there were no differences observed in antibody profiles among the samples obtained during active or inactive phases of the disease and no relationship was found between aCL, anti-β_2GPI or aPT positivity and ischemic manifestations (5). Interestingly, antibodies against phosphatidylserine-dependent PT (aPS/PT) have not yet been reported in GCA, which could provide added value in the future. A schematic representation of autoantibodies found in the circulation of GCA patients is presented in Fig. 1.

Ferritin-targeted autoantibodies

β2GPI autoantibodies against the full length ferritin heavy chain were detected in 22% (n=31/142) of untreated GCA/PMR patients using ELISA. Sensitivity increased to 92% when only the N-terminal 27 amino acids (AA) of ferritin heavy chain were used as antigen. During remission, the presence of antibodies against N-teminal 27 AA of ferritin heavy chain decreased from an initial 92% to 13% of GCA/PMR patients. These antibodies were, however, also present in the sera of patients with systemic lupus erithematosus (SLE) (29%;

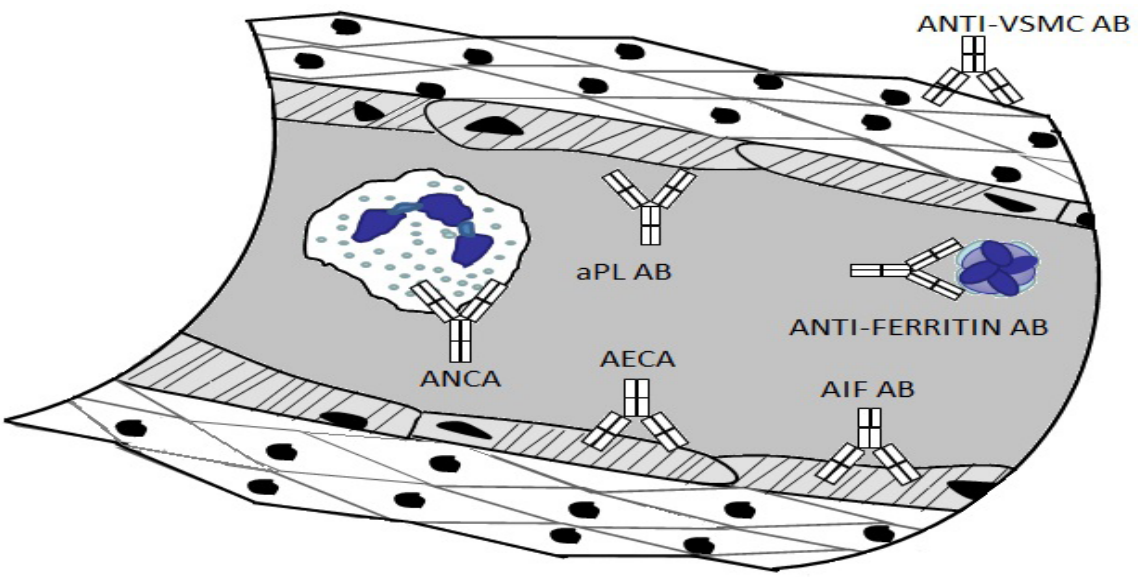

Fig. 1. *Autoantibodies identified in the circulation of GCA patients.*
Abbreviations. AECA: anti-endothelial cells antibodies; AIF: anti-intermediate filaments antibodies; ANCA: anti-neutrophil cytoplasmic antibodies; Anti-ferritin AB: anti-ferritin antibodies; Anti-VSMC AB: anti-vascular smooth muscle antibodies; aPL: anti-phospholipid antibodies.

n=11/38), rheumatoid arthritis (3%; n=1/36), ANCA-associated vasculitis (29%; n=19/66) and B non-Hodgkin's lymphoma (6.5%; n=3/46), but only in 1% (n=1/100) of HBDs (6) (Table II).

In addition to 19-45 AA of the N terminal heavy chain, other AA sequences (1-19, 52-78, 79-104, 105-143 and 145-183) of ferritin were tested as epitopes for autoantibodies revealing that anti-ferritin antibodies bound to different peptide epitopes. Antibodies against AA 19-45, 79-104 and 105-144 were observed with similar prevalence in sera of GCA/PMR patients (36%; n=25/70), however, when detecting positivity against any of the three epitopes, the prevalence increased to 66% in GCA (n=46/70), but was also shown in 27% of patients with fever (13/49) and in 25% (4/16) of patients with Wegener's granulomatosis (7) (Table II).

Antibodies against endothelial and vascular smooth muscle cells

Navarro et al. performed a large study on 216 patients with different autoimmune diseases and 100 age- and sex-matched HBDs. AECAs were detected in 33% of patients with GCA (n=13/39) by ELISA, using human umblical vein endothelial cells (HUVEC) as source of antigens. Sera of patients with other primary vasculitides (41%; n=28/68), SLE (64%; n=58/90) and Sjogren's syndrome (26%; n=5/19) also tested positive for the presence of AECAs, however, they were not detected in HBDs. GCA patients with AECAs were more likely to have active disease, compared to AECA-negative GCA patients. Moreover, the same group showed that in patients with Wegener's granulomatosis and polyarteritis nodosa, titers of AECA decreased during therapy-induced remission, indicating AECAs could represent a potential marker of disease activity (10).

IgG reactivity from sera of GCA patients (n=15) and HBDs (n=12) against antigens to HUVEC and mammary VSMC was reported using 2D electrophoresis and immunoblotting. IgG derived from 5 different pools of sera from each of 3 GCA patients showed reactivity towards 162±3 (mean ± SD) and 100±17 (mean ± SD) proteins spots in HUVEC and VSMC, respectively, as opposed to 79 and 94 protein spots from pooled sera of HBDs, respectively. Three differential spots identified lamin A/C, vinculin and mitochondrial fumarate hydratase as antigens by mass spectrometry. Although AECAs were detected in a number of systemic autoimmune diseases and HBDs, this was the first study to show the presence of anti-VSMC antibodies in a human disease (9).

Interestingly, using 2D electrophoresis and HUVEC antigens, Karasawa et al. identified reactivity of IgG against peroxiredoxin-2 (Prx-2) fusion protein in sera of GCA (n=2) and other vasculitis patients. The frequency of anti-Prx-2 antibodies tended to be higher in large vessel vasculitides, such as GCA, Takayasu arteritis and Behcet's disease, as compared to small vessel vasculitides. It was also shown that anti-Prx-2 antibodies upregulated secretion of inflammatory cytokines and chemokines from vascular endothelial cells, which indicated they could play a role in vascular injury. However, the number of GCA patients in this study was very small and a larger study would be needed to confirm this potentially important function (11).

Antibodies against other antigens

Chlamydophila pneumoniae (*C. pneumonia*) infection can induce immune reactivity against human heat shock protein 60 (hHSP60) expressed by VSMC, which shares extensive homology with the most immunogenic particle of *C. pneumoniae* (cHSP60). Levels of antibodies against hHSP-60, but not against *C. pneumoniae* were significantly increased in the sera of GCA patients with active untreated disease (n=17) compared to PMR patients (n=39) and HBDs (n=23). The levels of both (anti-hHSP60 and anti-*C. pneumoniae*) decreased significantly after therapy in GCA and PMR patients. Despite the homology between both HSP60 molecules, no correlation between the antibodies against *C. pneumoniae* and anti-hHSP60 was observed (13).

Among other antibodies, gastrointestinal autoimmune disease-associated antibodies have been proposed to be present in GCA and other autoimmune diseases. Three major antibodies studied in connection with GCA were anti-gliadin, anti-transglutaminase and anti-*Saccharomyces*

cerevisiae (*S. cerevisiae*). IgG antibodies against transglutaminase were present in 12% (n=3/26) of GCA patients compared to only 1% (n=3/338) of HBDs, while anti-transglutaminase IgA, as well as antibodies against gliadin and *S. cerevisiae* were absent (14).

Recently, antibodies against 14-3-3, a protein that binds cellular signaling molecules, have been proposed as a useful marker for presence of aortic aneurysm in patients with large vessel vasculitis, including GCA. Antibodies against all three isoforms of 14-3-3 (γ, ε and ζ) were detected in GCA patients (n=48), as well as in age-matched inflammatory and non-inflammatory controls (n=29), as determined by multiplexed bead-based assay. 71% (n=10/14) of GCA patients, positive for antibodies against 14-3-3ε had aortitis, compared to 29% (n=7/24) anti-14-3-3ε negative patients, suggesting anti-14-3-3 autoantibodies are involved in tissue damage. Interestingly, all three 14-3-3 isoforms have AA sequences 74-76% similar to a 14-3-3 homologue protein secreted by *Toxoplasma gondii* (*T. gondii*). Indeed, it has been shown that individuals with high levels of anti-14-3-3γ antibodies were more likely to be *T. gondii* seropositive than individuals with lower levels of anti 14-3-3 antibodies. Additionally, when comparing the differences in sequences between the three isoforms and *T. gondii* homologue, clusters of three AA, conserved between the *T. gondii* 14-3-3 and human 14-3-3γ protein, but not 14-3-3ε or 14-3-3ζ, were arranged in close proximity to each other, raising the possibility of molecular mimicry (15).

Some of the methods mentioned have previously been used in routine diagnostics (aCL, anti-β2GPI ELISA, ANCA IIF, anti-tissue transglutaminase multiplex assay), while others are still exploratory. Low levels of autoantibodies could be quantitated by high sensitivity ELISA, as well as multiplex assays.

In conclusion, the highest number of studies in GCA was reported on aPL, followed by AECA, anti-VSMC and anti-ferritin autoantibodies. The highest prevalence of autoantibodies in GCA patients was shown against AA of N-terminal ferritin heavy chain (92%), however, studies evaluating their pathogenicity are lacking. ANCA, aCL and antibodies against ferritin heavy chain may represent an added value, in combination with other clinical and laboratory parameters, for detecting relapses in GCA.

ACKNOWLEDGEMENTS

Funding for this work was obtained from the Slovenian Research Agency (ARRS) - National Research Grant #P3-0314. The mentioned received funding did not lead to any conflicts of interest regarding the publication of this manuscript.

REFERENCES

1. Samson M, Corbera-Bellalta M, Audia S, Planas-Rigol E, Martin L, Cid MC, Bonnotte B. Recent advances in our understanding of giant cell arteritis pathogenesis. Autoimmun Rev 2017; 16(8):833-44.
2. van der Geest KS, Abdulahad WH, Chalan P, et al. Disturbed B cell homeostasis in newly diagnosed giant cell arteritis and polymyalgia rheumatica. Arthritis Rheumatol 2014; 66(7):1927-38.
3. Liozon E, Roblot P, Paire D, Loustaud V, Liozon F, Vidal E, Jauberteau MO. Anticardiolipin antibody levels predict flares and relapses in patients with giant-cell (temporal) arteritis. A longitudinal study of 58 biopsy-proven cases. Rheumatology (Oxford) 2000; 39(10):1089-94.
4. Duhaut P, Berruyer M, Pinede L, et al. Anticardiolipin antibodies and giant cell arteritis: a prospective, multicenter case-control study. Groupe de Recherche sur l'Arterite a Cellules Geantes. Arthritis Rheum 1998; 41(4):701-9.
5. Espinosa G, Tassies D, Font J, Munoz-Rodriguez FJ, Cervera R, Ordinas A, Reverter JC, Ingelmo M. Antiphospholipid antibodies and thrombophilic factors in giant cell arteritis. Semin Arthritis Rheum 2001; 31(1):12-20.
6. Baerlecken NT, Linnemann A, Gross WL, et al. Association of ferritin autoantibodies with giant cell arteritis/polymyalgia rheumatica. Ann Rheum Dis 2012; 71(6):943-47.
7. Grosse K, Schmidt RE, Witte T, Baerlecken NT. Epitope mapping of antibodies against ferritin heavy chain in giant cell arteritis and polymyalgia rheumatica. Scand J Rheumatol 2013; 42(3):215-19.
8. Schmits R, Kubuschok B, Schuster S, Preuss KD,

Pfreundschuh M. Analysis of the B cell repertoire against autoantigens in patients with giant cell arteritis and polymyalgia rheumatica. Clin Exp Immunol 2002; 127(2):379-85.

9. Regent A, Dib H, Ly KH, et al. Identification of target antigens of anti-endothelial cell and anti-vascular smooth muscle cell antibodies in patients with giant cell arteritis: a proteomic approach. Arthritis Res Ther 2011; 13(3):R107.
10. Navarro M, Cervera R, Font J, et al. Anti-endothelial cell antibodies in systemic autoimmune diseases: prevalence and clinical significance. Lupus 1997; 6(6):521-26.
11. Karasawa R, Kurokawa MS, Yudoh K, Masuko K, Ozaki S, Kato T. Peroxiredoxin 2 is a novel autoantigen for anti-endothelial cell antibodies in systemic vasculitis. Clin Exp Immunol 2010; 161(3):459-70.
12. Gil H, Mauny F, Meaux-Ruault N, Magy-Bertrand N, Roncato-Saberan M, Hafsaoui C, Dupond JL. [Usefulness of antineutrophil cytoplamic antibodies in giant cell arteritis]. Rev Med Interne 2008; 29(10):780-84.
13. Lopez-Hoyos M, Alvarez L, Ruiz Soto M, Blanco R, Jose Bartolome M, Martinez-Taboada VM. Serum levels of antibodies to Chlamydia pneumoniae and human HSP60 in giant cell arteritis patients. Clin Exp Rheumatol 2008; 26(6):1107-10.
14. Shor DB, Orbach H, Boaz M, et al. Gastrointestinal-associated autoantibodies in different autoimmune diseases. Am J Clin Exp Immunol 2012; 1(1):49-55.
15. Kistner A, Bigler MB, Glatz K, et al. Characteristics of autoantibodies targeting 14-3-3 proteins and their association with clinical features in newly diagnosed giant cell arteritis. Rheumatology (Oxford) 2017; 56(5):829-34.

LETTER TO THE EDITOR

STATUS OF CATHELICIDIN LL-37, CYTOKINE TNF, AND VITAMIN D IN PATIENTS WITH PULMONARY TUBERCULOSIS

K. MAJEWSKI[1,2], J. AGIER[1], E. KOZŁOWSKA[1]
and E. BRZEZIŃSKA-BŁASZCZYK[1]

[1]Department of Experimental Immunology, Medical University of Lodz, Lodz, Poland; [2]Pulmonary Disease Hospital, Lodz, Poland

Received December 30, 2017 – Accepted February 16, 2018

Development of *Mycobacterium tuberculosis* (*Mtb*) infection depends on the ability of the host to elicit the protective immune response to the pathogen. Cathelicidin plays a role in antibacterial innate immunity mechanisms. This peptide contributes to the barrier function of respiratory epithelium and takes part in controlling pulmonary bacterial infections. LL-37 (leucine-leucine-37) is involved in host defense and innate immune response to mycobacterial infections, as well. This study aims to evaluate the serum concentrations of LL-37 in individuals with active pulmonary tuberculosis (TB) and to determine whether any correlations between peptide LL-37, tumor necrosis factor (TNF) and vitamin D serum levels exist. A total of 46 adults with pulmonary TB were recruited for the study. Sixty-one controls were randomly selected as control group. Serum concentrations of cathelicidin LL-37, vitamin D (25(OH)D), as well as TNF, were measured using an enzyme-linked immunosorbent assay (ELISA) kit. The mean (± SEM) level of LL-37 was significantly higher in the TB group (7.45±1.58) compared with healthy controls (1.41±0.22) ($p < 0.001$). Mean serum concentration of TNF was significantly higher in the TB group (8.51±1.92) compared with healthy controls (2.69±0.19) ($p < 0.001$). There was no significant difference in mean serum levels of vitamin D between healthy (26.10±1.74) and TB subjects (24.18±1.95). No correlations between LL-37, TNF, and vitamin D levels in patients with TB were observed. Our results indicated that serum levels of peptide LL-37 during TB is raised significantly, and this observation is compatible with the general view of the important role of this cathelicidin in defense mechanisms against *Mtb* infection.

To the Editor,

Tuberculosis (TB) is a global reason for morbidity and remains a significant cause of mortality toll worldwide. TB is an infectious disease caused by *Mycobacterium tuberculosis* (*Mtb*), a facultative intracellular bacterium, which infects macrophages and other myeloid cells. Exposure to *Mtb* results in active TB in only 5-10% of infected individuals and the vast majority of *Mtb* infections are controlled and clinically silent (latent TB infections), and can persist lifelong.

Development of *Mtb* infection depends on the ability of the host to elicit the protective immune response to the pathogen. Immune response to mycobacterial infection is mainly Th1-dependent, and the significant role is played by different cytokines, of which tumor necrosis factor (TNF) is the most essential (1). More and more data imply the role of cathelicidin leucine-leucine-37 (LL-37), a small amphipathic peptide, in antibacterial defense

Key words: cathelicidin LL-37, vitamin D; cytokine TNF, pulmonary tuberculosis, Mycobacterium tuberculosis

Mailing address:
Justyna Agier, Ph.D.,
Department of Experimental Immunology,
Medical University of Lodz,
92-213 Lodz,
Pomorska 251, Poland
e-mail: justyna.agier@umed.lodz.pl

0393-974X (2018)

(2), and there is information that this peptide is also involved in protection against *Mtb* infection (3). Lung epithelial cells, alveolar monocytes/macrophages, and neutrophils produce LL-37 in response to *Mtb* infection. *In vitro* LL-37 can inhibit the growth of *Mtb* strains and it exhibits bactericidal activity against this pathogen. LL-37 mediates activation of autophagy in macrophages and modulates macrophage activity during *Mtb* infection by influencing the expression of proinflammatory cytokines.

Vitamin D acts as a regulator of immune functions and influences immune response towards *Mtb* (4, 5). Vitamin D also regulates the expression of peptide LL-37 (5). Thus, our study aimed to evaluate the serum concentrations of LL-37 in individuals with active pulmonary TB and to determine whether any correlations between peptide LL-37 and TNF and vitamin D serum levels exist.

MATERIALS AND METHODS

Study population

A total of 46 adult patients with pulmonary TB from the Hospital of Lung Diseases in Lodz were enrolled in the study. As a contol group, sixty-one healthy subjects were randomly selected. All individuals were subjected to an initial evaluation that included: a clinical examination, radiological findings, general laboratory tests including ALAT, AspAT, total bilirubin, urea, creatinine, glucose, sodium, potassium, C-reactive protein (CRP), white blood cell (WBC) count, and microbiology standard laboratory methods. Subjects with chronic inflammatory diseases, systemic diseases, immunological disorders (AIDS, allergy), cancer, taking antibiotics for the previous three months, taking immunosuppressive or antihistamine agents were excluded from the study. TB diagnosis was made in accordance with the WHO standard TB case definition, and was based on respiratory symptoms, radiological findings, tuberculin skin test (TST) positivity, *Mtb* culture positivity, sputum acid-fast bacilli (AFB) smear, and history of contact with an active TB case. All patients included in the study were informed about its methods and aims and provided their written informed consent for participation. This study protocol was approved by the Bioethics Committee of the Medical University of Lodz (protocol No. RNN/785/13/KB), and written informed consent was obtained from all participants.

Measurement of LL-37, TNF, and vitamin D serum levels

Blood samples from all the participants were collected using serum separator tubes. Serum samples were

Table I. *Baseline characteristics of the study population.*

	Healthy controls	TB patients
n	61	46
Age (years)	46.8±1.49	50.6±2.09
Gender (M/F)	22 / 39	33 / 13
AspAT (U/L)	21.0±0.94	26.6±3.08
ALAT (U/L)	23.2±1.86	20.7±2.28
Total bilirubin (mg/dL)	0.5±0.03	0.6±0.03
Urea (mg/dL)	27.0±1.19	23.1±1.09
Creatinine (mg/dL)	0.8±0.02	0.6±0.01
Glucose (mg/dL)	81.5±1.67	103.4±2.37
Sodium (mmol/L)	134.5±0.53	135.3±0.59
Potassium (mmol/L)	4.78±0.07	4.7±0.07

Data are shown as means±SEM. AspAT: Aspartate transaminase; ALAT: Alanine transaminase

separated by centrifugation at 3500 rpm at 4°C for 10 min and then immediately stored at -80°C until analysis. Serum levels of cathelicidin LL-37, vitamin D (25(OH) D), as well as TNF, were measured using an enzyme-linked immunosorbent assay (ELISA) kit (MyBIOSource, San Diego, USA). Protocols for the assays were followed per the manufacturer product manuals.

Statistical analysis

Data management and statistical analyses were performed with Statistica 12.5 (Statsoft Inc., USA). Simple descriptive statistics (means, SEM) were generated for all continuous variables. Normality of distribution was tested with the Shapiro-Wilk test. Serum levels of LL-37, TNF, and vitamin D, as well as CRP levels and WBC counts, were compared with the use of the Mann-Whitney *U* test. The relationships between the serum concentrations of cathelicidin LL-37 and 25(OH)D, cathelicidin LL-37 and TNF, as well as between circulating levels of TNF and 25(OH)D were expressed as Spearman's correlation coefficients. $p < 0.05$ was considered statistically significant.

RESULTS

Baseline characteristics of participants

Baseline characteristics of all studied groups are shown in Table I. In the healthy group, the mean (± SEM) age was 46.8±1.49 years, and there were 22 men and 39 women. In the TB group, the mean age was 50.6±2.09 years, and the male/female ratio was 33/13. There were no statistical differences in

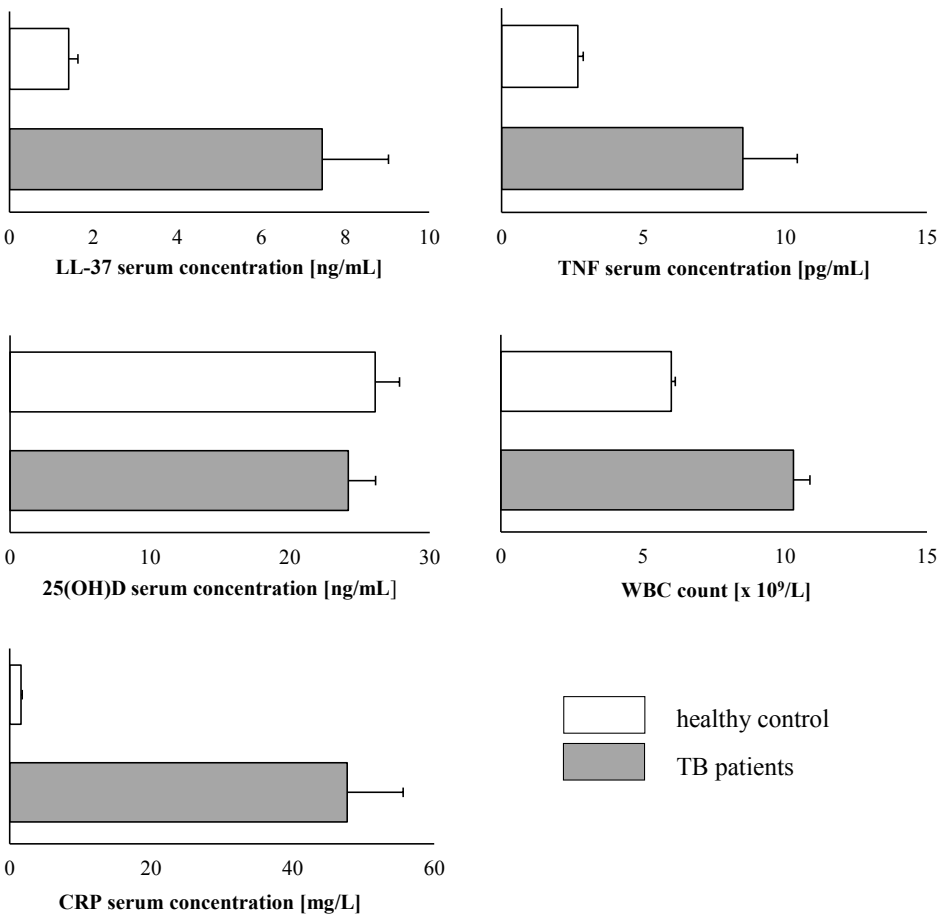

Fig. 1. *Serum concentrations of LL-37, TNF, 25(OH)D, and CRP, as well as WBC count in healthy controls and patients with pulmonary tuberculosis.*

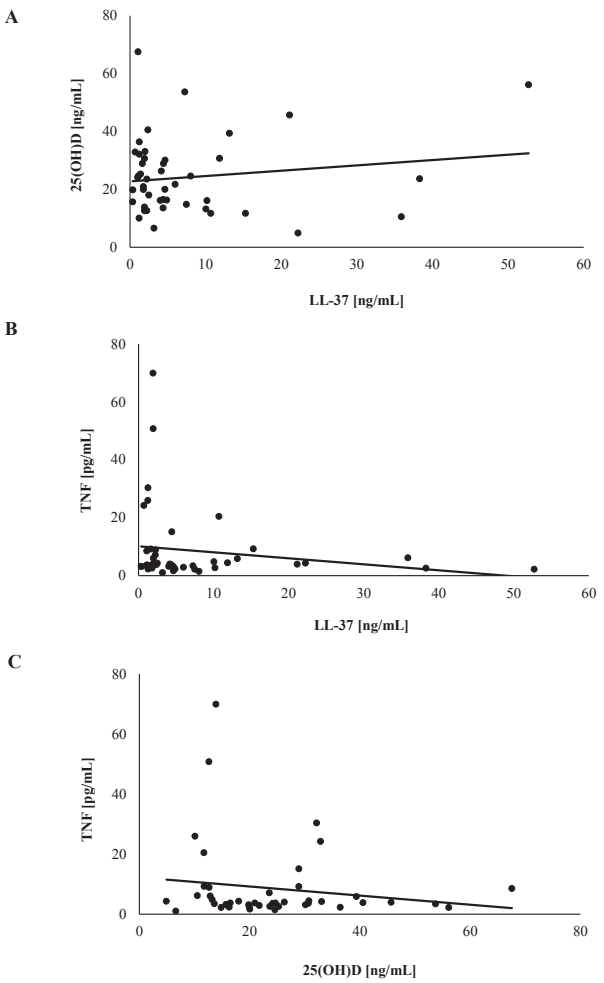

Fig. 2. *Correlation between circulating level of 25(OH)D and LL-37 level in patients with TB (**A**); the correlation between circulating level of TNF and LL-37 level in patients with TB (**B**); the correlation between circulating level of TNF and 25(OH)D level in patients with TB (**C**).*

age and sex distribution between the groups. In all groups, basic laboratory parameters, such as AspAT, ALAT, total bilirubin, urea, creatinine, glucose, sodium, and potassium were within normal ranges.

Circulating LL-37, TNF and vitamin D levels in studied groups

In healthy subjects LL-37 serum levels varied from 0.24 to 10.37 ng/mL, and in patients with TB serum levels of LL-37 ranged from 0.35 to 52.72 ng/mL. The mean (± SEM) level of LL-37 was significantly higher in the TB group compared with healthy controls ($p < 0.001$). In the healthy controls circulating TNF concentration ranged from 1.21 to 8.52 pg/mL. In TB patients TNF levels ranged from 1.02 to 69.9 pg/mL. Mean serum concentration of TNF was significantly higher in TB group compared with healthy controls ($p < 0.001$). Vitamin D serum levels ranged from 9.98 to 46.42 ng/mL in healthy and from 4.92 to 67.57 ng/mL in TB subjects. The concentration of vitamin D was at the same level in healthy control and TB group. There were no significant differences in mean serum levels of vitamin D between healthy and TB subjects (Fig. 1). In patients with TB no statistically significant correlations between serum LL-37 level and vitamin D concentration ($r = -0.078$; $p = 0.081$), between serum LL-37 concentration and TNF concentration ($r = -0.126$; $p = 0.414$), and between serum vitamin D concentration and TNF concentration ($r = -0.1212$; $p = 0.512$) were observed (Fig. 2).

Additionally, the mean WBC counts were significantly higher in TB patients, as compared with healthy controls ($p < 0.001$). Likewise, CRP concentrations in infected patients were substantially higher than in healthy subjects ($p < 0.001$). Elevated CRP levels and WBC counts in the TB group compared to the healthy controls, confirmed the ongoing infection.

DISCUSSION

There is data that cathelicidin LL-37 plays a role in mycobacterial infection (3), however the circulating level of the peptide in patients with pulmonary TB was estimated sparsely. Zhan and Jiang (6) noticed increased serum levels of LL-37 in adult patients with pulmonary TB, and Cakir et al. (7) observed elevated LL-37 levels in bronchoalveolar lavage (BAL) of children with *Mtb* infection. Herein, we stated that adult patients with active pulmonary TB demonstrate statistically significant higher circulating levels of this peptide than healthy subjects. Previously, we documented that serum LL-37 levels in subjects with *Mtb* infection is significantly higher not only than in healthy individuals but also in patients with bacteria-induced pneumonia (8, 9).

Given the critical role of TNF and vitamin D in the immune response against *Mtb* and cathelicidin

production (1, 4, 5), it was interesting to check whether any correlations between LL-37, TNF and vitamin D levels exist. We noticed that TNF levels in patients with TB were significantly higher than in healthy controls, and this observation is consistent with previous data (10-13). Previously, decreased vitamin D levels in patients with TB was observed (6). However, we noticed no differences in 25(OH) D serum levels between healthy and TB subjects. Moreover, we found no correlations between LL-37 and TNF levels, nor TNF and vitamin D levels in patients with TB. Other Authors previously observed the lack of clear correlation between systemic concentrations of vitamin D and LL-37/hCAP18 in patients with TB (6, 14, 15).

In conclusion, our results indicate that serum levels of peptide LL-37 during TB is raised significantly, and this observation is compatible with the general view of the vital role of LL-37 in defense against *Mtb* infection. While the significance of TNF and vitamin D in *Mtb* infection is known, the relationship between LL-37, TNF as well as vitamin D must be further investigated.

ACKNOWLEDGEMENTS

This work was supported by the Medical University of Lodz (grant No. 502-03/6-164-01/502-64-083). The authors would like to thank Karolina Wódz, PhD, who conducted the ELISA tests.

REFERENCES

1. Lin PL, Plessner HL, Voitenok NN, Flynn JL. Tumor necrosis factor and tuberculosis. J Investig Dermatol Symp Proc 2007; 12:22-25.
2. Vandamme D, Landuyt B, Luyten W, Schoofs L. A comprehensive summary of LL-37, the factotum human cathelicidin peptide. Cell Immunol 2012; 280:22-35.
3. Méndez-Samperio P. The human cathelicidin hCAP18/LL-37: a multifunctional peptide involved in mycobacterial infections. Peptides 2010; 31:1791-98.
4. Prietl B, Treiber G, Pieber TR, Amrein K. Vitamin D and immune function. Nutrients 2013; 5:2502-21.
5. Chun RF, Adams JS, Hewison M. Immunomodulation by vitamin D: implications for TB. Expert Rev Clin Pharmacol 2011; 4:583-91.
6. Zhan Y, Jiang L. Status of vitamin D, antimicrobial peptide cathelicidin and T helper-associated cytokines in patients with diabetes mellitus and pulmonary tuberculosis. Exp Ther Med 2015; 9:11-16.
7. Cakir E, Torun E, Gedik AH, Umutoglu T, Aktas EC, Topuz U, Deniz G. Cathelicidin and human β-defensin 2 in bronchoalveolar lavage fluid of children with pulmonary tuberculosis. Int J Tuberc Lung Dis 2014; 18:671-75.
8. Majewski K, Żelechowska P, Brzezińska-Błaszczyk E. Circulating cathelicidin LL-37 in adult patients with pulmonary infectious diseases. Clin Invest Med 2017; 40: E34-E39.
9. Majewski K, Agier J, Kozłowska E, Brzezińska-Błaszczyk E. Serum level of cathelicidin LL-37 in patients with active tuberculosis and other infectious diseases. J Biol Regul Homeost Agents 2017; 31:731-36.
10. Andrade Júnior DR, Santos SA, Castro Id, Andrade DR. Correlation between serum tumor necrosis factor alpha levels and clinical severity of tuberculosis. Braz J Infect Dis 2008; 12:226-33.
11. Deveci F, Akbulut HH, Turgut T, Muz MH. Changes in serum cytokine levels in active tuberculosis with treatment. Mediators Inflamm 2005; 2005:256-62.
12. Xiong W, Dong H, Wang J, et al. Analysis of plasma cytokine and chemokine profiles in patients with and without tuberculosis by liquid array-based multiplexed immunoassays. PLoS One 2016; 11:e0148885.
13. Bekker LG, Maartens G, Steyn L, Kaplan G. Selective increase in plasma tumor necrosis factor-alpha and concomitant clinical deterioration after initiating therapy in patients with severe tuberculosis. J Infect Dis 1998; 178:580-84.
14. Yamshchikov AV, Kurbatova EV, Kumari M, Blumberg HM, Ziegler TR, Ray SM, Tangpricha V. Vitamin D status and antimicrobial peptide cathelicidin (LL-37) concentrations in patients with active pulmonary tuberculosis. Am J Clin Nutr 2010; 92:603-11.
15. Larcombe L, Mookherjee N, Slater J, et al. Vitamin D, serum 25(OH)D, LL-37 and polymorphisms in a Canadian First Nation population with endemic tuberculosis. Int J Circumpolar Health 2015; 74:28952.

LETTER TO THE EDITOR

CORRELATION ANALYSIS OF *CD4* GENE POLYMORPHISM AND BLOOD ROUTINE INDEXES IN PIGS (*SUS SCROFA*)

J. XU[1], H. ZHANG[2], Y. GU[1], K. MEHMOOD[2,3], Q. ZHANG[4], M. IJAZ[5], R.Z. ABBAS[6], W. BABAR[3] and S. LI[1]

[1]College of Animal Science, Anhui Science and Technology University, Fengyang, China; [2]College of Veterinary Medicine, Huazhong Agricultural University, Wuhan, China; [3]University College of Veterinary and Animal Sciences, Islamia University of Bahawalpur, Bahawalpur, Pakistan; [4]College of Animal Science and Technology, China Agricultural University, Beijing, China; [5]Department of Clinical Medicine and Surgery, University of Veterinary and Animal Sciences, Lahore, Pakistan; [6]Departmet of Parasitology, University of Agriculture Faisalabad, Pakistan

Received December 8, 2017 – Accepted February 19, 2018

The first two Authors made equal contributions to this article

Cluster of differentiation 4 (*CD4*) is an important molecule in the immune system of animals, which participates in the processes of T-lymphocyte differentiation, maturation, immune response and signal transduction. During this study, we adopted the direct sequencing of PCR products and time-of-flight mass spectrometry methods for the detection of single nucleotide polymorphisms (SNPs) in 382 Yorkshire pigs. The linkage disequilibrium of *CD4* gene polymorphisms and their genetic effects on blood routine indexes were also analyzed. The results showed that SNP was screened in intron 1, intron 6 and exon 10, respectively, of the porcine *CD4* gene, and each SNP locus was detected in Yorkshire pigs, which had three genotypes with moderate polymorphism. The three SNPs were in strong linkage disequilibrium (r^2>0.8), and constituted only two major haplotypes, AGT and CAC (both frequencies accounted for about 97%). The association analysis showed that *CD4* gene polymorphisms were significantly correlated with white blood cell, lymphocyte and monocyte count in Yorkshire pigs (*P*<0.05). The white blood cell count and monocyte count in individual animals with CAC/CAC diplotype were significantly higher than those with AGT/CAC and AGT/AGT diplotypes (*P*<0.05). The lymphocyte count in animals with CAC/CAC diplotype were significantly higher than those with the AGT/AGT diplotype (*P*<0.05). This study indicates that *CD4* gene is significantly associated with partial blood routine indexes in pigs, and it can be considered as a candidate gene for the study of porcine disease resistance.

To the Editor,

At present, the prevention and control of disease is still an essential part of pig farming. The development of immune procedures and drug treatment can be studied from the perspective of genetic breeding to enhance the disease resistance of pigs. Different animals have different resistance to diseases, but there are still many difficulties in raising the disease resistance in pigs to resist pathogens (1). The composition of blood is stable in normal conditions

Key words: CD4 gene, single nucleotide polymorphisms, pig, haplotype, blood routine indexes

Mailing address:
Dr Shenghe Li,
College of Animal Science,
Anhui Science and Technology University,
Fengyang 233100, China.
Tel.: +86 13855046178
e-mail: lishhe2005@163.com

0393-974X (2018)

only if the physiology or pathology is unchanged. Therefore, the blood immunity parameter is closely related to the immune response in the body, which is the auxiliary index to measure and evaluate the health. The variation of blood index can reflect the changes of immune status in animals, therefore investigating the genetic variation that regulates blood immunological characters in the genome can help to promote the breeding of pig disease resistance (2).

Hematological parameters can reflect the immune status of the body and become an important auxiliary indicator for the clinical diagnosis of human medicine. At present, some porcine genomic regions related to blood routine have been located by quantitative trait loci (QTL) positioning and genome-wide association analysis (3, 4), but the functional genes that regulate blood routine parameters and their variation need more specific research.

Cluster of differentiation (CD) 4 molecules are mainly expressed in CD4+ T lymphocyte and its biological functions are related to T lymphocyte subgroup (5). The CD4 molecule is one of the important surface auxiliary T cell (T_H) proteins and its mutation could potentially impact T_H cell function. Previous studies have shown that gene polymorphism of *CD4* is significantly associated with human rheumatoid arthritis and somatic cell score of dairy cattle (6,7). In swine, *CD4* gene is located in chromosome V (8), and it is significantly associated with T lymphocyte subsets in peripheral blood of Yorkshire pigs (9). However, polymorphisms of other regions of the pig *CD4* gene and its correlation with blood routine have not been reported. This research was carried out to determine the correlation analysis of *CD4* gene polymorphism and blood routine indexes in pigs.

MATERIALS AND METHODS

Ethics approval

All the experiments were approved and conducted according to the guideline of Animal Welfare and Ethics Committee Chinese Agricultural University, Beijing, China following the national legislations regarding animal welfare.

Sample collection

A total of 382 samples from 10-day-old pigs (*Sus scrofa*) were collected randomly from local pig farms during 2015. During the experimental period, blood and ear tissues (used for extracting genomic DNA) were collected on days 20 and 35 for future analysis.

Table I. *Primer sequences of porcine CD4 gene.*

Primer	Amplification region	Primer sequence	Tm/°C	Product size /bp
P1	Partial intron 1, exon 2 and partial intron 2	F: CTGGCAAATCGGCTTCAT	57	693
		R: GGTGGTCAGGACTTGAGGTT		
P2	Partial intron 5, exon 6 and partial intron 6	F: TCTGCTCTTATCTCGTGCGG	56.5	831
		R: GGCTGCCTCTTGGATGTCA		
P3	Partial exon 10 and external sequence	F: ACTGACGGAGCCACAGACTC	57.5	668
		R: GGCTATCAACTTTCGCAGGA		

Hematological measurements

To study the physiological blood status of pigs, the blood indexes was measured by using an automatic hematology analyzer (CELL-DYN1500, Abbott) according to our previous study (10) to check the average white blood cell count, neutrophilic granulocyte count, neutrophilic granulocyte percentage, lymphocyte count, lymphocyte count percentage, monocyte count, monocyte count percentage, red blood cell count, hemoglobin, mean corpuscular hemoglobin concentration, mean corpuscular hemoglobin, hematocrit, red blood cell volume distribution width, mean corpuscular volume, platelets count, plateletocrit, platelet distribution width, and mean platelet volume.

Genetic polymorphism detection

Total DNA was purified from ear tissue using a TIANamp DNA Extraction Kit (TianGen, China) as per the manufacturer's instructions. The *CD4* gene was further amplified by using primers designed according to the database of Ensemble (ID: ENSSSCG00000000687). The PCR amplification approach was used to amplify the fragment of the *CD4* gene by the specific primers (I). The amplification was made using a PCR Kit (TianGen, China) with the previous specifications (11, 12). PCR products were separated on Agarose gel (1.5%) along with ethidium bromide (0.5μg/mL), followed by electrophoresis in 0.5×TBE buffer at 5 V/cm for 60 min. The obtained products were sequenced by a commercial company (Quintara Biosciences, Wuhan, China).

Genotyping and haplotype construction

Single nucleotide polymorphisms were screened using the DNAMAN 6.0 software. Three SNPs were detected in the porcine *CD4* gene by sequence comparison. Haploview 4.2 and Beagle 3.3.2 software were used to construct the

Table II. *Genotype, allele frequency, population genetic parameters, polymorphism, haplotype type and frequency of the CD4 gene in Yorkshire pigs.*

Name	**Genotype frequency (genotype)**	**Allele frequency**			**χ^2-value**
Intron 1	0.2435 (CC)	0.4660 (CA)	0.2906 (AA)	0.4764 (C)	0.5236 (A)	1.6634
Intron 6	0.2277 (AA)	0.4817 (AG)	0.2906 (GG)	0.4686 (A)	0.5314 (G)	0.4118
Exon 10	0.2461 (CC)	0.5026 (CT)	0.2513 (TT)	0.4974 (C)	0.5026 (T)	0.0106
Population genetic parameters and polymorphisms					
Name	Homozygosity	Heterozygosity	Number of effective allele	Polymorphism information content	
SNP1	0.5011	0.4989	1.9956	0.3744	
SNP2	0.5020	0.4980	1.9921	0.3740	
SNP3	0.5000	0.5000	1.9999	0.3750	
Haplotype type and frequency					
Type	Haplotype	Frequency (number of haplotype)			
Haplo 1	AGT	0.5026 (384)			
Haplo 2	CAC	0.4673 (357)			
Haplo 3	AGC	0.0196 (15)			
Haplo 4	CGC	0.0092 (7)			
Haplo 5	AAC	0.0013 (1)			

SNPs haplotype construction. The SNPs were genotyped using the time-of-flight mass spectrometry (Sequenom Mass Array).

Statistical analysis

All statistical analyses were performed using SPSS 19.0 software and the model is presented as $y=\mu+h+s+t+bx+e$ (y: blood routine index in day 35; μ: population mean; h: haplotype; s: gender; t: sampling time; b: blood routine index on day 20; x: regression coefficient of blood routine index on day 20; e: random error).

RESULTS

Polymorphism detection and classification of CD4 gene

The PCR products were sequenced and three SNPs were detected from *CD4* gene. The results showed that polymorphic sites were located in intron 1, intron 6 and exon 10, respectively named SNP1 (g. 6283C/A), SNP2 (g. 21659A/g) and SNP3 (g. 25827C/T) (Fig. 1). Each SNP was detected and three genotypes existed, introns 1 (CC, CA and AA), intron 6 (AA, GA and GG) and exons 10 (CC, CT and TT).

Genetic characteristics analysis of CD4

The genotype frequency and allele frequency analysis of 3 SNPs are shown in Table I. The results showed that the frequency of intron 1 was highest in CA>AA>CC, while the frequency of allele A was higher. The frequency of intron 6 was highest in AG>GG>AA, with higher frequency of allele G. Exon 10 genotype frequency was highest in CT>TT>CC, while the frequency of allele T was higher. Genetic parameter analysis of three SNPs in *CD4* gene were shown in Table II, the homozygosity of intron 1, intron 6 and exon 10 of the polymorphic sites was similar to that of heterozygosity (approximately

Table III. *Association between the CD4 gene polymorphism and blood routine indexes in Yorkshire pigs.*

Blood routine indexes	Diplotype (sample number)		
	CAC/CAC (86)	AGT/CAC (177)	AGT/AGT (96)
White blood cell count /($10^9 \cdot L^{-1}$)	18.90±0.68^a	16.59±0.52^b	15.54±0.61^b
Neutrophilic granulocyte count /($10^9 \cdot L^{-1}$)	4.65±0.34	3.90±0.26	4.03±0.31
Neutrophilic granulocyte percentage /%	24.21±1.65	23.92±1.26	26.30±1.48
Lymphocyte count/($10^9 \cdot L^{-1}$)	10.75±0.47^a	9.99±0.36^{ab}	9.04±0.42^b
Lymphocyte count percentage /%	60.53±1.63	61.94±1.24	59.66±1.46
Monocyte count /($10^9 \cdot L^{-1}$)	2.92±0.15^a	2.34±0.12^b	2.15±0.14^b
Monocyte count percentage /%	15.23±0.60	14.06±0.46	13.98±0.55
Red blood cell count /($10^{12} \cdot L^{-1}$)	5.57±0.15	5.76±0.11	5.61±0.13
Hemoglobin /($g \cdot L^{-1}$)	108.96±2.58	105.08±2.00	104.21±2.28
Mean corpuscular hemoglobin concentration /($g \cdot L^{-1}$)	319.37±4.42	318.29±3.41	323.07±4.08
Mean corpuscular hemoglobin /pg	18.06±0.21	17.73±0.17	18.01±0.20
Hematocrit /%	33.76±0.86	32.97±0.66	32.47±0.76
Red blood cell volume distribution width /%	20.96±0.52	20.61±0.40	20.72±0.45
Mean corpuscular volume /fL	55.22±0.47	54.43±0.37	54.46±0.41
Platelet count /($10^9 \cdot L^{-1}$)	531.18±28.83	530.82±22.37	552.51±26.03
Plateletocrit /%	0.47±0.02	0.45±0.02	0.46±0.02
Platelet distribution width /%	13.97±0.16	14.06±0.12	14.10±0.14
Mean platelet volume /fL	8.78±0.14	8.43±0.12	8.56±0.13

The same letters in the same row show no significant difference ($P>0.05$), the different letters show significant difference ($P<0.05$), data are shown least squares mean ± standard error.

0.5). The effective allele numbers were close to 2, which were in the moderate polymorphism (0.25< polymorphism information content <0.5).

Analysis of CD4 gene haplotypes

The linkage disequilibrium analysis showed that the *CD4* gene has a strong chain imbalance (r^2 >0.8), where the r^2 value of SNP1 and SNP2, SNP1 and SNP 3, SNP2 and SNP3 were 0.95, 0.92 and 0.89, respectively (Fig. 2). The haplotype frequency of AGT is 0.5026 and CAC is 0.4673, while the frequencies of rare haplotypes (AGC, CGC and AAC) are 0.0196, 0.0092 and 0.0013, respectively (Table II).

Correlation analysis of CD4 gene polymorphism and blood immune indexes

The polymorphisms of *CD4* were significantly

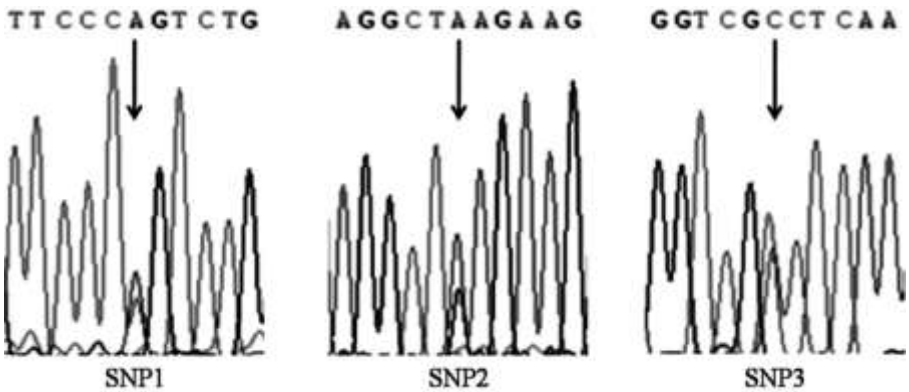

Fig. 1. *Detection of porcine CD4 gene polymorphisms.*

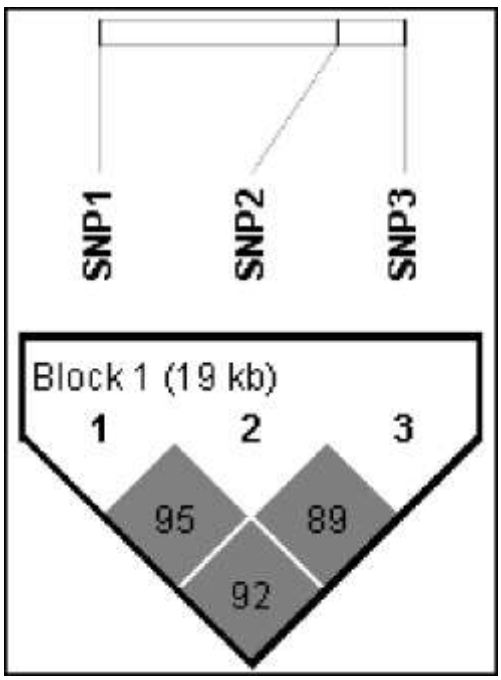

Fig. 2. *The linkage disequilibrium analysis of porcine CD4 gene polymorphisms. (The numbers represent r^2 (%), the larger the value (range of value is 0~1), the stronger the degree of linkage disequilibrium).*

correlated with white cells, lymphocytes, and monocytes in Yorkshire pigs ($p<0.05$), and there was no significant correlation with white blood cell, red blood cell and platelet ($p>0.05$). Meanwhile, the white blood and monocyte count in individual animals with the CAC/CAC diplotype were significantly higher than those with AGT/CAC and AGT/AGT diplotypes ($P< 0.05$). The number of lymphocytes in individual animals with the CAC/CAC diplotype was significantly higher than those with the AGT/AGT diplotype ($P< 0.05$), as shown in Table III.

DISCUSSION

Our previous studies found five missense mutations from the *CD4* coding region in pigs, and these have strong linkage disequilibrium state in SNPs in 16kb (9). In order to further analyze the variations of *CD4* gene, the polymorphisms were carried out in the same pig samples. The results showed that the *CD4* gene has genetic variations. Previous studies have found that the intron 1 of the *CD4* gene was contained silencer in mice (13), and the intron 1 of the *CD4* gene confirmed existence promoter in human (14). Furthermore, our study found that two SNPs in introns 1 and 6 were not involved in coding the CD4 protein, and potentially affected the expression of *CD4* gene. Our results suggest that *CD4* gene (19 kb) has a stronger degree of linkage disequilibrium ($r^2 >0.8$), which means that three SNPs have linkage with other mutations which can affect the *CD4* gene function.

It is now widely acknowledged that the routine blood test is closely associated with immune responses. Single SNP analysis was tedious and not comprehensive, so we adopted the haplotypes analysis to study the effects of SNPs (15). Our results show that three SNPs found in this experiment had strong linkage disequilibrium, so we analyzed two main haplotype (AGT and CAC) of *CD4* gene. The results showed that polymorphisms of the *CD4* gene had significant correlation with blood leucocyte indexes (white blood cells, lymphocytes and monocytes). The encoding protein of *CD4* gene was mainly expressed in *CD4* T lymphocytes and small part of *CD4* molecules were distributed in B lymphocytes and monocytes. This indicates that *CD4* gene polymorphisms significantly correlated with the number of monocytes. Our results indicated that polymorphisms of the *CD4* gene have an effect with leucocyte in blood. Our study showed that the number of white blood cells, lymphocytes and mononuclear cells in pigs with the CAC/CAC genotype was significantly higher than those of AGT/AGT. However, there is a difference in the immunity between CAC/CAC and AGT/AGT types of *CD4* gene, which requires further study in the future.

In conclusion, this study indicates that the *CD4* gene polymorphisms is significantly associated with partial blood routine indexes, therefore can be considered as a candidate gene in disease-resistant breeding of pigs.

ACKNOWLEDGEMENTS

This work was supported by the Provincial Natural Science Research Project of Anhui Colleges (KJ2017ZD43), the Anhui Provincial Science and Technology Major Special Project (16030701066 and 17030701008), and the Anhui Provincial Science and Technology Plan Project (1704a07020093).

REFERENCES

1. Stear MJ, Bishop SC, Mallard BA, Raadsma H. The sustainability, feasibility and desirability of breeding livestock for disease resistance. Res Vet Sci 2001; 71(1):1-7.
2. Mach N, Yu G, Lemonnier G, Lecardonnel J, Oswald IP, Estellé J, Rogel-Gaillard C. The peripheral blood transcriptome reflects variations in immunity traits in swine: towards the identification of biomarkers. BMC Genomics 2013; 14:894.
3. Wang JY, Luo YR, Fu WX, et al. Genome-wide association studies for hematological traits in swine. Anim Genet 2013; 44(1):34-43.
4. Zhang F, Zhang Z, Yan X, Chen H, Zhang W, Hong Y, Huang L. Genome-wide association studies for hematological traits in Chinese Sutai pigs. BMC Genet 2014; 15:41.
5. Vignali DA, Doyle C, Kinch MS, Shin J, Strominger

JL. Interactions of CD4 with MHC class II molecules, T cell receptors and p56lck. Philos Trans R Soc Lond B Biol Sci 1993; 342(1299):13-24.

6. He Y, Chu Q, Ma P, et al. Association of bovine CD4 and STAT5b single nucleotide polymorphisms with somatic cell scores and milk production traits in Chinese Holsteins. J Dairy Res 2011; 78(2):242-49.
7. Mohammed WJ, Sh B, Jasim NA, Jebur MS. Validity of CD4 enhancer gene polymorphism in susceptibility and severity of some Iraqi rheumatoid arthritis patients. Int J Adv Res 2016; 3:1200-05.
8. Matsubara T, Nishii N, Takashima S, et al. Identification and characterization of two CD4 alleles in Microminipigs. BMC Vet Res 2016; 12:222.
9. Xu J, Liu Y, Fu W, et al. Association of the porcine cluster of differentiation 4 gene with T lymphocyte subpopulations and its expression in immune tissues. Asian-Australas J Anim Sci 2013; 26(4):463-69.
10. Zhang H, Dong H, Mehmood K, et al. Physiological variations among blood parameters of domestic cats at high- and low-altitude regions of China. Arch Physiol Biochem 2018; doi: 10.1080/13813455.2018.1423623.
11. Zhang H, Li K, Wang Y, et al. Investigation and characterization of β-lactam resistance in Escherichia coli strains isolated from bamboo rats (Rhizomys sinensis) in Zhejiang province, China. J Vet Med Sci 2017; 79(10):1633-36.
12. Zhang H, Rehman, MU, Li K et al. Antimicrobial resistance of Escherichia coli isolated from Tibetan piglets suffering from white score diarrhea. Pak Vet J 2017; 37:43-46.
13. Siu G, Wurster AL, Duncan DD, Soliman TM, Hedrick SM. A transcriptional silencer controls the developmental expression of the CD4 gene. EMBO J 1994; 13(15):3570-79.
14. Rushton JJ, Zorich GP, Stolc V, Neudorf SM. Characterization of a promoter within the first intron of the human CD4 gene. Eur J Biochem 1997; 245(3):768-773.
15. Akey J, Jin L, Xiong M. Haplotypes vs single marker linkage disequilibrium tests: what do we gain? Eur J Hum Genet 2001; 9(4):291-300.

LETTER TO THE EDITOR

IMPORTANCE OF BASOPHILS IN EOSINOPHILIC ASTHMA: THE MURINE COUNTERPART

D. PODDIGHE[1,2], C.B. MATHIAS[3], I. BRAMBILLA[2], G.L. MARSEGLIA[2] and H.C. OETTGEN[4,5]

[1]Department of Medicine, School of Medicine, Nazarbayev University, Astana, Kazakhstan; [2]Department of Pediatrics, Università degli Studi, Pavia, Italy; [3]Department of Pharmaceutical and Administrative Sciences, College of Pharmacy, Western New England University, Springfield, MA, USA; [4]Department of Medicine, Boston Children's Hospital, Boston, MA, USA; [5]Department of Pediatrics, Harvard Medical School, Boston, MA, USA

Received December 19, 2017 – Accepted February 19, 2018

Several experimental studies in mice showed that basophils participate in the initiation of Th2 adaptive immune response, in addition to the effector phase. However, the role of basophils in allergic airway inflammation is less clear. The aim of this experiment was to assess the importance of basophils in recruiting inflammatory cells and, in particular, eosinophils in a murine model of asthma induced by *Aspergillus fumigatus* allergens. Additionally, bronchial reactivity was evaluated. Basophil depletion resulted in a reduction of inflammatory cells in the airways and eosinophil recruitment was significantly impaired. Also bronchial reactivity seemed to be impaired in basophil-depleted mice, but the result was not statistically significant. According to these preliminary data, basophils seem to influence the local eosinophilic response of allergic asthma.

To the Editor,

Allergic asthma is a chronic inflammatory process arising from a dysregulation of the immune response to some environmental allergens. Cytokines, such as interleukin (IL)-4, IL-5, IL-13, produced by CD4+ T cells polarized toward Th2 functional phenotype and activated mast cells, lead to IgE production and eosinophilic pulmonary inflammation associated to airway hyper-responsiveness, which are the main pathophysiological features of allergic asthma (1).

Initial mechanisms responsible for Th2 differentiation after contact with air allergens have not been completely elucidated. Local cytokine production along with antigenic activation of naïve T CD4+ cells is known to be an important factor to commit them toward one of several functional T helper subsets. In allergic diseases, early IL-4 production is supposed to be critical for Th2 differentiation, and the innate immune system has been demonstrated to play a fundamental role in this regard. Recently, the idea that basophils may be an important starting source of lymphocyte-priming IL-4 has gained ground progressively (2-3).

Despite their small number, basophils have been shown to contribute to the effector phase of host response to helminthes, chronic IgE-mediated skin reactions and acute IgG-mediated anaphylaxis; moreover, recent studies hypothesized a role of basophils in some autoimmune diseases. In general, novel mouse models have provided additional evidence supporting a remarkable role of basophils in triggering Th2 responses in allergy (4-7). A few

Key words: basophils, asthma, mouse, Aspergillus fumigatus, eosinophils, bronchial reactivity

Mailing address:
Dr. Dimitri Poddighe, M.D.
Department of Medicine,
School of Medicine, Nazarbayev University,
010000 Astana, Kazakhstan
Tel.: +7 347 7241851
e-mail: dimitri.poddighe@nu.edu.kz

0393-974X (2018)

years ago, we carried out a study on a murine model of allergic asthma induced by *Aspergillus fumigatus* (*Af*) allergens. Our previous findings from such a mouse model of eosinophilic asthma suggested that basophils promote the development of Th2 lymphocytes, as their depletion resulted in a lower percentage of Th2-lymphocytes at several sites, as well as in the impairment of the related cytokine and IgE immunoglobulin production. (8)

As a clinical counterpart, an increased number of basophils in lungs and airways of asthmatic patients has been described in several studies, and those cells are mainly implicated in eosinophilic asthma. Recently, Brooks et al. assessed the number of basophils in the sputum of patients with allergic asthma and found an increase of basophils, recovering the highest numbers in patients showing an eosinophilic endotype of asthma (9). Thus, in the light of recent advances about the biological importance of basophils, here we report some preliminary data collected in the context of experimental studies on basophil-depleted mice with allergic asthma induced by *Aspergillus fumigatus* (*Af*) allergens, which further support the influence of basophils in the recruitment of eosinophils in the inflamed respiratory mucosa and, as a consequence, in bronchial hyper-reactivity.

MATERIALS AND METHODS

Study design

A 50 µl sterile aqueous extract of *Af* was applied intra-nasally *(i.n.)* to BALB/c mice, according to a prolonged sensitization protocol, lasting 3 weeks (*3w*), as shown in Fig. 1 (10); the control group was treated with intra-nasal sterile saline solution (50 µl). Mice depleted of basophils received the intra-peritoneal (i.p.) administration of MAR-1 anti-FcεRI monoclonal antibody (10 µg/day for 3 days/week). Each experimental group included five mice. After the sensitization protocol, all mice underwent whole body plethysmography (through BUXCO equipment), in order to evaluate the bronchial reactivity to nebulized methacholine administered at progressively increasing concentrations (from 0 mg/ml up to 333 mg/ml). After this procedure, mice were sacrificed and a bronchoalveolar lavage (BAL) was performed, in order to count the inflammatory cells inside.

Mice and reagents

A sterile aqueous extract of *Aspergillus fumigatus* (1:10 w/v at 87.000 PNU/ml) was obtained from Greer Laboratories. BALB/c mice were purchased from Taconic Farms. Mice were housed in a specific pathogen-free environment and were 8-10 weeks old. All experiments were conducted in accordance with the Institutional Animal Care and Use Committee policies and procedures of the Children's Hospital Boston.

Collection and analysis of BAL specimen

For bronchoalveolar lavage (BAL), 1 ml of PBS was infused into the trachea and then retrieved. BAL fluid was cytocentrifugated onto slides and differential cellular analysis was performed by light microscopy, after staining with Wright-Giemsa (Richard-Allan Scientific).

Methacholine bronchial reactivity test

The whole-body single-chambered plethysmograph (freely moving animal) was purchased from BUXCO Electronics, New York, USA. Data were acquired in conscious mice using a BUXCO LS14 Biosystem Plethysmograph logging analyzer. Penh (PEF/PIF x Pause) was used as a main parameter to track the bronchial response to allergen challenge (11).

Statistical analysis

Differences in experimental parameters among the experimental groups were examined for significance with GraphPad Prism® software using ANOVA test, and values are presented as means ± standard error of the mean (SEM).

RESULTS

BAL cellularity

After sacrifice, the mice received bronchoalveolar lavage (BAL) in order to count the inflammatory cells from lower airways.

As shown in Fig. 2A, we observed a significant increase of cells recovered by BAL in mice sensitized with *Af* suspension compared to mice receiving sterile saline solution (638±52.1 $x10^3$/ml *vs* 52.5±8.5 $x10^3$/ml in saline-treated mice, $p<0.001$); importantly, basophil-depleted and *Af* sensitized mice showed a significant reduction of total cellularity in BAL (372±43.75 $x10^3$/ml,

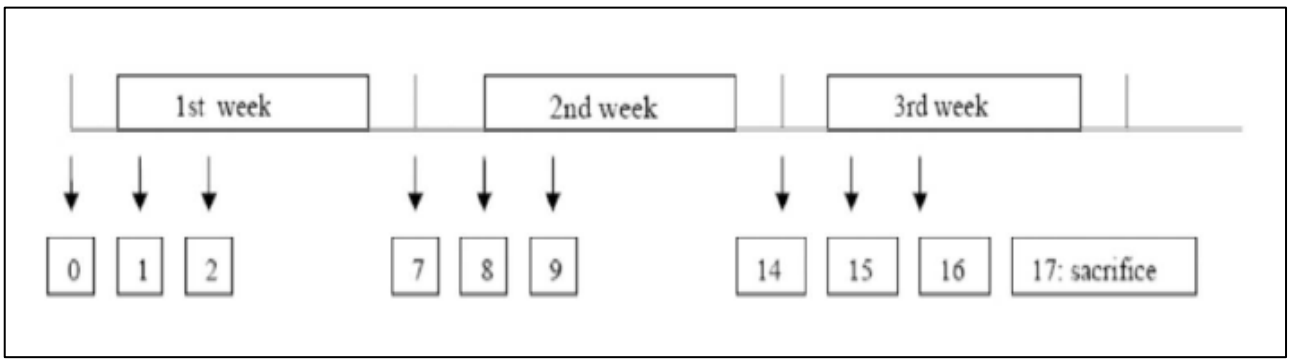

Fig. 1. *Sensitization protocol with Aspergillus fumigatus allergens (the arrows indicate days when the extract was administered intra-nasally).*

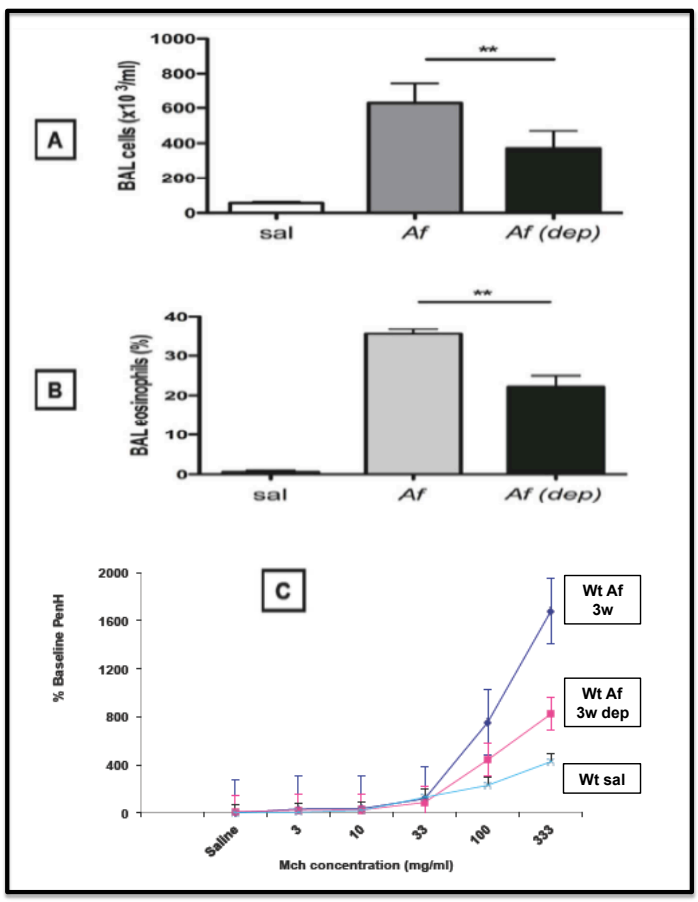

Fig. 2. *Summary of experimental data.* ***A****) BAL cellularity in the three groups of mice: wild-type mice receiving saline solution [sal], wild-type mice sensitized with Aspergillus fumigatus allergens [Af] and basophil-depleted wild-type mice sensitized with Aspergillus fumigatus allergens [Af (dep)].* ***B****) Percentage of eosinophils in BAL cells in the three experimental groups.* ***C****) Curves of bronchial resistances after methacholine nebulization for all three groups: wild-type mice receiving saline solution [WT sal], wild-type mice sensitized with Aspergillus fumigatus allergens [WT Af 3w] and basophil-depleted wild-type mice sensitized with Aspergillus fumigatus allergens [WT Af 3w dep].*

$p<0.01$) compared to the correspondent group untreated with MAR-1 anti-FcεRI monoclonal antibody.

Moreover, BAL eosinophils were specifically counted. Whereas the inflammatory infiltrate was characterized by many eosinophils in normal mice sensitized with *Af* (243±28.9 x10^3/ml), their number was significantly lower in the study group depleted of basophils (81.8±10.5 x10^3/ml, $p<0.001$). No eosinophil increase was seen in mice treated with saline solution. In order to assess the specific difference in eosinophil recruitment, we expressed these data in percentage of the total cellularity (Fig. 2B). Again, the percentage of eosinophils (35.8±1.1% *vs* 22.2±2.75%, $p<0.01$) resulted to be significantly lower in mice depleted of basophils.

Bronchial reactivity

The curves expressing bronchial resistance (obtained through the relative increase of the measured PenH at a specific concentration of nebulized methacholine, expressed in percentage of the correspondent basal value) for each experimental group of mice are shown in Fig. 2C. At the two highest concentrations of nebulized methacholine, namely 100 mg/ml and 333 mg/ml, differences among the three curves become evident: in particular, the bronchial resistance of basophil-depleted mice resulted to be less increased than normal mice, after the protocol of *Af* sensitization, but such a difference did not reach any statistical significance.

DISCUSSION

Basophils have been demonstrated to be amplifier/effector cells of allergic inflammation and Th2 responses, through IgE binding. Indeed, a number of studies appreciated the effector role of basophils in anaphylaxis and allergic skin inflammation. More recently, skin inflammation elicited by means of passive immunization with hapten-specific IgE, followed by intradermal challenge, implicated basophils also in the induction of IgE-mediated allergic inflammation. Subsequent investigations, using genetic strategies to obtain mouse models depleted of basophils, confirmed a block of the induction of IgE-driven skin inflammation. Finally, an experimental study reported that the induction of food allergy by means of epicutaneous antigen application is dependent on IgE antibodies and basophils (12-13).

Unfortunately, the role of basophils in allergic airway inflammation is less defined. However, basophil depletion in murine models of OVA-induced allergic airway inflammation supported their role in the recruitment of Th2 cells in the airways. (14) We also showed an impaired development of IL-4-producing Th2 lymphocytes and IgE responses after basophil depletion in our murine model of allergic asthma induced by *Aspergillus fumigatus* allergens. (8) Interestingly, as a human counterpart, Boita et al. demonstrated that *Aspergillus fumigatus* stimulation resulted to upregulate BAFF expression on the basophils of severe asthmatic patients and those affected with bronchopulmonary aspergillosis, suggesting that basophils may contribute to the Th2 adaptive immune response and, specifically, to the polyclonal production of IgE observed in these patients. (15)

Moreover, basophils resulted to be increased in lungs of asthmatics and, importantly, were detected in the lungs of fatal asthma patients, suggesting an important role in most severe forms (16). The recent article by Brooks et al. supported a prominent role of basophils in eosinophilic asthma, where airway inflammation is typically Th2-driven. In that study, the authors assessed the number of basophils in the sputum of patients with allergic asthma compared to healthy controls; they found an increase of basophils in all asthmatic patients, recovering the highest numbers of basophils in patients showing an eosinophilic asthma. However, they were not able to find a clear correlation with respiratory function tests and, probably, this lack of statistical significance could be related to the small number of patients included in each subgroup of asthma (9). In the light of these human findings, our preliminary data may represent the murine counterpart. In our murine model of allergic asthma induced by *Aspergillus fumigatus* allergens, mice subjected to repeated inhalation of *Af* displayed a vigorous IgE response accompanied by a robust expansion of mast cells in the bronchi, which was associated with a significant recruitment of eosinophils also in the airways (10). Thus, such a model could be assimilated to human eosinophilic asthma. After describing that basophil

depletion resulted in a significant impairment of Th2 adaptive immune response (8), here we assessed the bronchial inflammatory response and the bronchial reactivity to methacholine challenge. The cellularity of BAL resulted reduced in basophil-depleted mice and, importantly, the eosinophilic component was primarily compromised. Thus, our experimental data enriched this pathophysiological picture by showing that Th2 reduction, induced by basophil depletion, may impair the effector phase of the allergic immune response in the airways and the bronchial reactivity.

In conclusion, our data from a murine experimental model support the clinical observations of the importance of basophils in those endotypes of human asthma characterized by eosinophil infiltration, according to few available human studies. These findings might be an interesting extension of our previous studies, but further research is needed to clarify the biological relevance of basophils and their mechanisms, which are probably different among different forms of asthma, both in humans and animal models. Importantly, if this initial evidence could be confirmed by future research, basophils might represent an additional target for the therapy of allergic and eosiniphilic endotypes of asthma.

REFERENCES

1. Umetsu DT, Dekruyff RH. Immune dysregulation in asthma. Curr Opin Immunol 2006; 18:727-32.
2. Paul WE, Zhu J. How are T(H)2-type immune responses initiated and amplified? Nat Rev Immunol 2010; 10:225-35.
3. Thiriou D, Morianos I, Xanthou G, Samitas K. Innate immunity as the orchestrator of allergic airway inflammation and resolution in asthma. Int Immunopharmacol 2017; 48:43-54.
4. Obata K, Mukai K, Tsujimura Y, et al. Basophils are essential initiators of a novel type of chronic allergic inflammation. Blood 2007; 110:913-20.
5. Tsujimura Y, Obata K, Mukai K, et al. Basophils play a pivotal role in immunoglobulin-G-mediated but not immunoglobulin-E-mediated systemic anaphylaxis. Immunity 2008; 28:581-89.
6. Poddighe D, Marseglia GL. Commentary: Basophil activation-dependent autoantibody and interleukin-17 production exacerbate systemic lupus erythematosus. Front Immunol 2017; 8:787.
7. 7.Schwartz C, Eberle JU, Voehringer D. Basophils in inflammation. Eur J Pharmacol 2016; 778:90-95.
8. Poddighe D, Mathias CB, Freyschmidt EJ, Kombe D, Caplan B, Marseglia GL, Oettgen HC. Basophils are rapidly mobilized following initial aeroallergen encounter in naïve mice and provide a priming source of IL-4 in adaptive immune responses. J Biol Regul Homeost Agents 2014; 28:91-103.
9. Brooks CR, van Dalen CJ, Hermans IF, Gibson PG, Simpson JL, Douwes J. Sputum basophils are increased in eosinophilic asthma compared with non-eosinophilic asthma phenotypes. Allergy 2017; 72(10):1583-86.
10. Mathias CB, Freyschmidt EJ, Caplan B, et al. IgE influences the number and function of mature mast cells, but not progenitor recruitment in allergic pulmonary inflammation. J Immunol 2009; 182:2416-24.
11. Lomask M. Further exploration of the Penh parameter. Exp Toxicol Pathol 2006; 57:13-20.
12. Karasuyama H, Yamanishi Y. Basophils have emerged as a key player in immunity. Curr Opin Immunol 2014; 31:1-7.
13. Oettgen HC. Fifty years later: Emerging functions of IgE antibodies in host defense, immune regulation, and allergic diseases. J Allergy Clin Immunol 2016; 137:631-45.
14. Zhong W, Wu W, Zhang Y, et al. Basophils as a primary inducer of the T helper type 2 immunity in ovalbumin-induced allergic airway inflammation. Immunology 2014; 142:202-15.
15. Boita M, Heffler E, Pizzimenti S, et al. Regulation of B-cell-activating factor expression on the basophil membrane of allergic patients. Int Arch Allergy Immunol 2015; 166:208-12.
16. Marseglia GL, Caimmi S, Marseglia A, et al. Rhinosinusitis and asthma. Int J Immunopathol Pharmacol 2010; 23(Suppl 1):29-31.

LETTER TO THE EDITOR

CORRELATION BETWEEN CHILDHOOD ECZEMA AND SPECIFIC IgG ANTIBODY LEVEL

Y. LIU[1], H. YAN[2], F. SHAO[3], QH. LI[2] and M. CUI[2]

[1]Department of Dermatology, Taian Maternal and Child Health Care Hospital, Shandong, China; [2]Department of Pediatric Surgery, Taian City Central Hospital, Shandong, China; [3]Department of Pediatric Surgery, Taian Maternal and Child Health Care Hospital, Shandong, China

Received April 21, 2017 – Accepted February 21, 2018

Eczema, a common pediatric dermatosis with unclear pathogenesis, can seriously affect the life quality of children due to its recurrence and long course. Recent study has found that food specific IgG (sIgG) might be involved in the course of eczema. To analyze the correlation between childhood eczema and sIgG and evaluate the role of avoiding taking intolerance food in the treatment of childhood eczema, this study enrolled 216 children with eczema who were admitted to the Taian Maternal and Child Health Care Hospital, Shandong, China, between August 2014 and October 2015. They were divided into an eczema group (N = 140) and an allergy group (N = 76). Eighty healthy children who were admitted to the Department of Children Healthcare in the same period were selected as a control group. Enzyme-linked immuno sorbent assay (ELISA) was used to detect the serum sIgG level. The result showed that the sIgG positive rates of children in the eczema group and allergy group were 91.4% and 93.4%, respectively, and the difference had no statistical significance (P > 0.05). However, the sIgG positive rates of children in the eczema group and allergy group were significasntly higher than that in the control group (P < 0.05). Milk and eggs were the major allergy-causing food for children with sIgG positive rates higher than 70%. The sIgG test results revealed that eggs had the highest allergenicity, followed by milk, tomatoes and soybeans, and pork was not highly sensitive. Therefore, it can be concluded that sIgG positive rate of children with eczema is high, and examination of food sIgG antibody in serum is valuable in the diagnosis and treatment of childhood eczema.

To the Editor,

Allergic diseases, also known as anaphylactic diseases, are a group of inflammatory diseases caused by allergic reaction; allergens can induce allergy and the occurrence of allergic reaction via ingestion, injection, inhalation and direct contact (1, 2). Pediatric eczema, common among allergic skin diseases, is featured by complex pathogenesis and poor therapeutic outcome (3) and may evolve to other allergic diseases after most of the symptoms fade. Therefore, focusing on the pathogenesis of childhood eczema and giving early interventional treatment is of practical significance for its treatment.

In recent years, many scholars have found that food intolerance was associated with the incidence of many skin diseases and changes in disease conditions. Food intolerance is a repeatable IgG-mediated immune response induced by specific

Key words: childhood eczema, sIgG, food

Mailing address:
Dr Hua Yan,
Department of Pediatric Surgery,
Taian City Central Hospital,
Shandong, 271000, China
e-mail: yanh2233@163.com

0393-974X (2018)

food or ingredients, and manifests as symptoms across the whole body, mainly involving the skin and gastrointestinal tract (4, 5). One epidemiological study (6) has suggested that approximately 33% of allergic diseases are induced by food. It was also pointed out that more than 35% of the total population has late-phase sensitive positive reaction to one or more kinds of food (7). This study aimed to investigate the correlation between childhood eczema and sIgG in the serum and the role of avoiding taking sIgG-positive food.

MATERIALS AND METHODS

Study subjects

Two hundred and sixteen children, 116 boys and 100 girls (aged 9 months~13 years; average age 2.5±1.6 years), with childhood eczema who were admitted to Taian Maternal and Child Health Care Hospital, Shandong, China, between August 2014 and November 2015 were enrolled. There were, and the Moreover, 80 healthy children, 44 boys and 36 girls (average age 3.1±1.8 years), were selected from the Department of Child Healthcare of the same hospital as a control group. The children with eczema were divided into an eczema group (N = 140) and an allergy group (N = 76) based on the presence of allergic diseases. In the eczema group, there were 75 boys and 65 girls, with an average age of 3.8±1.3 years; in the allergy group, there were 43 boys and 33 girls, with an average age of 4.1±1.4 years. The level one or two immediate relatives of 120 out of 216 children with eczema had a family history of allergy. In the allergy group, there were 39 children with allergic rhinitis, 29 children with bronchial asthma, 24 children with urticaria, and 16 children with more than two allergic diseases. There was no significant differences in the general data between the three groups (P>0.05), therefore, the results were comparable.

In this study, selection of the subjects was in line with ethical requirements, the family members of the patients signed informed consent, and diagnosis of eczema was consistent with the diagnosis and treatment guidelines for eczema. Eczema was confirmed by laboratory or histopathological examinations. Children with symptoms similar to eczema, severe blood diseases, mental illness or acute diseases in infection period, those who had been recently treated with glucocorticoid and those who refused to coordinate with the treatment were excluded from the study.

Detection methods

The serum sIgG level was measured by enzyme-linked immuno sorbent assay (ELISA), and the children were given drugs for external use. The effect was analyzed after 2 months of not taking sIgG-positive food. 3 mL of venous blood was extracted after four to six hours of fasting and then placed aside for 30 min. Then the serum was centrifuged by a centrifugal machine at 3000 r/min. Finally it was transferred to a German Effendof tube and stored at 2~8°C. The detection finished within 2 days. The sIgG levels of beef, chicken, cod, corn, crab, eggs, mushrooms, milk, pork, rice, shrimp, soybeans, tomatoes and wheat were detected. Personal LAB TM (Adaltis, Italy) and food intolerance kit (Biomerica, USA) were used. The sIgG concentration of the specimens was determined based on the absorbance value, and the unit was $U \cdot mL^{-1}$. The determination criteria were as follows: allergy was determined as level 0 if the sIgG concentration was lower than 50 $U \cdot mL^{-1}$; level 1 (mild) if the sIgG concentration was between 50 and 100 $U \cdot mL^{-1}$; level 2 (moderate) if the sIgG concentration was between 100 and 200 $U \cdot mL^{-1}$; and level 3 (severe) if the sIgG concentration was higher than 200 $U \cdot mL^{-1}$.

Evaluation of treatment

Treatment effect was evaluated as cured, significantly effective, progressive or ineffective. The overall effective rate could be obtained by adding the cured rate with the significantly effective rate. The treatment effect were assessed one week after withdrawal, and was determined as cured if the eczema area improved for more than 90%, significantly effective if the eczema area improved for 60-90%, progressive if the eczema area improved between 20% and 60%, and ineffective if the eczema area was less than 20%.

Statistical analysis

Data were analyzed by SPSS ver. 21.0. Rates were compared using *Chi*-squared test. Difference was considered as statistically significant if $P < 0.05$.

RESULTS

Comparison of sIgG positive rate between the three groups

The difference of the sIgG positive rate between

the eczema group and allergy group was not statistically significant ($\chi^2 = 0.385$, P = 0.517); the difference of the sIgG positive rate between the eczema group and control group was statistically significant ($\chi^2 = 96.517$, P = 0.000); the difference of the sIgG positive rate between the allergy group and control group was statistically significant ($\chi^2 = 65.979$, P = 0.000) (Table I).

Categories and percentage of sIgG-positive foods in the eczema group

One hundred and twenty-eight patients had sIgG-positive results of 140 patients with eczema. Among the 128 patients, one kind of food taken by 29 patients was sIgG-positive (22.7%), two kinds of food taken by 38 patients were sIgG-positive (29.7%), three kinds of food taken by 18 patients were sIgG-positive (14.1%), and four or more kinds of food of 42 patients were sIgG-positive (32.8%).

Detection of serum sIgG of children in the eczema group after taking different kinds of food

The sIgG positive rate of milk was the highest (91.4%), followed by eggs (78.1%) and tomatoes (35.9%). The allergenicity of eggs was the highest (64.1%), followed by milk (61.7%), tomatoes (11.7%) and soybeans (7%), and pork was not highly sensitive (Fig. 1).

Therapeutic effects

Among the 216 children with eczema, 93 patients were cured, treatment of 96 patients was significantly effective, 10 patients had progressive disease condition, and treatment of 17 was ineffective; the overall effective rate was 87.5% (189/216).

DISCUSSION

Childhood eczema is the most common skin

Table I. *The comparison of food sIgG positive rate.*

Groups	Food sIgG		Total number	The positive rate (%)
	positive	negative		
Eczema group	128	12	140	91.4
Allergy group	71	5	76	93.4
Control group	13	67	80	16.3

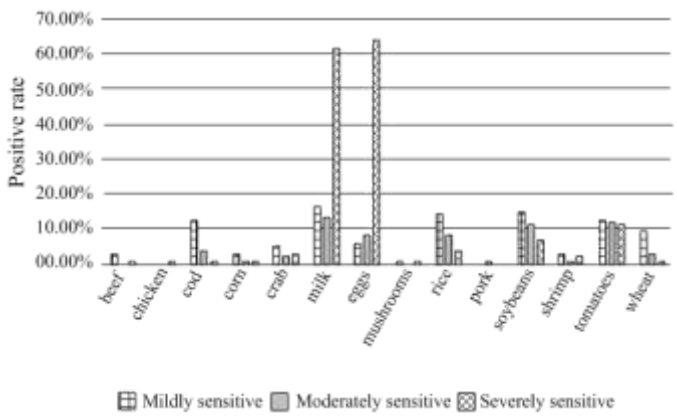

Fig. 1. *Food sIgG positive rates of fourteen kinds of food taken by patients in the eczema group.*

disease in pediatrics. In recent years, the incidence of childhood eczema has been increasing, and its pathogenesis is quite complicated. In addition to factors such as genetics, immunity, environment and endocrine, specific allergens are important external causes for childhood eczema. Eczema is reported associated to food intolerance (8). Foods which cannot be thoroughly digested by the human body, because of lack of some enzymes, enter into the intestinal tract in the form of peptides or other molecules and may be identified as foreign substances by the body, which may induce immune response and the generation of food specific IgG antibody (9). IgG antibody combines with food molecules to form immune complex, which blocks the renal filtration structure and induces a series of allergic symptoms.

A previous study (10) suggested that the sIgG positive rate of the patients with eczema was between 70% and 93%. The results of this study indicated that the sIgG positive rate of patients in the eczema group and allergy group was 91.4% and 93.4% respectively; the sIgG positive rate of milk was the highest, followed by eggs, tomatoes and soybeans, which indicated that sIgG is involved in the development of eczema.

Gary et al. (11) found that eliminating food influence was the only reliable method for Th1/Th2-mediated high sensitivity. The detection results of sIgG antibody suggested that mildly allergized food could be taken alternately; moderately and severely allergized food could be taken after two months of fasting if symptoms relieved. The current study found that most of the symptoms of eczema could be significantly alleviated and improved after avoiding taking sIgG-positive food.

REFERENCES

1. Isik S, Çaglar A, Eroglu-Filibeli B, Çaglayan-Sözmen S, Arikan-Ayyildiz Z, Asilsoy S, Uzuner N. Knowledge, perspectives and attitudes about allergen-specific immunotherapy for respiratory allergic disease among paediatricians in Turkey. Allergol Immunopath 2017; 45(2):193-97.
2. Lee CS, Kim HY, Lim YW, et al. Evaluation of the relationship between allergic diseases in school children at Seoul's roadside elementary schools and air pollution. Atmosp Pollut Res 2015; 6(6):1004-12.
3. Akelma AZ, Mete E, Bozkurt B. Effect of probiotic supplementation during pregnancy and breast-feeding on the allergic sensitization in the infantile eczema. J Allergy Clin Immunol 2013; 131(5):1447.
4. Bryniarski K, Ptak W, Jayakumar A, et al. Antigen-specific, antibody-coated, exosome-like nanovesicles deliver suppressor T-cell micro RNA-150 to effector T cells to inhibit contact sensitivity. J Allergy Clin Immunol 2013; 132(1):170-81.
5. Sicherer SH, Sampson HA. Food allergy: Epidemiology, pathogenesis, diagnosis, and treatment. J Allergy Clin Immunol 2014; 133(2):291-307.
6. Genuis SJ. Sensitivity-related illness: The escalating pandemic of allergy, food intolerance and chemical sensitivity. Sci Total Environ 2010; 408(24):6047-61.
7. Roduit C, Frei R, Depner M, et al. Increased food diversity in the first year of life is inversely associated with allergic diseases. J Allergy Clin Immunol 2014; 133(4):1056-64.
8. Zeng Q, Dong SY, Wu LX, et al. Variable food-specific IgG antibody levels in healthy and symptomatic Chinese adults. PLoS One 2013; 8(1):e53612.
9. Tkaczyk C, Okayama Y, Woolhiser MR, Hagaman DD, Gilfillan AM, Metcalfe DD. Activation of human mast cells through the high affinity IgG receptor. Mol Immunol 2002; 38(16-18):1289-93.
10. Saeed SA, Ali R, Ali SS, Ahmad N, Basit A, Urfy MZ. A closer look at food allergy and intolerance. J Coll Physicians Sung Pak 2004; 14(6):376-80.
11. Gray HC, Foy TM, Becker BA, Knutsen AP. Rice-induced enterocolitis in an infant: TH1/TH2 cellular hypersensitivity and absent IgE reactivity. Ann Allergy Asthma Immunol 2004; 93(6):601-5.

LETTER TO THE EDITOR

POSTERIOR HEMIVERTEBRA RESECTION IN COMBINATION WITH SCREW ROD INTERNAL FIXATION IN THE TREATMENT OF PEDIATRIC CONGENITAL SCOLIOSIS

YL. TIAN[1], J. GENG[2], F. WANG[3] and YP. ZHENG[4]

[1]Department of Pediatric Surgery, Binzhou People's Hospital, Shandong, China; [2]Department of Operating Room, Binzhou People's Hospital, Shandong, China; [3]Department of General Surgery, Binzhou People's Hospital, Shandong, China; [4]Department of Orthopedic Surgery, Qilu Hospital of Shandong University, Shandong, China

Received June 7, 2016 – Accepted February 21, 2017

Congenital scoliosis, a commonly seen disease occurring in children, can not only affect the growth, but also can uglify the individual which can severely affect the health and quality of life of children. To investigate the efficacy of posterior hemivertebra resection in combination with screw rod internal fixation in the treatment of congenital hemivertebra scoliosis, 115 patients were randomly divided into an observation group and a control group. Patients in the observation group were treated by posterior hemivertebra resection in combination with screw rod internal fixation, while patients in the control group were treated by posterior hemivertebra resection only. The surgical evaluation indicators, postoperative improvement of scoliosis and incidence of complications were recorded. The results demonstrated that the observation group had longer average operation time and less average blood loss compared to the control group, and the differences had statistical significance (P<0.05); the correction efficacy of the observation group was superior to that of the control group (P<0.05); the incidence of postoperative complications in the two groups had no significant difference, but the incidence of correction loss of the observation group was much lower than that of the control group (P<0.05). In conclusion, posterior hemivertebra resection in combination with screw rod internal fixation is a highly efficient and safe treatment which can significantly relieve the clinical symptoms and cause few complications.

To the Editor,

Congenital scoliosis, a congenital spine malformation, is a malformation in the bending direction and side direction on the coronal plane of spine which is induced by congenital developmental abnormality (1, 2). The pathogen of congenital scoliosis usually includes block vertebrae and spine formation failure, and hemivertebra is the most common cause (3). Congenital scoliosis can produce serious influence on the growth and development of children, and delayed treatment can result in spine malformation after body maturity, which can even induce spinal cord compression and multiple complications. Therefore, effective therapies for congenital scoliosis are always a focus in clinics.

Epiphysis block, internal fixation fusion and hemivertebra resection were frequently used to treat spine malformation (4). With the development of spinal surgery (5), posterior hemivertebra resection has been gradually applied in treating congenital

Key words: congenital scoliosis, posterior hemivertebra resection, screw rod internal fixation

Mailing address:
Dr Yanping Zheng,
No.107 Wenhua West Road,
Department of Orthopedic Surgery,
Qilu Hospital of Shandong University,
Jinan, Shandong, 250012, China
e-mail: zhengypbz@163.com

0393-974X (2018)

scoliosis. Hemivertebra resection fundamentally prevents the further progress of malformation and in combination with spinal internal fixation suggests a favorable corrective effect, therefore is more suitable for children. Yaszay et al. (6) also pointed out that hemivertebra resection in combination with vertebral resection could achieve a good result. Though the clinical application of the above combined regimen has been described in many papers (7, 8), the description is simple and only involves a small size of samples, and lacks analysis based on X-rays. This study selected one hundred and fifteen children with congenital scoliosis who were admitted to the hospital between January 2015 and January 2016, and treated with hemivertebra resection in combination with screw rod internal fixation, to analyze its efficacy and safety.

MATERIALS AND METHODS

General data

One hundred and fourteen patients with congenital hemivertebra scoliosis who were admitted to our hospital between January 2015 and January 2016 were selected as research subjects. They were randomly divided into an observation group and a control group. In the observation group, there were 30 males and 27 females, with an average age of 6.3±2.8 years; there were 27 cases of type I congenital scoliosis, 5 cases of mixed-type congenital scoliosis, 31 cases of tethered cord syndrome, 22 cases of diastematomyelia, and 4 cases of hip dysplasia. In the control group, there were 32 males and 25 females, with an average age of 6.6±3.1 years; there were 25 cases of type I congenital scoliosis, 8 cases of mixed-type congenital scoliosis, 34 cases of tethered cord syndrome, 26 cases of diastematomyelia and 3 cases of hip dysplasia. The difference of general data such as gender ratio, age and scoliosis type between the two groups suggested no statistical significance ($P>0.05$). Patients who were confirmed as scoliosis (Cobb angle of the major curve on the coronal plane > 90 degrees) by X-ray and whole spinal magnetic resonance imaging and had unilateral hemivertebra dysplasia, whose parents signed informed consent and who were aged from 3 years to 12 years were enrolled. Those who had severe mental disease or other serious diseases such as heart, liver and kidney failure or could not cooperate with doctors were excluded.

Therapeutic method

Patients in the control group underwent hemivertebra resection only. The detailed operation was as follows. After anesthesia, a line which was 5 cm long was drawn 1~2 cm away from the spinous process taking hemivertebra as the center. Then an incision was cut along the line, and the paravertebral muscle was detached to fully expose the vertebral plate, ribs adjacent to hemivertebra, spinous process-hemivertebra plane and upper and lower joint zygapophyseal joints. If nothing wrong was found by X-ray examination, the thoracic vertebra was detached, and the medial segment of rib was removed for bone grafting. Then the vertebral plate, pedicle of vertebral arch and transverse process were also removed. The anterolateral periosteum of the hemivertebra was detached to fully expose the hemivertebra, and the dura mater and spinal canal were marked. For patients who underwent eggshell hemivertebra resection, the anterior hemivertebra was scraped, then the interior hemivertebra. Cartilage shell was reserved. Bone grafting was performed inside the normal intervertebral disk and the cartilage shell of the hemivertebra. For those who underwent complete hemivertebra resection, the vertebral plate was removed firstly, and then the anterior hemivertebra was scraped. The posterior longitudinal ligament should not be exceeded when the posterior hemivertebra was scraped, avoiding damage to the venous plexus and spinal cord. The scraping stopped when reaching the nucleus pulposus. For patients with mixed congenital scoliosis upper and lower epiphyseal plate block was performed at the same time. After the upper and lower intervertebral discs were removed by a rongeur, cartilage plate was scraped until reaching the cancellous bone. Then cancellous bone was inserted into the vertebral defect site and hemivertebra to integrate the hemivertebra area, zygopophysis, upper and lower vertebral bodies, transverse process and vertebral plate. After surgery, the children were asked to lie on the bed and were forbidden to stand or sit. After being discharged, they wore braces for 5 to 7 months.

Patients in the observation group were treated by screw rod internal fixation in addition to posterior hemivertebra resection. A vertical incision was cut to expose the spinal cord until reaching the bilateral spinous processes, taking the position of hemivertebra that was confirmed by spinal computed tomography (CT) plain scan and three-dimensional reconstruction as the center. Corresponding

vertebral body was inserted with pedicle screws after target segment was confirmed. Patients observed with structural curvature underwent long-segment fixation, while two vertebral bodies above and below the hemivertebra were fixed for patients whose compensatory curvature was non-structural. Temporary rods were inserted on the concave side to stabilize the spinal cord after the screws inserted previously were confirmed stable, avoiding shearing-like injury caused by spinal twist during surgery. The braces were fixed for five to seven months after operation.

Observation index

The average duration of surgery and intraoperative blood loss of the two groups was recorded. The anteroposterior and lateral X-rays for the whole spinal cord were examined to measure the Cobb angle before and after surgery respectively, and the Cobb angle before surgery, one day after surgery and six months after surgery were recorded. The correction efficacy was evaluated based on correction rate, and the effects of the two regimens were compared. The formula of correction rate was: correction rate=(Cobb angle before operation-Cobb angle during follow-up)/ Cobb angle before surgery*100%. The incidences of complications were recorded during follow-up.

Statistical analysis

SPSS ver. 21.0 was used. Measurement data were expressed as mean±standard deviation (SD) and processed by *t*-test. Categorical data were expressed as percentage and processed by *Chi*-squared test. Difference was considered as statistically significant if $P<0.05$.

RESULTS

Comparison of correction efficacy

The Cobb angle was significantly improved in both groups after surgical correction, and the difference had statistical significance ($P<0.05$). The Cobb angle suggested no obvious changes in the reexamination performed in the 1st day and 6th

Table I. *Comparison of the correction efficacy between the two groups.*

Group		Observation group(N=57)	Control group (N=57)	χ^2	P
Cobb angle (°)	Before treatment	40.7±10.5	31.3±8.7	0.185	<0.05
	1 d after treatment	17.5±6.4	22.6±7.7	0.248	<0.05
	6 months after treatment	17.8±6.3	22.7±7.2	0.159	<0.05
Average correction rate (%)	Before treatment	-	-	-	-
	1 d after treatment	59.6	30.1	0.275	<0.05
	6 months after treatment	66.8	37.7	0.228	<0.05

Table II. *Comparison of average duration of operation and blood loss between the two groups.*

Group	Observation group(N=57)	Control group(N=57)	*t*	P
Average duration of operation (min)	278.9±48.1	189.7±26.2	0.196	<0.05
Average blood loss (mL)	258.7±34.4	125.8±36.9	0.219	<0.05

month after surgery. In the perspective of Cobb angle and average correction rate, the correction efficacy of the observation group was significantly superior to that of the control group, and the difference had statistical significance ($P<0.05$, Table I).

Comparison of duration of surgery and blood loss

The observation group had a longer average duration of operation and more average blood loss compared to the control group, and the differences had statistical significance ($P<0.05$, Table II).

Incidence of complications

The incidence of complication was 8.8% in the observation group; there were 4 cases of abdominal distention and pain and 1 case of incision infection. The incidence of complications in the control group was 10.5%; there were 4 cases of abdominal distention and pain, 1 case of incision infection and 1 case of lower limb discomfort. The comparison of incidence of complications between the two groups suggested no statistically significant difference ($\chi^2=1.315$, $P>0.05$). Four patients in the control group had loss of correction, while there was no case of loss of correction in the observation group. The fixation effect of the observation group was significantly superior to that of the control group ($^2=2.216$, $P<0.05$).

X-rays of typical scoliosis of the observation group

The X-rays suggested hemirertebra deformity in block vertebrae type on the right side of T4 before surgery (Fig. 1a); the instant correction effect was favorable after posterior hemivertebra resection in combination with screw rod internal fixation was used. The X-rays obtained after one-year follow-up suggested favorable correction maintenance, no loss and no obvious secondary deformity (Fig. 1b).

DISCUSSION

Congenital spinal deformity is mainly caused by the defects in the process of spinal segmentation and formation. Its incidence is 10%~20% among spinal deformity diseases. The pathogenesis of congenital spinal deformity may be correlated to vertebral segmentation defects, vertebral formation defects or mixed malformation (9, 10). Hemivertebra-induced congenital scoliosis is the most common among

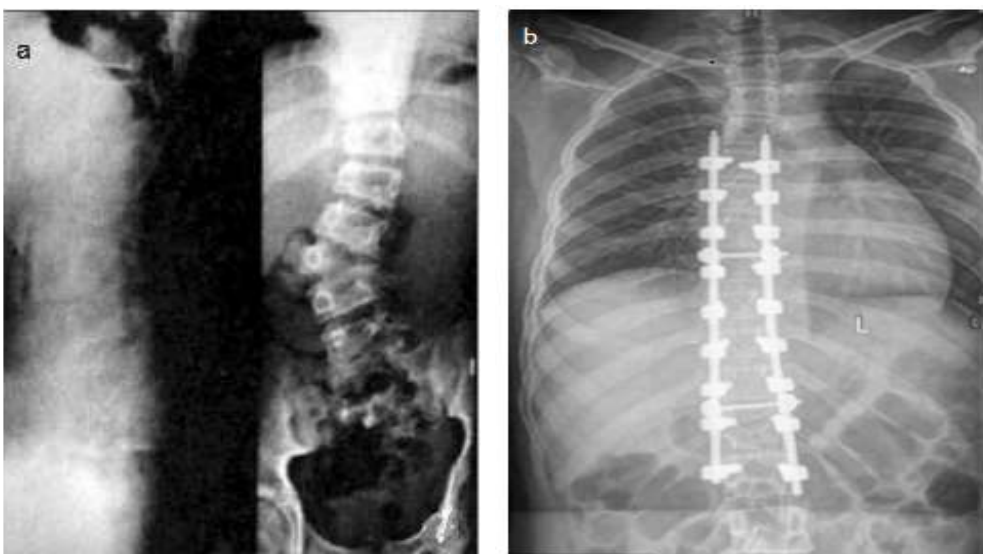

Fig. 1. *Anteroposterior and lateral X-rays of one case before and after surgery.* ***a)*** *anteroposterior and lateral X-ray before surgery;* ***b)*** *anteroposterior and lateral X-rays one year after surgery.*

different subtypes (11). The treatment principles are preventing the development of scoliosis and improving malformation.

The research results demonstrated that the Cobb angle significantly improved after surgical correction, and the observation group had better Cobb angle improvement and higher average correction rate compared to the control group after, which was because the pedicle screw intemal fixator reinforced the major correction curvature and increased the stability of the spinal cord. Therefore, hemivertebra resection in combination with screw rod internal fixation is more effective than hemivertebra resection alone in the treatment of spinal scoliosis. Moreover, the incidence of complications of the two groups had no remarkable difference. Four cases in the control group and 0 cases in the observation had correction loss, suggesting the correction and fixation efficacy of the regimen of the observation group was better than that of the control group in the long term. The observation group had longer average duration of surgery and more average blood loss compared to the control group, indicating the surgical regimen in the observation group was simpler and less harmful.

In conclusion, hemivertebra resection in combination with screw rod internal fixation has advantages of favorable fixation effect, less complications and high reliability and safety in the treatment of congenital scoliosis. However, the follow-up period was short; whether there was recurrence during the growth and development of the children or not should be observed, and whether further treatment is needed remains to be discussed.

REFERENCES

1. Mladenov K, Kunkel P, Stuecker R. Hemivertebra resection in children, results after single posterior approach and after combine anterior and posterior approach: a comparative study. Eur Spine J 2012; 21(3):506-13.
2. Weiss HR, Moramarco M. Congenital scoliosis (Mini-review). Curr Pediatr Rev 2016; 12(1):43-47.
3. AlBakri A, Karaoui M, Alkuraya FS, Khan AO. Congenital ptosis, scoliosis, and malignant hyperthermia susceptibility in siblings with recessive RYR1 mutations. J AAPOS 2015; 19(6):577-79.
4. Balioglu MB, Albayrak A, Akman YE, Atici Y, Kargin D, Kaygusuz MA. The effect of vertical expandable prosthetic titanium rib on growth in congenital scoliosis. J Craniovertebr Junction Spine 2015; 6(4):200-205.
5. Zhang H, Chu Ge, Pan C, Huang J, Hu W, Aikemu-Kahaer. Treatment of congenital kyphoscoliosis with selective-partial hemivertebra resection and instrumentation via posterior approach. Chin J Reparat Reconstr Surg 2015; 29(3):315-20.
6. Yaszay B, O'brien M, Shufflebarger HL, et al. Efficacy of hemivertebra resection for congenital scoliosis: a multicenter retrospective comparison of three surgical techniques. Spine 2011; 36(24): 2052-60.
7. Gu Z, Qiu G, Zhang Y. Genetic association analysis between polymorphisms of hairy-and-enhancer-of split-7 and congenital scoliosis. Int J Clin Exp Med 2015; 8(9):16714-18.
8. Ranade A, Samdani AF, Williams R, et al. Feasibility and accuracy of pedicle screws in children younger than eight years of age. Spine 2009; 34(26):2907-11.
9. Tauchi R, Tsuji T, Cahill PJ, et al. Reliability analysis of Cobb angle measurements of congenital scoliosis using X-ray and 3D-CT images. Eur J Orthop Surg Traumatol 2016; 26(1):53-57.
10. Schulze A, Schrading S, Betsch M, Quack V, Tingart M. Adolescent scoliosis: From deformity to treatment. Orthopade 2015; 44(11):836-44.
11. Wang S, Zhang J, Qiu G, Li S, Yu B, Weng X. Posterior hemivertebra resection with bisegmental fusion for congenital scoliosis: more than 3 year outcomes and analysis of unanticipated surgeries. Eur Spine J 2013; 22(2):387-93.

JOURNAL OF BIOLOGICAL REGULATORS & HOMEOSTATIC AGENTS Vol. 32, no. 2, 351-355 (2018)

LETTER TO THE EDITOR

THREE-VESSEL-TRACHEA VIEW IN THE DIAGNOSIS OF FETAL CARDIAC GREAT VESSEL MALFORMATION

KB. CHEN, Q. GU, T. XIA, X. LU and ZD. ZHANG

Cardiovascular surgery, Tai'an City Central Hospital, Tai'an, Shandong, China

Received June 21, 2017 – Accepted February 21, 2018

Fetal cardiac great vessel malformation is attracting increasing attention in the prenatal ultrasonic diagnosis of fetal congenital heart disease. To investigate the clinical diagnostic values of three-vessel-trachea view (3VT view) in the ultrasonic diagnosis of this malformation, the present study analyzed the echocardiographic examination results of 77 fetuses with great vessel malformation, retrospectively analyzed the echocardiographic characteristics in the three-vessel-trachea view, and followed up the enrolled cases. The results suggest that great vessel malformation had characteristic manifestations, such as abnormal arrangement order, inner diameter, blood flow direction and branch. Color Doppler flow imaging found V, O, C, U, Ioo and oVo structures. There were 20 cases of blood vessel position abnormality, 38 cases of abnormal blood vessel diameter, and 19 cases of abnormal number of blood vessels. The detection rate of abnormal blood vessel diameter was 95%, which was the highest; the detection rate of abnormal blood vessel position was 97.4%, and that of abnormal number of blood vessels was 84.2%. It is concluded that the 3VT view can indicate fetal cardiac great vessel malformation. The 3VT view is beneficial to timely prenatal diagnosis, relief of body pain and improvement of quality of birth.

To the Editor,

Congenital heart disease is a main cause for infant death (1). Prenatal diagnosis of congenital heart disease can effectively change pregnancy outcome and improve the living quality and health level of infants and pregnant women (2). Great vessels coming in and going out of the heart of fetuses mainly include aorta, pulmonary artery, superior and inferior vena cava and pulmonary vein, and the dysplasia of great vessels manifests as abnormal position, number, diameter, branch and hemodynamics of blood vessels. Four-chamber view (3) is well known and has been extensively applied in conventional prenatal screening. Four-chamber view can find most cardiac malformations, but does not include great vessel malformation. Three-vessel-trachea view (3VT view) (4, 5) plays an indispensable role in determining the spatial arrangement, diameter and number of cardiac great vessels, blood flow direction and the correlation between blood vessel distribution and trachea; hence, it has been gradually and extensively applied in clinics. This study investigated the clinical values of 3VT view in the ultrasonic diagnosis of fetal cardiac great vessel malformation

Key words: three-vessel-trachea view, fetal heart, great vessel malformation

Mailing address:
Dr Zhidong Zhang,
No.29, Longtan Road,
Cardiovascular surgery,
Tai'an City Central Hospital,
Tai'an, Shandong, 271000, China
e-mail: zhangzdongta@163.com

0393-974X (2018)

by retrospectively analyzing the fetuses with cardiac great vessel malformation in Tai'an City Central Hospital, Shandong, China, during two years.

MATERIALS AND METHODS

Research data

Two hundred pregnant women who underwent fetal ultrasonic screening in Tai'an City Central Hospital, Shandong, China, between February 2015 and December 2016, were selected as research subjects. The fetuses of seventy-seven pregnant women were diagnosed as cardiac great vessel malformation by examination of the 3VT view. The included pregnant women were aged from 22 years to 36 years (average 28.7±3.5 years). They had been pregnant for 17~35 weeks (average 25.7±3.6 weeks), and all were singleton pregnancies. Gestational weeks were determined based on the last menstrual period or by early ultrasonic examination. All of them signed informed consent to participate in the study.

Method

Philips ie33 and iu22 color Doppler ultrasonic systems which were installed with abdominal convex array probes were used. Firstly, the peripheral vascular conditions of the fetuses, such as number of umbilical arteries, distribution of umbilical veins, and presence of venous duct and spectromorphology of venous duct were probed. Then sequential examination was performed on eight fetal cardiac examination-associated views including upper abdominal cross view, four-chamber cardiac view, left ventricular outflow tract view, right ventricular outflow tract view, 3VT view, long axis view of the aortic arch, long axis view of arterial duct and superior and inferior vena cava view.

The fetal heart was measured in the eight views and, moreover, a color Doppler and spectral Doppler were used for further screening. 3VT view was obtained by moving the probe towards the head of the fetus based on the four-chamber cardiac view. In a normal 3VT view, three blood vessels are distributed in a straight line from left front to right rear, and the views are aortopulmonary oblique view, ascending aorta cross view and superior vena cava cross view. The inner diameter decreased from left to right. The ain pulmonary artery connected with the rear descending aorta via the arterial duct. Tracheal cross view manifested a tube-like echo-free area which ought to be in the right rear side of arcus aortae and the left rear side of the superior vena cava under normal conditions. Keeping the display of the main pulmonary artery and arterial duct unchanged in the 3VT view, the probe on the side of aorta was slightly turned towards the head of the fetus to obtain the oblique cross view of the arcus aortae. Moreover, the oblique cross views of the arterial duct arch and arcus aortae arch, which were distributed in a V-shape, were also displayed, and both of them located on the left side of the trachea. The blood in the arterial duct and arcus aortae both flowed towards the descending aorta.

During examination, if the position of the fetus and the display of fetal heart were poor, the pregnant women were asked to do off-bed activities and undergo repeated examinations until a clear view was obtained. Ultrasonographic features in the 3VT view were observed, any abnormality of vessel position was recorded, and the detection rates of abnormalities of vessel position, diameter and number in the 3VT view were calculated. Cases with abnormal heart conditions were suggested to undergo genetic tests; for fetuses which had stopped growing, autopsy was performed if the family members of the pregnant women agreed, and the fetuses which continued growing were reexamined on the 50th day after birth.

RESULTS

Comparison of 3VT view with postnatal echocardiography or autopsy results

Seventy fetuses were re-examined by the superior hospital or reviewed by autopsy. As to blood vessel position abnormality, 20 cases were diagnosed before delivery and 1 case of mirror image dextrocardia was missed; as to blood vessel diameter abnormality, 38 cases were diagnosed before delivery, and 1 case of tetralogy of fallot was missed; with regard to blood vessel number abnormality, 19 cases were diagnosed before delivery, 1 case of double outlet right ventricle was misdiagnosed as persistent truncus arteriosus, and 2 cases of persistent left superior vena cava were misdiagnosed. The detection rates of abnormality of blood vessel diameter, position and number were 95%, 97.4% and 84.2%, respectively (Table I).

Echocardiographic performance of great vessel malformation

Great vessel malformation had characteristic performance, such as abnormal arrangement order, diameter, blood flow and branches of great vessels in the 3VT view. Color Doppler flow imaging found blood flow in shapes of V, O, C, U, Ioo and oVo. Echocardiography of typical great vessel malformation is shown in Fig. 1.

Fetal great vessel malformation in combination with intracardiac and extracardiac abnormality

Of the seventy-seven cases, twenty-one cases were re-examined, 41 cases stopped growing, and 15 cases were followed up via telephone calls. There were 4 cases of mirror image dextrocardia, 11 cases of persistent left superior vena cava, 4 cases of complete transposition of great arteries and 1 case of right aortic arch, and none of the cases were foundwith intracardiac abnormality. Of 33 cases of abnormality in 3VT view in combination with extracardiac malformation, there were 1 case of holoprosencephaly, 5 cases of situs inversus viscerum, 4 cases of cleft lip and palate, 3 cases pf Danday-Walker malformation, 4 cases of limb deformity, 1 case of multicystic dysplastic kidneys, 1 case of gastroduodenal stenosis, 2 cases of right umbilical vein, 2 case of hydrocephalus, 1 case of

Table I. *Abnormality detection by three-vessel-trachea view.*

Category	Classification	Cubic structure abnormality	Number of cases
Three vessel position abnormality	Order abnormality	Transposition of great artery	14
		Mirror image dextrocardia	5
	Abnormality in the correlation with the position of the trachea	Right aortic arch	2
	Pulmonary artery abnormality	Pulmonary stenosis	20
Blood vessel diameter abnormality	Aorta abnormality	Aortic stenosis	12
		Coarctation of Aorta	5
		Arterial duct circuity	1
Blood vessel number abnormality	Increase of number	Persistent left superior vena cava	14
		Anomalous pulmonary venous drainage	2
	Decrease of number	Persistent truncus arteriosus	2

pleural effusion, 1 case of spina bifida, 3 cases of single umbilical artery, 2 cases of polyhydramnios, 2 cases of oligohydramnion and 1 case of retrocollic cystic hygroma. Seven fetuses underwent chromosome examination, in which 5 cases were normal and the remaining 2 cases were trisomy 18.

DISCUSSION

Currently, the incidence of fetal congenital heart disease ranks the first among all fetal malformations. Combined congenital heart disease is one of the main causes for the death of perinatal infants (6, 7). Fetal four-chamber cardiac view is the simplest and most important approach for screening congenital heart disease; however, it is unable to screen all malformations (8) and is also difficult to diagnose double outlet right ventricle, transposition of great artery, great artery malformation and persistent *truncus arteriosus*. 3VT view plays an important role in determining the diameter, number and percentage of blood vessels, spatial arrangement of great vessels of cardiac base, correlation between the trachea and blood vessel distribution and blood flow direction (9-11). The ultrasonic features of fetal 3VT view include blood flow of aortic arch, ascending aorta, arterial duct and pulmonary artery towards descending aorta; the cross views of ascending aorta, main pulmonary artery and superior vena cava distribute in a straight line, and the trachea locates between superior vena cava and ascending aorta. Abnormalities in blood flow direction and anatomical structure are prone to be found.

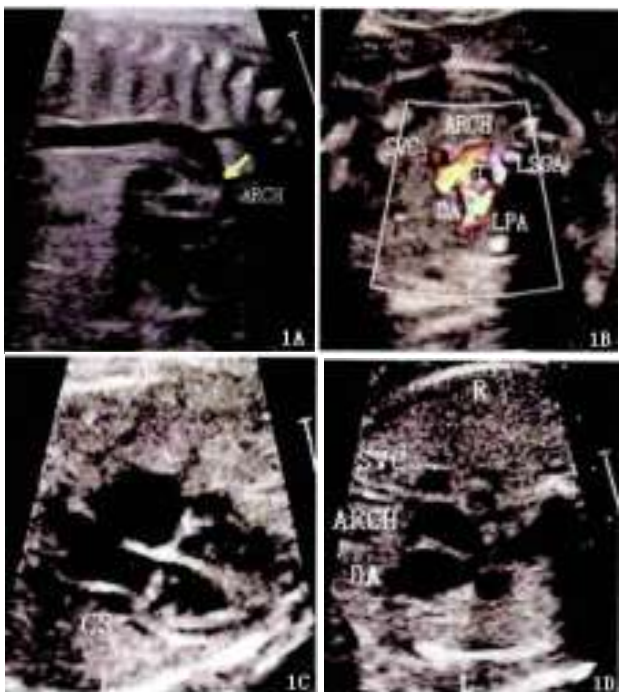

Fig. 1. *Echocardiography of typical great vessel malformation.* ***A)*** *Echocardiography suggested stenosis of aortic arch behind the left common carotid artery and left subclavian artery.* ***B)*** *Echocardiography suggested that the trachea was wrapped by the right aortic arch, right duct arch and left subclavian artery in a C-shape.* ***C)*** *Echocardiography suggested persistent left superior vena cava, and there were left superior vena cava, arterial duct, aortic arch and superior vena cava in 3VT view from left to right (in oVo shape).* ***D)*** *Echocardiography suggested arterial duct circuity. R: right; L: left; SVC: superior vena cava; LSA: left subclavian artery; ARCH: aortic arch; DA: Ductus arteriosus; T: trachea; CS: coronary sinus; PA: pulmonary artery.*

The results of this study suggested that the detection rates of abnormality of blood vessel diameter, position and number were 95%, 97.4%, 84.2% respectively, indicating that the 3VT view could effectively detect fetal cardiac great vessel malformation. Different cardiac malformations had different performances in the 3VT view, which were prone to be observed.

In conclusion, 3VT view can enhance the diagnostic rate of great vessel malformation of fetuses, help make early prenatal diagnosis for pregnant women, relieve their physical and mental pain, and improve quality of birth. However, this study has some limitations. The cardiac examination results of the fetuses might be affected by probe frequency, amniotic fluid depth and fetal position; hence technical means need to be improved and the sample size should be greater in future studies.

REFERENCES

1. Thangaratinam S, Brown K, Zamora J, Khan KS, Ewer AK. Pulse oximetry screening for critical congenital heart defects in asymptomatic newborn babies: a systematic review and meta-analysis.

Lancet 2012; 379(9835):2459-64.
2. Furenäs E, Eriksson P, Wennerholm UB, Dellborg M. Effect of maternal age and cardiac disease severity on outcome of pregnancy in women with congenital heart disease. Int J Cardiol 2017; 243:197-203.
3. Weissmann-Brenner A, Pretorius DH, Achiron R, Gindes L. Fetal echocardiography: the four-chamber view, the outflow tracts, and the contribution of the cardiac arches. Ultrasound Clin 2012; 7(1):1-13.
4. Sinkovskaya E, Berkley E, Abuhamad A. Abnormalities in anatomic components of the three-vessel-trachea view in various congenital heart defects. Am J Obst Gynecol 2009; 201(6):S137.
5. Yagel S, Arbel R, Anteby EY, Raveh D, Achiron R. The three vessels and trachea view (3VT) in fetal cardiac scanning. Ultrasound Obstet Gynecol 2002; 20(4):340-45.
6. International Society of Ultrasound in Obstetrics & Gynecology. Cardiac screening examination of the fetus: guidelines for performing the basic and extended basic cardiac scan. Ultrasound Obstet Gynecol 2006; 27(1):107-3.
7. Desai DK, Moodley J, Naidoo DP. Echocardiographic assessment of cardiovascular hemodynamics in normal pregnancy. Obstet Gynecol 2004; 104(1):20-29.
8. Allan L. Antenatal diagnosis of heart disease. Heart 2000; 83(3):367-70.
9. Singh K, Feldman D, Rad S, Burk C, Peterman J, Esakoff T, Rotmensch S. The "three vessel and trachea view" as part of the routine fetal anatomic survey: analysis of success rates, technical quality, and time requirements. Am J Obstet and Gynecol 2013; 208(1):S165-66.
10. Jeanty P, Chaoui R, Tihonenko I, Grochal F. A review of findings in fetal cardiac section drawings Part 3: The 3-vessel-trachea view and variants. J Ultrasound Med 2008; 27(1):109-17.
11. Palatnik A, Gotteiner NL, Grobman WA, Cohen LS. Is the "I-Sign" in the three-vessel and trachea view a valid tool for prenatal diagnosis of d-transposition of the great arteries? J Ultrasound Med 2015; 34(7):1329-35.

LETTER TO THE EDITOR

EFFECT OF BRANCHED CHAIN AMINO ACIDS ON PERIOPERATIVE TEMPERATURE, GLUCOSE LEVEL AND FAT METABOLISM IN PATIENTS WITH GASTROINTESTINAL TUMORS

LY. WEN[1], YS. ZHANG[1], X. ZHOU[1], G. LI[2], CY. HU[1], Y. LI[1] and LJ. JIN[1]

[1]Department of Anesthesiology, Affiliated HongQi Hospital of Mudanjiang Medical University, Mu Danjiang, China; [2]Department of Orthopedics, Affiliated HongQi Hospital of Mudanjiang Medical University, Mu Danjiang, China

Received December 21, 2017 – Accepted February 6, 2018

This study aimed to investigate the effect of branched chain amino acids (BCCAs) on perioperative temperature, glucose and fat metabolism in patients with gastrointestinal tumors. Fifty-six patients undergoing gastrointestinal tumor surgery were included in the study and randomly divided into two groups of 28 patients each: an experimental and a control group. During surgery, the experimental group received 5.64mL·Kg^{-1}·h^{-1}(4KJ·Kg^{-1}·h^{-1}) of BCCAs intravenously, through an infusion pump, and the control group received an equal volume of NaCl 0.9%. Vital signs were continuously monitored during the operation. Nasopharynx temperature levels of glucose, insulin, free fatty acid and ketone bodies in the blood were determined 30 min before anesthesia (t 0), after anesthesia and before surgery (t 1), 30 min after the start of surgery (t 2), 2 h after start of surgery (t 3) and 1 h after the end of surgery (T4). Patients' shivering intensity (Wrench grading) and pain degree [Visual analogue scale (VAS)]) were estimated 1 h after the endotracheal tube was removed. Nasopharynx temperature was decreased (p<0.05) in both groups after anesthesia induction, while 1 h after the tube was removed it was higher in the experimental group than the control group (p<0.05); compared with pre-surgery values, blood glucose levels were increased during surgery in both groups, but the experimental group had a lower increasing trend compared to the control group, though without statistical significance (p>0.05). Insulin levels were significantly different between the two groups at all time-points during surgery (p <0.05). However, the rising trend of the experimental group was more dramatic during the period from t 0 to t 3. One hour after surgery (t 4), the insulin levels varied, but still at higher levels than pre-surgery, with a significant difference (p<0.05); levels of free fatty acids had a downward trend in both groups, and levels in the experimental group continued to decline until 1 h after surgery. Patients who received branched chain amino acids had less temperature decrease during surgery. Moreover, blood glucose levels were not increased, which limits fat mobilization and leads to production of ketone bodies, reduces the shivering and its intensity after surgery.

To the Editor,

Both anesthesia and surgery can cause stress responses (1, 2). Decline of the patient's temperature during operation with anesthesia is common because narcotism, among others, leads to the decreased ability of the body for temperature regulation and body fluid loss (3). Traditionally, sugar, fat and amino acids cannot be supplemented during surgery

Key words: branched chain amino acids, gastrointestinal tumor, temperature, glucose metabolism, fat metabolism

Mailing address:
Dr Lianjin Jin,
Department of Anesthesiology,
Affiliated HongQi Hospital of Mudanjiang Medical University,
Tongxiang Road No. 5, Mu Danjiang City,
HeiLongjiang Province, China
e-mail: dr_jinlianjinjlj@126.com

0393-974X (2018)

with anesthesia, but the effect of branched chain amino acid infusion into the human vein on body metabolism has been studied in recent years (4, 5). It has been suggested that branched chain amino acid infusion during the perioperative period has some responses, including stimulating insulin secretion, raising blood glucose in advance, and restoring temperature levels during the perioperative period. Branched chain amino acids (BCAAs) belong to essential amino acids playing an important role in body metabolism as signaling molecules. They are involved in glucose metabolism, fat metabolism and energy balance through many signal transductions, but BCAAs cannot be synthesized in human bodies (6, 7). Current research has shown that the content of BCAAs in the compound amino acid solution for clinical use is low. As BCAAs are beneficial to patients with liver dysfunction, an increase of BCAAs in the compound amino acid solution to 100% is expected to have a beneficial effect in postoperative patients. This study aimed to investigate the effect of compound BCAA treatment on the temperature and metabolism of patients with gastrointestinal tumors.

MATERIALS AND METHODS

Patients

Fifty-six patients who underwent gastrointestinal tumor surgery at the Affiliated Hong Qi Hospital of Mudanjiang Medical University during March 2016-February 2017 were included in the study. All patients volunteered to participate in the study and signed the informed consent form. The medical ethics committee of the hospital discussed this research and agreed with all the procedures.

Inclusion crieteria: ASA (American Society of Anesthesiologists) I-II, age between 18-65, BMI(Body Mass Index) between 18-24kg/m2; gastroenteric tumor operation was performed under epidural block combined with general anesthesia, and surgery duration between 120-240 min.

Exclusion criteria: patients using medicines that affect metabolism, such as glucocorticoids, before surgery; patients who had contraindication or allergic history of using branched chain amino acids; hypertension or diabetes without control; severe disease of cardio-pulmonary function, abnormal heart rate, hepatic and renal dysfunction or alcoholism; patients whose plasma albumin was lower than 35g/L or had anemia; pregnant or breast feeding women; patients with abnormal blood coagulation function before; unresectable malignant tumor or disease in terminal stage; patients who had taken part in other clinical trials recently; patients who refused to sign informed consent.

Grouping

The selected patients were randomly divided into an experimental group and a control group, 28 patients in each group. The experimental group received a concentration of 4.26% branched chain amino acids that refers to energy expenditure of the human body in the state of basic metabolism (about $4KJ \cdot Kg^{-1} \cdot h^{-1}$). 5.64mL·Kg-1·h-1(4KJ·Kg-1·h-1) branched chain amino acids were infused intravenously through an infusion pump from induction to the removal of the endotracheal tube. The control group received 5.6mL·Kg-1·h-1 NaCl injection with 0.9% concentration i.v. through an infusion pump from induction to removal of the endotracheal tube.

Main experimental instruments and medicines

Experimental instruments: arteriovenous catheter (Kabushiki gaishaHAKKO); monitor (Henan Million Medical Electronic Co., Ltd.); anesthesia machine (Beijing Fulian Medical Co., Ltd.); infusion pump (Beijing KellyMed Co., Ltd.); portable blood glucose meter (GermanACCU-CHEK); temperature probe (Shanghai NijingElectronic Technology Co., Ltd.); automatic biochemical analyzer (Xuzhou Meikang Electronic Equipment Co., Ltd.); automatic electrochemical luminescence analyzer (Jinan Biobase Biotechnology Co., Ltd.).

Medicines: branched chain amino acids [3AA, elements: every 1000 ml contains 12.6 g L-$C_5H_{11}NO_2$, 16.5g L-$C_6H_{13}NO_2$ and 13.5g L-$C_6H_{13}NO_2$); they were purchased from Anhui Pharmaceutical Co., Ltd.]; NaCl injection with 0.9% concentration (HengshuiChanglong Medical Commercial and Trading Co., Ltd.); compound electrolyte injection (Plasmalyte-A, purchased from Anhui Pharmaceutical Co., Ltd); hydroxyethyl starch 130/0.4 NaCl injection (GermanFresenius Kabi); sevoflurane for inhalation (Guangzhou LaiyuBiotechnology Co., Ltd.); fentanyicitrate injection (Yichang Humanwell Pharmaceutical Co., Ltd.); lidocaine hydrochloride

injection (Jinan Jiage Biological Technology Co., Ltd.); bupivacaine hydrochloride Injection (ZhejiangJiuxu Pharmaceutical Co., Ltd.); remifentanil hydrochloride for Injection (Langfang Branch Office of China National Pharmaceutical Industry Corporation Co., Ltd.); tropisetronmesylate Injection (BeijingHwellso Pharmaceutical Co., Ltd.); atropine sulfate injection (Hubei Kelun Pharmaceutical Co., Ltd.).

Anesthesia schemes

Preparation before anesthesia: patients were not allowed to take food, water or drugs for 6-8 h before surgery. The temperature in the operating room was maintained around 23-25°C. Epidural puncture tube (chest: 8-12 level, depth of tube: 4-6cm), vena jugularis interna and radial artery puncture tubes were prepared to monitor patients' electrocardiogram (ECG), heart rate (HR), pulse oxygen saturation of blood (SpO_2), nasopharynx temperature, and artery blood pressure (ART). Patients were given 3L pure oxygen/min.

Anesthesia induction: Preliminary oxygen was given with mask for 3 min, before anesthesia was induced. Target-controlled infusion of propofol with 4ug/ml plasma concentration, 0.2ug·Kg^{-1}·min^{-1}remifentanil, fentanyl 3ug/kg, 0.6mg/kg rocuronium bromide and 60 mg lidocaine were mixed. Then trachea cannula was linked to the respirator adjusted to maintain carbon dioxide of end-respiratory air at 40±5mmHg.

Anesthesia maintenance: sevoflurane was continuously inhaled to keepMinimum alveolar concentration (MAC) between 0.8-0.9. At the same time, propofol target controlled infusion and remifentanil pump infusion were stopped. If necessary, 2ug/kg fentanyl and 0.2mg/kg rocuronium bromide were added.

Epidural management: 3 ml lidocaine testing dose with 2% concentration was injected in epidural space; 8-12ml bupivacaine with 0.5%concentration was added before surgery, and 3-5ml bupivacaine with 0.5%concentration was added every hour for epidural space in order to get a better regional nerve block, and was stopped 30 min before the end of surgery.

Tube drawing: 6mg tropisetron was given i.v. before the end of surgery. Antagonism of muscle relaxation was given routinely after skin suture: 0.05mg/kg neostigmine and 0.02-0.03mg/kg atropine are compatibility of medicines for i.v. injection. The tubes were drawn until patients were totally clear and their muscle force recovered.

Postoperative analgesia: after the tubes were removed, the patients given 0.125% bupivacaine and 2ug/ml

Fig. 1. *VAS scale.*

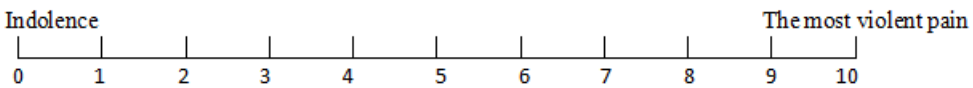

Table I. *Wrench grading.*

Grading	Clinical features
0	No shiver
I	Flesh creep or peripheral vessel shrink or peripheral cyanosis, but without muscular fibrillation
II	Only one muscle group has muscular fibrillation
III	More than one muscle group has muscular fibrillation
IV	The whole body has muscular fibrillation

fentanyl to control epidural analgesia at the speed of 3ml/h. Bolus 4 ml was given every 10 min.

Liquid management

Patients were did not undergo infusion after going into the operating theatre until 30 min before anesthesia induction. $4mL \cdot Kg^{-1} \cdot h^{-1}$ multiple electrolytes were given i.v. 30 min before anesthesia induction to remove endotracheal tubes. Blood loss volume was restored at the ratio of 1:1 with 130/0.4NaCl hydroxyethyl starch injection during surgery. If necessary, blood was transfused to bring blood volume to normal levels.

Data acquisition

Thirty min before anesthesia was the time-point t 0; and after the induction of anesthesia and before surgery was the time-point t 1; 30 min after the beginning of surgery was the time-point t 2; 2 h after the beginning of surgery was time-point t 3; and 1 h after the end of surgery was time-point t 4. Selected patients' HR, blood pressure (BP), SpO2, pressure of end-tidal carbon dioxide (PETCO2), MAC and nasopharynx temperature were monitored from the time of entering the operating room up to 1 h after removing the tube. Blood sampling was performed at the five timings and then blood glucose (finger peripheral blood), insulin, free fatty acid and ketone bodies (vena ductus venosus blood) were monitored. Pain degree and postoperative shiver intensity were assessed after tubes were removed. Visual analogue scale (VAS) was adopted to assess pain degree after removing the tubes. According to their own pain degree, patients marked the position of pain degree according to the following scale where 0-10 represents different degrees of pain, 0 for no pain and 10 for the most violent pain: 0-2 is excellent, 3-5 is fine, 6-8 is not bad and 9-10 is bad (Fig. 1).

Wrench grading standard was used to assess postoperative shiver intensity, which is shown in Table I.

Statistical analysis

Data were analyzed using the SPSS 20.0 statistical software. Measurement data are expressed as mean ± standard deviation ($\bar{x} \pm s$). If the repeated measurements followed a normal distribution, the comparison within groups or among groups will adopt analysis variance with repeated measurement data; if the data do not follow a normal distribution, it will be indicated with quartiles; if the data follow a normal distribution, non-parametric test and Mann-Whitney U were used for comparison. Correlation between the basic information and the statistical data of patients was assessed with *chi*-squared test, and differences of measurement data were analyzed with two-sided *t*-test. Values $P<0.05$ were considered statistically significant

Table II. *General clinical statistics of selected patients.*

Index	Experimental group	Control group	*p*
Gender (male/female)	17/11	18/10	0.87
Age (years)	54.21±9.69	53.56±8.10	0.46
BMI(kg/m^2)	23.34±2.12	22.76±2.21	0.91
Type of operation (stomach/intestines)	11/17	8/20	0.68
Duration of operation (min)	145.89±2.87	136.68±37.28	0.34
Fluid infusion volume during operation (mL)	2611.56±237.36	2458.91±283.63	0.31
Input of intervened solution (mL)	897.25±165.32	949.91±310.03	0.57
Urine volume during operation (mL)	216.33±130.09	249.25±218.93	0.68
Blood loss volume during operation (mL)	75.45±45.67	70.57±38.54	0.31

RESULTS

General clinical data

The patients of the experimental and the control groups had no statistical significant differences regarding the clinical data, as shown in Table II (p>0.05).

Effect of infusing branched chain amino acid on nasopharynx temperature, blood glucose, insulin, ketone bodies and free fatty acid during surgery

Nasopharynx temperature fell remarkably (p<0.05) after the operation, in both groups, compared with the temperature before the surgery but there was no obvious difference between the experimental and control groups (p>0.05). Moreover, patients' temperatures tend to fall continuously as the operation time extends. However, 1 h after surgery, their temperature begins to rise again.

Compared with t 0, blood glucose of the two group was on the rise at time-point t 4 (P<0.05). the increased rate of the control group was higher than experimental group, but data between two groups had no statistical significant difference from the overall data (P>0.05). In addition, insulin levels of the experimental group was higher than the control group (P<0.05), but insulin levels at every time-point during the operation in the two groups was significantly different (P<0.05).

The concentration of ketone bodies between the two groups was normally distributed. When non-parametric test and Mann-Whitney U test were applied in comparing data from the two groups, the concentration difference of ketone bodies had no statistical significance (P>0.05) (Table III).

After removing the tubes, the pain scores of all patients were between 0-2. As shown in Table IV, shiver intensity of patients concentrates on 0-II, and occurrence rate of muscular fibrillation in the experimental group was lower than the control group (p<0.05) as well as their shiver intensity (p <0.05).

DISCUSSION

In this study, nasopharynx temperature of patients in the control group clearly falls after anesthesia

Table III. *Changes in levels of nasopharynx temperature, blood glucose, insulin, ketone bodies and free fatty acid during surgery.*

Group		t0	t1	t2	t3	t4
Nasopharynx temperature (□)	Experimental group	36.79±0.36	36.53±0.28#	36.24±0.33#	35.92±0.41#	36.41±0.37*#
	Control group	36.63±0.35	36.35±0.36#	36.16±0.43#	35.84±0.58#	36.07±0.47#
Blood glucose (mmol/L)	Experimental group	5.18±0.90	5.43±0.74#	5.83±0.88#	5.98±0.92#	6.11±1.32#
	Control group	4.80±0.91	5.16±0.96#	5.94±1.41#	6.07±2.11#	7.08±1.78#
Insulin (uU/L)	Experimental group	4.79±2.37	6.82±4.31*#	6.89±4.66*#	12.67±7.71*#	10.59±5.47*#
	Control group	3.36±2.34	3.19±2.99	2.18±2.03	2.56±1.64	4.07±2.81
Ketone bodies (Median [25%,75%], mmol/L)	Experimental group	0[0,0]	0[0,0.49]	0[0,0.49]	0.245[0,0.49]	0.245[0,0.49]
	Control group	0[0,0.49]	0[0,0.49]	0[0,0.49]	0.49[0,0.98]	0.49[0,0.98]
Free fatty acid (mmol/L)	Experimental group	0.85±0.28	0.64±0.25#	0.46±0.15#	0.41±0.17*#	0.35±0.17*#
	Control group	0.95±0.27	0.76±0.23#	0.57±0.24#	0.76±0.35#	0.88±0.35

Note: compared with control group, p <0.05; compared with fundamental value (t 0) in the same group, # p <0.05.*

Table IV. *Statistical table of shiver intensity one hour after surgery.*

Group	0	I	II	III	IV
Experimental group	18	8	2	0	0
Control group	14	4	7	2	1

because thermoregulation function is lowered by general anesthesia through core and periphery effects in a dose-dependent manner. Some studies (8, 9) suggest that amino acid infusion during the perioperative period can lead to temperature fall about 0.5°C. In our study, branched chain amino acid infusion during surgery increased the temperature of the patients 1 h after removing tubes compared to the control group (but still lower than the value at t 0). The thermal effects of BCAAas began 3 h after infusion and the effect may be more evident in longer time periods.

Treatment with BCAAs resulted in increased insulin levels of patients during surgery, but 1 h after surgery, the levels fell again (still higher than the value at t 0). Therefore, BCAAs had no effect on the levels of blood glucose in the two groups which increased similarly. This result suggests that BCAAs can stimulate the secretion of insulin during surgery, but would become invalid if infusing was stopped after surgery. BCAAs can lower sensitivity of insulin and strengthen insulin resistance. It was demonstrated that blood glucose was higher in the experimental group than in the control group (10, 11). After BCAAs were used to intervene, blood glucose had no clear changes, due to the given dose of BCAAs, study subjects and duration of time (12).

Generally, concentration of FFAs in serum would rise with operative stress, However, FFAs in the control group were decreased, probably because the patients adopted epidural block combined with general anesthesia. Insulin concentration of the experimental group clearly rose during surgery in this study, and insulin has a function to restrict fat mobilization and tissue and release FFAs (13). Ketone body is an intermediate metabolite when liver disassembles oxidation (14). Normally, blood contains few ketone bodies, but with diabetes, hunger and stress occur and ketogenesis is increased (15). Here, BCAA solution infusion had no clear effect on the concentration of ketone bodies of patients during surgery, demonstrating that although fat mobilization and ketone bodies are increased during anesthesia and surgery, they do not exceed the normal range.

REFERENCES

1. Pan X, Yuan L, Yang M, Liu C. Effects of propofol on the differentiation of normal spleen dendritic cells to immune cells and its mechanism of action. Farmacia 2017; 65(3):429-34.
2. Pan YS, Hu YF, Tian FB, Xu K. Effects of epidural preemptive analgesia on stress reaction in retroperitoneal laparoscopic adrenalectomy surgery: a randomized controlled study. Int J Clin Exp Med 2015; 8(6):9862-8.
3. Wang XT, Lv M, Guo HY. Effects of epidural block combined with general anesthesia on antitumor characteristics of T helper cells in hepatocellular carcinoma patients. J Biol Regul Homeost Agents 2016; 30(1):67-77.
4. Ma W, Zhu YM, Zhou H, Fu GQ, Pan H, Shen WD. Protecting action of acupuncture-drug compound anesthesia with different frequency electroacupuncture on stress reaction in pneumonectomy. Zhongguo Zhen Jiu 2011; 31(11):1020-4.
5. Liu Q, Wang JJ, Yan HY, Wang YQ, Qin CW, Li ML. Safety and pharmacodynamic mechanism of ropivacaine lumbar anesthesia in Cesarean section. J

Biol Regul Homeost Agents 2017; 31(1):71-76.
6. Valerio A, D'Antona G, Nisoli E. Branched-chain amino acids, mitochondrial biogenesis, and healthspan: an evolutionary perspective. Aging (Albany NY) 2011; 3(5):464-78.
7. Serralde-Zúñiga AE, Martha GC, Tovar AR, Herrera-Hernández MF, Noriega LG, Granados O, Torres N. Omental adipose tissue gene expression, gene variants, branched-chain amino acids, and their relationship with metabolic syndrome and insulin resistance in humans. Genes Nutr 2014; 9(6):431.
8. Li XS, Liu L,Jin YL, Luo FF, Li L, Zhu J, Xie Q. Accompanying mild hypothermia significantly improved the prognosis of septic mice than artificial mild hypothermia. Am J Emerg Med. 2015; 33(11):1651-58.
9. Sander M, Heymann C V, Spies C. Implementing the International Liaison Committee on Resuscitation guidelines on hypothermia after cardiac arrest. The German experience: still a long way to go? Crit Care 2006; 10(2):407.
10. Muoio DM, Newgard CB. Mechanisms of disease: Molecular and metabolic mechanisms of insulin resistance and beta-cell failure in type 2 diabetes. Nat Rev Mol Cell Biol 2008; 9(3):193-205.
11. Krebs M, Brehm A, Krssak M, et al. Direct and indirect effects of amino acids on hepatic glucose metabolism in humans. Diabetologia 2003; 46(7):917-25.
12. Zanchi N E, Guimarães-Ferreira L, de Siqueira-Filho M A, Felitti V, Nicastro H, et al. Dose and latency effects of leucine supplementation in modulating glucose homeostasis: opposite effects in healthy and glucocorticoid-induced insulin-resistance states. Nutrients 2012; 4(12):1851-67.
13. Chmielewska J, Szczepankiewicz D, Skrzypski M, Kregielska D, Strowski MZ, Nowak KW. Ghrelin but not obestatin regulates insulin secretion from INS1 beta cell line via UCP2-dependent mechanism. J Biol Regul Homeost Agents 2010; 24(4):397-402.
14. Kitagawa M, Haji S, Amagai T. High serum essential amino acids as a predictor of skeletal muscle depletion in patients with cachexia and advanced gastrointestinal cancers. Nutr Clin Pract 2017; 32(5):645-51.
15. Zawar BP, Mehta Y, Juneja R, Arora D, Raizada A, Trehan N. Nonanalgesic benefits of combined thoracic epidural analgesia with general anesthesia in high risk elderly off pump coronary artery bypass patients. Ann Card Anaesth 2015; 18(3):385-91.

LETTER TO THE EDITOR

ABILITY OF COMPUTED TOMOGRAPHY TO PREDICT RIGHT HEART STRAIN ON AN ECHOCARDIOGRAM IN PATIENTS WITH ACUTE PULMONARY EMBOLUS

A. SHAMS[1], J. HUNG[2] and A. BAHL[1]

[1]Department of Emergency Medicine, Beaumont Health System, Royal Oak, Michigan, United States of America; [2]Department of Biomedical Sciences, Oakland University William Beaumont School of Medicine, Rochester, Michigan, United States of America

Received January 14, 2018 – Accepted February19, 2018

Patients with submassive pulmonary embolism (PE) resulting in right heart strain (RHS) have an increased risk of mortality compared to those with a preserved right ventricular function. This study aimed to investigate the predictive value of computed tomography pulmonary angiogram (CTPA) findings of right heart strain in patients with computed tomography (CT)-proven PE for the diagnosis of right heart strain by echocardiogram (ECHO). The institutional review board (IRB) approved retrospective chart review of the adult emergency department patients diagnosed with an acute PE between 2012 and 2016. A total of 128 patients diagnosed with RHS by CT who had received an ECHO during their hospitalization were included in the study. Descriptive statistics were run for the variables of interest. The majority of patients (101 patients) with reported findings of RHS on CT had similar findings on ECHO. In our cohort, a finding of enlarged right atrium (RA) on CT was 100% predictive of RHS diagnosis on ECHO, whereas having interventricular septal bowing alone on CT was the least predictive of RHS on subsequent ECHO (61%). The 2 remaining subgroups: right ventricle (RV) enlargement alone and RV enlargement with either interventricular septal bowing/hepatic vein blood reflux or both lies somewhere in between, with 80% of these patients showing strain on ECHO. We found that signs of RHS on CT are predictive of strain on an ECHO (78%) and RA enlargement in any combination was the most predictive finding of RHS on ECHO (100%). Future prospective randomized investigations are needed to confirm such findings.

To the Editor,

Acute pulmonary embolism (PE) is a life-threatening condition that emergency physicians encounter regularly. Pulmonary embolism can be classified as non-massive, submassive and massive PE. This study focused on massive and submassive PE, which are defined as PE with cardiovascular shock, and PE with evidence of right heart strain (RHS) but no shock, respectively (1). Patients in the massive and submassive groups have an increase in mortality and morbidity compared to hemodynamically stable PE (2). The management of massive PE consists of systemic fibrinolytic therapy, catheter-directed interventions, and/or surgery, however, the definitive treatment for submassive PE remains unclear (3). Therefore, the early diagnosis of acute PE and risk stratification including measurement of right heart function guide the management of these patients.

Currently, transthoracic echocardiography (TTE) plays an important role in the diagnosis of RHS

Key words: pulmonary embolus, computed tomography, ECHO, right heart strain

Mailing address:
Dr A. Shams,
Department of Emergency Medicine,
Beaumont Health System,
3601 W 13 Mile Rd,
Royal Oak, MI, 48073, USA
Tel.: +1 248 325 4831
e-mail: alishams75@gmail.com

0393-974X (2018)

in patients with PE while computed tomographic pulmonary angiography (CTPA) is the first-line imaging to study patients with suspected PE (5). TTE can identify RHS by looking for right ventricular dysfunction, dilatation, or hypokinesis (5). However, TTE can be time-consuming, user-dependent and may not be readily available in all emergency departments. As a result, CTPA is being increasingly used to diagnose RHS due to its high accuracy and accessibility in many emergency departments (4). To date, few studies with small sample size have shown that CTPA can be a clinically reliable tool compared to echocardiography (ECHO) for identifying RHS in patients with acute PE (4, 5) but more data are needed. In this study, we aimed to investigate the predictive value of CTPA as a diagnostic modality of RHS in patient with CT-proven PE in comparison to TTE

MATERIALS AND METHODS

This was an Institutional Review Board-approved retrospective descriptive chart review of emergency department patients diagnosed with an acute pulmonary embolus between 2012 and 2016 at three suburban hospitals within a large health system. One site is a Level 1 trauma tertiary care academic center while the other two sites are Level 2 trauma centers in the community.

Electronic charts were queried for International Classification of Diseases 9 (ICD-9) diagnoses consistent with acute PE in patients aged 18 years and over. A total of 1,208 cases were found. Patients were further queried for those who had received both a CTPA diagnosing acute PE in the emergency department and those who had had a TTE during their hospitalization, totaling 444 cases. We further narrowed the pool of patients to 128 by including only patients with evidence of RHS mentioned in the findings and/or impression section of the CT report (Fig. 1). As absence of RHS was not reported consistently by all radiologists reading PE studies and generally not reported for most cases, these cases were excluded which is a limitation of this study. Future prospective studies should be aimed at addressing this discrepancy and designed in a way where radiologists are expected to address the presence or absence of signs of RHS on every CTPA they assess. Signs of RHS on CTPA include; right ventricle enlargement, right atrial enlargement, interventricular septal bowing, and reflux of contrast into hepatic veins. Study personnel used the abstraction form (Appendix A) to collect data, no blinding was performed; however, the principal investigator reviewed 15% of cases to assess adequacy

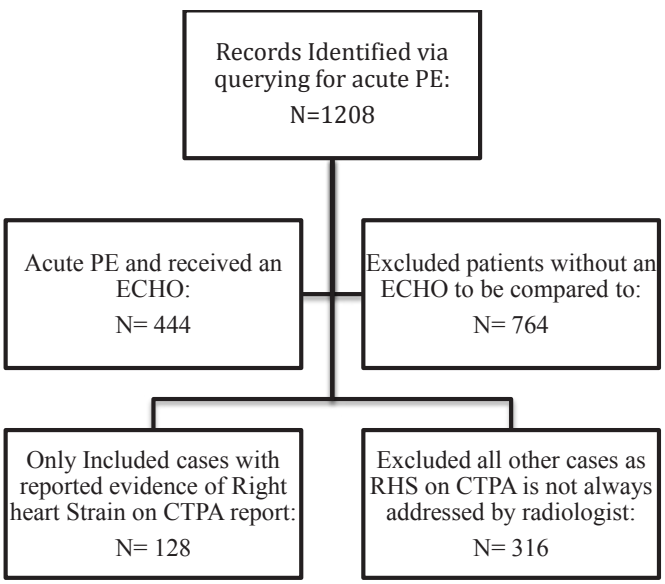

Fig. 1. *Flow chart for patient selection.*

of data collection and had a 100% inter-rater reliability.

Descriptive statistics were run for the variables of interest. A Pearson *chi*-squared test was performed to determine the association between the CTPA subgroup and strain on TTE. All analyses were conducted using SAS version 9.3 for Windows and R version 2.15.1 for Windows.

RESULTS

One hundred twenty-eight subjects showed signs of RHS reported on CTPA. Radiologists reported 4 signs of right heart strain on CTPA: right atrial (RA) enlargement, right ventricle (RV) enlargement, septal bowing and reflux of contrast into hepatic veins in different combinations (Table I). In addition, 6 of the 128 subjects had the nonspecific term "evidence of right heart strain" reported on their report. Table I shows the frequency distribution for strain on CTPA.

The majority of patients (101 patients/78.90%) with reported findings of RHS on CT had evidence of strain on TTE. Echocardiographic findings suggestive of RHS included any of the following combinations: RA/RV enlargement, RV hypokinesis, and elevated RV pressure, moderate to severe tricuspid (TC) regurgitation, septal bowing, and dilated inferior vena cava. Table II shows the frequency distribution for whether or not the subject had RHS on TTE.

Furthermore, the 16 combinations of signs of right heart strain mentioned above were divided into 4 major subgroups. We looked at the association of the 4 subgroups separately with their TTE findings. The four major subgroups are listed in Table III.

It was found that having an enlarged RA in any combination on CTPA is 100% indicative of strain on TTE, whereas having septal bowing alone on CTPA was the least indicative of strain on subsequent ECHO (61%). The two remaining subgroups: RV enlargement alone and RV enlargement with septal bowing, reflux or both, lie somewhere in between, with 80% of these patients showing strain on TTE. The relationship between CTPA subgroup and strain on TTE was statistically significant (p=0.0084).

Table I. *Frequency of specific CT findings association with strain.*

Strain on CT	Frequency	Percent
RA enlargement	1	0.78
RA + RV enlargement	8	6.25
RA + RV enlargement + Reflux	2	1.56
RA + RV enlargement + Reflux + Septal bowing	2	1.56
RA + RV enlargement + Septal bowing	4	3.13
RA + RV enlargement + Septal bowing	1	0.78
RA enlargement + Reflux + Septal bowing	1	0.78
RA enlargement + Septal bowing	1	0.78
RV enlargement	41	32.03
RV enlargement + Reflux	5	3.91
RV enlargement + Reflux + Septal bowing	2	1.56
RV enlargement + Septal bowing	18	14.06
Reflux	3	2.34
Reflux + Septal bowing	2	1.56
Right heart strain	6	4.69
Septal bowing	31	24.22

Table II. *Strain on CT correlation to TTE.*

Strain on TTE	Frequency	Percent
No	27	21.01
Yes	101	78.90

Table III. *CT subgroup findings correlation to strain on TTE.*

CT Subgroup	Strain on ECHO		
Frequency **Row Pct**	**No**	**Yes**	**Total**
All combinations with RA Enlargement	0 0.00	20 100.00	20
RV enlargement Alone	8 19.51	33 80.49	41
Septal Bowing Alone	12 38.70	19 61.29	31
RV enlargement + Septal Bowing/Reflux or Both	5 20	20 80	25
Total	25	92	117

Frequency Missing = 11

The rate of tissue plasminogen activator (TPA) administered to patients was also reviewed. The frequency distribution for TPA is given below. The majority (97 subjects; 76%) did not have TPA (Table IV). Out of the 31 subjects who received TPA, the majority (28 subjects) had a strain on both CTPA and TTE documented (Table V).

DISCUSSION

In this retrospective study, we found that the majority of patients (78%) with signs of right heart strain on CTPA also had RHS confirmed by TTE. By dividing the patients into different subgroups, it was found that any RA enlargement on CTPA was highly (100% of patients) indicative of RHS, whereas interventricular septal bowing was the least indicative with 61% of patients (Table III). Septal bowing is significantly affected by the cardiac cycle (systole *vs* diastole) and the timing of the image taken, which may explain a poorer correlation with echocardiographic findings when compared to other signs of RHS (6).

Previous studies have found that RV enlargement is a useful predictor for right heart strain, but these studies did not examine RA enlargement as a potential predictor (5, 6, 11-13). Further prospective studies comparing RA enlargement seen on CTPA and TTE need to be performed in order to determine the utility of this findings in clinical practice.

The major limitation of this work is the absence of any data on patients with CTPA studies without evidence of RHS which precludes calculation of common measures of diagnostic accuracy such as sensitivity, specificity, and even more useful, positive and negative likelihood ratios. The reason outcomes

Table IV. *TPA administration for PE.*

TPA	Frequency	Percent
No	97	75.78
Yes	31	24.21

Table V. *TPA administration correlation to strain.*

Frequency Received TPA	Strain on both	Percent
3	No	9.67
28	Yes	90.32

were measured only among a select patient population is mentioned above in the methods section.

Additional limitations of this study include how findings of RHS are sometimes subjective and operator-dependent when reading TTE. Inter-rater reliability of the CT and ECHO reports was not assessed in this retrospective analysis. The extent that radiographers were more likely to comment upon the presence of signs of RHS in patients exhibiting more dramatic manifestations of these features was not measured, and it is possible that the positive predictive value is overstated (12, 13). Also patients with comorbidities such as congestive heart failure, chronic obstructive pulmonary disease, or pulmonary hypertension were not excluded. These patients may already have had a component of RHS prior to their acute PE.

This study concludes that signs of RHS on CTPA are indicative of strain on an ECHO (78%) and of all the different signs of RHS on CT, RA enlargement in any combination was the most indicative of right heart strain on ECHO (100%).

REFERENCES

1. Guidelines on diagnosis and management of acute pulmonary embolism. Eur Heart J 2000; 21(16):1301-36.
2. Sanchez O, Trinquart L, Colombet I, Durieux P, Huisman MV, Chatellier G, Meyer G. Prognostic value of right ventricular dysfunction in patients with haemodynamically stable pulmonary embolism: a systematic review. Eur Heart J 2008; 29:1569-77.
3. Konstantinides SV, Torbicki A, Agnelli G, et al. 2014 ESC Guidelines on the diagnosis and management of acute pulmonary embolism. Eur Heart J 2014; 35(43):3033-73.
4. İn E, Aydın AM, Özdemir C, Sökücü SN, Dağlı MN. The efficacy of CT for detection of right ventricular dysfunction in acute pulmonary embolism, and comparison with cardiac biomarkers. Jpn J Radiol 2015; 33(8):471-78.
5. Cok G, Tasbakan MS, Ceylan N, Bayraktaroglu S, Duman S. Can we use CT pulmonary angiography as an alternative to echocardiography in determining right ventricular dysfunction and its severity in patients with acute pulmonary thromboembolism? Jpn J Radiol 2013; 31(3):172-78.
6. Park JR, Chang SA, Jang SY, et al. Evaluation of right ventricular dysfunction and prediction of clinical outcomes in acute pulmonary embolism by chest computed tomography: comparisons with echocardiography. Int J Cardiovasc Imaging 2012;

28(4):979-87.
7. Konstantinides S, Geibel A, Heusel G, Heinrich F, Kasper W: Management Strategies and Prognosis of Pulmonary Embolism-3 Trial Investigators. Heparin plus alteplase compared with heparin alone in patients with submassive pulmonary embolism. N Engl J Med 2002; 347(15):1143-50.
8. Witty LA, Krichman A, Tapson VF. Thrombolytic therapy for venous thromboembolism. Utilization by practicing pulmonologists. Arch Intern Med. 1994; 154(14):1601-4.
9. Goldhaber SZ. Thrombolytic therapy for patients with pulmonary embolism who are hemodynamically stable but have right ventricular dysfunction: pro. Arch Intern Med 2005; 165(19):2197-9-5.
10. Kang DK, Thilo C, Schoepf UJ, et al. CT Signs of right ventricular dysfunction. JACC Cardiovasc Imaging 2011; 4(8):841-49.
11. Quiroz R, Kucher N, Schoepf UJ, Kipfmueller F, Solomon SD, Costello P, Goldhaber SZ. Right ventricular enlargement on chest computed tomography: prognostic role in acute pulmonary embolism. Circulation 2004; 109(20):2401-4.
12. Becattini C, Vedovati MC, Agnelli G. Right ventricle dysfunction in patients with pulmonary embolism. Intern Emerg Med 2010; 5(5):453-55.
13. Jaff MR, McMurtry MS, Archer SL, et al. Management of massive and submassive pulmonary embolism, iliofemoral deep vein thrombosis, and chronic thromboembolic pulmonary hypertension: a scientific statement from the American Heart Association. Circulation 2011; 123(16):1788-830.

LETTER TO THE EDITOR

DETECTION OF HAND-FOOT-MOUTH DISEASE AND ITS SPATIAL-TEMPORAL EPIDEMIOLOGICAL CHARACTERISTICS WITH GIS PLATFORM

XJ. XU, Z. TANG, LR. ZENG, H. LUO, QY. CHEN, L. LI, Q. LOU and XJ. HE[1]

Information and Management School, Guangxi Medical University, Nanning, Guangxi, China

Received December 21, 2017 – Accepted February 8, 2018

The aim of this study is to investigate the main category of hand-foot-mouth (HFM) virus and analyze the distribution characteristics and susceptible population of HFM disease in China. Infants who have had HFM disease for less than 7 days were selected from the First Affiliated Hospital of Guangxi Medical University, Guangxi, China. Various specimens were collected from the infants, and EV71 and CA16 nucleic acid detections were performed using fluorescence quantitative assay. The positive results of the specimens were compared to determine the components of the pathogen. Moreover, the data of the target cases were analyzed based on Geographic Information System (GIS) to obtain the spatial-temporal epidemiological features of HFM disease in China. The detection rate of HFM virus in the throat swab, feces, bleb fluid and cerebrospinal fluid were 75%, 81.13%, 85.71% and 25%, respectively, indicating that the detection rate of virus in the bleb fluid was the highest. When the detection was based on more than one specimen, it was found that the positive rate was higher compared to detection based on a single specimen. The positive detection rate of EV71 in the target specimens was significantly higher than that of CA16 and mixed infection. Moreover, CA16 infection was usually accompanied by EV71 infection. As to spatial-temporal distribution, hand-foot-month disease broke out in the South of China in April, then spread to the north, and diminished in July. There was a notable difference in the number of cases between different provinces. EV71 and CA16 are the main viruses inducing HFM disease, especially EV71. Fluorescence quantitative polymerase chain reaction with high sensitivity can be used to detect the copy number of viruses, which is applicable to the early diagnosis of HFM disease. The incidence of HFM disease is notably different according to the influence of time, geographical space, gender and the living conditions of the children. Early diagnosis and treatment based on scientific methods are needed to reduce the incidence of severe diseases and avoid death.

To the Editor,

Hand-foot-mouth (HFM) disease is induced by enterovirus (EV) from the *Picornaviridae* family (1). More than 20 kinds of EV can induce HFM disease, among which coxsackievirus A16 (CA16) and EV71 are the most common. HFM disease, which usually occurs in infants (2), has complex and diversified clinical manifestations. The most common symptoms are fever, general weakness, depression and poor appetite. HFM-associated herpes usually appear on the tongue, root of tooth, palm, arch of the foot and hip. Most cases can be

Key words: HFM disease, virus detection, GIS analysis, distribution characteristics

Mailing address:
Master Xijia He,
Information and Management School,
Guangxi Medical University,
No. 22, Shuangyong Road,
Nanning City, Guangxi, 530021, China
e-mail: xjhegx@126.com

0393-974X (2018)

self-cured, but some have severe pathological changes such as myocarditis and pulmonary edema, which may be life-threatening. HFM disease has broken out many times in China in recent years, and the number of cases involved is increasing. Wang et al. (3) considered that this disease is one of the current severe public issues in China, and has greatly affected the safety of children. Mirand et al. (4) determined the potential new virus variants through analyzing the phylogenetic relationship. Lott et al. (5) carried out a study on connecting HFM disease with CA6. Thus, it can be seen that the population threatened by HFM disease has become increasingly larger (6), however there are few studies concerning its pathogen. To early diagnose and timely treat HFM disease in infants, the main pathogen should be found to provide clinical support. The variation of HFM disease along with time should be explored based on the analysis and statistical processing of case data to provide theoretical support and assistance for the formulation of comprehensive measures and to develop a vaccine, which can prevent an epidemic outbreak.

MATERIALS AND METHODS

Study subjects

Eighty infants diagnosed with HFM disease by the department of infection of the First Affiliated Hospital of Guangxi Medical University, Guangxi, China who had suffered the disease for no more than 7 days were selected as study subjects. The parents of the infants were informed with the study protocol and signed informed consent.Throat swab specimens, stool specimens and cerebrospinal fluid were collected from all the infants. In the study of spatial-temporal epidemiological characteristics, data of 1 million and 0.5 million cases of HFM disease in China in 2015 and 2016 were selected. This study was approved by the ethics committee.

Main reagents and instruments for virus detection

Reagents included RNA extraction kit, fluorescence quantitative polymerase chain reaction (FQ-PCR) kits for enterovirus-universal (EV-U), CA16 and EV71, chloroform, 75% ethyl alcohol and normal saline. Negative quality control was prepared using normal saline, and positive quality control was inactivated EV nutrient solution. Virus preservation solution and sampling tubes were also used.

The instruments included quantitative PCR amplifier, imager, electrophoresis tank, centrifugal machine, oscillator, biohazard safety equipment, workbench, ultralow temperature water tank and pipettor.

EV, EV71 and CA16 primer sequences and fluorescent probes are shown in Table I.

Collection of specimens

Before detection, the throat swab specimens were preserved at 4°C temporarily or processed by nucleic acid extraction immediately after collection.

The stool specimens were processed into stool suspension using normal saline. Then the specimens were preserved in a biological safety cabinet.

One bleb fluid specimen could be collected from more than one bleb. Firstly the blebs were disinfected by ethyl alcohol and then broken. The bleb fluid was corrected for testing.

Cerebrospinal fluid was collected within three days after the occurrence of neurological problem. Nucleic acid extraction was directly performed without processing.

EV is an RNA virus (7). During nucleic acid extraction, the pollution of RNA enzyme should be considered, and the activity of RNA enzyme should be reduced. In this study, viral RNA was extracted directly by the RNA kit (8).

Methods

The sequences of primers used in the detection which was performed to determine the existence of EV, EV71 or CA16 specific RNA fragments in the specimens were carried out according to the manufacturer's instructions. The sequence length of PE, EV71 and CA16 was 116, 226 and 208, respectively.

The PCR product of EV71 was connected with carriers (9). The carriers were mixed with the fragments in a mole ratio between 1:3 and 1:8. The experimental substances were mixed by

mildly stirring centrifuged. The reaction liquid was preserved at 16°C overnight. The centrifuge tube was placed on ice after the reaction. For CA16, the amount of the PCR product could be increased or decreased, but 4 μl was the limit. The carriers were mixed with the fragments in a ratio of 1:7, followed by 12 min of reaction at 25°C. The centrifuge tube was placed on ice after the reaction.

PCR amplification

The product was processed by 2% agarose gel electrophoresis. Specific bands were determined as positive EV results, and some bands which could not be definitely determined were processed by sequencing analysis. All the experiments were repeated at least thrice.

The reaction results were preserved after reaction. The baseline start value, stop value and Value were debugged to optimize the state of standard curve, $r^2 \geq 0.99$ and recorded.The numerical values of the speciments were recorded.

The amplification curve of the negative controls

Table I. *Primer sequences*

Category of primer	Name of primer	Sequence of primer
PE	Upstream	5-TCC GGC CCC TGA ATG CGG CTA ATC C-3’
	Downstream	5-ACA CGG ACA CCC AAA GTA GTC GGT CC-3’
EV71	Upstream	5-GCA GCC CAA AAG AAC TTC-3’
	Downstream	5-ATT TCA GCA GCT TGG AGT-3’
CA16	Upstream	5-ATT GGT GCT CCC ACT ACA-3’
	Downstream	5-TCA GTG TTG GCA GCT GTA-3’
Fluorescent probe		5-AAC ACA CAC CGA TCA ACA GTC AGC GTG G-3’

Table II. *The positive rates of different combinations of the specimens*

Combination mode		No. of positive cases	Positive rate (%)
Throat swabs + stool (42 cases)	Throat swabs	32	76.19
	stool	31	73.81
Stool + bleb fluid (5 cases)	stool	4	80
	Bleb fluid	4	80
Throat swabs + stool + cerebrospinal fluid (4 cases)	Throat swabs	3	75
	stool	4	100
	Cerebrospinal fluid	1	25
Throat swabs + stool + bleb fluid (2 cases)	Throat swabs	2	100
	stool	2	100
	Bleb fluid	2	100

was not S-shaped or was blank at Ct value. As to the Ct values of critical positive controls, the standard curve was controlled and $r^2 \geq 0.99$. If the above conditions could not be satisfied in the study, it was determined as ineffective, and then a new experiment was initiated with the step of sample processing.

Analysis of spatial-temporal distribution characteristics

The data of cases of HFM disease in China in 2016 given by the Chinese disease control and prevention information system were taken as source data for the analysis of the regional and temporal distribution conditions of HFM disease (10). HFM disease has a high infection rate but a low death rate (11). To ensure the reliability of the experiment, the present addresses of the patients were regarded as the geographical location, and the onset date of HFM disease was regarded as the occurrence time; statistical cycle was one month. Stata software was used to test the target data. Different epidemic curves were drawn. Moreover, different layers were divided according to the epidemic intensity. arcGIS was used to establish trend diagrams of spatial distribution.

RESULTS

Detection of HFM virus infection

71.03% of the detected nucleic acid samples were EV-positive. The detection rate of virus in the cerebrospinal fluid, stool, bleb fluid and throat swab were 50.00%, 62.26%, 85.71% and 73.4%, respectively (Fig. 1).

Combination of specimens

In this test, 53 target cases were selected. The positive rates of different combinations of the specimens of throat swabs, stool, bleb fluid and cerebrospinal fluid were calculated. The experimental results are shown in Table II. The positive rate was approximately 75% when throat swab was in combination with stool; the positive rate was 80% when stool was in combination with bleb fluid; the positive rate was 81.5% when throat swab was in combination with stool and cerebrospinal fluid; the positive rate was 100% when throat swab was in combination with stool and bleb fluid. The results of the detection based on single specimen and multiple specimens further verified that HFM disease was induced by EV. Detection based on the combination of specimens could improve the positive rate and greatly reduce the rate of missed diagnosis, which made the study results more authoritative. Furthermore, experiments based on multiple methods could enhance the sensitivity of experiments as well as the reliability and accuracy of the results.

Epidemiological characteristics in different provinces of China

Data of cases of HFM disease in 2016 were collected, and the incidence of HFM disease was analyzed according to different indicators. The distribution of patients with HFM disease in different provinces is shown in Fig. 2.

All the provinces in China have been invaded by HFM disease, indicating that HFM disease was not regional. But it mostly happened in the East and South China, and seldom happened in the West and North China.

A remarkable difference was observed in the incidence of HFM disease between different provinces. The incidence rates of HFM disease in thirteen provinces or municipalities such as Beijing, Shanghai, Hainan, Guangdong and Zhejiang were higher than the average incidence rate, and the incidence rates of the other provinces were lower than the average incidence rate.

The distribution of death cases was significantly different between different provinces. The death rates of HFM disease in eleven provinces such as Anhui, Hainan, Guangdong and Guangxi were higher than the average death rate. No death cases were found in ten provinces or municipalities such as Tibet and Qinghai.

The above probability statistics and indicators were evaluated comprehensively. It was found that the prevalence of HFM disease mainly concentrated on three areas, i.e. the three provinces in the north, the three provinces in the south and east coastal provinces.

The large-scale analysis of the research data suggested that the number of cases in different cities

in the same province differed significantly. Cities with large population which are more developed had faster transmission speed of HFM disease than cities with small population. Taking Guangdong as an example, the incidence of HFM disease mainly concentrated on Guangzhou, Shenzhen and Dongguan.

Temporal distribution characteristics

The data of the cases of HFM disease were analyzed, and then the statistical diagrams of cases of HFM disease were drawn.

Fig. 3 suggests that HFM disease in China had a high incidence between April and July.

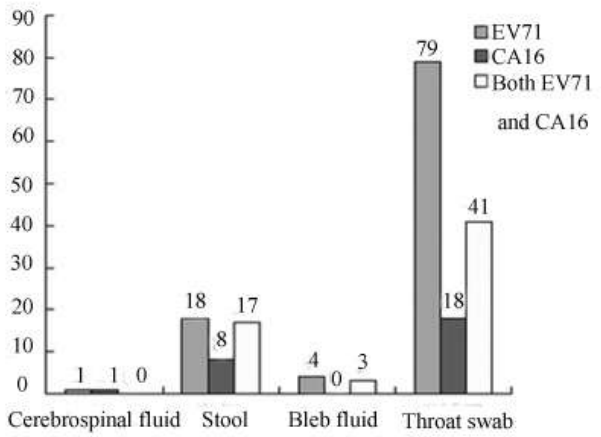

Fig. 1. *The test results and detection rates of the target samples*

Fig. 2. *The distribution of cases of HFM disease in China in 2016*

Spatial-temporal dynamic variation characteristics

From the above analysis, it was concluded that HFM disease had the following incidence characteristics in China: the concentrated and dispersed distribution conditions of HFM disease in China were different in different years; the number of reported cases in different provinces began to increase sharply from April - the period between April and July was the frequently occurring period, and the number of cases began to decrease in August; in May and June, the number of cases increased in the north, and the high-incidence area gradually moved toward the north.

Overall, the number of cases was large in cities such as Beijing and Shanghai.

Population distribution

According to the statistical data of cases of HFM disease, the ratio of males to females was 1.75:1, the percentage of scattered children was 64.72%, the percentage of kindergarten children was 26.93%, and the percentage of students was 5.39%. The total percentage of the three groups was 97.04%.

The differences between different cities in the same province were also significant. The percentages of scattered children and kindergarten children had a significant difference. For example, the ratio of scattered children to kindergarten children with HFM disease was 1.25 in one city, but the ratio in the neighboring city was 8.88, which was associated to the proportions of scattered children and kindergarten children in different cities.

DISCUSSION

HFM disease is induced by EV. 68 ~ 72 categories of EV have been discovered to date, among which, 20 categories, especially CA16, EV72 and echovirus, can induce the disease. These viruses may spread worldwide, and most of the patients are newborn infants with an immature immune system (12).

In this study, the nucleic acids of EV71 and CA16 were detected in the specimens collected from the patients, which directly suggested that EV71 and CA16 were the main infective pathogens (13). FQ-PCR specific amplification found that 65.9% of the

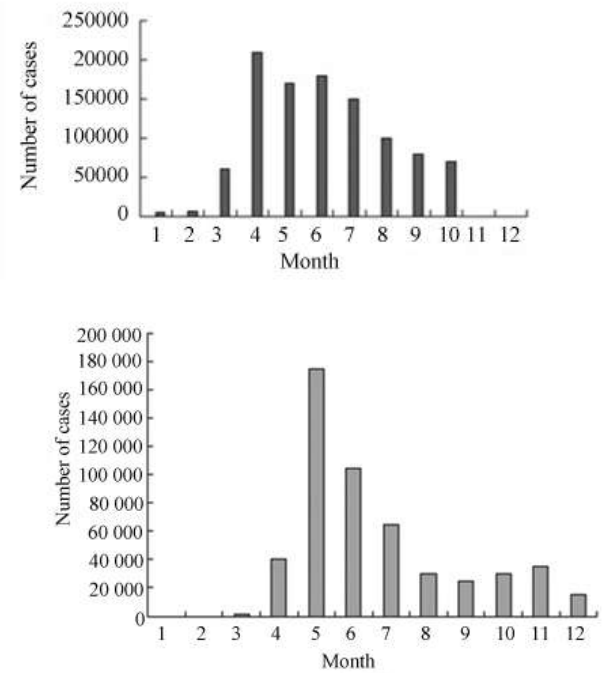

Fig. 3. *The statistical diagrams for cases of HFM disease*

cases were induced by EV71.

The analysis of data of HFM disease in China in 2015 and 2016 suggested that new cases appeared every year and covered a large area. The number of patients increased in mid-to-late March; in April, the number of patients increased rapidly in provinces in the south; in July, it spread from the south to the north; in August, the epidemic situation weakened and diminished gradually. Regarding spatial distribution, the incidence rate of in the three provinces in the north, the three provinces in the south and the coastal region were higher than that in other areas, which was because the population density and migrant population of those areas were higher than those of the other areas. Moreover, HFM disease is transmitted via the digestive tract, respiratory tract and contact.

CA16 and EV71 were the main viruses inducing HFM disease. In this study, the incidence induced by EV71 infection was higher than that induced by CA16 infection, and CA16 was usually accompanied by EV71. Patients with infection of both CA 16 and EV71 had a high death rate (14). It was found that the detection rate of bleb fluid was the highest, and the difference of the positive detection rate between different specimens had no statistical significance. Basing on different categories of specimens could enhance the detection rate.

In this paper, the spatial-temporal distribution characteristics of HFM disease in China at the macro level were explained based on medical statistical data, and a medical assessment was made at the geographical level. GIS technology was applied in the medical field to promote the cross development of medicine and geography. Some conclusions may be not convictive due to the one-sidedness of data. Therefore, further analysis on more precise data is needed to provide a scientific basis for the control of HFM disease.

ACKNOWLEDGEMENTS

This study was supported by the Special Research Project of Education Reformation and Development of Degree and Graduate Student (2017) (Project No.: JGY2017038).

REFERENCES

1. Cheng BN, Jin YL, Chen BQ, Zhu LY, Xu ZC, Shen T. Serum cholinesterase: a potential assistant biomarker for hand, foot, and mouth disease caused by enterovirus 71 infection. Infect Dis Povert 2016; 5(1):27.
2. Park KS, Lee BH, Baek KA, et al. Enteroviruses isolated from herpangina and hand-foot-and-mouth disease in Korean children. Virol J 2012; 9(1):205.
3. Wang Q, Zhang W, Zhang Y, et al. Clinical features of severe cases of hand, foot and mouth disease with EV71 virus infection in China. Arch Med Sci 2014; 10(3):510.
4. Mirand A, Henquell C, Archimbaud C, Ughetto S, Antona D, Bailly JL, Peigue-Lafeuille H. Outbreak of hand, foot and mouth disease/herpangina associated with coxsackievirus A6 and A10 infections in 2010, France: a large citywide, prospective observational study. Clin Microb Infect 2012; 18(5):E110.
5. Lott JP, Liu K, Landry ML, Nix WA, Oberste MS, Bolognia J, King B. Atypical hand-foot-and-mouth disease associated with coxsackie virus A6 infection. J Am Acad Dermatol 2014; 19(12):20745.

6. Wu JS, Zhao N, Pan H, et al. Patterns of polymorphism and divergence in the VP1 gene of enterovirus 71 circulating in the Asia-Pacific region between 1994 and 2013. J Virol Meth 2013; 193(2):713-28.
7. Huang SW, Wang YF, Yu CK, Su IJ, Wang JR. Mutations in VP2 and VP1 capsid proteins increase infectivity and mouse lethality of enterovirus 71 by virus binding and RNA accumulation enhancement. Virology 2012; 422(1):132-43.
8. Nishimura N, Nakayama H, Yoshizumi S, et al. Detection of noroviruses in fecal specimens by direct RT-PCR without RNA purification. J Virol Meth 2010; 163(2):282-86.
9. Chen J, Li HL, Dong JY, Wang FJ, Wang AG, Wang JY. Preparation of the FQ-PCR standard reference varied the quantification of gene expression. Chin J Biochem Mol Biol 2012; 28(11):1064-68.
10. Cao C, Li G, Zheng S, et al. Research on the environmental impact factors of HFM Disease in Shenzhen, China using RS and GIS technologies. Geosci Remote Sens Symp IEEE 2012; 53(60):7240-43.
11. Zhao JN, Xue C, Zhong LF, Zhao JJ. Analysis of contact rates and force of infection of HFM disease in Chongqing, China. Chin Sci Bull 2016; 61;2475-82.
12. Lai CC, Jiang DS, Wu HM, Chen HH. A dynamic model for the outbreaks of hand, foot, and mouth disease in Taiwan. Epidemiol Infect 2016; 144(7):1500-11.
13. Zhang C, Zhu R, Yang Y, et al. Phylogenetic analysis of the major causative agents of hand, foot and mouth disease in Suzhou city, Jiangsu province, China, in 2012–2013. Emerg Microb Infect 2015; 4(2):e12.
14. Mo JJ. Surveillance and analysis on hand foot and mouth disease in Guangxi Zhuang Autonomous Region in 2011. Occupat Health 2012.

LETTER TO THE EDITOR

ROLE OF FUNGAL-INDUCED STRESS IN BIOCHEMICAL AND PHYTOCHEMICAL PROFILING OF *PEGANUM HARMALA*

M. AFZAL [1], M. SHAHID[2], M. RIAZ[3], M.A. SALEEM[1], J.I. WATTOO[1], B. ZESHAN[1] and M. NAVEED[1]

[1]Faculty of Life Science, University of Central Punjab, Lahore, Pakistan; [2]Department of Biochemistry, University of Agriculture Faisalabad, Pakistan; [3]Department of Chemistry, University of Sargodha, Women Campus, Faisalabad, Pakistan

Received July 27, 2017 – Accepted December 20, 2017

The current study was designed to evaluate bioactive compounds under the influence of biotic stress on seedlings of *Peganum harmala*. Biologically active compounds were determined by using different techniques. The HPLC and GC-MS analyses detected the significant amount of phenolic acids and active biological compound. Total protein content, activity of proteases, α-amylases, catalases and peroxidases were observed to be accelerated under fungal stress. The seedling extracts exhibited prominent antifungal and antimicrobial activity against selected strains. The present study showed that *P. harmala* is a good candidate to be used in natural therapies and medicine.

To the Editor,

Plants have been used as a routine medicine to cure several diseases. *Peganum harmala,* commonly known as Syrian rue, is a flowering plant which is widely distributed in Central Asia, North Africa and the Middle East (1). The plant is well-known owing to medicinal importance in Pakistan, India and southern parts of Iran. Phenolic-rich plants are considered beneficial for human use either directly as food or as medicinal constituents. Several studies indicated the presence of important components of this plant in essential oil which could be responsible for its potential role in health. *P. harmala* contains several other chemical constituents besides phenolics that are known to play key roles in maintaining health (2). The seed extracts of plants contain alkaloids, steroids, fatty acids, amino acids and carbohydrates and are commonly used as an analgesic and anthelmintic component to treat high bilirubin level, lumbar pain, nervous and stomach disorders (3).

The potential role of *P. harmala* in cardiovascular, nervous system, gastrointestinal, antimicrobial, antifungal, antidiabetic, osteogenic, immunomodulatory and antitumor activities have been well documented in recent studies (4). Many biotic and abiotic stresses influence the secondary metabolite production in plants. Recent studies have reported that stress induction augments the food value and metabolites in many nutritional and medicinal plants (5). The objectives are to study the bio-active compounds in *P. harmala* under the influence of biotic stress of *Aspergillus niger* and analysis of plant extracts at seedling stage to evaluate antioxidants, antifungal and antimicrobial compounds.

Key words: P. harmala, biotic stress, phenolic acids, pharmacological activity, antimicrobial activity

Mailing address:
Dr. Muhammad Afzal,
Assistant Professor, Faculty of Life Science,
University of Central Punjab,
Lahore, Pakistan
Tel.: +92-336-7373573
e-mail: dr.afzal@ucp.edu.pk

0393-974X (2018)

MATERIALS AND METHODS

For characterization of antimicrobial peptides/proteins in *P. harmala,* SDS-Polyacrylamide gel electrophoresis (PAGE), Specific activities of Catalase (CAT) and Peroxidase (POD) and alpha amylase were used following the reported method for the study of the total protein contents (6). Antifungal and antibacterial activity of sample against selected strains was determined by using disc diffusion (7). Minimum inhibitory concentration (MIC) of different collected samples was determined by micro dilution (8). Phytochemical screening of extract of *P. harmala* was studied to detect the presence of glycosides, flavonoids, alkaloids and saponins following the reported methods (9). TPC contents were estimated using standard methods (10). The identification and concentration of phenolics were calculated from standard curves calibrated using phenolic standards. GC-MS analysis was studied by Super Critical Fluid Extraction (SCFE) method (11).

Statistical analysis

To find the accuracy in the data, regression analysis was performed using statistical software STATISTICX version 8.1 (Stat soft Inc, Tulsa, Oklahoma, USA).

RESULTS

The protein contents of *P. harmala* increased up to 4 dpi and then started decreasing which was observed at 5 dpi (Fig. 2). The decrease was due to a thick growth of fungus that causes stress. Similar to protein, the metabolically important enzymes involved in germination were also found to be accelerated under fungal stress. The maximum activity of proteases, amylase, and catalase (CAT) was observed at dpi 4 and 5 and then decreased at 6 and 7 dpi (Fig. 1). Antioxidants, such as peroxidase (POD) and catalase (CAT), were also investigated under stress conditions. The highest specific activity of POD was recorded at 4 dpi for *P. harmala* and the lowest at 7 dpi (Fig. 1). The antibacterial activity results in Table I showed that maximum activity of *P. harmala* extract was measured against *Staphylococcus aureus* at dpi 1 and 2, which were 22±2 and 23±1.15, respectively, while the minimum was 10±1.15 recorded at dpi 7. The zone of inhibition was measured against *Bacillus subtilis* that were 23±1.15 mm at dpi 3 and 4 while 9±1.15 mm at dpi 7. Minimum Inhibitory Concentration (MIC) was measured against selected strains and the least value of the MIC was observed at dpi 3 against *Staphylococcus aureus* that was 18±0.18 mg/mL and the highest value of the MIC was at dpi 2 and 6 against *Bacillus subtilis*. The results were shown in Table II. Finally, the data of MICs of seedling extracts of the medicinal plant at different dpi showed that dpi 3, 4 and 5 extracts were potent for detailed studies. These values were in the range of MICs of the selected medicinal plants to inhibit the growth of the bacterial strains (12). The flavonoids (28%), alkaloids (5.6%) and saponin were also observed in plant extract. HPLC results were expressed in parts per million (ppm) where *P. harmala* contained a large amount of hydroxymethoxy benzoic acid, in leaf, stem and root 26.20±0.519, 18.62±0.369 and 4.152±0.644, respectively. *P. harmala* leaf, stem and root extract contained a good amount of Gallic acid, as 16.89±0.412, 11.63 364±0 and 3.483±0.284. Chlorogenic acid and Syringic acid were detected only in leaf extract. The most abundant phenolic acids, like caffeic acid (10.51±0.331), m-coumeric acid and ferrulic acid were also detected in *P. harmala* extracts. Optimization of acidic conditions for the hydrolysis of flavonoid glycosides in a range of fruits, vegetables, and beverages has already been described (13). GC-MS analysis of *P. harmala oil* exhibited the presence of chemical constituents as 2-piperidinone, epiglobulol, veridiflorol, surfynol, 3, 6-dimethyl-4-octyne-3, 6-diol, nerolidiolisobutyrate and 1-nonanoyl-3-octanoyl-glycerol.

DISCUSSION

The results of previous studies indicated that medicinal plants have potential antimicrobial activity in terms of organic extracts and essential oils (14). The present study shows that *P. harmala* plant extracts possess substantial antimicrobial and antifungal activity (Table III) due to the presence of potent bioactive compounds. The study is quite novel as no previous studies report the detection of phenolic contents in *P. harmala*. The potent antimicrobial

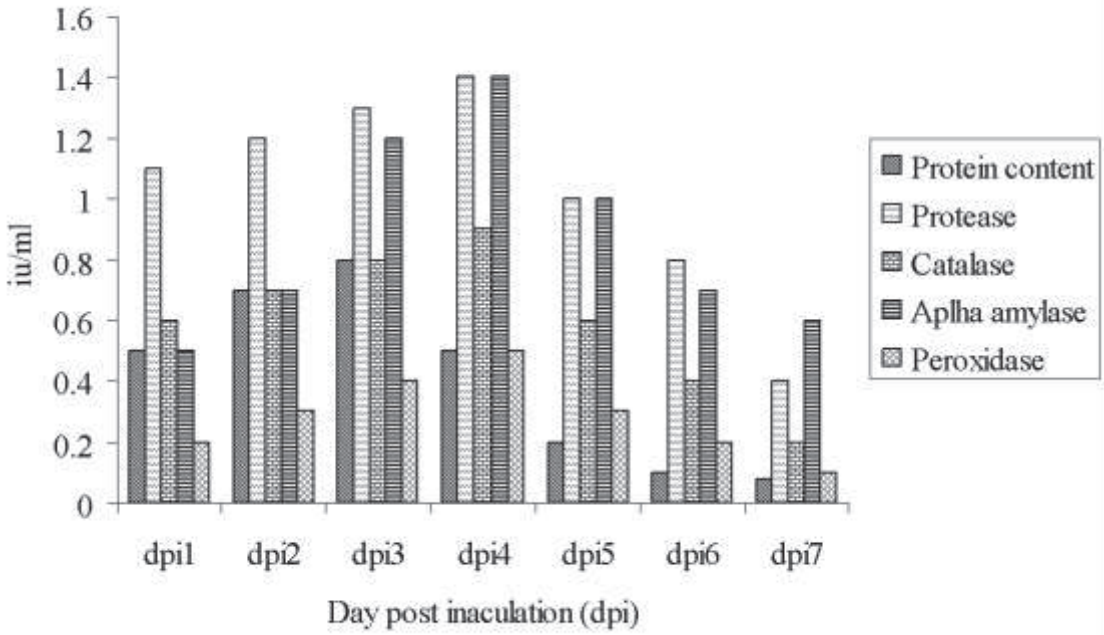
1.6
1.4
1.2
1
0.8
0.6
0.4
0.2
0
iu/ml
dpi1
dpi2
dpi3
dpi4
dpi5
dpi6
dpi7
Day post inaculation (dpi)
Protein content
Protease
Catalase
Aplha amylase
Peroxidase

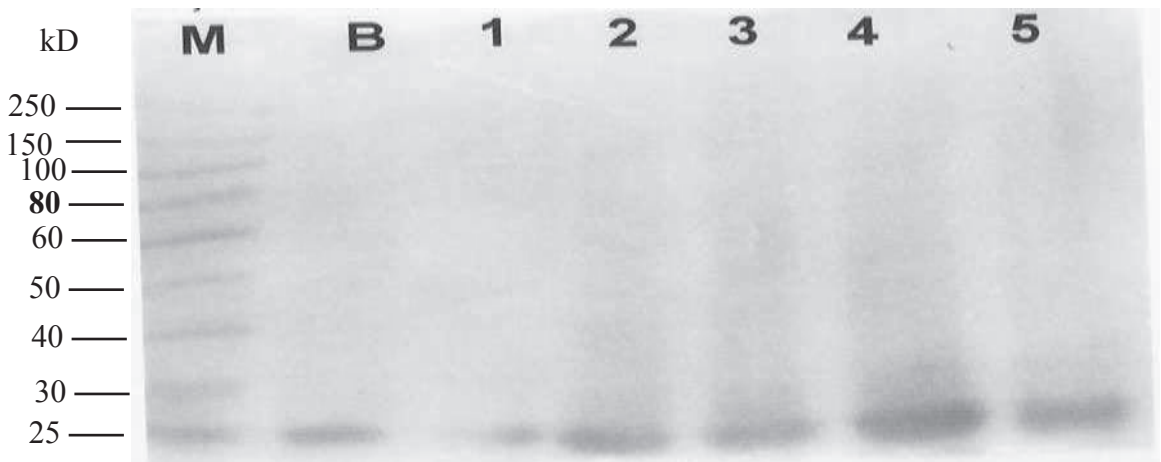
kD
M
B
1
2
3
4
5
250
150
100
80
60
50
40
30
25

Table I. *Antibacterial activity of extracts of P. harmala induced by Asparagus niger.*

Bacterial strains		***Staphylococcus aureus***	***Escherichia coli***	***Pasturella multocida***	***Bacillus subtilis***
dpi	0	$21^{a} \pm 1.15$	$12 \pm 1.12^{-}$	$15^{a} \pm 1.15$	$7^{a} \pm 1.15$
	1	$22^{a} \pm 2.00$	$14 \pm 1.13^{-}$	$17^{a} \pm 1.15$	$11^{a} \pm 1.15$
	2	$23^{a} \pm 1.15$	$08 \pm 1.10^{-}$	$14^{a} \pm 1.15$	$13^{a} \pm 1.15$
	3	$19^{a} \pm 1.15$	$18 \pm 1.11^{-}$	$21^{a} \pm 1.15$	$23^{a} \pm 1.15$
	4	$16^{a} \pm 2.00$	$22 \pm 1.15^{-}$	$23^{a} \pm 1.15$	$23^{a} \pm 1.15$
	5	$6^{a} \pm 1.15$	$24 \pm 1.08^{-}$	$13^{a} \pm 1.15$	$12^{a} \pm 1.15$
	6	$6^{a} \pm 1.15$	$16 \pm 1.00^{-}$	$11^{a} \pm 1.15$	$18^{a} \pm 3.02$
	7	$6^{a} \pm 1.15$	$10 \pm 0.86^{-}$	$10^{a} \pm 2.20$	$9^{a} \pm 1.15$
+ve control		24 ± 0.940	23 ± 0.94	$23^{a} \pm 0.94$	$23^{a} \pm 0.94$

One-way Anova results indicate that there is no significant difference between groups at 5% level of probability.

Table II. *Phenolics from P. harmala determined by HPLC method.*

Phenolic compound	**Leaf (ppm)**	**Stem (ppm)**	**Root (ppm)**
Chromatotropic acid	ND	ND	ND
Gallic acid	$16.89_{A}{}^{b} \pm 0.412$	$11.63_{B}{}^{b} \pm 0.321$	$3.483_{C}{}^{a} \pm 0.284$
Caffeic acid	$10.51_{A}{}^{c} \pm 0.331$	$4.726_{B}{}^{c} \pm 0.264$	$1.085_{C}{}^{b} \pm 0.241$
Vanillic acid	$3.725_{A}{}^{e} \pm 0.286$	$0.861_{B}{}^{d} \pm 0.485$	ND
Hydroxymethoxybenzoic acid	$26.20_{A}{}^{a} \pm 0.519$	$18.62_{B}{}^{a} \pm 0.369$	$4.152_{C}{}^{a} \pm 0.644$
Chlorogenic acid	$2.583^{e} \pm 0.439$	ND	ND
Syringic acid	$0.825^{f} \pm 0.537$	ND	ND
m-Coumeric acid	$7.847_{A}{}^{c} \pm 0.643$	$5.163_{B}{}^{c} \pm 0.321$	$1.733_{C}{}^{b} \pm 0.174$
Ferrulic acid	$5.841_{A}{}^{d} \pm 0.521$	$4.038_{B}{}^{c} \pm 0.124$	$0.369_{C}{}^{c} \pm 0.243$

Least significant test (LSD) was used to compare means. Means followed by different letters are different at 5% level of probability. Capital letters (A to C) describe the significant difference among rows, whereas small letters (a to f) indicate significant difference among columns.

Table III. *Antifungal activity of extracts of P. harmala induced by fungal stress.*

P. harmala		***A. niger***	***T. harzianum***	***F. solanai***	***H. myedis***
dpi	0	17^{a}±1.24	7^{b}±1.24	16^{c}±1.63	16^{d}±1.63
	1	14^{a}±1.63	13^{b}±0.81	22^{c}±1.63	12^{d}±0.94
	2	14^{a}±2.86	16^{b}±1.24	9^{c}±0.94	0^{d}.0±0
	3	22^{a}±0.47	17^{b}±1.24	0^{c}.0±0	14^{d}±1.63
	4	26^{a}±1.63	8^{b}±1.63	0^{c}.0±0	13^{d}±0.81
	5	11^{a}±0.94	14^{b}±1.63	8^{c}±1.63	0^{d}.0±0
	6	8^{a}±1.63	0^{b}.0±0	0^{c}.0±0	0^{d}.0±0
	7	13^{a}±0.81	13^{b}±0.81	14^{c}±1.63	0^{d}.0±0
Control (+)		25^{a}±1.24	22^{b}±0.47	24^{c}±1.24	26^{d}±2.49

Means were compared for different fungal strains. Least significant test (LSD) was used to compare means.

potential of *P. harmala* makes it a good candidate to be used in natural therapies and medicine.

REFERENCES

1. Hilal HS, Young ken HW. Certain poisonous plants of Egypt. In Pharmaceutical Society of Egypt, Ed. Dokki: the National Information and Documentation Centre. Cairo, Egypt, 1983; p. 88.
2. Chatterjee A, Ganguly M. Alkaloidal constituents of peganum harmala and synthesis of the minor alkaloid deoxyvascinone. Phytochem 1968; 7:307-311.
3. Marwat SK, Rehman Fu. Medicinal and Pharmacological Potential of Harmala (Peganum harmala L.) Seeds. Nuts and Seeds in Health and Disease Prevention. San Diego Academic Press, 2011; p. 585.
4. Dube A, Misra P, Khaliq T, Tiwari S, Kumar N, Narender T. Therapeutic potential of harmala (Peganum harmala L.) seeds with an array of pharmacological activities. In: Preedy VR, Watson RR, Patel VB, eds, Nuts and Seeds in Health and Disease Prevention. London, England: Academic Press, 2011; p585.
5. Suzuki N, Rivero RM, Shulaev V, Blumwald E, Mittler R. Abiotic and biotic stress combinations. New Phytol 2014; 203:32-43.
6. Lee HC, Aarhus R. ADP-ribosyl cyclase: an enzyme that cyclizes NAD+ into a calcium-mobilizing metabolite. Cell Regul 1991; 2:203-9.
7. Riaz M. Rasool N. Bukhari I, et al. Antioxidant Studies Using Sunflower Oil as Oxidative Substrate and DNA Protective Assay by Antirrhinum majus. Oxid Commun 2013; 36:542-52.
8. Ashraf A, Sarfraz RA, Rashid MA, Shahid M. Antioxidant, antimicrobial, antitumor, and cytotoxic activities of an important medicinal plant

(*Euphorbia royleana*) from Pakistan. J Food Drug Analy 2015; 23:109-15.

9. H.O.Edeoga,D.E.Okwu,B.O.Mbaebie.Phytochemical constituents of some Nigerian medicinal plants. Afr J Biotechnol 2005; 4:685-88.
10. Tsao R, Yang R. Optimization of a new mobile phase to know the complex and real polyphenolic composition: towards a total phenolic index using high-performance liquid chromatography. J Chromatogr 2003; 1018:29-40.
11. De Melo MMR, Oliveira ELG, Silvestre AJD, Silva JCM. Supercritical fluid extraction of triterpenic acids from Eucalyptus globulus bark. Supercritical Fluids 2012; 70:137-45.
12. Nenaah G. Antibacterial and antifungal activities of (beta)-carboline alkaloids of Peganum harmala (L) seeds and their combination effects. Fitoterapia 2010; 81:779-82.
13. Asghari G, Lockwood GB. Stereospecific biotransformation of phenylethyl propionate by cell culture of Peganum harmala. Iranian Biomed J 2002; 6:43-46.
14. Razmavar S. Abdulla MA, Ismail SB, Hassandarvish P. Antibacterial activity of leaf extracts of Baeckea frutescens against methicillin-resistant Staphylococcus aureus. BioMed Res Int 2014; 2014:521287.

LETTER TO THE EDITOR

EXTRACORPOREAL SHOCKWAVE THERAPY *VERSUS* EXERCISE PROGRAM IN PATIENTS WITH LOW BACK PAIN: SHORT-TERM RESULTS OF A RANDOMISED CONTROLLED TRIAL

A. NOTARNICOLA[1,2], G. MACCAGNANO[1], M.F. GALLONE[3], L. MASTROMAURO[4], F. RIFINO[1], V. PESCE[1], I. COVELLI[1] and B. MORETTI[1,2]

[1]Orthopedics Section, Department of Medical Sciences of Basis, Neurosciences and Organs of Sense, Faculty of Medicine and Surgery, University of Study of Bari, General Hospital, Bari, Italy; [2]Course of Motor and Sports Sciences, Department of Medical Sciences of Basis, Neurosciences and Organs of Sense, Faculty of Medicine and Surgery, University of Study of Bari, Bari, Italy; [3]Department of Biomedical Sciences and Human Oncology, Faculty of Medicine and Surgery, University of Study of Bari, General Hospital, Bari, Italy; [4]Centro Polivalente di Riabilitazione Frangi, Segesta-Korian, Acquaviva delle Fonti, Bari, Italy

Received September 20, 2017 – Accepted January 23, 2018

The physiotherapy treatment of low back pain (LBP) with physical stimulation offers different possibilities of application. Until now, the physical therapies used in LBP are laser therapy, ultrasonotherapy and currents. We conducted a clinical trial in order to verify whether shockwave therapy, which is very effective in treating tendinopathies and fracture consolidation delays, leads to clinical and electromyographic improvement in patients affected by LBP. We randomized thirty patients affected by LBP treated with shock waves (shockwave group) or a standard protocol characterized by rehabilitative exercises (control group). At one and three months, the patients treated with shockwave therapy showed clinical improvement measured by VAS scales (p=0.002; p= 0.02), and disability evaluated with Roland scales (p=0.002; p=0.002) and Oswestry (p=0.002; p=0.002). At three months, the patients treated with shock waves, showed a significant improvement in terms of values of amplitude of the sensory nerve conduction velocity (SNCV) of the plantar medialis nerve (left: p=0.007; right: p=0.04), the motor nerve muscular conduction (MNCV) of the deep peroneal nerve (left: p=0.28; right: p=0.01) and recruitment of motor units of finger brevis extensor (left: p = 0.02; right: p=0.006). In the control group, there was a trend to increase the clinical and electromyographic results without statistical significance. The preliminary results suggest a good applicability of shockwave therapy in the treatment of LBP, in accordance with the anti-inflammatory, antalgic, decontracting effects and remodeling of the nerve fiber damage verified in previous studies conducted on other pathological models. Future research will allow us to verify the integration of this therapy into a rehabilitation protocol combined with other physical therapies.

To the Editor,

The prevalence of low back pain in the adult is 37% (1). New studies permit to increase our knowledge about the different components responsible for low back pain (LBP) symptomatology (2). The arthritis and disc degeneration can start a local inflammatory process. There emerges a mechanical compression of root and radiculopathy. The spinal

Key words: shock wave, electromyographic exam, low back pain

Mailing address:
Dr Angela Notarnicola,
Orthopedics Section, Department of Medical Sciences of Basis, Neurosciences and Organs of Sense, Faculty of Medicine and Surgery, University of Study of Bari, General Hospital, Piazza Giulio Cesare 11, 70124 Bari, Italy
Tel./fax.: +39 080 5592938
e-mail: angelanotarnicola@yahoo.it

0393-974X (2018)

muscle becomes hypertonic, causing pain due to development of atrophy and fat degeneration of muscle fiber. Furthermore, chronic pain may cause central neuroplasticity. The LBP treatment is multidisciplinary, as multiple treatments can be administered simultaneously or in series (3-5). The shock waves (SW) represent innovative treatment of LBP. This therapy is characterized by anti-inflammatory, anti-oedema, decontracturant, antalgic, neuro-modulation and neurotrophic effects (6, 7). In lumbar pain these actions are able to manage the various pathological components. In the literature two preliminary trials have compared the SW protocol and exercises with a thermotherapy protocol and exercises in LBP treatment (8, 9). The results showed a progressive clinical improvement over time, with better outcomes in patients treated with extracorporeal shockwave therapy (ESWT).

The present study aimed to examine three goals based on the aforementioned information: i) to determine the effectiveness of ESWT without exercise for the patients with low back pain; ii) to compare this treatment with the exercises performed alone; iii) to analyze the effects, not only with subjective pain degree (VAS) and disability (Roland Morris Disability Questionnaire and Oswestry Low Back Pain Disability Questionnaire), but also by electromyographic values of the affected muscles and nerves of the lower limb. By improving the knowledge of this therapy we will be able to prescribe an efficacious SW therapy integrated with rehabilitation protocol for the patient with LBP.

MATERIALS AND METHODS

Thirty patients were recruited from our Orthopedic Unit. The study was approved by the local Ethics Committee. Prior informed consent to take part was given by all participants. Inclusion criteria were age >18 years old, a diagnosis of chronic low back pain or low back pain and leg pain lasting at least 12 weeks, made on the basis of clinical symptoms and instrumental tests, and a functional VAS score >/=4*;* computed tomography (CT) or nuclear magnetic resonance (MRI) documented discopathy or disk hernia. Patients were excluded from the study if they had contraindications to SW therapy. Furthermore, they were excluded if they had the presence of active vertebral fractures, a history of previous spine surgery, rheumatic diseases such as rheumatoid arthritis, infections and systemic diseases that could affect pain perception (diabetes, etc) or local injections (local anesthetic and/or corticosteroids; O2O3, etc) or physiotherapy administered within the previous 4 weeks. At the recruitment the study protocol included the collection of medical history and clinical visit, as in our previous experience (10). Clinical results were evaluated using visual analogic scale (VAS), Roland Morris Disability Questionnaire and Oswestry Low Back Pain Disability Questionnaire at the time of recruitment (T0) and at the follow-up (FU) visits at 1 and 3 months (FU) (T1 and T2). All subjects had an electromyography study carried out by an electromyographer blinded to the subjects' treatment. The work by Dillingham and colleagues (11) showed that the electromyography study of the legs was able to detect 94-98% of subjects with a radiculopathy. At T0 and T2, each patient was evaluated by electroneuromyographic exam in order to record the sensitivity nerve conduction velocity (SNCV) of the plantar medialis nerve (the data were expressed as amplitude in microVolts), of the motor nerve muscular conduction (MNCV) of deep peroneal nerve motor and the recruitment of the muscular motor units of the finger brevis extensor (the data were expressed as amplitude in milliVolts).

In the SW group, ESWT was administered with an electromagnetic generator equipped with in-line ultrasound guidance (Minilith SL1, Storz, Swiss), during three sessions (1 session per week). Under ultrasound guidance, the depth of the probe was adjusted to treat muscular structures, which represent the main affected sides in LBP, mainly the quadratus lumborum muscle, the gluteus maximus muscle, the gluteus medius muscle, the gluteus minimus muscle, and the piriform muscle. We used a low-medium energy level (0.03 mJ/mm2), which was consistent with the patient pain tolerance level, during the treatment. We administered 2000 impulses. In the control group, all participants received individual exercise treatment sessions of 50 min, generally 5 times per week, for a total of 4 weeks.

All information was collected in a spreadsheet and data were analyzed using Stata MP12 statistical software. The proportions in the three treatment groups were compared using *chi*-squared test. For the evaluation of functional

score variation over the time in each single treatment group, median scores were compared using Wilcoxon sign-rank test and comparing two times at a time (T0 *vs* T1; T1 *vs* T2). In order to evaluate differences between the two treatment groups with regard to functional scores measured at single time of follow-up, median scores were compared using Wilcoxon-Mann-Whitney test for independent samples. For each test we considered a value of $p<0.05$ as statistically significant. The z-value was the value of the statistical test. The data were not normally distributed.

RESULTS

In the study, 30 patients were recruited and randomized to the two groups. Six patients (2 in the SW group and 4 in the exercise group) dropped out of the study. At the last follow-up we analyzed 24 patients: 13 in the SW group (6 males and 7 females), and 11 in the control group (6 males and 5 females). The average age was 61.8±14.2 years (exercise group: 54.4±10.3 years, SW group: 68.2±14.3 years). As regards epidemiological characteristics and clinical features, the two groups were homogeneous. Weight, height and Body Mass Index (BMI) were 75.5±13.2 kg, 166±7.5 cm and 27.4±4.5 kg/cm2, respectively. 8.3% of the population were smokers. The Lasegue and Wasserman tests were positive in 50% and 25% of the recruited population, respectively. 16.7% of patients presented a sensitivity alteration, 29.2% were characterized by a deficit of one or more tendon-bone of reflexes at the lower limb, and 4.2% had a modification of the muscular tone of the lower limb muscle.

Clinical-functional data and electromyography

Regarding the VAS scores at recruitment, the two groups were not homogeneous, with a higher value in the group treated with SW (T0: z=-3.15, p=0.002). At the two consequent follow-ups, a reduction emerged of the values for both groups, which was statistically significant in the SW group (T0-T1: z = 3.1, p=0.002; T1-T2: z=2.4, p=0.02).

Regarding the Roland scores, at T0 the two groups were homogeneous. There was a progressive reduction of disability at the two following follow-ups which was statistically significant only in the SW group (T0-T1: z=3.1, p=0.002; T1-T2: z=3, p=0.002). At T2 there was a significant difference between the two groups in favor of the SW group (z=2.82; p=0.005).

With regard to the Oswestry score, at T0 the two groups were homogeneous. There was a progressive reduction of disability, which was statistically significant for the SW group (T0-T1: z=3.15, p=0.002; T1-T2: z=3.13, p=0.002). At T2 by comparison of the two groups, the SW group showed better values than the exercise group (z=2.73, p=0.006).

At T0, the analysis of the electromyographic evaluation detected that the MNCV amplitude of the deep peroneal nerve, finger brevis extensor was homogeneous between the two treatment groups for the lower left limb (z=1.48, p=0.14), whilst we observed higher values in the SW group for the lower right limb which were statistically significant (z=-2.4, p=0.01). At T2 there emerged a significant increase in the SW group for both lower limbs (left: z =-2.38, p=0.02, right: z=-2.76, p=0.006).

At T0, regarding the value of MNCV of deep peroneal nerve, we did not detect any statistically significant differences between the two groups (left: z=-0.46, p=0.64; right: z=-1.65, p=0.10). At T2 there emerged a significant increase of the values in the SW group on the right (z=-2.55, p=0.01), but not on the left (z=-1.08, p=0.28).

At T0 the value of amplitude of SNCV of the plantar medialis nerve showed higher values in the exercise group (left: z=2.06, p=0.04; right: z=2.69, p=0.007). At T2 we detected a significant improvement in the SW group (left: z=-2.69, p=0.007; right: z=-2.06, p=0.04).

DISCUSSION

The results of this study show that SW could be useful in management of low back pain, allowing a clinical improvement and a functional electromyographic recovery. The rationale of this application in LBP is to modulate the inflammation and involvement of the muscular-nervous structures involved locally. We verified an improvement in the clinical and functional pain and disability score

already at the end of the treatment and T2, which was statistically significant in the SW group. Furthermore, in the SW group, the electromyographic values also demonstrated a significant recovery of SNCV of the plantar medialis nerve, the MNCV of the deep peroneal nerve and the recruitment of the muscular motor units of the finger brevis extensor. The analysis of the results highlighted the clinical-functional improvement and neuro-muscular properties in LBP according to the effects of SW. The *in vivo* studies on the animal model of SW stimulation on the sciatic nerve allowed to analyze the electro-neuro-myographic effects (12). The evaluations carried out within 14 weeks showed a reduction of motor nervous conduction (61% of reduction). After a muscular nerve traumatic event, the SW application was able to guarantee the regeneration of the damaged nerve and recovery of muscular function (13). A first SW model application for nerve fiber disorders is carpal tunnel syndrome. In carpal tunnel syndrome, the application of SW compared to placebo (12) and orthosis treatment (14) determined a significant recovery of disability and nervous function and pain remission, persistent at 12 weeks. The comparison of SW application and neurotrophic administration in carpal tunnel syndrome treatment showed similar results (15).

These results are due to the different effects of SW which are responsible for decreasing muscular tension and improving local perfusion in muscle contracted areas. Furthermore, the clinical effects are related to the decrease of algogenic substance production and inhibition of muscular nociceptors. This selective effect is responsible for decreasing metabolic demand.

In conclusion, due to the biological effect of shock waves and our clinical experience, ESWT may represent a new strategy in the treatment of low back pain. Further research will able to verify the effectiveness of integrated protocol of this therapy combined with therapeutic exercises.

ACKNOWLEDGEMENTS

The authors thank Brian John Molloy B.A. for language revision.

REFERENCES

1. Schmidt-Wilcke T, Leinisch E, Gänssbauer S, Draganski B, Bogdahn U, Altmeppen J, May A. Affective components and intensity of pain correlate with structural differences in gray matter in chronic back pain patients. Pain 2006; 125(1-2):89-97.
2. Beattie PF. Current understanding of lumbar intervertebral disc degeneration: a review with emphasis upon etiology, pathophysiology, and lumbar magnetic resonance imaging findings. J Orthop Sports Phys Ther 2008; 38(6):329-40.
3. Haldeman S, Dagenais S. A supermarket approach to the evidence-informed management of chronic low back pain. Spine J 2008; 8(1):1-7.
4. Notarnicola A, Maccagnano G, Tafuri S, Gallone MF, Moretti L, Moretti B. High level laser therapy for the treatment of lower back pain: clinical efficacy and comparison of different wavelengths. J Biol Regul Homeost Agents 2016; 30(4):1157-1164.
5. Fiore P, Panza F, Cassatella G, et al. Short-term effects of high-intensity laser therapy versus ultrasound therapy in the treatment of low back pain: a randomized controlled trial. Eur J Phys Rehabil Med. 201; 47(3):367-73.
6. Iannone F, Moretti B, Notarnicola A, Moretti L, Patella S, Patella V, Lapadula G. Extracorporeal shockwave increase interleukin-10 expression by human osteoarthritic and healthy osteoblasts in vitro. Clin Exp Rheumatol 2009; 27(5):794-9.
7. Moretti B, Iannone F, Notarnicola A, Lapadula G, Moretti L, Patella V, Garofalo R. Extracorporeal shockwave down-regulate the expression of interleukin-10 and tumor necrosis factor-alpha in osteoarthritic chondrocytes. BMC Musculoskelet Disord 2008; 9:16.
8. Notarnicola A, Maccagnano G, Gallone MF, Covelli I, Tafuri S, Moretti B. Short term efficacy of capacitive-resistive diathermy therapy in patients with low back pain: a prospective randomized controlled trial. J Biol Regul Homeost Agents 2017; 31(2):509-515.
9. Lee S, Lee D, Park J. Effects of extracorporeal shockwave therapy on patients with chronic low back pain and their dynamic balance ability. J Phys Ther Sci 2014; 26(1):7-10.
10. Han H, Lee D, Lee S, Jeon C, Kim T. The effects of

extracorporeal shockwave therapy on pain, disability, and depression of chronic low back pain patients. J Phys Ther Sci 2015; 27(2):397-9.

11. Dillingham TR, Lauder TD, Andary M, et al. Identifying lumbosacral radiculopathies: an optimal electromyographic screen. Am J Phys Med Rehabil 2000; 79:496-503.
12. Wu YT, Ke MJ, Chou YC, et al. Effect of radial shockwave therapy for carpal tunnel syndrome: A prospective randomized, double-blind, placebo-controlled trial. J Orthop Res 2016; 34(6):977-84.
13. Mense S, Hoheisel U. Shockwave treatment improves nerve regeneration in the rat. Muscle Nerve 2013; 47(5):702-10.
14. Raissi GR, Ghazaei F, Forogh B, Madani SP, Daghaghzadeh A, Ahadi T. The effectiveness of radial extracorporeal shockwave for treatment of carpal tunnel syndrome: A Randomized Clinical Trial. Ultrasound Med Biol 2017; 43(2):453-460.
15. Notarnicola A, Maccagnano G, Tafuri S, Fiore A, Pesce V, Moretti B. Comparison of shockwave therapy and nutraceutical composed of Echinacea angustifolia, alpha lipoic acid, conjugated linoleic acid and quercetin (perinerv) in patients with carpal tunnel syndrome. Int J Immunopathol Pharmacol 2015; 28(2):256-62.

LETTER TO THE EDITOR

ORAL LICHEN PLANUS

L. GIANNETTI[1], A.M. DELLO DIAGO[1] and E. SPINAS[2]

[1]University of Modena and Reggio Emilia, Department of Surgery, Medical, Dental and Morphological Sciences with Interest in Transplantation, Oncology and Regenerative Medicine, Modena, Italy; [2]Department of Surgical Sciences, University of Cagliari, Cagliari, Italy

Received December 21, 2017 – Accepted February 12, 2018

Oral Lichen planus (OLP) is the most frequent mucosal localization of Lichen planus, affecting about 1-2% of the population. It is associated with skin lesions in 60-70% of cases, while occurring as the only manifestations in 15-25% of patients. Six clinical forms of OLP are identified: reticular (the most common), plaque, papular, atrophic, vesicles/bullous and erosive. The evolution is chronic, especially in the erosive form. A 1% incidence of squamous-cell carcinoma has been reported, thus considering OLP as a potential premalignant condition. The etiopathogenesis is still not completely understood: genetic (HLA-DR2), immunologic (T cell-mediated) and infectious (association with viral hepatitis C, differences in oral microbiota in OLP, and bacteria internalization into infiltrating T cells and oral epithelial cells) are considered the main predisposing or provoking factors. Management is based on the severity of the lesions; topical steroids are the first-line therapy and oral glucocorticoids are used for severe erosive lesions.

To the Editor,

Lichen planus (LP) is a benign mucocutaneous inflammatory disease of unknown origin. The skin and mucous membranes are the most frequently involved areas, and rarely LP can be localized on the scalp and nails. Among the mucous membranes, oral mucosa is the most frequently affected; Oral lichen planus (OLP). In some instances, the oral manifestations may be the exclusive expression of the disease, and can involve a single or several oral areas, either concomitantly or sequentially. OLP was clinically first described by Wilson in 1869 (1) as a chronic mucocutaneous illness and was documented histologically by Dubreuilh in 1906 (2).

Epidemiology

The Incidence of LP is estimated to be between 0.1-0.8% of the general population (3). OLP is associated with skin lesions in 60-70% of cases but can occur as the only manifestation of the disease in 15-25% of patients (4). LP is more common among the female population, with 60-75% of OLP patients being female. The mean age at diagnosis is between 50 and 60 years (5).

Etiopathogenesis

Several predisposing or provoking factors have been considered, including genetic, infectious and immunologic factors.

Genetic factors

Associations with HLA-DR1, DRB10101, and DQ1 have been proven in association with LP, but no such associations have been detected in OLP

Key words: Lichen planus, bullous vesicles, squamous-cell-carcinoma, oral diseases, oral mucosa

Mailing address:
Prof. Luca Giannetti,
U.O.C. Odontoiatria e Chirurgia Oro-Maxillo-Facciale,
Università degli Studi di Modena e Reggio Emilia,
Via del Pozzo, 71, 41124 Modena, Italy
Tel.: +39 059 422 4325
e-mail: luca.giannetti@unimore.it

0393-974X (2018)

(6). However, in a study performed on a Jewish population affected by erosive OLP, a significant association with HLA-DR2 and its variant alleles was demonstrated (7).

PATHOGENESIS

Hepatitis C virus

Polymerase chain reaction (PCR) has detected the presence of Hepatitis C Virus (HCV) RNA in a significant number of OLP patients in studies performed on both Japanese and Mediterranean populations (8). This HCV is associated with HLA-DR6.

Bacteria; microbioma

Oral microbial communities are distinct from those of other barrier sites and are among the most diverse in terms of community membership. The dominant phyla detected in oral mucosa are firmicutes, proteobacteria, actinobacteria and bacterioidetes. At the species level, over 600 prevalent taxa have been demonstrated in oral mucosa. Analyses of the mucosal microbiota from OLP patients revealed a decrease in Streptococcus and an increase in gingivitis/periodontitis-associated bacteria within the OLP lesions (9). At the genus level, fusobacterium, leptotrichia, and lautropia were found to be in abundance in OLP patients compared to healthy subjects. Few differences have been found between erosive and non-erosive OLP. Bacteria are abundant throughout the epithelium and lamina propria of OLP tissue, which exhibits positive correlations with the levels of infiltrated CD3+, CD4+, and CD8+ cells. Furthermore, bacteria are detected within the infiltrated T cells; some are internalized into epithelial cells or T cells and induce the production of T-cell chemokines CXLCL10 and CCL5. Therefore, intracellular bacteria could trigger T-cell infiltration and provide target antigens, playing a potential role in the pathogenesis of OLP (10).

Contact allergens

The role of a variety of metals (mercury, copper and gold) has been described in the exacerbation or induction of OLP (local lichenoid reaction), examples of which include exposure to metallic dental restorations or constructions. Positive patch test results and the eventual regression or complete clearing of OLP symptoms after removal of the sensitizing metal, and eventual replacement with other materials have been reported (11).

Immunologic factors

Structurally, the oral mucosa possesses a stratified squamous epithelium; the lamina propria underlying the epithelium is composed of loose connective tissue, which contains blood and lymphatic vessels. The oral mucosa forms a mechanical barrier, which is thicker and denser than gastrointestinal mucosa. From an immunological point of view, oral mucosa is considered to be a specialized part of mucosal-associated lymphoid tissue (MALT).

The oral mucosa exploits various mechanisms to protect the host against invading pathogens. The lamina propria provides resistance to tear and compression forces, thus maintaining tissue integrity; protection from microorganisms is also afforded by cell shedding from the surface layer, therefore minimizing colonization. Furthermore, salivary secretion aids in keeping the oral mucosa moist and limiting excessive bacterial accumulation. In addition, the oral mucosa contains an elaborate immune system which is thought to be pro-tolerogenic in nature as the oral mucosa remains in a relative state of health despite the heavy microbial load (12). Moreover, an inflammatory infiltrate composed mainly of lymphocytes and neutrophils can be regularly detected in the gingiva, even in those considered clinically healthy. In human normal oral mucosa, the majority of dendric cells (DCs) is represented by Langerhans cells (LCs) namely found in the vestibulum, buccal, palate and lingual tissues (13).

There is growing evidence that T cell-mediated immunity plays a fundamental role in the pathogenesis of LP and OLP, and that damaged basal keratinocytes express altered self-antigens on their surface. In the induction phase, DC present self-peptide modified by exogenous antigens (viruses, medications, and contact allergens) to antigen-specific naïve T cells in the lymph nodes; the latter differentiate into effector T cells. In the evolution phase, effector T cells migrate into the inflammatory

site and are activated, releasing proinflammatory cytokines and cytotoxic molecules, causing epidermal injury.

OLP is characterized by massive lymphocyte infiltration in the lamina propria and results in an abnormal epithelial keratinization cycle and the destruction of the epithelium basal layer. It has been shown that Th1 and Th2 cells contribute to inflammation and mucosa lesion formation (14). Proinflammatory cytokines, including IL-6, IL-17 and TNF-alpha are increased in the serum and saliva of OLP patients (15). On the contrary, TGF-beta and IL-10 are decreased in the sera of OLP patients. Interestingly, lower serum IL-10 levels have been correlated with IL-10 polymorphisms in a Chinese population. Activated LCs/DCs infiltrate OLP and suggest their involvement in disease progression. Besides myeloid (mDCs), plasmacytoid dendritic cells (pDs) were observed in OLP; they secrete IFN-alpha and contain granzyme B, facilitating DC maturation. pDs are accumulated in the submucosa and co-localized with lymphocytes. Such cellular organization might allow the ongoing presentation of self antigen to T cells to facilitate tissue destruction.

Clinical features

Andreasen (16) described six clinical forms of LP:

i) the reticular form, consisting of lace-like keratotic lesions, is the most common and characteristic form of LP. It predominantly affects the buccal mucosa (Fig. 1), near the last molars, but also the tongue, gums, palate, and lips. Clinically, it manifests with a whitish reticulated network, described as "fern leaf", symmetric in distribution. Lesions of the dorsum of the tongue (Fig. 2) tend to be subtle. Gingival involvement is common with typical aspects of chronic desquamative gingivitis. This form is usually asymptomatic;
ii) the plaque form appears as slightly raised, white solitary lesions, with higher incidence amongst tobacco smokers;
iii) the papular form is characterized by slightly elevated white lesions, approximatively 0.5-1.0 mm in diameter;
iv) the atrophic form combining erythema plus reticular keratosis, is a controversial entity, difficult to differentiate from leukoplakia in case of unilaterality. A biopsy is mandatory in such cases;
v) the bullae and vesicles are rarely found in the oral cavity because it is a trauma-intense environment;
vi) the erosive form (Fig. 3) is characterized by areas, more or less extensive, of ulcerated mucosa; the lesions are often bleeding, burning, and painful, especially with the ingestion of hot or spicy foods.

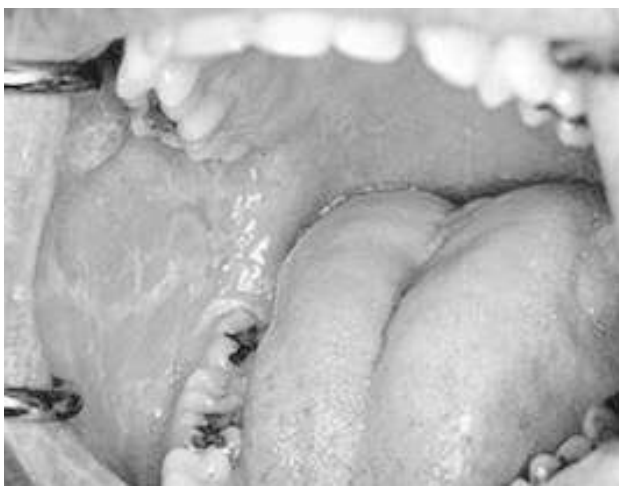

Fig. 1. *Lesions of buccal mucosa.*

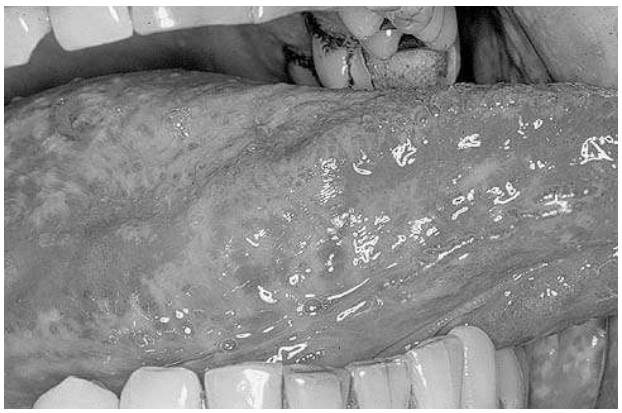

Fig. 2. *Lesion of the dorsum of the tongue.*

Associations

OLP has been significantly associated with the erosive form of LP, along with chronic liver disease, particularly due to HCV infection, as reported in meta-analyses researches. Some authors

found that HCV-seropositive was five times more frequently found in LP patients as compared to control populations, and that LP was 2.5 to 4.5 times more likely to develop in HCV-seropositive patients. Moreover, associations of LP (including OLP) with other diseases of similar immune origin, such as alopecia areata, vitiligo, inflammatory bowel disease, myasthenia gravis, and thymoma have been reported (17). The etiology of OLP (18) is unclear; however, we found a positive and statistically significant correlation between OLP and thyroid disease. From this, we can assume that thyroid disease may be involved in the pathogenesis of OLP, or that OLP is a clinical manifestation of thyroid disease.

Histopathology

Despite different clinical manifestations, the histopathology of LP is fairly uniform. The primary features are hyperkeratosis, focal increases in the granular cell layer, irregular acanthosis with a "saw tooth" appearance, liquefactive degeneration of the basal layer, and a band-like lymphocytic infiltrate at the dermo-epidermal junction. Colloid bodies representing apoptotic or dyskeratotic keratinocytes are usually present in the lower levels of the epidermis and the superficial dermis.

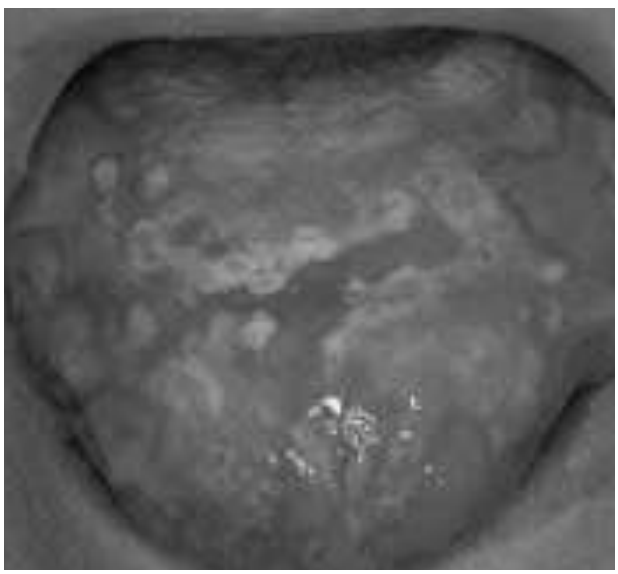

Fig. 3. *Erosive form of the tongue.*

Vacuolar changes within the basal cell layer may become confluent and result in small separations between the epidermis and the dermis. In OLP, lesions often show parakeratosis rather than hyperkeratosis, and the epidermis frequently becomes atrophic.

Course

Mucosal lesions have a chronic evolution both in the leukokeratotic form and, especially, in the erosive form. The chronicity is related to a poor therapeutic response and to an often associated immune disorder or chronic liver disease.

OLP is generally considered a potentially premalignant condition; a 1% incidence of squamous-cell carcinoma has been reported among patients with this condition in both retrospective and prospective cohort studies. However, the true risk remains controversial (18).

TREATMENT

Reticular OLP is usually asymptomatic and does not require treatment. For erosive OLP, the treatment goal is to heal erosive lesions and to lessen pain and the associated difficulty in eating and drinking (19,20).

Corticosteroids

Topical steroids are the first-line therapy. In two randomized, placebo-controlled trials, (one with fluocinonide and the other with betamethasone valerate) the rate of cure or attenuation were significantly higher in the active-treatment group.

Oral corticoids are used for erosive lesions that do not respond to topical corticoids.

Retinoids

Topical retinoids are used as first-line treatment in papular and plaque-like OLP; however, they are less effective than topical steroids.

Miscellanea

Systemic drugs, such as griseofulvin, dapsone, hydroxychloroquine, thalidomide, and levamisole have been used with modest results.

REFERENCES

1. Wilson E. Oral lichen planus. J Cutaneous Med Dis Skin. 1869; 3:117-32.
2. Dubreuilh W. Histologie du lichen plan des muqeuses. Ann Dermatol Venereol1906; 7:123-26.
3. Mc Cartan BE, Healy CM. The reported prevalence of oral lichen planus: a review and critique. J Oral Pathol Med 2008; 37:337-53.
4. Carbone M, Arduino PG, Carrozzo M, et al. Course of oral lichen planus: a retrospective study of 808 northern Italian patients. Oral Dis 2009; 15:235-43.
5. Bernejo-Fenoll A, Sanchez-Siles M, Lopez-Jornet P, Bamacho Alonso F, Salazar-Sabchez N. A retrospective clinic-pathological study of 550 patients with oral lichen planus in south-eastern Spain. J Oral Pathol Med 2010; 39:4919-6.
6. La Nasa G, Cottoni F, Mulargia G, et al. HLA antigen distribution in different clinical subgroups demonstrates genetic heterogeneity in lichen planus. Br J Derm 1995; 132:897-900.
7. Roitberg-Tambur A, Friedmann A, Korn S, Markitziu A, Pisanti S, Safirman C, Nelkon D, Brauthar D. Serologic and molecular analysis of the HLA system in Israel Jewish patients with oral erosive lichen planus. Tissue Antigens 1994; 43:219-23
8. Rebora A, Rongioletti F, Canepa A. Chronic active hepatitis and lichen planus. Acta Derm Venereol 1982; 62:351-52.
9. Choi Y C, Kim Y, Yoon H-J, Baek KJ, Alan J, Park HK, Choi Y. The presence of bacteria within tissue provide insights into the pathogenesis of oral lichen planus. Sci Rep 2016; 6:29186.
10. He Y, Gong D, Shi C, Shao F, Shi J, Fei J. Dysbiosis of oral buccal mucosa microbiota in patients with oral lichen planus. Oral Dis 2017; 23(5):674-82.
11. Laine J, Kalimo K, Happonen RP. Contact allergy to dental restorative materials in patients with oral lichenoid lesions. Contact Dermatitis 1997; 36:141-46.
12. Moutsopoulos NM, Konkel JE. Tissue-specific immunity and the oral mucosal barrier. Trends in Immunology 2017; S1471-4906(17). 301697-2.
13. Hovav A-H. Dendritic cells of the oral mucosa. Immunology 2014; 7:27-36.
14. Scully C, Carrozzo M. Oral mucosal disease: lichen planus. Br J Oral Maxillofac Surg 2008; 46(1):15-21.
15. Bai J, Jiang L, Lin M, et al. Association of polymorphisms in the TNF-alfa and IL-10 genes with OLP: a study in a Chinese cohort with Han ethnicity .J Interferon Cytokine Res 2009; 29(7):381-88.
16. Andreasen JO. Oral lichen planus: 1. A clinical evaluation of 115 cases. Oral Surg Oral Med Oral Pathol 1968; 25:31-42.
17. Le Cleach L, Chosidow O. Lichen planus. N Engl J Med 2012; 366; 8: 723-32.
18. The association of thyroid disease and oral lichen planus: a literature review and meta-analysis. Li D, Li J, Li C, Chen Q, Hua H Front Endocrinol (Lausanne). 2017; 8:310.
19. Rajentheran R, McLean NR, Kelly CG, Reed MF, Nolan A. Malignant transformation of oral lichen planus. E J Surg Oncology 1999; 25:520-23.
20. García-Pola MJ, González-Álvarez L, Garcia-Martin JM. Treatment of oral lichen planus. Systematic review and therapeutic guide. Med Clin (Barc) 2017; 149(8):351-62.

LETTER TO THE EDITOR

COMPARISON OF CORONAL LEAKAGE OF DIFFERENT ROOT CANAL FILLING TECHNIQUES: AN *EX VIVO* STUDY

A. LIBONATI[1], V. DI TARANTO[2], C. D'AGOSTINI[3,4], M.M. SANTORO[3], D. DI CARLO[3], D. OMBRES[4], G. GALLUSI[2], C. FAVALLI[1,3,4], G. MARZO[5] and V. CAMPANELLA[2]

[1]Department of Surgical Sciences, Dental School, Catholic University of Our Lady of Good Counsel of Tirane, Tirane, Albania; [2]Department of Clinical Sciences and Translational Medicine, Dental School, University of Rome "Tor Vergata", Rome, Italy; [3]Department of Experimental Medicine and Surgery, University of Rome "Tor Vergata", Rome, Italy; [4]Laboratory of Clinical Microbiology and Virology, University Hospital of Rome "Tor Vergata", Rome, Italy; [5]Department of Life, Health and Environmental Sciences, Dental School, University of L'Aquila, L'Aquila, Italy

Received October 6, 2017 – Accepted February 5, 2018

The aim of this study was to compare the quality of the coronal seal, using an *in vitro* bacterial invasion test, of three different root canal filling systems. Twenty-seven freshly extracted mandibular premolars were selected and divided into three experimental groups (G1, G2 and G3 n=7) and two control groups (Ct+ and Ct- n=3). All teeth in the experimental groups were prepared using NiTi Mtwo rotating instruments and then the endodontic treatments were completed using the three-tested warm guttapercha root filling techniques: Microseal (G1), Thermafil (G2) and System B (G3). All root filling techniques were performed using the same endodontic sealer (Pulp Canal Sealer). Three teeth were instrumented and not filled, serving as positive controls (Ct+) and the last three teeth, with intact crowns and no endodontic treatment, served as negative controls (Ct-). All samples were mounted in a two-chamber apparatus and exposed to *Enterococcus faecalis* performing a bacterial infiltration test. All samples were observed for a maximum period of 60 days checking for turbidity of the BHI broth on a daily basis recording when contamination occurred. A quantitative evaluation of the bacterial CFU/ml was performed using the URO-QUICK™ system. On day 32 an overall value was recorded of contamination of 42.85% for group G1, 71.42% for G2 and 42.85% for G3; after 60 days, the final contamination result was 85.71% for group G1, and 100% for both G2 and G3 groups. Considering the number of contaminated samples at the end of the observation period, the three techniques showed no statistically significant differences. The study highlighted the bacterial permeability of gutta-percha/seal barrier, underlining the importance of an effective coronal restoration to ensure a durable seal after root canal treatment.

To the Editor,

In literature, there are many *in vitro* studies that tested coronal infiltration of root filling materials. The most common test for infiltration is dye penetration however, since this largely used method gave a great variability of results in similar studies its clinical relevance has been questioned (1). Different test strategies present in literature are positive pressure

Key words: biocompatibility, zoe sealer, guttapercha, filling method, leakage, bacteria

Mailing address:
Prof. Vincenzo Campanella,
Department of Clinical Sciences and Translational Medicine,
Dental School, University of Rome "Tor Vergata",
Via Montpellier, 1 - 00133 Rome, Italy
Tel.: +39 0620900396
e-mail: vincenzo.campanella@uniroma2.it

0393-974X (2018)

fluid filtration, electro-chemical infiltration and dye infiltration in a vacuum-sealed system (2). All these kinds of tests were also questioned as they foresee the forced passage of a fluid. In order to better simulate what happens clinically, other testing techniques used penetration of bacterial toxins (3, 4) or human saliva (5). Our test design is based on bacterial infiltration since, even if not exempt from criticism, it seems to be the closest to clinical evidence (3).

There is a wide range of bacteria found to be responsible for secondary infection (6) of endodontically treated teeth (*Actinomyces*, *Enterococcus*, *Propionibacterium*) (6), (*Streptococcus*, *Stafilococcus*, *Peptostreptococcus*, *Lactobacillus* and *Eubacterium*) (6, 7), but one of the most commonly found is *Enterococcus faecalis* (6, 8) and for this reason we selected it for our infiltration test.

Our null hypothesis is that there is no difference in the coronal sealing abilities of three different root warm guttapercha canal filling techniques. This study compares the coronal seal of three currently-used root canal filling techniques [Microseal (9), Thermafil (10) and System B (11)] using a bacterial invasion *ex vivo* test. The test simulates a situation in which, as a consequence of a correctly performed endodontic therapy, the tooth is left without a coronal restoration, and is therefore subject to a continuous bacterial infection from the oral cavity (12).

MATERIALS AND METHODS

Sample selection

Twenty-seven freshly extracted human, single rooted, mandibular premolars were selected for the study. All teeth received a mesio-distal and bucco-lingual X-ray projection, in order to control the endodontic anatomy and exclude presence of multiple canals or complexities. Twenty-four of the selected teeth were sectioned to remove the crown and expose the canal leaving root portions of 15 mm in length. The remaining three samples were left intact to be used as negative control.

Tooth preparation

The patency of each canal was confirmed using a size 10 K-file (Dentsply/Maillefer, Baillaigues, Switzerland) to the length of the root apex and Working Length (WL) was stated as 0.5 mm shorter. Each tooth was instrumented with the Mtwo technique (Sweden and Martina, Italy) (basic sequence: 10.04/ 15.05/ 20.06/ 25.06 and/or 25.07 for System B samples) irrigating the canal between each file with 5% NaOCL (Niclor Ogna, Italy) and 10% EDTA (Tubuliclean Ogna, Italy). The preparation was completed with manual instruments (K-file 30 to working length, 35 to 0.5 mm from the foramen and 40 to 1 mm), used for the finishing of the apical zone. After instrumentation, a final prolonged irrigation with NaOCL and EDTA was performed to remove the smear layer; canals were rinsed with saline, and stored in sterile glass test-tubes containing the same solution.

Before mounting the samples into the test chambers, in order to remove any bacteria or contaminants, every tooth was singularly sterilized in autoclave (134°C, 1 h to 2 atm) (13).

Root canal filling techniques

The instrumented teeth were randomly divided into three experimental groups of 7 teeth each. The three groups were treated with three different root canal filling techniques:

- Group 1 (G1): Microseal
- Group 2 (G2): Thermafil
- Group 3 (G3): System B

All filling techniques were performed operating in a sterile environment (work station, instruments and sterile gloves), under a hood and using the same endodontic ZOE-sealer: Pulp Canal Sealer (PCS) (Kerr Italia spa, Italy).

Group 1- Microseal

A master cone size 40 taper 02 was inserted into the canal 1 mm shorter than working length (WL) and checked for appropriate tug back. After a last rinse, the canal was dried with sterile paper points, the PCS was placed to WL with the tip of a paper point and the master cone was placed at the desired length. A mounted engine spreader (taper 04 size 25 length 25 mm, SybronEndo, California, USA) was used at 300 rpm to condense the guttapercha up to 2 mm shorter than WL. The root filling was then completed using a NiTi obturation instrument (PacMac taper 04 size 25 length 25 mm, SybronEndo, CA, USA) in three takes to fill the canal with warm guttapercha (Microseal Guttapercha, SybronEndo, CA, USA) at a 6,000 rpm. Between each one

of the three filling phases the engine spreader was used still as a vertical condenser (9).

After completion of the root filling, mesio-distal and bucco-lingual X-ray projections were taken, in order to control the root filling homogeneity, and to check for the presence of visible gaps or voids.

In order to let the PCS set completely, each completed sample was stored in a sterile test-tube, wrapped in sterile gauze soaked in physiological solution for 7 days prior to proceeding with the experimental test.

Group 2- Thermafil

Having verified the correct fitting, a Thermafil Obturator measure 35 was selected (Dentsply, Bellaigues, Switzerland). After a last rinse, the canal was dried with sterile paper points and the PCS was placed to WL with the tip of a paper point. Then the heated Obturator was placed approximately 0.5 mm shorter of the WL using a firm apical pressure and the carrier was cut with a diamond bur flush with the access cavity of the canal completing the root canal filling (10).

Mesio-distal and bucco-lingual X-ray projections were taken, in order to control the root filling homogeneity, and to check for the presence of visible gaps or voids.

In order to let the PCS set completely, each completed sample was stored in a sterile test-tube, wrapped in sterile gauze soaked in physiological solution for 7 days prior to proceeding with the experimental test.

Group 3- System B

All tooth samples were instrumented as in group 1 and 2 with the only difference of using an Mtwo 25.07 as the last shaping instrument. For the root filling using System B 25.06 MtwoGutta guttapercha points (Sweden and Martina, Italy) cut with a gauge to a tip diameter of 35 were used. After a last rinse, the canal was dried with sterile paper points, the PCS was placed to working length with the tip of a paper point and the master cone was placed at the desired length.

For the continuous wave of condensation, the System B "B-Plugger" (50.04) was set 4 mm short of the working length and heated up to 300°C to fill the apical third of the root canal with warm gutta-percha and PCS (11).

For back-packing an Obtura II injectable plasticized gutta-percha syringe (Obtura Spartan Corporation, CA, USA) was used and then vertically compacted with Schilder's standard pluggers.

Mesio-distal and bucco-lingual X-ray projections were taken, in order to control the root filling homogeneity, and to check for the presence of visible gaps or voids.

In order to let the PCS set completely, each completed sample was stored in a sterile test-tube, wrapped in sterile gauze soaked in physiological solution for 7 days prior to proceeding with the experimental test.

Positive Controls (Ct+)

Three samples were instrumented without performing any root canal filling and leaving the canal empty.

Negative Controls (Ct-)

Three elements with intact crowns were used as negative controls. The cusps were cut with a diamond bur; the structure of the dental elements and the integrity of the pulp chamber were maintained. Two coats of nail varnish were applied to the external surface and on apical foramen.

Microbial leakage apparatus

The apparatus used to evaluate bacterial leakage consisted of an upper chamber and a lower chamber (Fig. 1). The upper chamber was formed by a glass pipe, obtained by a vial of anaesthetic emptied of its content, and the coronal portion of the sample was the deep end. The lower chamber was constituted by a Teflon container, obtained by a diffuser, in which the root was lodged, and it had an exhaust valve. The two chambers were assembled through wax and cold-polymerization resin, in order to obtain a hermetic system and to prevent any external access.

The external surface of the bottom of the upper chamber was sand-blasted and the coronal surface was etched. The cyanocrylate (SuperAttak®) was applied on the glass surface to foster the bond with the composite, and it was also applied on dental surfaces. A mass of dental composite was used to connect the dental element to the bottom of the upper chamber, being careful not to ruin the center of the root canal in the diameter of the cylinder in glass, and to avoid the exposure of the composite inside the chamber. Two coats of nail varnish were applied on the surface of glass-composite interface, one on the composite and one on the root surface, with the exception of the last three apical millimeters. In this

way, the whole system was isolated except for the portion that was interesting for the study. The upper chamber, in contact with the coronal portion of the filled sample, operates as reservoir of a bacteria stock of *Enterococcus faecalis* (ATCC 29912). In accordance with this intention, a protocol of cold-sterilization was set (without altering the thermoplastic characteristics of the materials), that needed detergents and disinfectants (Table I) for pre-arranged times. The lower chamber was instead sterile, because it was simply pulled out of its packing, and therefore there were less steps. The medium culture used during the tests was the Brain Heart Infusion (BHI) and its initial concentration with *Enterococcus faecalis* was 1.5 McFarland. Keeping the environment sterile, the upper chamber was contaminated under an extractor hood with medium culture (1 ml) and the lower chamber with sterile medium culture (3 ml).

Table I. *Disinfection and sterilization protocol of the test apparatus.*

UPPER CHAMBER	
Sterilization solution	**Time**
Sodium Hypochlorite 5%	20’
Pera-Safe surfactant diluted to the concentration of 16.2 g/l	20’
Alcoholic Neoxinal® (chlorhexidine gluconate 0.5% ethyl alcohol 70%)	20’
Physiological saline	20’
LOWER CHAMBER	
Sterilization solution	**Time**
Sodium Hypochlorite 5%	1h
Physiological saline	30’

The samples were incubated in oven at about 37°C, for a period of observation of 60 days. To guarantee the vitality of the bacterial stock, keeping a constant temperature, every 4 days the renovation (refresh) of the contaminated sample in the upper chamber was performed. The test of the coronal bacterial infiltration is constituted by the appearance of turbidity in the medium culture in the lower chamber. When the microorganisms succeed in reaching the apex of the dental elements, migrating in crown-apical sense through the filled root canal, they determine the alteration of the transparency of the BHI, that will appear turbid, manifesting the presence of bacterial deposits, and underlining therefore the contamination and the alteration of the apical seal.

Microbial count

The use of traditional culturing methods in the evaluation of microbial counts is more intensive, because it is not possible to use blood-culturing systems. The URO-QUICK™ system is the mean through which microbial growth is studied in fluid samples (14).

The URO-QUICK™ system is used widely for bacteriuria-screening in urine samples and other liquid samples, such as pleural liquid, bronchus lavages, cerebrospinal fluid (as long as they are limpid), with the aim of verifying the presence of bacterial count.

Statistical analysis

All the analyses were performed using the statistical open source environment R (version 3.4.1).

Probability and time of coronal infiltration

To estimate the time and probability of coronal infiltration Kaplan-Meier curves were used. Curves were stratified according to the three different techniques (Microseal, Thermafil and System B) and they were compared by using the long-rank test. Curves were also compared by pairwise tests, adjusting p-values by Benjamini-Hockberg correction (15).

Correlation between levels of contamination and time of experiencing coronal infiltration

The levels of contamination at the moment of the

event of coronal infiltration were compared between the three different techniques by using Kruskal-Wallis test. Pairwise tests were also performed by using Mann-Whitney test, adjusting p-values by Benjamini-Hockberg correction. Spearman's rank correlation test was performed to detect potential statistical correlation between the levels of contamination and the time of experiencing coronal infiltration. Analysis of correlation was stratified according to the three different techniques.

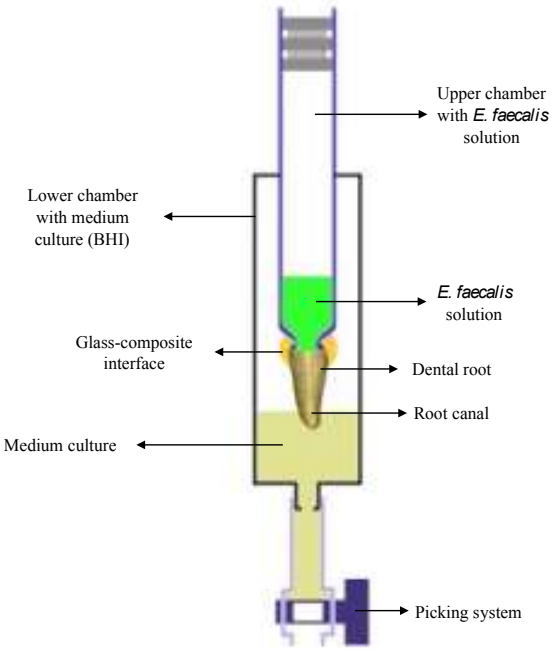

Fig. 1. *Experimental apparatus diagram for bacterial infiltration test.*

RESULTS

The samples were observed for a period of 60 days, during which, as previously described, the renovation of the contaminated medium culture was performed every 4 days. In Table II it is possible to see the results of the experimentation.

During the period of study, 100% of the negative controls did not show signs of contamination; after 24 hours, the BHI of the positive controls showed formation of bacterial deposits, a clear sign of the coronal infiltration.

The first positive (T7) samples were observed on the sixteenth day. The other samples showed positive results on the twenty-fourth and sixtieth days, with the exception of one element (M5) belonging to Group 1 (Microseal), that did not show signs of contamination during the period of observation.

Taking as a reference the periods of observation at days 32 and 60, it is possible to affirm that on the 32nd day the samples of G1 were 42.85% contaminated, the samples of G2 were 71.42% contaminated and

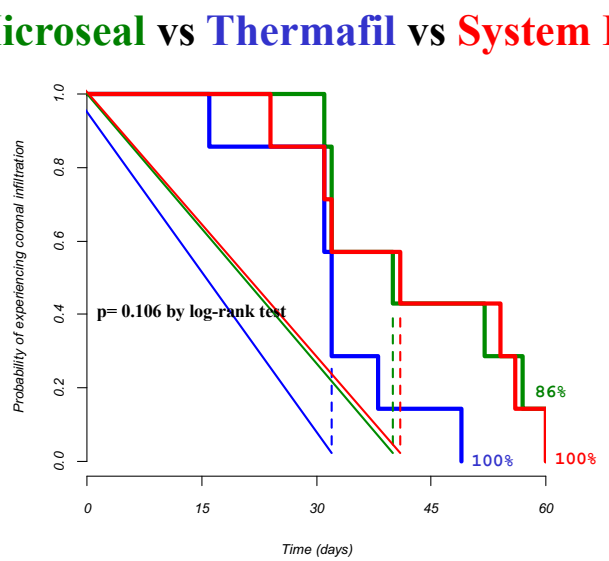

Fig. 2. *Bacterial infiltration curves based on observation time.*

Table II. *Bacterial infiltration test results.*

		Group																										
		G1							G2							G3							Ct+			Ct-		
		M1	M2	M3	M4	M5	M6	M7	T1	T2	T3	T4	T5	T6	T7	S1	S2	S3	S4	S5	S6	S7	+1	+2	+3	-1	-2	-3
Time	1	-	-	-	-	-	-	-	-	-	-	-	-	-	-	-	-	-	-	-	-	-	+	+	+	-	-	-
	16	-	-	-	-	-	-	-	-	-	-	-	-	-	+	-	-	-	-	-	-	-				-	-	-
	24	-	-	-	-	-	-	-	-	-	-	-	-	-		-	+	-	-	-	-	-				-	-	-
	31	-	+	-	-	-	-	-	-	+	-	-	-	+		-		-	-	-	-	+				-	-	-
	32	+		+	-	-	-	-	+		-	-	+			-		-	-	-	+					-	-	-
	38				-	-	-	-			-	+				-		-	-	-						-	-	-
	40				-	-	-	+			-					-		-	-	-						-	-	-
	41				-	-	-				-					-		-	+	-						-	-	-
	49				-	-	-				+					-		-		-						-	-	-
	52				+	-	-									-		-		-						-	-	-
	54					-	-									-		-		+						-	-	-
	56					-	-									-		+								-	-	-
	57					-	+									-										-	-	-
	60					-										+										-	-	-

Table III. *Results of bacterial counts with URO-QUICK™.*

G1			G2			G3		
Sample	*Day*	*CFU/ml*	*Sample*	*Day*	*CFU/ml*	*Sample*	*Day*	*CFU/ml*
M1	32	~1,000	T1	32	~10,000	S1	60	20,000
M2	31	~1,000	T2	31	~10,000	S2	24	<1,000
M3	32	~1,000	T3	49	50,000	S3	56	15,000
M4	52	<10,000	T4	38	20,000	S4	41	~5,000
M5	-	-	T5	32	~10,000	S5	54	15,000
M6	57	10,000	T6	31	~10,000	S6	32	1,000
M7	40	5,000	T7	16	5,000	S7	31	1,000

the samples of G3 were 42.85% contaminated, while on the 60th day 85.71% of G1 was contaminated, and both G2 and G3 were 100% contaminated.

Once verified the contamination, the BHI of each element was taken and injected into the URO-QUICK™ test-tube, in order to obtain the microbial count.

In the first group (G1), at day 31, the BHI of the element M2 showed approximately 1,000 CFU/ml; at day 32, the sample M1 showed approximately 1,000 CFU/ml, like M3; at day 40, the sample M7 showed 5,000 CFU/ml; at day 52, the M4 specimen showed less than 10,000 CFU/ml; in the end, at day 57, the M6 specimen showed 10,000 CFU/ml.

With regard to the second group (G2), the first contamination was already present at day 16 for the T7 specimen; then, examining the medium culture with the URO-QUICK™ system, it resulted contaminated by 5,000 CFU/ml. At day 31, samples T2 and T6 resulted positive with an approximate presence of 10,000 CFU/ml. At day 32, samples T1 and T5 resulted positive with an approximate presence of 10,000 CFU/ml; at day 38, sample T4 showed a microbial count of 20,000 CFU/ml; in the end, at day 49, the element T3 showed 50,000 CFU/ml.

In the third group (G3), at day 24, the sample S2 showed less than 1,000 CFU/ml; at day 31, the sample S7 showed 1,000 CFU/ml. At day 32, the sample S6 showed also 1,000 CFU/ml. At day 41, the S4 the contamination was around 5,000 CFU/ml. At day 54, the sample S5 showed 15,000 CFU/ml; at day 56, also the sample S3 showed 15,000 CFU/ml. In the end, at day 60, the sample S1 resulted contaminated by 20,000 CFU/ml (Table III).

Probability and time of coronal infiltration

Overall, the median [95% Confidential Interval, 95% CI] time of achieving coronal infiltration after inoculation was 32 [32-54] days. By 60 days after contamination, the overall probability of coronal infiltration was 95%, corresponding to a total number of 20 events. Samples treated with Microseal technique showed the lowest probability of coronal infiltration, even though without any statistical significance, probably due to the low number of samples analyzed (Microseal: 86%; Thermafil: 100%; System B: 100%) (p=0.106) (Fig. 2). By comparing curves with pairwise tests, there were no significant differences according to time and probability of experiencing coronal infiltration between Microseal and System B (p=0.683), while a trend toward statistical significance was observed by comparing Thermafil and System B (p=0.105) and Thermafil and Microseal (p=0.058).

Correlation between levels of contamination and time of experiencing coronal infiltration

At the time of coronal infiltration, the level of contamination was higher in samples treated with Thermafil technique (median [95% CI] of contamination, Microseal: 3,000 [1,000-8,750]; Thermafil: 10,000 [10,000-15,000]; System B: 5,000 [1,000-15,000]; p=0.119). The main differences between techniques according to levels of contamination were observed by comparing with pairwise tests Microseal and Thermafil (p=0.102).

A strong correlation between time of experiencing coronal infiltration and levels of contamination was observed in all the three techniques (Microseal: rho=0.939, p=0.005; Thermafil: rho=0.923, p=0.003; System B: rho=0.954, p=0.001).

DISCUSSION

In our study, it was possible to observe how a treated element in more than one month, deprived of suitable post-endodontic restoration, can be subject to bacterial contamination, and therefore subject to failure. This was observed especially in the specimens filled with the Thermafil technique, in comparison with the Microseal and System B groups. Thermafil was the subject of many studies in relationship with the sealing ability through the canal walls and the root apex. A contact was frequently observed between the carrier and the walls in the middle third and in the cervical third, and an asymmetrical distribution of the different components in the apical third. The carrier, in certain circumstances, results without gutta-percha and deprived of endodontic seal (16). Micalizzi et al. (17) studied the results of fillings effected with the Thermafil system: in this study, examined by SEM, there is a crack between the dentinal walls and the filling material. A probable cause can be the contraction of the gutta-percha during the phase of cooling. This could be the reason why the roots filled with Thermafil were the first ones to result positive to the bacterial infiltration *in vitro*. In our study, less than half of the filled roots through the Microseal (9) and System B techniques (11) resulted positive after a period of observation of 32 days, therefore showing that the techniques are more efficient over time. Moreover, it is worth noticing that, after one month, the same number of elements of G1 and G3 was contaminated; both the techniques of filling in gutta-percha behaved in the same way. At the end of the period of observation (60 days), the results obtained by our study agree with the study of Yucel (18) for the System B and Thermafil techniques, according to which the examined techniques of filling introduce the contamination on the sixtieth day of control (18). Nevertheless, in our case, at the end of the 60th day, an element (M5) of Group 1, filled with Microseal technique, did not show positive results, underlining a better behavior. However, it is not possible to reproduce *in vitro* the complex peri-apical system. In fact, the study of the seal of the endodontic filling materials, even when conducted with a microbiologic method, essentially consists in a test of hydraulic seal.

In the tests of microbiologic infiltration, it is possible to propose the various bacterial species implicated in the endodontic relapses (13) and their growth conditions. The clinical answer to the treatment with gutta-percha is not reproducible *in vitro* because it depends on the biological answer of the peri-apical complex. According to this study, it is possible to outline basic guidelines for the success of the endodontic treatment, as a correct three-dimensional filling in gutta-percha and a good apical seal, underlined by a good behavior of the techniques of filling, in which the control and the adaptation of the gutta-percha/seal system in the apical zone is guaranteed by the application of a hydraulic pressure in the compacting phase.

Therefore, we can conclude that during the period of study, 100% of the negative controls did not show signs of contamination; after 24 hours from the bacteria infiltration, the BHI of the positive controls showed formation of bacterial deposits, a clear sign of the coronal-apical infiltration.

After 60 days all the elements, except one (M5), showed positive results. Considering therefore the number of contaminated samples at the end of the period of observation, the three techniques did not show meaningful differences in the long period. However, it is necessary to underline that the roots filled with Thermafil showed bacterial contamination after a shorter period in comparison to the roots treated with the two other techniques. In fact, the elements filled with Thermafil all resulted positive on the 49th day. Microseal and System B therefore showed a great resistance, in terms of time, to the bacterial infiltration in comparison to the Thermafil (Microseal is more involved in terms of resistance to the bacterial infiltration). Further studies on a larger sample size should be performed to confirm these findings.

Our study also underlines the bacterial permeability of the barrier guttapercha/seal over a period of 60 days, despite the techniques used, confirming the necessity of a coronal restoration to protect the filled endodontic system.

REFERENCES

1. Wu MK, Wesselink PR. Endodontic leakage studies reconsidered. Part I. Methodology, application and relevance. Int Endod J 1993; 26(1):37-43.
2. Karagenç B, Gençoglu N, Ersoy M, Cansever G, Külekçi G. A comparison of four different microleakage tests for assessment of leakage of root canal fillings. Oral Surg Oral Med Oral Pathol Oral Radiol Endod 2006; 102(1):110-12.
3. De Deus G, Murad CF, Reis CM, Gurgel-Filho E, Coutinho Filho T. Analysis of the sealing ability of different obturation techniques in oval-shaped canals: a study using a bacterial leakage model. Braz Oral Res 2006; 20(1):64-69.
4. Torabinejad M, Ung B, Kettering JD. In vitro bacterial penetration of coronally unsealed endodontically treated teeth. J Endod 1990; 16(12):566-69.
5. De Deus G, Audi C, Murad C, Fidel S, Fidel RA. Sealing ability of oval-shaped canals filled using the System B heat source with either gutta-percha or Resilon: an ex vivo study using a polymicrobial leakage model. Oral Surg Oral Med Oral Pathol Oral Radiol Endod 2007; 104(4):e114-19.
6. Molander A, Reit C, Dahlén G, Kvist T. Microbiological status of root-filled teeth with apical periodontitis. Int Endod J 1998; 31(1):1-7.
7. Mummolo S, Marchetti E, Giuca MR, Gallusi G, Tecco S, Gatto R, Marzo G. In-office bacteria test for a microbial monitoring during the conventional and self-ligating orthodontic treatment. Head Face Med 2013; 9:7.
8. D'Ercole S, Filippakos A, De Toledo Leonardo R, Pameijer CH, Tripodi D. Enterococcus faecalis leakage of root canal sealers: an ex vivo study. J Biol Regul Homeost Agents 2012; 26(3):545-52.
9. McSpadden. Endodontic Techniques. Bradford, UK: Prestige. 1995.
10. Johnson WB. A new gutta-percha technique. J Endod 1978; 4(6):184-88.
11. Buchanan LS. The continuous wave of obturation technique: 'centered' condensation of warm gutta percha in 12 seconds. Dent Today 1996; 15(1):60-2, 64-7.
12. Mummolo S, D'Ercole S, Marchetti E, Campanella V, Martinelli D, Marzo G, Tripodi D. Oral antiseptic and periodontitis: a clinical and microbiological study. Oral Healt Dent Manag 2014; 13(3):698-702.
13. Sedgley CM, Lennan SL, Appelbe OK. Survival

of Enterococcus faecalis in root canals ex vivo. Int Endod J 2005; 38(10):735-42.
14. Fontana C, Favaro M, Minelli S, Bossa MC, Altieri A, Favalli C. A novel culturing system for fluid samples. Med Sci Monit 2008; 14(12): BR1-BR6.
15. Benjamini Y, Hochberg Y. Controlling the false discovery rate: a practical and powerful approach to multiple testing. J R Statist Soc B 1995; 57(1):289-300.
16. Yücel AC, Ciftçi A. Effects of different root canal obturation techniques on bacterial penetration. Oral Surg Oral Med Oral Pathol Oral Radiol Endod 2006; 102(4):e88-92.
17. Canonica M, Favatà M. Sistema Thermafil nelle otturazioni canalari: valutazioni cliniche. Associazione Italiana Ododntoiatri 2004.
18. Micalizzi A, Briguglio R, Miragliotta S. Otturazione canalare con il sistema Thermafil. Dental Cadmos 1999; 4:31-34.

JOURNAL OF BIOLOGICAL REGULATORS & HOMEOSTATIC AGENTS Vol. 32, no. 2, 407-413 (2018)

LETTER TO THE EDITOR

EFFECT OF BIOPHYSICAL THERAPY ON ARTICULAR PAIN IN A PRIMARY CARE SETTING COMPARED TO IBUPROFEN AND PLACEBO: A RANDOMIZED CONTROLLED TRIAL

A. FOLETTI[1,2], C.G. EGAN[3] and P. BARON[1]

[1]Clinical Biophysics International Research Group, Lugano, Switzerland; [2]Institute of Translational Pharmacology, National Research Council-CNR, Rome, Italy; [3]CE-Medical Writing, Pisa, Italy

Received November 4, 2017 – Accepted February 7, 2018

Articular pain is one of the most frequent complaints practitioners face in their daily work. With an aging population, many patients have multiple comorbidities that are associated with the presence of chronic diseases, while others experience allergies, side effects or do not respond to standard medications or procedures. Therefore, there is an urgent need for new effective and safe strategies to manage articular pain, especially in its chronic manifestations. This randomized controlled trial was designed to assess the efficacy of a single therapy session using a biophysical procedure matched with a common non-steroidal anti-inflammatory drug (ibuprofen) and placebo. Biophysical therapy was performed using a Med Select 729 device. One hundred fifty patients (mean age 56±15.6 years) diagnosed with acute or chronic articular pain at different locations were randomized into 3 groups and the Numeric Pain Rating Score (NPRS) was used to measure pain at baseline, after one week, one month, and three months. While no difference in NPRS was observed at baseline among the 3 groups, a statistically significant difference was observed at all subsequent time points, respectively, after one week ($p<0.05$), one month ($p<0.001$), and three months ($p<0.01$), for both ibuprofen and biophysical groups *vs* placebo. Biophysical treatment of articular pain was shown to be as effective as a conventional non-steroidal anti-inflammatory treatment over a period of 3 months compared to placebo and could, therefore, represent an integrative, safe and long-lasting therapy to be considered for the management of acute and particularly chronic articular pain in current medical practice.

To the Editor,

Articular pain management is a leading burden in general practice setting (1) and each patient requires personalized treatment (2). Often, patients show multiple comorbidities, multiple pharmacological treatment, and frailty due to aging, increasing the complexity of their management (3) due to possible cross drug reactions and possible side effects from non-steroidal anti-inflammatory drugs (NSAID). Pain, indeed, seems to play the role of an homeostatic emotion in the response to stress (4) and to increase allostatic load (5). Thus, pain must to be considered not only from a symptomatic viewpoint but also from a holistic perspective (6). For these reasons, an effective non-pharmacological strategy to cope with pain in an efficient and safe way would benefit many patients. Biophysical therapies using electro-medical devices (such as Med Select 729 in this trial) allow to perform a very personalized treatment based on endogenous electromagnetic signals of the patient and is consistent with the raising concept of personalized medicine (2). It has been previously

Key words: biophysical therapy, electromagnetic information transfer, aqueous system, articular pain, ibuprofen

Mailing address:
Alberto Foletti, MD
Clinical Biophysics International Research Group,
Via Maggio, 21
6900 Lugano, Switzerland
Tel.: +41 787578783 - Fax: +41 919724042
e-mail: albertofolettimd@gmail.com

0393-974X (2018)

DISCLOSURE: ALL AUTHORS REPORT NO CONFLICTS OF INTEREST RELEVANT TO THIS ARTICLE.

shown that the integration of an electromagnetic paradigm into biology and medicine could offer an additional potential when translated into clinical application (7). The biophysical protocol integrates an Electromagnetic Information Transfer Through Aqueous System (EMITTAS) procedure which has been shown to be effective in a range of biological and clinical settings including chronic kidney disease, refractory gynaecological infections (8), and psoriasis (9). Furthermore, we have previously demonstrated the beneficial effects of biophysical therapy in the treatment of pain after 1 week in a three-arm randomized pilot trial matching a biophysical protocol, a placebo, and a drug (ibuprofen) (10), as well as in the treatment of low back pain in a pilot report (11). A limitation of these previous studies was the lack of long-term follow-up, the small sample size, and the heterogeneous nature of the disease treated.

MATERIALS AND METHODS

Study objectives and design

A randomized, double-blind, three-arm study was designed in order to test the potential effect of a biophysical protocol integrating an Electro Magnetic Information Transfer Through Aqueous System (EMITTAS) procedure (8) in the treatment of articular pain in a general practice setting. Randomization was performed through the website http://www.randomization.com. The primary outcome of the study was to evaluate the effectiveness of a biophysical therapy following daily sublingual administration of drops of the recorded aqueous solution (Nomabit Base) to patients with acute or chronic articular pain in a general practice setting compared with a negative and a positive control. The secondary outcome was to assess the duration of the effect on pain over time at one week, one month and up to three months as endpoint. The third outcome was to assess the safety and compliance of the biophysical procedure.

Patients

Patients presenting with joint pain within the general practice outpatient clinic of Poliambulatorio San Marco, Palmanova, Italy were enrolled. Informed consent was obtained from all the participants and the study was performed in accordance with the declaration of Helsinki.

The subjects of the study were patients with symptoms of acute or chronic articular pain. Inclusion criteria were the following: (i) presence of articular pain symptoms; (ii) aged between 18 and 70 years; (iii) fluent Italian speaking; (iv) legal capacity to consent to the treatment; (v) unchange of any other general unrelated medications throughout the study.

Exclusion criteria were the following: (i) presence of psychiatric disorders; (ii) cognitive disorders such as dementia; (iii) inadequate comprehension of written and spoken Italian language; (iv) drug or alcohol abuse; (v) current pregnancy; (vi) presence of any autoimmune or rheumatic disease (e.g. rheumatoid arthritis or gout) or (vii) currently undertaking any anti-inflammatory or pain relieving medication.

Treatment arms and randomisation

The biophysical therapy protocol was offered to patients who met the inclusion criteria, with an explanation of the aims of the study and declaration of the possibility that they would be assigned by random allocation to the experimental group of treatment or to one of the control groups (50 patients in each group). If they agreed, they signed the informed consent and, immediately, were randomly assigned to Group 1 (placebo as negative control), Group 2 (ibubrofen as positive control), or Group 3 (biophysical protocol) respectively. The sequence of randomization was determined by an independent statistical consultant using Randomization.com. Patients assigned to Group 1 constituted of the placebo group as negative control and received the Nomabit Base (Named, Italy) solution as treatment to be administered as sublingual drops according to the weekly plan as previously described (10-11). Patients assigned to Group 2 constituted of the positive control group and received ibuprofen (600 mg) twice daily on a full stomach for ten days, as usual non-steroidal anti-inflammatory treatment.

Biophysical treatment

Patients assigned to Group 3 (biophysical group) were treated following a 2-step biophysical protocol using a commercially available electro-medical device, MedSelect 729 (Wega, Germany) (10). This medical device operates in the low frequency range (between 0 and 20 KHz) using a magnetic field with an intensity

similar to the Earth's magnetic field with a maximum of 50 μT (MicroTesla). This device is capable of recording bio-signals, mainly electrical signals, in the order of millivolts, similar to electrocardiographic and electroencephalographic recording procedures. The device is a simple recording and reemitting unit committed to recording a predefined 5 second signal pattern and then to reemit the same pattern repeated along the settled delivery time. It allows to record input signals using two electrodes and to send output signals to the patient through two magnetic electrodes for local use, in this case, at the pain site, or through a magnetic carpet where the patient can lie down (in this way the entire body of the patient can be treated). Therefore, the device can offer a local and systemic treatment simultaneously. The programs used for the 2-step treatment were preloaded in the apparatus and included: a) the 1st step which consisted of selecting the program 'regulation therapy' on the touch screen of the Med Select 729 device to record the endogenous input signals at the painful region of each patient and of delivering the therapeutic electromagnetic output signals to an electromagnetic, full body-sized carpet on which the patient lay for 10 min. Then, in the second step, b) the program 'pain therapy' was selected from the touch screen of the MedSelect 729 to record the endogenous input signals at the painful region and deliver the therapeutic output signals at the pain site for 10 min. These output therapeutic signals were recorded on a commercially available aqueous system (Nomabit Base) by placing the solution into a special output coil built-in in the Med Select 729 device. The aqueous solution in which signals were recorded was inserted into a coil present in the device. The recording circuit and procedures are described in detail (8). The Nomabit Base aqueous solution is composed of oligo-minerals: it presents the advantage of already being provided with a dropper and stored in a cardboard coated aluminium container, which ensures that the signal is preserved on the aqueous solution and is protected from thermal shock and environmental electromagnetic pollution. After the first and second step treatment phase (day 1), patients followed a weekly self-administration protocol, as previously described (10, 11). Briefly, the once a day self-administration protocol of the recorded Nomabit Base, for the placebo and the biophysical group therapy was identical, according to a weekly plan as follows: 1 drop on Monday, 2 drops on Tuesday, 3 drops on Wednesday, 4 drops on Thursday, 5 drops on Friday, 6 drops on Saturday, pause with no drops on Sunday. Both the placebo and biophysical groups obtained sublingual drops and application of electrodes, but in Group1

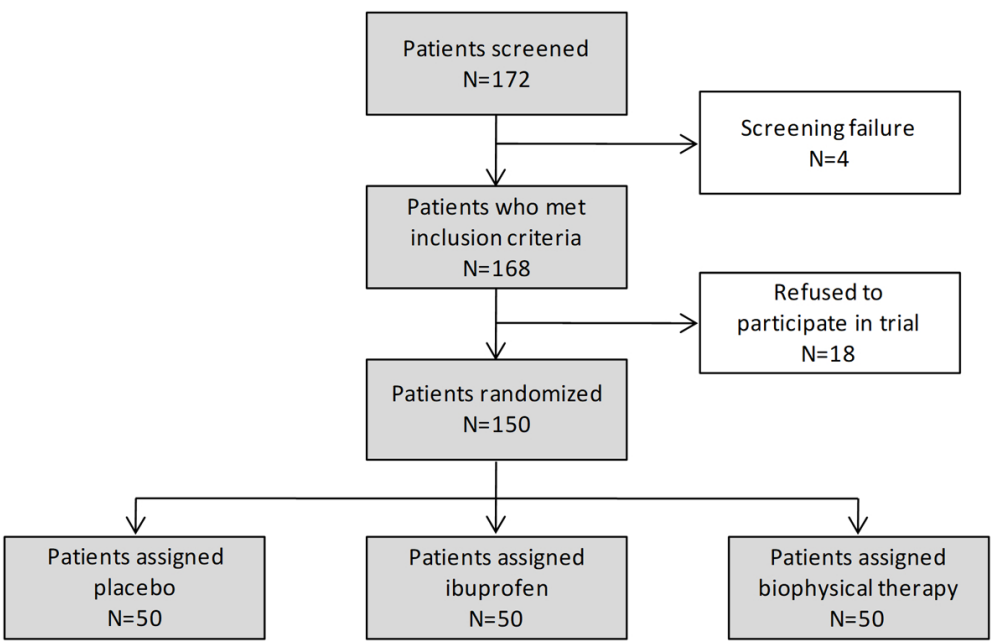

Fig. 1. *Study patients.*

Table I. *Baseline clinical characteristics.*

Characteristic	Placebo (N=50)	Ibuprofen (N=50)	Biophysical therapy (N=50)	P-value
General				
Age (years)	56.3±13.2	55.9±18.7	55.6±14.7	0.98
Female patients, n	30	29	30	0.97
Female patients, (%)	60	58	60	0.97
Acute pain, n (%)	18 (36)	23 (46)	12 (24)	0.07
Chronic pain, n (%)	32 (64)	27 (54)	38 (76)	0.07
Baseline NPRS	6.44±1.5	6.75±1.8	7.1±1.44	0.15
Characterisation of pain				
Burning	9 (18)	7 (14)	8 (16)	0.86
Stabbing	16 (32)	17 (34)	20 (40)	0.68
Dull	22 (44)	25 (50)	23 (46)	0.83
At rest	9 (18)	18 (36)	13 (26)	0.13
During movement	36 (72)	30 (60)	32 (64)	0.44
Intense movement	1 (2)	3 (6)	2 (4)	0.59
Location of pain				
Temporomandibular	3 (6)	2 (4)	0 (0)	0.24
Upper limbs and shoulders	11 (22)	13 (26)	12 (24)	0.89
Dorsal	1 (2)	2 (4)	0 (0)	0.36
Neck and back	21 (42)	15 (30)	28 (56)	**0.03**
Lower limbs	13 (26)	18 (36)	8 (16)	0.07
Other site	1 (2)	0 (0)	2 (4)	0.36

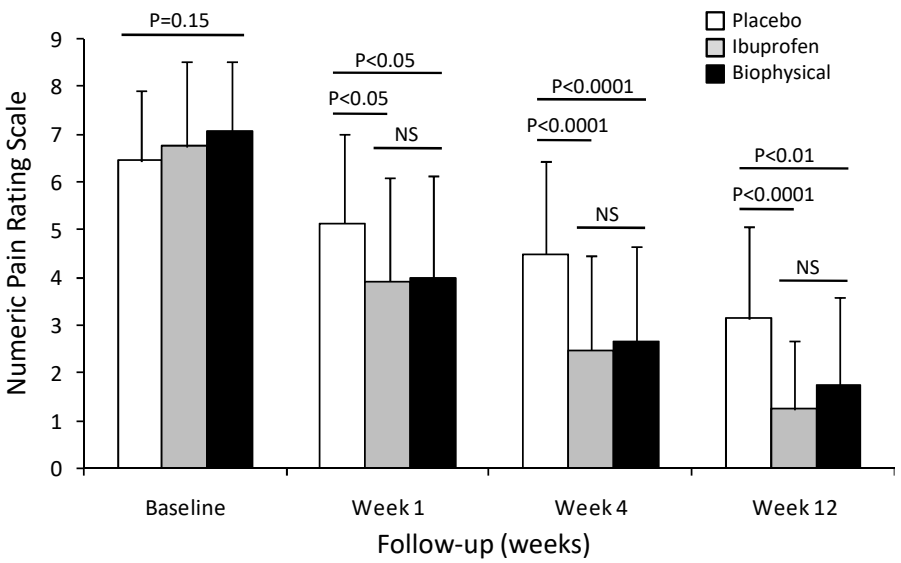

Fig. 2. *Numeric Pain Rating Scale in patients with articular pain at baseline, 1 week, 4 weeks and 12 weeks after ibuprofen (grey columns) or biophysical treatment (black columns) and placebo control (white columns). Data are presented as mean±SD. P-values denote level of statistical significance.*

(placebo) it was an untreated solution (Nomabit Base) and no biophysical treatment was applied; whereas in Group 3 (biophysical) it was biophysically treated solution and electrodes were active: this way the patients were blinded as to which group they were assigned to.

Pain assessment

The Numeric Pain Rating Score (NPRS) was employed for scoring pain (12) at baseline, after one week, one month and three months. It is a segmented numerical version of the visual analoge scale (VAS) in which a respondent selects a whole number (0–10 integers), higher scores indicating greater pain intensity (12).

Statistical analysis

Data are presented as mean±standard deviation or number and percent. Comparisons between the three treatment arms was performed using 1-way ANOVA followed by Bonferroni post-hoc for continuous variables or the *Chi*-squared test for dichotomous variables. Univariate analysis was also used to evaluate the presence of associations between change in NPRS and clinical characteristics. Statistical analysis was performed using Instat Software (GraphPad, La Jolla, CA, USA). A p-value of <0.05 was considered statistically significant.

RESULTS

Patient disposition

A total of 172 patients were screened during the recruitment period and 168 met inclusion criteria of whom 150 participated in the study (Fig. 1). Fifty patients were randomized to the placebo control group (negative control), 50 to the pharmacological treatment with ibuprofen (positive control group), and 50 patients to the experimental condition with the biophysical protocol. No patients dropped out of the study and all patients who enrolled completed the follow-up period.

Baseline clinical characteristics

Baseline clinical characteristics of patients who participated in the study are summarized in Table I. The study included patients presenting with both acute and chronic articular pain and approximately 60% were female (Table I). Mean age of the patients was 56±15.6 years and age was similar across the 3 arms. At baseline, mean NPRS was 6.8±1.6 for all patients, no difference being observed among the 3 study groups. Pain characteristics and pain localisation were also similar across the 3 groups (Table I).

Effect of biophysical and ibuprofen vs placebo on NPRS

NPRS was significantly decreased (1-way ANOVA, $p<0.0001$) over the 3 visits compared to baseline for all 3 treatment arms (including placebo). No difference among the three treatments was observed on NPRS at baseline ($p=0.15$, 1-way ANOVA) (Fig. 2). In contrast, after just 1 week, a significant difference was observed among the 3 groups (1-way ANOVA, $p<0.0049$); NPRS in patients treated with ibuprofen and the biophysical group afforded a similar reduction, while both were significantly decreased compared to placebo group ($p<0.05$). After 1 month, the difference in NPRS in patients treated with ibuprofen and biophysical-treated groups compared to the placebo group was even more pronounced (1-way ANOVA, $p=0.0001$), both groups being significantly reduced to the same extent ($p<0.0001$) compared to the placebo control. At the 3 month time-point, NPRS was also significantly different among the 3 groups (1-way ANOVA, $p=0.0001$): a statistically significant reduction in both the ibuprofen ($p<0.0001$) and biophysical therapy groups ($p<0.01$) was observed compared to patients randomized to placebo (Fig. 2). Univariate analysis also revealed that change in NPRS over the follow-up period was not associated with age, gender or baseline NPRS (data not shown).

DISCUSSION

The benefit afforded by biophysical therapy has already been demonstrated in patients suffering from low-back pain and with general pain (10, 11). We extended these findings further to include a larger sample size (N=150) using a randomized, double-blind, 3-arm, placebo-controlled trial design with longer follow-up period. Our findings demonstrate that the improvement in pain following one single

session of biophysical treatment is identical to that provided by 600 mg ibuprofen twice daily for 10 days in patients with acute and chronic joint pain. Pain reduction, as measured by NPRS, was detected as early as 1 week and persisted up to 3 months. Furthermore, no adverse effects were observed in patients in either treatment arm. The majority of patients who participated in this study presented with chronic joint pain localised to the neck and back, the pain being pronounced during movement. These characteristics reflect an increasing population of patients who present in the general practice clinic. The long-term adverse effects of pain-relieving non-steroidal anti-inflammatory drugs (NSAIDs) such as high dose ibuprofen are well established (13). Regardless of whether any potential placebo effect may exist or not (14), both ibuprofen and biophysical therapy significantly reduced NPRS at each of the time points (2-fold). This study confirms previous pilot reports (10–11) and demonstrates that a biophysical protocol integrating an electromagnetic procedure through an aqueous system can be effective and efficient in the management of both acute and chronic joint pain in the general-practice setting. The biophysical approach presented here represents a novel alternative integrative strategy to effectively and reliably manage these patients in a cost-effective and timely manner. This method is consistent with the emerging field of bioelectronic medicine (15) and warrants further studies on other inflammatory diseases.

ACKNOWLEDGEMENTS

The authors wish to thank their colleagues Alfio Rinaudo MD, Giuseppe Bucci MD, and Roberto Rocco MD, for providing valuable help in the realization of this study.

REFERENCES

1. Palazzo C, Ravaud J-F, Papelard A, Ravaud P, Poiraudeau S. The burden of musculoskeletal conditions. PLoS One 2014; 9(3):e90633.
2. Hamburg MA, Collins FS. The path to personalized medicine. N Engl J Med 2010; 363(4):301-4.
3. Henney AM. The promise and challenge of personalized medicine: aging populations, complex diseases, and unmet medical need. Croat Med J 2012; 53(3):207-10.
4. Craig AD. A new view of pain as a homeostatic emotion. Trends Neurosci 2003; 26(6):303-7.
5. McEwen BS. Stress, adaptation, and disease. Allostasis and allostatic load. Ann N Y Acad Sci 1998; 840:33-44.
6. Carlson RJ. Holism and reductionism as perspectives in medicine and patient care. West J Med 1979; 131(6):466-70.
7. Liboff AR. Toward an electromagnetic paradigm for biology and medicine. J Altern Complement Med 2004; 10(1):41-47.
8. Foletti A, Ledda M, Lolli MG, Grimaldi S, Lisi A. Electromagnetic information transfer through aqueous system. Electromagn Biol Med 2017; 36(3):289-94.
9. Del Giudice E, De Filippis A, Del Giudice N, et al. Evaluation of a method based on coherence in aqueous systems and resonance-based isotherapeutic remedy in the treatment of chronic psoriasis vulgaris. Curr Top Med Chem 2015; 15(6):542-48.
10. Foletti A, Baron P, Sclauzero E, Bucci G, Rinaudo A, Rocco R. Assessment of biophysical therapy in the management of pain in current medical practice compared with ibuprofen and placebo: a pilot study. J Biol Regul Homeost Agents 2014; 28(3):471-79.
11. Foletti A, Pokorný J. Biophysical approach to low back pain: a pilot report. Electromagn Biol Med 2015; 34(2):156-59.
12. Hawker GA, Mian S, Kendzerska T, French M. Measures of adult pain: Visual Analog Scale for Pain (VAS Pain), Numeric Rating Scale for Pain (NRS Pain), McGill Pain Questionnaire (MPQ), Short-Form McGill Pain Questionnaire (SF-MPQ), Chronic Pain Grade Scale (CPGS), Short Form-36 Bodily Pain Scale (SF-36 BPS), and Measure of Intermittent and Constant Osteoarthritis Pain (ICOAP). Arthritis Care Res 2011; 63 (S11):S240-52.
13. Tramèr MR, Moore RA, Reynolds DJ, McQuay HJ. Quantitative estimation of rare adverse events which follow a biological progression: a new model applied to chronic NSAID use. Pain 2000; 85(1–2):169-82.
14. Hróbjartsson A, Gøtzsche PC. Is the placebo

powerless? An analysis of clinical trials comparing placebo with no treatment. N Engl J Med 2001; 344(21):1594-602.

15. Birmingham K, Gradinaru V, Anikeeva P, et al. Bioelectronic medicines: a research roadmap. Nat Rev Drug Discov 2014; 13(6):399-400.

LETTER TO THE EDITOR

CLINICAL COURSE OF SEVERE COLITIS: A COMPARISON BETWEEN CROHN'S DISEASE AND ULCERATIVE COLITIS

E. SINAGRA[1,2,3], A. ORLANDO[1], A. SCALISI[1], F. MOCCIARO[1,4], V. CRISCUOLI[1,5], L. OLIVA[1], S. MAISANO[1], M. GIUNTA[6], F. LA SETA[7], G. SOLINA[8], A.G. RIZZO[9], A. LEONE[10], G. TOMASELLO[3,11], F. CAPPELLO[11] and M. COTTONE[1]

[1]DIBIMIS, Ospedali Riuniti Villa Sofia – Vincenzo Cervello, Division of Internal Medicine, Palermo, Italy; [2]Gastroenterology & Endoscopy Unit, Fondazione Istituto San Raffaele Giglio, Cefalù, Italy; [3]Euro-Mediterranean Institute of Science and Technology (IEMEST), Palermo, Italy; [4]UOC Gastroenterologia, ARNAS Ospedale Civico Palermo, Italy; [5]UOC Medicina Interna, ARNAS Ospedale Civico Palermo, Italy; [6]Unit of Gastroenterology, Ospedali Riuniti Villa Sofia – Vincenzo Cervello, Palermo, Italy; [7]Unit of Radiology, Ospedali Riuniti Villa Sofia – Vincenzo Cervello, Palermo, Italy; [8]Unit of Surgery, Ospedali Riuniti Villa Sofia – Vincenzo Cervello, Palermo, Italy; [9]Unit of Pathology, Ospedali Riuniti Villa Sofia – Vincenzo Cervello, Palermo, Italy; [10]BIONEC, Section of Histology, University of Palermo, Palermo, Italy; [11]BIONEC, Section of Anatomy, University of Palermo, Palermo, Italy

Received June 12, 2017 – Accepted February 21, 2018

Few data are available about the clinical course of severe colonic Crohn's disease (CD). The aim of this study is to describe the clinical course of severe Crohn's colitis in a patient cohort with isolated colonic or ileocolonic CD, and to compare it with the clinical course of patients with severe ulcerative colitis (UC). Thirty-four patients with severe Crohn's colitis were prospectively identified in our cohort of 593 consecutive hospitalized patients through evaluation of the Crohn's Disease Activity Index score and the Harvey-Bradshaw Index. One hundred sixty-nine patients with severe ulcerative colitis were prospectively identified in our cohort of 449 consecutive hospitalized patients through evaluation of the Lichtiger score and the Truelove-Witts score. We evaluated the following data/aspects: response to steroids, response to biologics, colectomy rate in acute, colectomy rate during follow-up, megacolon and cytomegalovirus infection rate. We did not find significant differences in the response to steroids and to biologics, in the percentage of cytomegalovirus infection and of megacolon, while the rate of colectomy in acute turned out to be greater in patients with severe Crohn's colitis compared to patients with severe UC, and this difference appeared to be the limit of statistical significance (*Chi*-squared 3.31, p = 0.069, OR 0.39); the difference between the colectomy rates at the end of the follow-up was also not significant. In the whole population, by univariate analysis, according to the linear regression model, a young age at diagnosis is associated with a higher overall colectomy rate (p = 0.024) and a higher elective colectomy rate (p = 0.022), but not with a higher acute colectomy rate, and an elevated ESR is correlated with a

Key words: severe colitis, Crohn's disease, ulcerative colitis

Mailing address:
Dr Emanuele Sinagra,
Fondazione Istituto G. Giglio,
Contrada Pietrapollastra Pisciotto,
90015 Cefalù, Palermo, Italy
Tel.: ±39 3270193383 - Fax: ±39 921920406
e-mail: emanuelesinagra83@googlemail.com

0393-974X (2018)

higher overall colectomy rate (p = 0.014) and a higher acute colectomy rate (p = 0.032), but not with a higher elective colectomy rate. This correlation was significant on multivariate analysis. The overall rate of colectomy in the cohort of patients with severe Crohn's colitis was greater than that of the cohort of patients with severe UC, but this figure is not supported by a different clinical response to steroid therapy or rescue therapy with biologics. The clinical course of severe Crohn's colitis requires to be clarified by prospective studies that include a larger number of patients in this subgroup of disease.

To the Editor,

Few data are available on the clinical course of severe Crohn's colitis, compared to those of ulcerative colitis (UC) (1, 2). Approximately 15% of patients with UC have a severe attack requiring hospitalization for intravenous (IV) corticosteroid therapy at some time during their illness (3). This treatment leads to remission in only 60% of patients, and patients who do not have a response usually require total colectomy (4, 5). The advent of cyclosporine and infliximab has not eliminated the risk of colectomy in UC patients, also in our experience (6).

The aim of this study is to describe the clinical course of severe CD in a patient cohort with isolated colonic or ileocolonic CD from a tertiary referral centre and to compare it with the clinical course of severe UC in a patient cohort from the same centre in the same period of time.

MATERIALS AND METHODS

Patient characteristics

Patients with severe Crohn's colitis were prospectively identified, through evaluation of the Crohn's Disease Activity Index (CDAI) score (> 450) and the Harvey-Bradshaw Index (> 8), from our cohort of 593 consecutive patients, hospitalized in the Division of Internal Medicine at the "Villa Sofia - V. Cervello" Hospital. Diagnosis was made according to the Binder criteria. We also evaluated the Lichtiger Score, a score created for UC and applied to Crohn's colitis. Severity of Crohn's colitis was also evaluated through proctosigmoidoscopy: endoscopic severity was assessed by both presence or absence of deep colonic ulcers, by SES-CD criteria.

Patients with severe UC were prospectively identified through the Truelove and Witts' Criteria and the Lichtiger Score in our cohort of 449 consecutive patients, hospitalized in the same division. Severity was assessed also by proctosigmoidoscopy, according to both presence or absence of deep colonic ulcers, in accordance with the Mayo Clinic Criteria and the Baron Criteria.

On admittance, according to the protocol, all patients were evaluated clinically, with abdominal X-ray, full blood count, blood chemistry [including erythrocyte sedimentation rate (ESR), C-reactive protein (CRP) and albumin], arterial blood gas analysis and abdominal ultrasonography in order to exclude toxic megacolon or perforation and to establish the approximate extent of colitis. Human cytomegalovirus (HCMV) detection in rectal biopsies and peripheral blood was also examined, in order to exclude citomegalovirus infection (in the presence of a positive test we treated the patient with antiviral therapy before the standard treatment), as recommended. All patients were tested for enteric stool pathogens and *Clostridium difficile* toxins. Furthermore, we alerted the patients and the surgeons about the risk of colectomy.

On admittance, our cohort of patients was treated with intravenous (IV) corticosteroids according to the Oxford regimen (21), together with IV antibiotics and total parenteral nutrition.

IV steroid responsive patients [as defined by response to an adequate dose (1 mg/kg) of steroids within 5-7 days] were switched to oral corticosteroid, with concurrent starting of azathioprine at the dosage of 2.5 mg/Kg daily and progressive tapering of corticosteroid. If previous intolerance or failure of immunosuppressants had been reported, maintenance treatment with azathioprine was excluded.

IV steroid resistant patients [as defined by a lack of response to an adequate dose of steroids (1 mg) within 5-7 days] were treated with biological drugs, using the standard induction regimen [infliximab at the dosage of 5mg/kg iv or adalimumab 160 mg subcutaneously (adalimumab for CD)], after conventional screening for infection or malignant disease. All patients signed a written informed

consent before starting both treatments. The choice of the biological treatment was based on the possible failure of previous biological treatments, on the physicians' judgment and on the patients' preferences. Patients who responded to infliximab, and showed no clinical signs of intolerance, completed the induction phase with infusion at weeks 2 and 6 followed by scheduled infusion (5 mg/kg every 8 weeks). Patients who responded to adalimumab, and showed no clinical signs of intolerance, completed the induction phase with infusion at week 2 (80 mg sc) followed by scheduled infusion (40 mg sc every 2 weeks). The biological treatment was extended for one year. In some patients treated with biological drugs, azathioprine at the dosage of 2.5 mg/Kg daily was started soon after the last infusion in the acute phase.

Only in one patient with IV steroid and infliximab refractory UC, IV cyclosporine at the dosage of 2 mg/Kg/die was administered after a joint medical-surgical decision, adjusting the dosage according to the cyclosporine blood levels (therapeutic range: 200-250 mcg/L). The IV cyclosporine responsive patient was switched to oral cyclosporine at the dosage of 5 mg/Kg/

Table I. *Baseline characteristics of severe UC colitis patients (n=169).*

Variable	Value
Mean age at diagnosis in years	37.4±17.1
Mean age at admission for severe colitis in years	43.5±17.6
Sex, no. (%) 53) Male 54) Female	 92 (54.4%) 77 (45.6%)
Extraintestinal manifestations, no (%) 55) Articular 56) Erithema nodosum 57) Pyoderma gangrenosum 58) Sclerosing cholangitis 59) Uveitis	 16 (42.1%) 6 (15.8%) 4 (10.5%) 2 (5.3%) 3 (7.9%)
Haemoglobin at admission (g/dL)	11.6±2.3
Albumin at admission (g/dL)	2.8±0.5
Smoker, no (%)	35 (20.7%)
Perianal disease, no (%)	2 (1.2%)
Disease extension, no (%) 60) Pancolitis 61) Left colitis 62) New diagnosis	 66 (39%) 87 (51.5 %) 16 (9.4%)
Median Relapse rate/year for each patient	2 (0-9)
Median disease duration in months	48 (1-552)
Median number of hospitalizations before admission	1 (0-20)
Median number of hospitalizations after admission	-114 not hospitalized again - 32: 1 hospitalization after severe colitis - 23: ≥ 2 hospitalization after severe colitis
First episode of severe colitis / Relapse, no (%)	30 (17.8%) / 139 (82.2%)
Previous thiopurine treatment, no (%)	58 (34.3%)
Previous biologic treatment, no (%)	17 (10.1%)
Follow up in days	1530±73.9
Patients who needed transfusions, no (%)	20 (11.8%)

Table II. *Baseline characteristics of severe Crohn's colitis patients (no =34).*

Variable	Value
Mean age at diagnosis in years	29.1±12.2
Mean age at admission for severe colitis in years	34.1±12.8
Sex, no (%) 63) Male 64) Female	14 (41.2%) 20 (58.8%)
Extraintestinal manifestations, no (%) 65) Articular 66) Erythema nodosum	16 (47.1%) 13 (81.2%) 3 (18.8%)
Haemoglobin at admission (g/dL)	10.9±1.8
Albumin at admission (g/dL)	2.96±0.54
Smokers, no (%)	22 (64.7%)
Perianal disease, n (%)	6 (17.6%)
Disease behaviour, no (%) 3) Inflammatory 4) Stenosing 5) Fistulizing 6) New diagnosis	28 (82.4%) 3 (8.8%) 2 (5.9%) 1 (2.9%)
Disease extension, no (%) 7) Ileocolonic 8) Colonic 9) New diagnosis	12 (35.3%) 21 (61.8%) 1 (2.9%)
Relapse/year	1 (0-4)
Median disease duration in months	36 (1-186)
Median number of hospitalization before admission	4 (0-18)
Median number of hospitalization after admission, no/ hospitalizations	- 21: not hospitalized again - 6: < 2 hospitalizations after severe colitis - 7: ≥ 2 hospitalizations after severe colitis
First episode of severe colitis / Relapse, no (%)	9 (26.5%) / 25 (73.5%)
Previous thiopurine treatment, no (%)	10 (29.4%)
Previous biologic treatment, no (%)	9 (26.5%)
Follow-up in days	1238±217.9
Patients who needed transfusions, no (%)	4 (11.8%)
Mean SES-CD	31.9±4.9

die after 14 days (for no more than 3 months), together with maintenance treatment with azathioprine.

Patients whose condition worsened or failed to respond to treatment underwent colectomy. In the individual patient, performing colectomy was a joint medical-surgical decision.

Statistical analysis

Data were analyzed using the software package SPSS 15 (SPSS Inc., Chicago, IL, USA). Continuous variables were summarized as mean (± standard deviation (SD)) or median (range) according to their distribution. Categorical variables were summarized as frequency and percentage.

Table III. *Outcome evaluation, compared using the Chi-squared test.*

	Severe Crohn's colitis (N=34)	Severe UC (N=169)	P-value
CRP	18.7±9.6	11.4±5.4	ns
Response to corticosteroids, n (%)	23/34 (67.6%)	124/169 (73.4%)	ns
HCMV infection, no (%)	1/34 (2.9%)	12/169 (7.1%)	ns
Response to biologic treatment, no (%)	6/7 (85.7%)	24/27 (88.9%)	ns
Megacolon, no (%)	3/34 (8.8%)	27/169 (16%)	ns
Acute colectomy rate, no (%)	6/34 (17.6%)	13/169 (7.7%)	ns
Elective colectomy rate, no (%)	7/34 (20.6%)	22/169 (13%)	ns

Significant differences were calculated using a *Chi*-squared test for categorical variables and a Student's *t*-test for continuous variables.

Through the *Chi*-squared test the percentage of response to IV steroids, the prevalence of HCMV infection, the percentage of response to biological drugs, the megacolon rate and the colectomy rate after acute flare-up and at the end of follow-up were compared.

Time to colectomy was illustrated with a Kaplan-Meier plot. Actuarial curves of colectomy in both diseases were compared by the long rank test.

Demographic and disease variables were related to the main outcome using the logistic regression model at 3 and 12 months and the Mantel Cox model at the end of follow-up. We considered the following variables: sex, age, smoking habit, family history, dosage of corticosteroids till admittance, taking of biological drugs till admittance, number of hospitalizations before and after acute flare-up, ESR, CRP, white blood cell count, haemoglobin level, albuminaemia and disease duration.

RESULTS

The main outcome was the change in the colectomy rate after the acute flare-up and at the end of follow-up in both cohorts. Secondary outcomes were the prevalence of HCMV infection, response to IV corticosteroids, response to biological drugs and the rate of toxic megacolon in both diseases. All responder patients were followed up in our outpatients' clinic in order to monitor their clinical conditions, their relapse rate requiring hospitalization or not, the need for colectomy or any drug adverse events. Patients were examined more

frequently in the first month after discharge and then at 2-monthly intervals. At each examination general well-being, physical examination and blood analysis were obtained and recorded in an electronic file. All patients had a minimum follow-up of 12 months.

Severe UC

In our cohort of 449 patients requiring hospitalization, 169 patients were classified as presenting a severe UC (37.6%). Patients' characteristics are reported in Table I.

Severe UC was more common in males (54.4% *vs* 45.6%, *p* value not significant), who were non-smokers (79.3% *vs* 20.7%, *p* value < 0.001). Sixty-six out of 169 (39.1%) patients had pancolitis on admittance, while the others had more distal involvement; 16 (9.4) out of 169 patients presented with a disease onset, and therefore it was not possible to evaluate the extent before hospitalization. The mean age at the episode of severe UC was 43.5±17.6 years and the median disease duration was 48 months (range 1-552). The median Lichtiger score on admittance was 13 (range 10-19).

None of the patients tested positively for enteric pathogens or *Clostridium difficile* toxin, while HCMV infection was detected in rectal biopsies and peripheral blood in 12 patients (7.1%): these patients were treated with IV gancyclovir, except one who developed a toxic megacolon responding to oral valgancyclovir. Among the patients with HCMV infection, only one (8.3%) underwent surgery.

In 6 (3.6%) out of 169 patients HCMV was only detected in rectal biopsies: these patients were not treated with antiviral therapy. Among these, one patient underwent surgery because of megacolon.

One hundred twenty-four out of 169 patients (73.4%) responded to IV corticosteroids, thus avoiding total colectomy. Twenty-seven out of 169 (16%) received biologic agents (infliximab): 24 of them responded, thus avoiding colectomy. Furthermore, 5 patients (3%) received IV cyclosporine (one of them after infliximab failure) and 4 of them responded, thus avoiding colectomy; 13 out of 169 (7.7%) underwent acute surgery (total

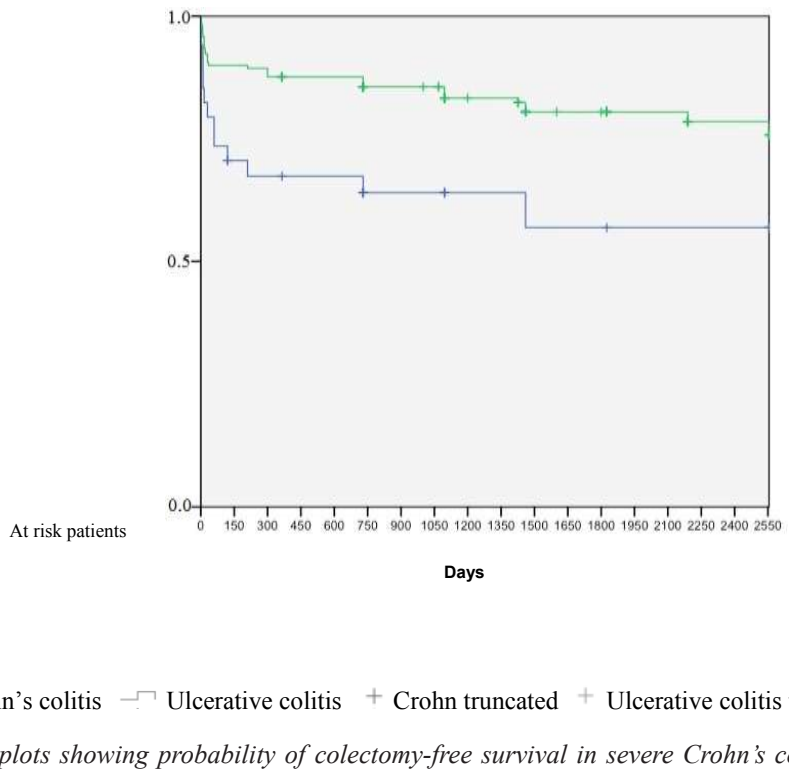

Fig. 1. *Kaplan-Meier plots showing probability of colectomy-free survival in severe Crohn's colitis and severe UC in relation to time.*

colectomy) because of medical therapy failure: 2 after infliximab failure, 1 after cyclosporine failure, 8 because of toxic megacolon and 2 because of fulminant colitis. At the end of the follow-up after the acute event (51±2 months), 13 patients were treated only with the standard induction regimen, 14 were on scheduled biological treatment, 28 switched to azathioprine or 6-MP after steroid discontinuation, 79 switched to mesalazine after steroid discontinuation (previous azathioprine intolerance or failure), and 14 discontinued infliximab because of failure, undergoing surgery, while 1 patient received IV cyclosporine as rescue therapy and 7 patients had maintenance treatment with azathioprine, as reported in Fig. 1. Twenty-seven patients (16%) developed megacolon during hospitalization: 8 of them underwent acute surgery.

The acute colectomy rate was 7.7%, while the colectomy rate at the end of the follow-up was 20.7%. Sixteen patients (45.7%), among those who underwent surgery, developed pouchitis after 14.5±5.9 months and are currently receiving VSL#3 as maintenance treatment (7). Three patients (1.8%) died within the follow-up period: one of them died because of fulminant colitis, but surgery was contraindicated because of age and comorbidity. Adverse events and side effects of biological treatment were: 2 interstitial lung diseases, 1 cutaneous herpes zoster, and 9 anaphylactic reactions between the second and the third infusions.

Severe Crohn's colitis

In our cohort of 593 CD patients requiring hospitalization, a total of 34 patients were classified as presenting severe Crohn's Colitis (5.7%). The patients' characteristic are reported in Table II (8). Severe Crohn's colitis was more common in females (females: 58.8% vs males: 41.2%, p value not significant), smokers (64.7% vs 35.3%, $p < 0.001$) and isolated colonic disease (61.8% vs 35.3%, $p = 0.002$). The mean age at the episode of severe Crohn's colitis was 34.1±12.8 years and the median disease duration was 36 months (range 1-186).

Mean SES-CD, in patients who underwent colonoscopy, was 31.9±4.9. Six patients (17.6%) had perianal disease. Mean CDAI, at admission, was 468±12.

One patient out of 34 (2.9%) had a *C. difficile* intestinal infection, while HCMV was detected in rectal biopsies and peripheral blood only in one patient (2.9%), who was treated with oral valgancyclovir before starting adalimumab (9).

Twenty-three patients out of 34 (67.6%) responded to IV corticosteroids, thus avoiding total colectomy. Seven patients out of 34 (20.6%) received biological drugs (6 infliximab, 1 adalimumab) due to steroid failure: 1 of them (14.3%) underwent colectomy, while 3 patients (8.8%) developed megacolon during hospitalization (1 of them underwent colectomy).

Six out of 34 (17.6%) underwent acute surgery (total colectomy) because of refractory colitis: 4 after IV steroid failure, 1 after infliximab failure, and 1 because of toxic megacolon. At the end of the follow-up after the acute event (41.3 7.3 months), 13 out of 28 not acutely operated patients (46.4%) received biological drugs as maintenance treatment (six patients received biological drugs after severe colitis because of development of severe perianal disease) but 7 patients (25%) discontinued it because of failure and underwent elective surgery; 7 (25%) switched to azathioprine after steroid discontinuation; 8 (28.6%) switched to mesalamine after steroid discontinuation (previous azathioprine intolerance or failure). The acute colectomy rate was 17.6% while the cumulative colectomy rate at the end of the follow-up was 38.2%. One patient (2.9%), among those who underwent total colectomy, died of post-surgical sepsis due to *Klebsiella pneumoniae*. Neither severe adverse events nor side effects of biological treatment were observed.

All the operated patients received mesalamine as maintenance treatment, while 2 patients were treated with adalimumab.

Outcome evaluation

a) Response to IV steroids was similar in our two cohorts: clinical remission was achieved in 73.4% of severe UC patients *vs* 67.6% of Crohn's colitis patients. The difference between the two cohorts was not significant ($p = 0.49$).

b) The HCMV infection rate was higher in UC patients (7.1%) than in CD patients (2.9%), but this difference was not statistically significant ($p = 0.36$).

c) The response to biological drugs was similar

in our two cohorts: clinical remission was achieved in 88.9% of severe UC patients *vs* 85.7% of Crohn's colitis patients. The difference between the two cohorts was not statistically significant (p = 0.84).

d) The megacolon rate was 16% in UC patients *vs* 8.8% in CD patients. This difference was not statistically significant (p = 0.28).

e) The acute colectomy rate was higher in severe Crohn's colitis patients (17.6%) than in severe UC patients, but this is a difference of borderline statistic significance (Chi-squared 3.31, p = 0.069, OR 0.39). The elective colectomy rate was 20.6% in severe Crohn's colitis patients and 13% in severe UC patients, but this difference was not statistically significant (p = 0.2).

Considering the whole patient population (both UC patients and CD patients), the linear regression model shows that a young age at diagnosis is associated with a higher overall colectomy rate (p = 0.024) and a higher elective colectomy rate (p = 0.022), but not with a higher acute colectomy rate, and an elevated ESR is correlated with a higher overall colectomy rate (p = 0.014) and a higher acute colectomy rate (p = 0.032), but not with a higher elective colectomy rate. These facts are also confirmed by multivariate analysis.

Considering the whole patient population (both UC patients and CD patients), the univariate analysis with the Mantel Cox model shows that no variables were significantly related to a higher overall colectomy rate or to a higher acute or elective colectomy rate.

Fig. 1 shows a comparison between the risk of colectomy in relation to time for the two diseases: severe UC patients have a lower cumulative risk of colectomy than severe Crohn's colitis patients (HR 0.4, IC 0.23-0.82, p = 0.01), but there are no differences between severe UC and severe Crohn's colitis as regards the risk of acute colectomy (p = 0.07) and the risk of elective surgery (p = 0.07).

Table III shows a comparison between the outcomes evaluated.

DISCUSSION

This prospective study shows that severe UC and severe Crohn's colitis have a different clinical course, although their clinical presentation may be similar. We compared two cohorts of patients requiring hospitalization for severe colitis in the same period of time. The clinical management of severe colitis was applied from 2003 to both diseases alike.

Focusing our attention on the colectomy rate, it was 38.2% in severe Crohn's colitis patients at the end of the follow-up. Our data are slightly different from those of Hancock's cohort (10), where the colectomy rate was 20.7%, but this cohort also included patients with mild and moderate CD.

The colectomy rate in our severe UC cohort was 20.7%. Our UC population was treated mostly with Infliximab and the colectomy rate we reported is different from the rate of a previous cohort that also received cyclosporine. This observation confirms that biological drugs (11) as rescue therapy have not eliminated the risk of colectomy, as also shown by the recent CYSIF trial (12).

The main limitation of this study is the small number of patients with severe Crohn's colitis included in the analysis.

At present, this is the first study that evaluates the clinical course of severe Crohn's colitis and compares it with that of severe UC. Our data show a higher cumulative colectomy rate in the severe Crohn's colitis cohort than in the severe UC one, but this evidence is not associated with differences between the two diseases referring to clinical response to IV corticosteroids and rescue therapy with biological drugs. The different colectomy rates could be explained by a higher biological aggressiveness of CD, as shown by the demographic and clinical characteristics of our cohort of patients, most likely because of the transmural involvement of CD in contrast to the mucosal involvement of UC.

The course of severe Crohn's colitis needs to be clarified by prospective studies including a larger number of patients with this subset of disease.

REFERENCES

1. Mills S, Stamos MJ. Colonic Crohn's Disease. Clin colon rectal surg 2007; 20(4):309-13.
2. Mortensen C, Caspersen S, Christensen NL,

Svenningse L, Thorsgaard N, Christensen LA. Treatment of acute ulcerative colitis with infliximab, a retrospective study from three Danish hospitals. J Crohn's Colitis 2011; 5:28-33.

3. Edwards FC, Truelove SC. The course and prognosis of ulcerative colitis: part 1: short term prognosis. Gut 1963; 4:300-8.
4. Jarnerot G, Rolny P, Sandberg-Gertzen H. Intensive intravenous treatment of ulcerative colitis. Gastroenterology 1985; 89:1005-13.
5. Meyers S, Sachar DB, Goldberg JD, Janowitz HD. Corticotropin versus hydrocortisone in the intravenous treatment of ulcerative colitis: a prospective, randomized, double-blind clinical trial. Gastroenterology 1983; 85:351-57.
6. Mocciaro F, Renna S, Orlando A, Rizzuto G, Sinagra E, Orlando E, Cottone M. Cyclosporine or Infliximab as rescue therapy in severe refractory ulcerative colitis: Early and long-term data from a retrospective observational study. J Crohns Colitis 2012; 6:681-86.
7. Sinagra E, Tomasello G, Cappello F, et al. Probiotics, prebiotics and symbiotics in inflammatory bowel diseases: state-of-the-art and new insights. J Biol Regul Homeost Agents 2013; 27(4):919-33.
8. Sinagra E, Aragona E, Romano C, et al. The role of portal vein thrombosis in the clinical course of inflammatory bowel diseases: report on three cases and review of the literature. Gastroenterol Res Pract 2012; 2012:916428.
9. Sinagra E, Renna S, Mocciaro F, Olivo M, Cottone M, Orlando A. Early postoperative recurrence of severe Crohn's disease, with colonic involvement and associated human cytomegalovirus infection, treated with oral valganciclovir and adalimumab. Inflamm Bowel Dis 2011; 17(6):E43-44.
10. Hancock L, Beckly J, Geremia A, et al. Clinical and molecular characteristics of isolated colonic Crohn's disease. Inflamm Bowel Dis 2008; 14(12):1667-77.
11. Sinagra E, Perricone G, Romano C, Cottone M. Heart failure and anti tumor necrosis factor-alpha in systemic chronic inflammatory diseases. Eur J Intern Med 2013; 24(5):385-92.
12. Laharie D, Bourreille A, Branche J, et al.: Groupe d'Etudes Thérapeutiques desAffections Inflammatoires Digestives. Ciclosporin versus infliximab in patients with severe ulcerative colitis refractory to intravenous steroids: a parallel, open-label randomised controlled trial. Lancet 2012; 380(9857):1909-15.

LETTER TO THE EDITOR

ETIOLOGICAL PERIODONTAL TREATMENT WITH AND WITHOUT LOW LEVEL LASER THERAPY ON IL-1β LEVEL IN GINGIVAL CREVICULAR FLUID: AN *IN VIVO* MULTICENTRIC PILOT STUDY

F. MASTRANGELO[1], A. DEDOLA[1], F. CATTONI[2], F. FERRINI[2], F. BOVA[2], M. TATULLO[3], E. GHERLONE[2] and L. LO MUZIO[1]

[1]Department of Clinical and Experimental Medicine, University of Foggia, Italy; [2]San Raffaele Dental Clinic University, Ateneo Vita e Salute, Milano, Italy; [3]Tecnologica Research Institute - Research and Development in Biomedicine - Crotone, Italy

Received January 31, 2018 – Accepted March 13, 2018

Cytokine proteins may have important roles during different human physiological and pathological processes. In the oral cavity, the bone loss and periodontal tissue pathology was related to inflammatory process activation. The aim of the present study was to assess the effects of etiological periodontal therapy with and without the use of Low Level Laser Therapy (LLLT) on clinical periodontal parameters and interleukin(IL)-1β level in gingival crevicular fluid (GCF) from chronic periodontitis (CP) patients. Thirty non-smoker CP patients were selected from the Foggia University Dental Clinic and other 2 private dental clinics. All patients were divided into two homogeneous randomized groups: 15 patients were treated with only scaling and root planing (group 1) and 15 patients with scaling and root planing etiological treatment and LLLT (group 2). In all sites, at baseline before treatment, the periodontal pocket depth (PPD) and bleeding on probing (BOP) were measured. In the PPD sites, the GCF samples were collected from 30 deep (≥5 mm) and shallow (≤3 mm) sites and IL-1β were evaluated at baseline, after 10 days and 1 month. In all the samples at baseline, the IL-1β concentration in GCF and BOP rate were significantly higher at deep PPD sites than at the shallow ones. After 10 days in all samples no PPD improvement was observed in the BOP rate but the IL-1 β level was statistically significantly improved ($p<0.005$) in group 2 compared to group 1. At 10 days and 1 month, in all deep PPD sites, PPD and BOP improvements were observed. At same time, IL-1β levels were lower and statistically significantly ($p<0.005$) improved in group 2 compared to group 1. The results confirmed that the periodontal etiology treatment of deep PPD sites with or with-out associated LLLT promotes periodontal health. Etiological treatment associated with LLLT, improves BOP and inflammation in periodontal disease. Moreover, the IL-1β concentration changes in GCF suggest these cytokines as a predictable marker of gingival inflammation in chronic periodontitis patients.

To the Editor,

Chronic periodontitis (CP) is one of the most common inflammatory diseases derived from multifactor pathological etiology and is focally or uniformly distributed in the oral cavity (1). The presence in periodontal tissue of bacteria clusters including *Aggregatibacter actinomycetemcomitans, Tannerella forsythus* and *Porphyromonas gingivalis* associated

Key words: chronic periodontitis, IL-1β, gingival crevicular fluid, etioogy periodontal therapy, low laser therapy

Mailing address:
Filiberto Mastrangelo MD, DDS, PhD
Oral Surgery Specialist,
Researcher TDB, Aggregate Professor,
Dental Clinic, Dept Clinical and Experimental Medicine,
University of Foggia, Foggia, Italy
e-mail: filibertomastrangelo@hotmail.com

0393-974X (2018)

with an altered immuno-response, increase the risk of periodontitis (2). Moreover, inflammation plays a crucial role in periodontal tissue destruction and the pro-inflammatory cytokines appear to have a critical role during different phases of the periodontal pathogenesis (3). The clinical pathological condition is a bone and gingival attachment level loss with periodontal tissue destruction and pocket depth formation (2). Several studies reported how interleukin(IL)-1β is an important mediator of inflammatory response in various physiological and pathological conditions involving cell proliferation, differentiation, and apoptosis (4, 5) Recent studies reported a correlation between IL-1β levels in gingival tissues and gingival crevicular fluid (GCF) with periodontitis and osteoclastic bone resorption mediated to prostaglandin E_2 (PGE_2) release (6, 7). Therefore, the clinical diagnosis of periodontal disease requires periodontal probing pocket depth (PPD), clinical attachment level (CAL), gingival bleeding on probing (BOP) and gingival inflammation index (GI) evaluation (8, 9). Low level laser therapy (LLLT) has been used in several physiological and pathological conditions *in vitro* and *in vivo* experiments to promote cell proliferation and tissue healing (10, 11). LLLT photo-bio-stimulation and modulation showed the reduction of pain and tissue inflammation, increasing collagen synthesis, fibroblast proliferation and cell scar activities (11, 12). Several studies have suggested that all clinical effects are related to mitochondrial adenosine triphosphate (ATP) increasingly activated by laser absorbed energy cells (13). However, the LLLT fine mechanisms are not yet understood for many factors that act in the different tissue healing stages and for the different strength, dose and time of laser irradiation. Oral lesions, dentine hypersensitivity, implant exposure and bacteria reduction in endodontic and periodontal therapies are found in oral surgery (11).

The aim of the present study was to assess the effects of scaling and root planing treatment with and without LLLT on clinical periodontal parameters and IL-1β level in two different CP patient groups.

MATERIALS AND METHODS

Thirty non-smoker CP patients (mean age, 48.4±2.7 years) were selected and included in this study. Ten patients received instruction and were treated in Foggia University Dental Clinic and other 20 patients in two different private dental clinics. The present study was structured following the clinical indications approved by the unified Scientific Committee of Foggia University Dental Clinic. The patients were randomized into 2 different groups. Inclusion criteria was, all patients were in good general health and had no history of periodontal treatment or antibiotic therapy within the 3 months before this study started. Written informed consent was obtained from each patient and periodontal parameters were assessed by measuring probing pocket depth (PPD) and bleeding on probing (BOP) with Hu-Friedy CP11 probe (Chicago, IL, USA). The study included only patients with CP with a presence of at least two sites with a PPD ≥5mm and periodontal attachment loss of >5mm.

Totally, 15 patients were treated only with scaling and root planing-SRP (group 1) and 15 patients with SRP and following LLLT (group 2). Before treatment, the plaque was gently removed with sterile cotton pellets, thirty specimens of gingival GCF were collected from two PPD periodontal sites (≤3 mm and ≥5 mm), and IL-1β was evaluated at baseline, after 10 days and 1 month. The GCF was collected from each insertion site, with periopaper (Oraflow, New York, NY, USA) retained for 20 s. For IL-1β evaluation, the periopaper was measured with a Periotron 8000 device and the GCF samples were pooled and stored in microcentrifuge tubes at -80°C.

Low level laser therapy

In several clinical conditions, different laser light sources such as gallium-aluminium-arsenide, helium-neon and diode were used. Diode lasers have shown higher penetration depth energy compared with other types. In the present study laser wave length range was between 600-1000 nm and 0.04 - 60 J/cm^2 energy density for 3 sec spotlights (L.E.O. Diode - Garda Laser, VR, Italy).

Enzyme-linked immunosorbent assay

All GCF samples were collected by a periopaper (Oraflow, New York, NY, USA), preserved in dry ice and immediately sent to the laboratory of Foggia University Dental Clinic. Commercially ELISA antibody sandwich assay (IBL International GMBH, Hamburg, Germany) was used to count the IL-1β concentration. After IL-1β samples collected the specimens were incubated with human

specific monoclonal antibody for 2 h. Then, the samples were primarily washed with 200 µL of anti-IL-1β conjugate added to each well for 1 h, and then 200 µL of substrate solution was added to each well for 20 min. Finally 50 µL of stop solution was added to each well, with reading at 450 nm. The IL-1β sensitivity has 1 pg/mL.

Statistical analysis

After initial periodontal treatment the *chi*-squared for independence test, confirmed by Fisher's exact probability test, was used to determine the improved BOP. At 10 days and 1 month after therapy, significant differences between baseline values for periodontal parameters and IL-1β level were analyzed using ANOVA test.

RESULTS

At baseline (T0), before therapy, thirty CP patients (21 male and 9 female; average age 48 years) with only 11-12-13-14-15-21-22-23-24-25 teeth (FDI numbers) were included. PPD, BOP and IL-1β levels in GCF from shallow (≤3 mm) and deep (≥5 mm) PPD site parameters of the CP patients were recorded (Table I).

At T0, the PPD shallow sites of group 1 were 2.56±0.13 mm (Fig. 1A) with 34% positive BOP sites (Fig. 2A) and the IL-1β concentration was 1.16±0.11 pg/µL (1.58±0.12 pg/site) (Fig. 3A). The deep sites of group 1 were 5.41±0.14 mm (Fig. 1B) with 94% positive BOP sites (Fig. 2B) and 2.15±0.44 pg/µL (5.38±1.05 pg/site) (Fig. 3B). At the same time, group 2 PPD shallow sites were 2.46±0.12 mm (Fig. 1A) with 38% positive BOP sites (Fig. 2A) and the IL-1β concentration was 1.19±0.14 pg/µL (1.56±0.12 pg/site) (Fig. 3A). The group 2 deep sites were 5.48±0.17 mm (Fig. 1b) with 91% positive BOP sites (Fig. 2B) and 2.16±0.48 pg/µL (5.58±1.11 pg/site) (Fig. 3B). At T0, in both groups, all parameters were significantly higher at deep PPD sites rather than at shallow ones (Table I).

Ten days after initial periodontal treatment (T1) PPD shallow sites in group 1 showed 1.80±0.11 mm (Fig. 1A) with 8% positive BOP sites (Fig. 2A) and the IL-1β concentration was 0.48±0.15 pg/µL (0.18±0.12 pg/site) (Fig. 3A). In group 2 the parameters were respectively 1.64±0.12 mm (Fig. 1A) with 6% positive BOP sites (Fig. 2A) and the IL-1β concentration was 0.49±0.15 pg/µL (0.17±0.14 pg/site) (Fig. 3A). At T1 group 1 PPD deep sites were 2.88±0.18 mm with (Fig. 1B) 36% positive BOP sites (Fig. 2B) and the IL-1β concentration was 0.98±0.30 pg/µL (0.20± 0.10 pg/site) (Fig. 3B) and group 2 parameters showed 2.59±0.21 mm PPD (Fig. 1B) with 33% BOP positive (Fig. 2B) and 0.71±0.36 pg/µL (0.19±0.12 pg/site) of IL-1β concentration (Fig. 3B) (Table I).

One month after periodontal treatment (T2) group 1 shallow site parameters detected PPD 1.72±0.12 mm (Fig. 1A) with only 3% positive BOP sites (Fig. 2A) and 0.52±0.13 pg/µL (0.26±0.12 pg/site) IL-1β concentration (Fig. 3A). At the same time, group 2 showed 1.50±0.12 mm PPD value (Fig. 1A), 2% BOP positive sites (Fig. 2B) and 0.47±0.12 pg/µL (0.26±0.11 pg/site) IL-1β concentration (Fig. 3A). At T2 in group 1, the deep sites showed PPD 2.8±0.14 mm (Fig. 1B) with only 12% positive BOP sites (Fig. 2B) and 0.90±0.13 pg/µL (0.41±0.16 pg/site) IL-1β concentration (Fig. 3b). In group 2 the deep site values were PPD 2.38± 0.11 mm (Fig. 1B) with only 11% positive BOP sites (Fig. 2B) and 0.75±0.23 pg/µL (0.38±0.11 pg/site) IL-1β concentration (Fig. 3B) (Table I).

After 10 days (T1) and 1 month (T2), in both shallow and deep PPD sites, the results of scaling and root planing treatment with or without LLLT on clinical parameters (PPD and BOP) were significantly improved. While, in the same conditions, the effects of etiological therapy with or with-out LLLT on biological parameters were significantly decreased at T1 and T2.

DISCUSSION

Inflammatory cytokines were critically observed in periodontal disease pathogenesis, and elevated cytokine levels were detected in periodontal sera during different phases of gingivitis and periodontitis. (14) Some studies observed no significant correlation among GCF volume, shallow or deep periodontal pockets and IL-1β in periodontitis patients. Furthermore, IL-1β concentration in GCF did not differ at baseline or

Table I. *Evaluation of probing pocket depth, bleeding on probing, and interleukin-1 beta in chronic periodontitis non-smoking patients.*

	T0 GROUP 1	T0 GROUP 2	T1 GROUP 1	T1 GROUP 2	T2 GROUP 1	T2 GROUP 2
PPD SHALLOW SITES	2.56 ±0.13	2.46±0.12	1.80±0.11	1.64±0.12	1.72±0.12	1.50±0.12
PPD DEEP SITES	5.41±0.14	5.48±0.17	2.88±0.18	2.59±0.21	2.80±0.14	2.38±0.11
BOP SHALLOW SITES	34%	38%	8%	6%	3%	2%
BOP DEEP SITES	94%	91%	36%	33%	12%	11%
IL-1β SHALLOW SITES	1.16±0.11	1.19±0.14	0.48±0.15	0.49±0.15	0.52±0.13	0.47±0.12
IL-1β DEEP SITES	2.15±0.44	2.16±0.48	0.98±0.30	0.7±0.36	0.90±0.13	0.75±0.23

Group 1: Patients treated with scaling and root planning; Group 2: Patients treated with scaling and root planning and LLLT. T0: Baseline; T1: after 10 days; T2: after 1 month of periodontal treatment PPD: probing pocket depth; BOP: bleeding on probing; IL-1β: interleukin-1 beta; CP: chronic periodontitis

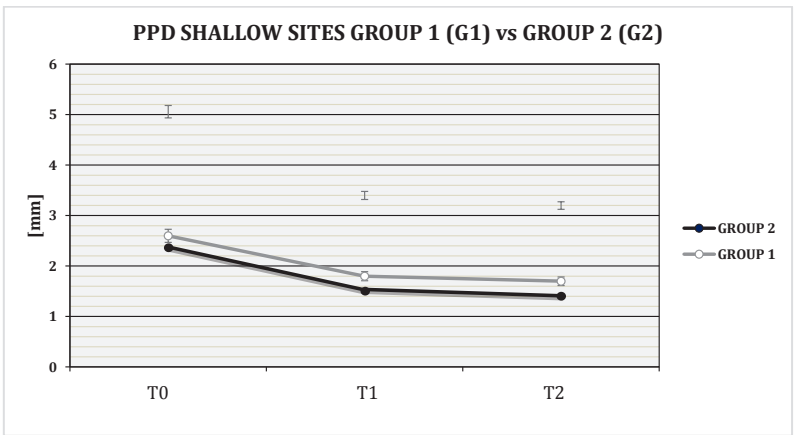

B

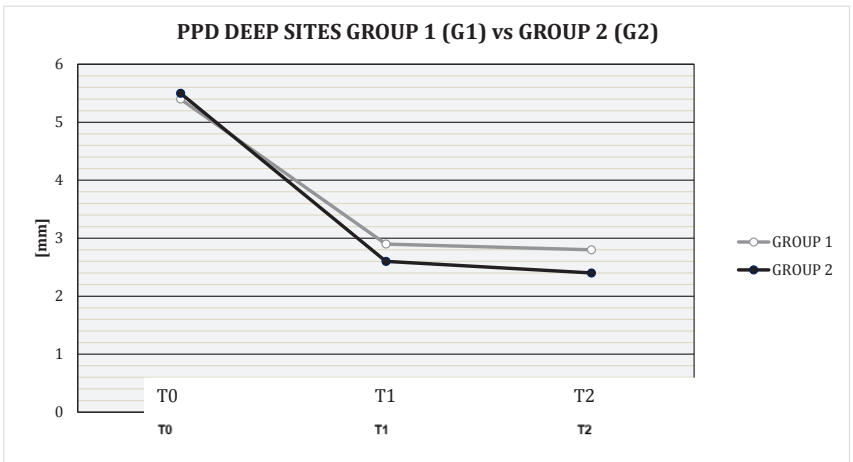

Fig. 1. *PPD values in shallow (**A**) and deep (**B**) sites of group 1 vs group 2 at T0, T1 and T2.*

after initial periodontal therapy between CP patients and healthy control patients. However, several studies based on crevicular IL-1β level, showed it closely related with severe periodontal disease and periodontal pocket inflammation. Moreover, previous studies observed how, in patients with periodontitis and gengivitis, the GCF IL-1β level was significantly higher in deep periodontal pocket sites than in shallow ones and healthy gingival sites. In this study, the high PPD reduction in all treated sites after 10 days and 1 month suggested how the etiological treatment of periodontal pockets is an effective therapy, capable of orienting the disease towards healing. Furthermore, the drastic reduction of BOP as well as of the concentration of the IL-1β in the crevicular fluid confirms how the periodontal treatment is able to reduce the inflammatory process and that this plays a key role in the pathogenesis and control of periodontal disease.

However, deep sites showed a significant decrease in probing depth and bleeding compared to surface sites. In addition, IL levels were significantly reduced after only 10 days and stabilized after 1 month. The periodontal etiologic therapy treatment and associated LLLT showed an improved clinical response of periodontal tissues with PPD and BOP significantly reduced compared to scaling and root planing treatment alone. The drastic reduction of

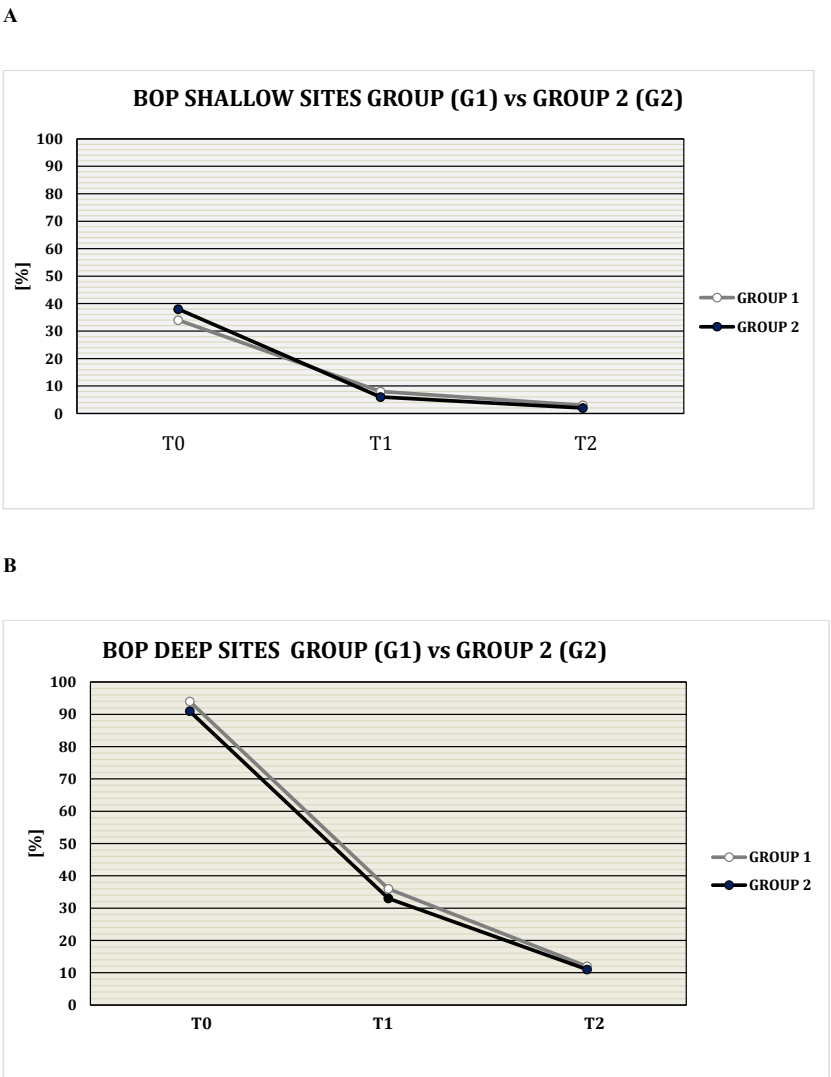

Fig. 2. *BOP values in shallow (**A**) and deep (**B**) sites of group 1 vs group 2 at T0, T1 and T2.*

A

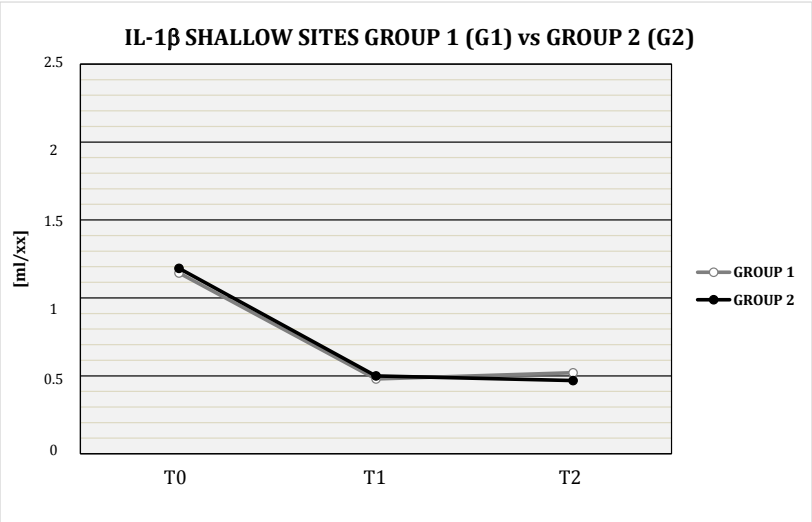

B

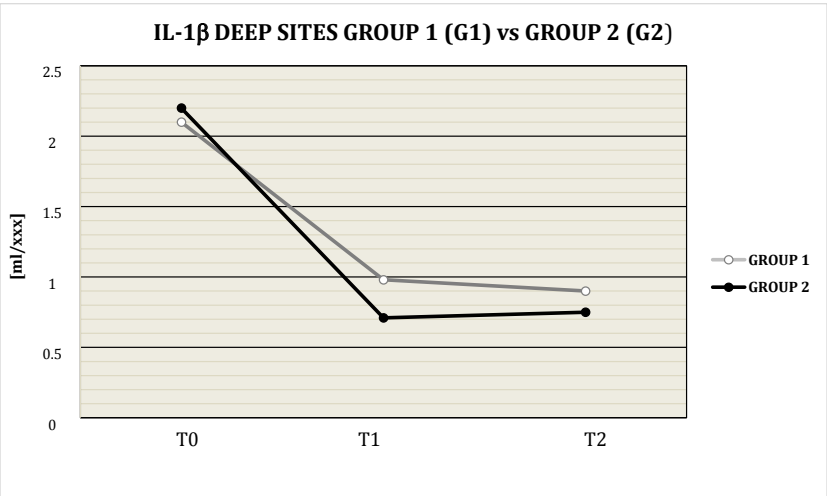

Fig. 3. IL-*1β concentration in shallow (**A**) and deep (**B**) sites of group 1 vs group 2 at T0, T1 and T2. *P < 0.001, **P < 0.005, ***P < 0.07, mean ± SE. PPD: probing pocket depth, BOP: bleeding on probing; GCF: gingival crevicular fluid*

IL-1β in patients treated with LLLT associated with etiologic therapy confirmed a better biological response of tissues in the short and long term (15).

In the light of the results obtained, it is possible to support how the association between LLLT and periodontal etiological therapy allows a drastic improvement of the clinical and biological parameters of superficial and deep periodontal defects and therefore could be suggested for use in all patients with chronic periodontitis.

REFERENCES

1. Bjordal JM, Lopes-Martins RA, Joensen J, Couppe C, Ljunggren AE, Stergioulas A, Johnson MI. A systematic review with procedural assessments

and meta-analysis of low level laser therapy in lateral elbow tendinopathy (tennis elbow). BMC Musculoskelet Disord 2008; 9:75.

2. Bjordal JM, Couppé C, Chow RT, Tunér J, Ljunggren EA. A systematic review of low level laser therapy with location-specific doses for pain from chronic joint disorders. Aust J Physiother 2003; 49(2):107-16.
3. Brosseau L, Robinson V, Wells G, et al. Low level laser therapy (Classes I, II and III) for treating rheumatoid arthritis. Cochrane Database Syst Rev 2005; 19(4):CD002049.
4. Jamtvedt G, Dahm KT, Christie A, Moe RH, Haavardsholm E, Holm I, Hagen KB. Physical therapy interventions for patients with osteoarthritis of the knee: an overview of systematic reviews. Phys Ther 2008; 88(1):123-36.
5. Chow R, Johnson M, Lopes-Martins R, Bjordal J. Efficacy of low-level laser therapy in the management of neck pain: a systematic review and meta-analysis of randomised placebo or active-treatment controlled trials. Lancet 2009; 374 (9705):1897-908
6. Tumilty S, Munn J, McDonough S, Hurley DA, Basford JR, Baxter GD. Low level laser treatment of tendinopathy: a systematic review with meta-analysis. Photomed Laser Surg 2010; 28(1):3-16.
7. van Middelkoop M, Rubinstein SM, Kuijpers T, Verhagen AP, Ostelo R, Koes BW, van Tulder MW. A systematic review on the effectiveness of physical and rehabilitation interventions for chronic non-specific low back pain. Eur Spine J 2011; 20(1):19-39.
8. Cobb CM. Lasers in periodontics: a review of the literature. J Periodontol 2006; 77(4):545-64.
9. da Silva JP, da Silva MA, Almeida AP, Lombardi Junior I, Matos AP. Laser in the tissue repair process: a literature review. Photomed Laser Surg 2010; 28(1):17-21.
10. Lapchak PA. Taking a light approach to treating acute ischemic stroke patients: transcranial near-infrared laser therapy translational science. Ann Med 2010; 42(8):576-86.
11. Chung H, Dai T, Sharma SK, Huang YY, Carroll JD, Hamblin MR. The nuts and bolts of low-level laser (light) therapy. Ann Biomed Eng 2012; 40(2):516-33.
12. Prindeze NJ, Moffatt LT, Shupp JW. Mechanisms of action for light therapy: a review of molecular interactions. Exp Biol Med (Maywood) 2012; 237(11):1241-48.
13. Ferraresi C, Kaippert B, Avci P, Huang YY, de Sousa MV, Bagnato VS, Parizotto NA, Hamblin MR. Low-level laser (light) therapy increases mitochondrial membrane potential and ATP synthesis in C2C12 myotubes with a peak response at 3-6 h. Photochem Photobiol 2015; 91(2):411-16.
14. Cantore S, Mirgaldi R, Ballini A, et al. Cytokine gene polymorphisms associate with microbiogical agents in periodontal disease: our experience. Int J Med Sci 2014; 11(7):674-79.
15. Ballini A, Mastrangelo F, Gastaldi G, et al. Osteogenic differentiation and gene expression of dental pulp stem cells under low-level laser irradiation: a good promise for tissue engineering. J Biol Regul Homeost Agents 2015; 29(4):813-22.

LETTER TO THE EDITOR

IL-1 HAPLOTYPE ANALYSIS IN PERIODONTAL DISEASE

A. BALLINI[1,2,3,4], S. CANTORE[1,2,3], A. DEDOLA[5], L. SANTACROCE[6], L. LAINO[7], M. CICCIÙ[8] and F. MASTRANGELO[5]

[1]Department of Basic Medical Sciences, Neuroscienes and Sense Organs, University of Bari Aldo Moro, Bari, Italy; [2]City Unity College, Athens, Greece; [3]BPP School of Health, University Faculty of Dentistry, Birmingham, United Kingdom; [4]World Academy of Growth Factors & Stem Cells in Dentistry, Athens, Greece; [5]Department of Clinical and Experimental Medicine, University of Foggia, Italy; [6]Ionian Department University of Bari Aldo Moro, Bari, Italy; [7]Multidisciplinary Department of Medical-Surgical and Dental Specialties, University of Campania Luigi Vanvitelli, Naples, Italy; [8]Departments of Biomedical and Dental Sciences and Morphological and Functional Imaging, Messina University, Messina, Italy

Received March 13, 2018 – Accepted March 20, 2018

Numerous studies have established statistical associations of the IL-1 gene cluster polymorphisms with various inflammatory diseases. Deriving from that, the present study was intended to determine whether single-nucleotide polymorphisms (SNPs) in these gene are also associated with periodontal disease in a Linkage disequilibrium analysis. This investigation also created two haplotype blocks, both consisting of two different SNPs. Recent theoretical analyses indicate that research with an interpretation of periodontal disease as a complex, oligogenic disorder, with IL-1 genetic variation contributes an important but not exclusive influence on disease risk. Further studies are needed to confirm these results and to understand the mechanisms behind the observed association between IL-1 SNPs and periodontal disease.

Dear Editor,

Periodontal disease (PD) is characterized by loss of connective tissues within the periodontium and destruction of (alveolar) bone support (1, 2). The most prevalent form of PD is chronic periodontitis, which is an inflammatory disease initiated by pathogenic bacteria in the subgingival plaque biofilm (1, 3). Furthermore, a prominent, localized inflammatory cell infiltrate involving neutrophils, monocytes and both T and B lymphocytes is another characteristic of PD (1). These cells are further sources of matrix metalloproteinases (MMPs) and the cytokines that regulate them (Fig. 1).

The host responds to periodontal infections with an array of events involving both innate and adaptive immunity, and association of periodontal infection with organ systems, such as cardiovascular, endocrine, reproductive, and respiratory, makes it a complex multiphase disease (1).

Interleukin(IL)-1 is an effective pro-inflammatory mediator that is primarily released by monocytes, macrophages and dendritic cells (4). The genes encoding the proteins IL-1A, IL-1B and interleukin receptor antagonist (RA) are located in close proximity in the IL-1 gene cluster at chromosome position 2q13-21. Single-nucleotide polymorphisms (SNPs) for IL-1A-889 (in linkage disequilibrium with

Key words: periodontal disease, single nucleotide polymorphisms, Interleukin-1, genetic factors, haplotype analysis

Mailing address:
Prof. Filiberto Mastrangelo, MD, DMD, PhD,
Department of Clinical and Experimental Medicine,
University of Foggia, Italy,
via Rovelli 48, 70011 Foggia, Italy
Tel.: +39 0881 55941 - Fax: +39 0881 55941
e-mail: filibertomastrangelo@hotmail.com

0393-974X (2018)

+4845, IL-1B -511 (in linkage disequilibrium), IL-1B +3954 (also referred to as +3953) and RA gene IL-1RN VNTR [variable number of tandem repeats, in linkage disequilibrium (LD) with +2018] are at present studied in periodontal research (Table I) (4, 5).

With respect to biallelic markers, the most common statistics to measure LD in a population are the difference between the observed and expected (under linkage equilibrium) haplotype frequencies (D), the proportion of D relative to the expected maximum value in the population (D'), and the square of the correlation between the values of alleles at two loci (r2) (6).

Cytokines, such as IL-1, and differences in their expression have critical roles in hard tissue injury which could explain the relationship of SNPs between the persistent populations (4). In industrialized countries, oral health care based on private or public systems is available to the population, but many developing regions have few oral health services.

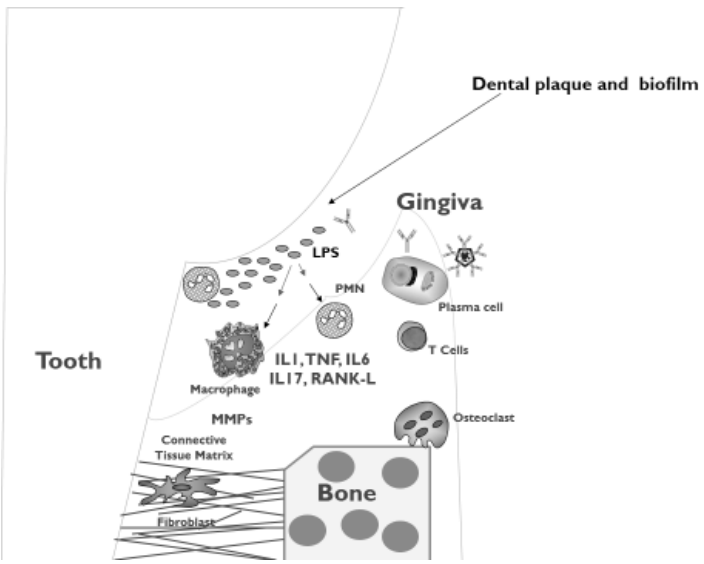

Fig. 1. *Host response can be both protective and destructive. Production of inflammatory biochemical mediators, collectively known as "cytokines" (e.g., IL-1, TNF-alpha). Cytokines signal other cells, such as fibroblasts, to produce PGE2 and MMPs, which have been associated with bone destruction and connective tissue degradation, respectively.*

Table I. *Genetic control of IL-1. Genes and Locus of SNPs associated with controlling IL-1 biological activity.*

Genes	Polymorphism Locus	Current Locus assessed with test	Controlled product
IL-1A	Allele 2 -889	Allele 2 IL-1A +4845	IL-1 alpha
IL-1B	Allele 2 +3953	Allele 2 IL-1B +3954	IL-1 beta
IL-1RN			Protein receptor antagonist (impedes IL-1 alpha and beta)

Genetic Susceptibility Test for periodontitis: tests for the presence of at least one copy of allele 2 at the IL-1A +4845 loci and at least one copy of allele 2 at the IL-1B +3954 locus.

**IL-1A +4845 is being used because it is easier to identify than IL-1A -889 and is essentially concordant with it.*

*** IL-1B +3953 has been now renumbered as IL-1B +3954 because the current convention indicates that the numbering of the transcription should begin at +1 instead of zero.*

Thus, the need for risk factor-based periodontitis preventive strategies has increased.

The aim of the present study was to investigate associations between one IL-1A and 1L-1B single-nucleotide polymorphism (SNP) and relative haplotype frequencies, on the incidence of chronic PD among a sample size of Caucasian subjects.

MATERIALS AND METHODS

Study sample

The characteristics of cases and controls (total 40 Caucasian subjects) are shown in Table II. There were no statistical differences between cases and control subjects with regard to age at oral examination, education, smoking, toothbrushing frequency, or use of an interdental brush.

This study was conducted in accordance with the Declaration of Helsinki and written informed consent was obtained from all participants.

Genomic analysis

Analysis of blood samples was carried out in a blinded fashion. Five milliliters of venous blood were drawn from the antecubital vein and transferred to a vacutainer containing ethylenediaminetetraacetic acid (EDTA; 3%) to prevent coagulation and stored at −20°C.

Genomic DNA was extracted by the salting out method (5, 6): DNA was aliquoted in distilled water and were stored at 4°C; DNA integrity was also tested, by running genomic DNA through 0.8% agarose gel, and visualized with ethidium bromide.

Table II. *Characteristics of the study population.*

	Cases	***Controls***
Age (years)	**SD: 38.7±15.6 yr**	**SD: 36.8±16.1 yr**
Male	8	7
Female	10	13
Smokers	14	4
Non-smokers	6	16

Unrelated patients (n = 20; 8 males; 10 females; mean age ± SD: 38.7±15.6 yr) with chronic periodontitis were enrolled in the study along with healthy control subjects (n = 20; 7 males; 13 females; mean age ± SD: 36.8±16.1 yr) from the Caucasian population.

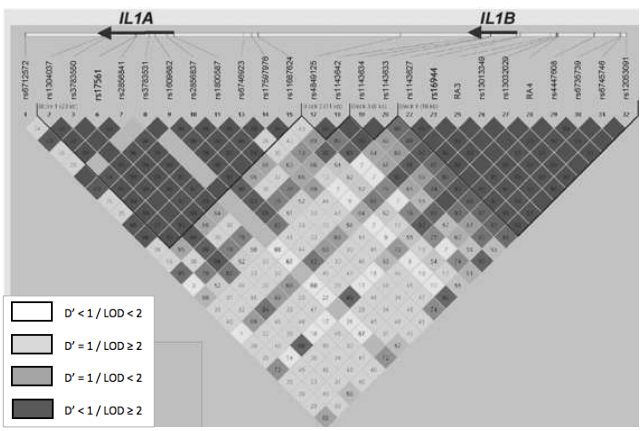

Fig. 2. *Characteristics of the study population. Unrelated patients (n = 20; 8 males; 10 females; mean age ± SD: 38.7±15.6 years) with chronic periodontitis were enrolled in the study along with healthy control individuals (n = 20; 7 males; 13 females; mean age ± SD: 36.8±16.1 years) from the Caucasian population.*

Statistical analysis

Epidata 3.02 software was used to establish a database, and the double-entry method was used for data input and logic error detection. The SPSS 17.0 statistical package was used for the *chi*-squared test and univariate logistic regression analysis (SPSS, Inc., Chicago, IL, USA). SHEsis software (http://analysis.bio-x.cn/myAnalysis.php) was used for haplotype analysis, and Phase software was used for linkage disequilibrium analysis. The frequency of alleles was determined by direct counting. Hardy-Weinberg equilibrium (HWE) was assessed in both the patient and control groups using SNPStats (http://bioinfo.iconcologia.net/index.php?module=Snpstats).

Linkage disequilibrium blocks and haplotypes were identified using Haploview version 4.2 (7). For the statistical tests, the significance level for P values was set at 0.05. Estimations of crude odds ratios (ORs) and 95% confidence intervals (CIs) for PD associated with the SNPs under study were made by means of logistic regression analysis, with the reference category being the homozygote of the major allele. Haplotypes and their frequencies were inferred according to the expectation maximization algorithm.

RESULTS

Analysis of the IL-1A and IL-1B, genes was performed according to the pairwise LD pattern observed within each of these genes (cases + controls, n = 40).

The LD analysis indicated the existence of two recombination sites in the IL-1 gene cluster, the first between rs6712572 and rs11687624 of IL-1a (|D'| = 0.25) and the second between rs1143627 and rs12063091of IL-1B (|D'| = 0.09). This also created two haplotype blocks, one containing rs17561, and rs16944 (the first SNPs from IL-1A and the second SNP from IL-1B gene; |D'| 0.91–0.97) as shown in Fig. 2, demonstrating that the rs17561 and rs16944 polymorphisms (D' = 0.9149/0.9024, R2 = 0.6 680/0.6845) showed linkage disequilibrium.

In the control group, the distribution of genotypes was in HWE (P = 0.41). When haplotypes with a frequency of less than 1% in either case or control subjects were deleted, three haplotypes remained; however, none of these were significantly related to the risk of PD.

DISCUSSION

In the present study we examined multiplicative interaction between the SNPs and haplotypes in regard to the risk of PD. The multiplicative interaction was estimated by introducing a multiplicative term into a multiple logistic regression model. This highlights that the carriage rate of genetic polymorphisms may vary among ethnic populations (1). Therefore, probable positive associations among a genetic polymorphism and disease within one population cannot be certainly generalized to other populations (4, 5).

For multi-factorial diseases, such as chronic PD, no single gene mutation will allow a definitive diagnosis or certain risk prediction. In such a complex disease model, a single functional gene polymorphism can modulate disease progression over time but is not solely sufficient to cause PD. Genetic testing would therefore be most useful for subjects with PD as one component of a spectrum of diseases which might be targeted for intervention for risk reduction at the gene environment level. At this level the information gained from genetic testing could assist health professionals to personalise the treatment of their patients.

Our study had methodological advantages: study subjects were homogeneous in gender and age and several confounders were checked. Important weaknesses in the present study should be taken into consideration. Firstly, our subjects were probably not a representative sample of Caucasian in the general population. Secondly, the current study size was rather small for a valid genetic association study. The lack of significant relationships between the other SNPs and PD might be attributable to an insufficient statistical power. Thirdly, a correction for multiple testing, an appropriate element in initial exploratory analyses, was not performed in this study. As this is a hypothesis testing study, and as part of the current findings is a replication of previously published results, we think that correction for multiple testing could lead us to underestimate our results. Fourthly, although adjustment was made for some confounders, residual confounding effects could not be ruled out.

The search for the 'master gene' responsible for periodontitis in an otherwise healthy individual is still continuing. The multifactorial nature of the disease makes the investigations more challenging and demanding, moving researchers towards different clinical treatments, as well as new insight, i.e. low level laser therapy, stem cells, and endo-perio approaches, within their actual limits (8-12). The evidence to date suggests that PD occurs as complex interactions among host factors, genetics, and the environment. Thus, as well as interpretation of genotype status, other factors must also be used in the treatment regime and for maintenance schedules. Future studies should focus on finding the confirmed etiologies and their exact role in the disease development and progression. Genetic studies may play a major role in solving this aspect.

REFERENCES

1. Ballini A, Cantore S, Farronato D, et al. Periodontal disease and bone pathogenesis: the crosstalk between cytokines and porphyromonas gingivalis. J Biol Regul Homeost Agents 2015; 29:273-81.
2. Ballini A, Tetè S, Scattarella A, et al. The role of anti-cyclic citrullinated peptide antibody in periodontal disease. Int J Immunopathol Pharmacol 2010; 23:677-81.
3. Cantore S, Ballini A, Mori G, et al. Anti-plaque and antimicrobial efficiency of different oral rinses in a 3-day plaque accumulation model. J Biol Regul Homeost Agents 2016; 30:1173-78.
4. Cantore S, Mirgaldi R, Ballini A, et al. Cytokine gene polymorphisms associate with microbiogical agents in periodontal disease: our experience. Int J Med Sci 2014; 11:674-79.
5. Crincoli V, Ballini A, Fatone L, Di Bisceglie MB, Nardi GM, Grassi FR. Cytokine genotype distribution in patients with periodontal disease and rheumatoid arthritis or diabetes mellitus. J Biol Regul Homeost Agents 2016; 30:863-66.
6. Rohlfs RV, Weir BS. Distributions of Hardy-Weinberg equilibrium test statistics. Genetics. 2008; 180:1609-16. (Erratum in: Genetics 2009; 183:756).
7. Barrett JC, Fry B, Maller J, Daly MJ. Haploview: analysis and visualization of LD and haplotype maps. Bioinformatics 2005; 15:263-265
8. Scattarella A, Ballini A, Grassi FR, et al. Treatment of oroantral fistula with autologous bone graft and application of a non-reabsorbable membrane. Int J Med Sci 2010; 11:267-71.
9. Ballini A, Mastrangelo F, Gastaldi G, et al. Osteogenic differentiation and gene expression of dental pulp stem cells under low-level laser irradiation: a good promise for tissue engineering. J Biol Regul Homeost Agents 2015; 29:813-22.
10. Grassi FR, Pappalettere C, Di Comite M, et al. Effect of different irrigating solutions and endodontic sealers on bond strength of the dentin-post interface with and without defects. Int J Med Sci 2012; 9:642-54.
11. Ballini A, Scattarella A, Crincoli V, et al. Surgical treatment of gingival overgrowth with 10 years of follow-up. Head Face Med 2010; 6:19.
12. Crincoli V, Scivetti M, Di Bisceglie MB, Pilolli GP, Favia G. Unusual case of adverse reaction in the use of sodium hypochlorite during endodontic treatment: a case report. Quintessence Int 2008; 39:e70-73.